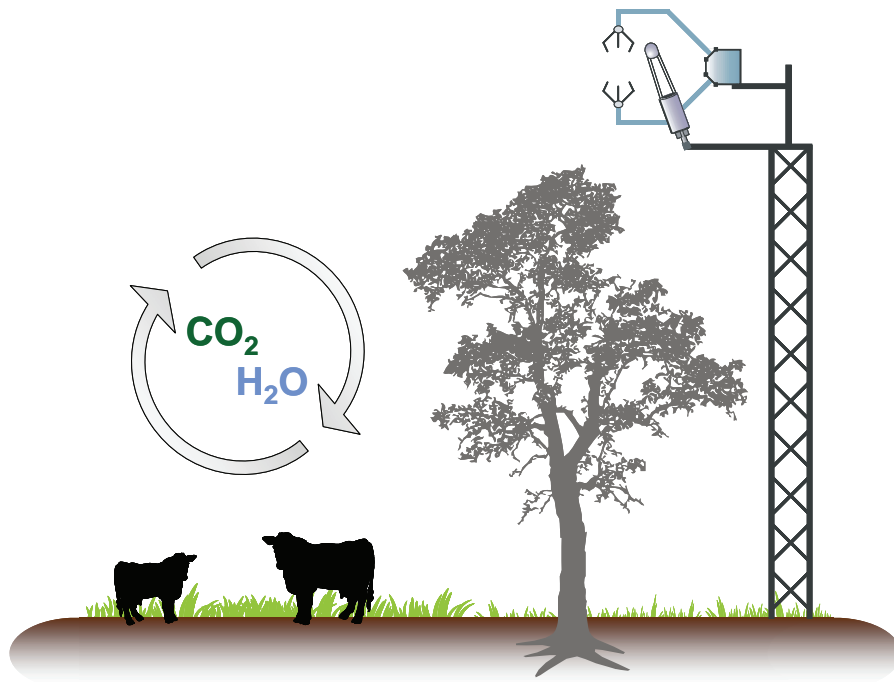


Carbon dioxide and water vapour fluxes of tropical pasture and afforestation: seasonal variations of net ecosystem exchange and carbon sequestration potentials

SEBASTIAN WOLF



Dissertation for the Degree of Doctor of Sciences

DISS. ETH NO. 19415

**CARBON DIOXIDE AND WATER VAPOUR FLUXES
OF TROPICAL PASTURE AND AFFORESTATION:
SEASONAL VARIATIONS OF NET ECOSYSTEM EXCHANGE
AND CARBON SEQUESTRATION POTENTIALS**

A dissertation submitted to

ETH ZURICH

for the degree of

Doctor of Sciences

presented by

SEBASTIAN WOLF

Dipl.-Geogr., Dresden University of Technology

born 25 December 1978

of German nationality

Prof. Dr. Nina Buchmann, examiner

PD Dr. Werner Eugster, co-examiner

Prof. Dr. Nicolas Gruber, co-examiner

2010

”Not everything that can be counted counts,
and not everything that counts can be counted”
(ALBERT EINSTEIN)

For my parents

Für meine Eltern

Contents

List of Tables	IV
List of Figures	V
List of Abbreviations	VI
Abstract	VII
Zusammenfassung	IX
1 Introduction	1
1.1 Biosphere-atmosphere interactions.....	1
1.2 Tropical ecosystems and land-use change.....	2
1.3 Terrestrial carbon sequestration.....	3
1.4 The Sardinilla research site.....	4
1.5 Eddy covariance technique	5
1.6 Objectives	7
1.7 Thesis outline.....	7
2 Seasonal variations in net ecosystem carbon dioxide exchange	9
2.1 Introduction	10
2.2 Materials and Methods	12
2.2.1 Site description	12
2.2.2 Instrumentation and data acquisition	14
2.2.3 Data processing and corrections	15
2.2.4 Separation of seasons.....	16
2.2.5 Auxiliary measurements	16
2.2.6 Energy Balance Closure.....	17
2.2.7 Statistical analyses and general conventions	18
2.3 Results	18
2.3.1 Seasonality in climate	18
2.3.2 Seasonal variations of NEE	22
2.3.3 Diurnal variations of NEE	22
2.3.4 Nighttime soil and ecosystem respiration.....	24
2.3.5 Environmental controls of CO ₂ fluxes.....	24
2.3.6 Quality assessment of flux data	26
2.3.7 Phenology	26
2.4 Discussion.....	28
2.5 Conclusions	31

3	Carbon sequestration potential of pasture compared to afforestation	33
3.1	Introduction	34
3.2	Materials and Methods	36
3.2.1	Site description	36
3.2.2	Instrumentation and data acquisition	36
3.2.3	Flux data processing	37
3.2.4	LAI, biomass, grazing and soil measurements	39
3.2.5	Statistical analyses and general conventions	40
3.3	Results	41
3.3.1	Intra- and inter-annual variations in precipitation	41
3.3.2	Seasonal patterns in GPP, TER and NEE	43
3.3.3	Carbon budgets	46
3.3.4	Environmental controls of GPP, TER and NEE	47
3.3.5	Management controls of GPP and TER	48
3.3.6	Inventory data	50
3.4	Discussion	52
3.5	Conclusions	56
4	Evapotranspiration of tropical pasture and afforestation	59
4.1	Introduction	61
4.2	Materials and Methods	62
4.2.1	Site description	62
4.2.2	Instrumentation	63
4.2.3	Data processing	64
4.2.4	Gap Filling	65
4.2.5	Supplementary measurements	65
4.2.6	Statistical analyses and general conventions	65
4.3	Results	66
4.3.1	Ecosystem water budgets	66
4.3.2	Seasonal and inter-annual variations in ET	68
4.3.3	Diurnal cycles of ET	68
4.3.4	Environmental controls of ET	71
4.3.5	Soil infiltrability	71
4.4	Discussion	72
4.5	Conclusions	75
5	Synthesis	77
5.1	Main results	77
5.2	Carbon stocks and fluxes	78
5.3	Implications for the tropics	79
5.4	Outlook	82

References.....	83
Appendixes	95
Appendix A – Schneebeli et al. (2008).....	97
Appendix B – Schneebeli et al. (accepted).....	101
Appendix C – Potvin et al. (in press).....	113
Appendix D – GIS Maps	125
Acknowledgements.....	141
Curriculum Vitae	143

List of Tables

Tab. 2.1:	Flux tower site characteristics for the pasture and the afforestation sites	13
Tab. 2.2:	Season lengths and climatic conditions at Sardinilla	19
Tab. 2.3:	Seasonal averages of midday and nighttime NEE.....	23
Tab. 2.4:	Mean cumulative seasonal NEE.....	24
Tab. 3.1:	Monthly values of GPP, TER, NEE and meteorological data.....	42
Tab. 3.2:	Season length, meteorology and total seasonal NEE.	45
Tab. 3.3:	Above and belowground standing biomass at the Sardinilla afforestation ..	51
Tab. 3.4:	Topsoil characteristics at the Sardinilla pasture and afforestation	51
Tab. 3.5:	Summary of ecosystem CO ₂ flux studies in the tropics	57
Tab. 4.1:	Site characteristics for the pasture and afforestation flux towers.....	64
Tab. 4.2:	Seasonal overview of meteorological variables at Sardinilla.....	67
Tab. 4.3:	Seasonal averages of daily total evapotranspiration.....	69

List of Figures

Fig. 1.1:	The global carbon cycle	1
Fig. 1.2:	Location of the Sardinilla site in Central Panama	4
Fig. 1.3:	Maps of the Sardinilla site	5
Fig. 1.4:	Ecosystem flux measurements using the eddy covariance technique.....	6
Fig. 1.5:	Biosphere-atmosphere net ecosystem CO ₂ exchange	6
Fig. 2.1:	Weekly precipitation, SWC, VPD and PPFD.....	20
Fig. 2.2:	Diurnal cycles of seasonally averaged PPFD	20
Fig. 2.3:	Diurnal cycles of seasonally averaged air temperature and VPD.....	21
Fig. 2.4:	Inter-annual and seasonal variations of weekly midday NEE	21
Fig. 2.5:	Diurnal cycles of seasonally averaged NEE	23
Fig. 2.6:	Mean nighttime soil respiration and total ecosystem respiration.....	25
Fig. 2.7:	Seasonal energy balance closure.....	27
Fig. 2.8:	Footprint estimates for dry and wet season.....	27
Fig. 2.9:	Leaf area index during February to July 2009	28
Fig. 3.1:	Daily total GPP, TER and NEE	43
Fig. 3.2:	Flux fingerprints of gap filled net ecosystem exchange	45
Fig. 3.3:	Cumulative annual net ecosystem exchange from 2007 until 2009	46
Fig. 3.4:	Seasonally averaged light response curves	47
Fig. 3.5:	Aboveground green biomass and grazing at the Sardinilla Pasture.....	49
Fig. 4.1:	Climate diagram of Sardinilla.....	63
Fig. 4.2:	Mean annual course of daily total evapotranspiration	67
Fig. 4.3:	Daily total ET and meteorological data from June 2007 to January 2010...	69
Fig. 4.4:	Relationship between daily total ET of pasture and afforestation	70
Fig. 4.5:	Diurnal cycles of seasonally averaged evapotranspiration	70
Fig. 4.6:	Seasonal variability in the functional relationship of ET and PPFD	72
Fig. 5.1:	Carbon stocks and fluxes in the Sardinilla in 2008.....	79

List of Abbreviations

ACP	Panama Canal Authority
AirT	Air temperature
A_{sat}	Maximum photosynthetic capacity
BCI	Barro Colorado Island
C	Carbon
C_3	Carbon fixation pathway where CO_2 is first fixed by RuBisCO
C_4	Carbon fixation pathway where CO_2 is first fixed by PEP-Carboxylase
CO_2	Carbon dioxide
CWD	Coarse woody debris
d_B	Bulk density
DOC	Dissolved organic carbon
DOY	Day of year
EBC	Energy balance closure
EC	Eddy covariance
ENSO	El Niño Southern Oscillation
ET	Evapotranspiration
GPP	Gross primary production
H_2O	Water vapour
IRGA	Infrared gas analyzer
LAI	Leaf area index
LCP	Light compensation point
LRC	Light response curve
LU	Livestock unit
MNR	Midday-Night ratio
N	Nitrogen
NEE	Net ecosystem exchange
P	Precipitation
PPFD	Photosynthetic photon flux density
R_G	Incoming shortwave radiation (global radiation)
R_N	Net radiation
R_{Soil}	Soil respiration
SD	Standard deviation
SWC	Soil water content
TER	Total ecosystem respiration
u^*	Friction velocity
VPD	Vapour pressure deficit
$\delta^{13}\text{C}$	Carbon isotope ratio referred to standard

Abstract

Tropical forest ecosystems play an important role in regulating the global climate, yet deforestation and land-use change indicate that the tropical carbon and water cycle are increasingly influenced by agroecosystems and pastures. It is not yet fully understood how the carbon and water cycle in the tropics respond to land-use change, particularly in managed ecosystems such as pasture and afforestation. Therefore, it is crucial to investigate the biosphere-atmosphere interactions of these alternative land-use types in the tropics. This thesis aims to improve our understanding of the interactions between land use and climate on ecosystem carbon dioxide (CO₂) and water vapour (H₂O) fluxes of tropical pasture and native tree species afforestation, with the main focus on seasonal variations and carbon sequestration potentials.

Comparative eddy covariance measurements of ecosystem CO₂ and H₂O fluxes were performed in a tropical C₄ pasture and adjacent afforestation with native tree species in Sardinilla (Panama) from 2007 to 2009. Pronounced seasonal variations were observed in gross primary production (GPP), total ecosystem respiration (TER) and net ecosystem exchange (NEE), which were closely related to radiation, soil moisture and C₃ *versus* C₄ plant physiology. The pasture ecosystem was more susceptible to water limitations during the dry season and thus, the conversion from pasture to afforestation reduced seasonal variations in GPP, TER and NEE. Furthermore, El Niño Southern Oscillation (ENSO) events and associated increases in precipitation variability were found to have a strong impact on seasonal variations of CO₂ fluxes, particularly on the pasture ecosystem. Soil respiration contributed about half of TER during nighttime, with only small differences between ecosystems or seasons. Temperature was found to have no effect on ecosystem and soil respiration in Sardinilla.

Annual GPP was higher in the pasture (2345 g C m⁻² yr⁻¹) than in the afforestation ecosystem (2082 g C m⁻² yr⁻¹) but overall lower than reported from tropical forests. Substantial carbon sequestration was found in the afforestation (-442 g C m⁻² yr⁻¹, negative values denote ecosystem carbon uptake) during 2008, which was in good agreement with biometric observations (-450 g C m⁻² yr⁻¹) revealing a total carbon stock of 2122 g C m⁻² in above and belowground biomass. Furthermore, estimates for 2007 and 2009 indicated also strong carbon uptake by the afforestation ecosystem. In contrast, the pasture ecosystem was a similarly strong carbon source in 2008 and 2009 (261 g C m⁻²) and carbon losses were predominantly associated with high stocking densities and periodical overgrazing. The carbon losses from the pasture originated primarily from soil organic matter. Stable isotope (δ¹³C) analysis indicated rapid carbon turnover following the land conversion from C₄ pasture to C₃ afforestation. The soil carbon stock (0–100 cm) in the pasture (5350 g C m⁻²) was significantly lower than in the afforestation (7640 g C m⁻²) suggesting differences in land management before the establishment of the afforestation in 2001. The afforestation of tropical pasture only

marginally affected annual ecosystem-scale evapotranspiration (ET; 1114 vs. 1034 mm yr⁻¹ in 2008), but reduced the seasonal variations in ET and largely increased the soil infiltration potential. About half of the annual precipitation was returned to the atmosphere by ET from both ecosystems.

In summary, this thesis presents the first multi-year eddy covariance measured CO₂ and H₂O fluxes for tropical pasture and afforestation in Panama, is one of the very few ecosystem flux studies from Central America, and emphasizes the significance to investigate alternative land-use types in the tropics. The results underline the substantial carbon sequestration potential of tropical afforestation and show the impact of overgrazing on carbon losses from a pasture. Moreover, the land-use change from pasture to afforestation can reduce the seasonal variations of CO₂ and H₂O fluxes and enhance the ecosystem resilience to seasonal drought.

Zusammenfassung

Tropische Waldökosysteme spielen eine wichtige Rolle bei der Regulierung des globalen Klimas. Abholzung und Landnutzungsänderungen haben zur Folge, dass der tropische Kohlenstoff- und Wasserkreislauf zunehmend von Agrarökosystemen und Weiden geprägt wird. Es ist noch nicht vollständig geklärt, welche Auswirkungen Landnutzungsänderungen auf den tropischen Kohlenstoff- und Wasserkreislauf haben. Dies gilt insbesondere für bewirtschaftete Ökosysteme wie Weiden und Aufforstungen. Daher ist es unerlässlich, die Wechselwirkungen zwischen Biosphäre und Atmosphäre dieser alternativen Landnutzungsarten in den Tropen zu untersuchen. Das Ziel dieser Arbeit war es, die Wechselwirkungen zwischen Landnutzung und Klima zu analysieren und ihren Einfluss auf die Ökosystemflüsse von Kohlendioxid (CO₂) und Wasserdampf (H₂O) in tropische Weiden und Aufforstungen besser zu verstehen. Der Schwerpunkt lag dabei auf saisonalen Schwankungen und dem Potential der Kohlenstoffspeicherung. Auf einer tropischen C₄-Weide und einer angrenzenden Aufforstung mit einheimischen Baumarten in Sardinilla (Panama) wurden von 2007 bis 2009 vergleichende Messungen dieser Ökosystemflüsse mit der Eddy-Kovarianz-Methode durchgeführt. Ausgeprägte saisonale Schwankungen in der Primärproduktion (GPP), der Ökosystematmung (TER) und des Netto-Ökosystem-Austausches (NEE) standen in einem starken Zusammenhang mit der Einstrahlung, der Bodenfeuchte sowie der C₃/C₄ Pflanzenphysiologie. Während der Trockenzeit war das Weide-Ökosystem empfindlicher gegenüber Wassermangel. Daher verringerten sich mit der Landnutzungsänderung von einer Weide zu einer Aufforstung die saisonalen Schwankungen von GPP, TER und NEE. Darüber hinaus hatten Ereignisse der El Niño Southern Oscillation (ENSO) und die damit verbundene Zunahme der Niederschlags-Variabilität einen starken Einfluss auf die saisonalen Schwankungen der CO₂-Flüsse, insbesondere im Weide-Ökosystem. Die Bodenatmung machte etwa die Hälfte der gesamten Ökosystematmung aus, wobei die Unterschiede zwischen beiden Ökosystemen und zwischen den Jahreszeiten gering waren. Es wurden keine Temperaturabhängigkeiten der nächtlichen Boden- und Ökosystematmung in Sardinilla festgestellt.

Die jährliche Primärproduktion war auf der Weide (2345 g C m⁻² yr⁻¹) höher als in der Aufforstung (2082 g C m⁻² yr⁻¹), jedoch insgesamt niedriger als in tropischen Regenwäldern. Die Aufforstung ging im Jahr 2008 mit einer starken Kohlenstoffsénke einher (-442 g C m⁻² yr⁻¹). Forstinventardaten zeigten eine gute Übereinstimmung mit den Flussmessungen (-450 g C m⁻² yr⁻¹) und quantifizierten mit 2122 g C m⁻² den gesamten Kohlenstoffspeicher in Form von unter- und oberirdischer Biomasse. Abschätzungen für 2007 und 2009 zeigten ebenfalls eine starke Kohlenstoffaufnahme durch die Aufforstung. Die Weide war in den Jahren 2008 und 2009 eine starke Kohlenstoffquelle (261 g C m⁻²), wobei die Kohlenstoffverluste im Wesentlichen durch eine starke Beweidung und regelmässige Überweidung bedingt waren.

Die Kohlenstoffverluste auf der Weide stammten hauptsächlich aus der organischen Bodensubstanz. Die Auswertung von stabilen Isotopen ($\delta^{13}\text{C}$) zeigte eine sehr schnelle Verarbeitung des Kohlenstoffs im Boden während der Landnutzungsänderung von einer C_4 -Weide zu einer C_3 -Aufforstung. Der Bodenkohlenstoff-Speicher (0–100 cm) war in der Weide signifikant niedriger (5350 g C m^{-2}) als in der Aufforstung (7640 g C m^{-2}). Dies deutet auf unterschiedliche Bewirtschaftungen beider Flächen vor dem Beginn der Aufforstung im Jahre 2001 hin. Die Aufforstung der tropischen Weide hatte kaum einen Einfluss auf die jährliche Verdunstung ($1114 \text{ vs. } 1034 \text{ mm yr}^{-1}$ in 2008), verringerte jedoch ihre saisonalen Schwankungen. Das Infiltrations-Potential des Bodens wurde hingegen stark erhöht. Die Verdunstung transportierte ungefähr die Hälfte der jährlichen Niederschlagsmenge zurück in die Atmosphäre.

Diese Arbeit präsentiert die ersten mehrjährigen Messungen für tropische Weiden und Aufforstungen mit der Eddy-Kovarianz-Methode in Panama. Sie ist eine der wenigen Ökosystem-Flussmessungen in Zentralamerika und betont die Notwendigkeit der Untersuchung von alternativen Landnutzungstypen in den Tropen. Die Ergebnisse bestätigen das erhebliche Potential der Kohlenstoffspeicherung in tropischen Aufforstungen und verdeutlichen den starken Einfluss von Überweidung auf die Kohlenstoffverluste einer Weide. Darüber hinaus zeigen die Ergebnisse, dass diese Landnutzungsänderung die saisonalen Schwankungen der CO_2 - und H_2O -Ökosystemflüsse verringert und die Widerstandsfähigkeit gegenüber jahreszeitlicher Trockenheit verbessert.

Chapter 1

1 Introduction

1.1 Biosphere-atmosphere interactions

The biosphere-atmosphere exchange of carbon and water is of major importance for the global climate system. Terrestrial ecosystems are critical constituents of this exchange, sequester 2 Pg C yr^{-1} or 34% of the fossil fuel emission (Sarmiento and Gruber, 2006; Fig. 1.1) and return 60% of the annual land precipitation back to the atmosphere via evapotranspiration (Oki and Kanae, 2006). This interaction between terrestrial ecosystems and the atmosphere induces biophysical (e.g. albedo change) and biogeochemical (e.g. CO_2 fertilization) feedbacks that directly affect the climate system (Arneeth et al., 2010; Moorcroft, 2003). It remains highly uncertain how the terrestrial carbon sink will behave in the future (Sarmiento et al., 2010) but there are indications that the sink strength of the biosphere is declining in response to climate change (Canadell et al., 2007; Le Quere et al., 2009). Moreover, the feedbacks of the hydrological cycle to a changing climate are not well understood (Bates, 2008; Jung et al., 2010), but evidence indicates that climate change causes an intensification of the water cycle (Huntington, 2006).

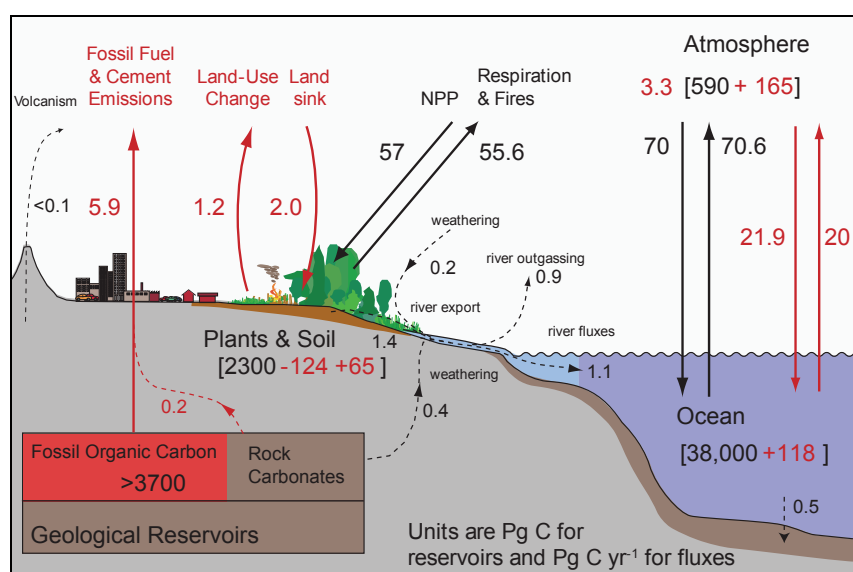


Figure 1.1. The global carbon cycle. Black arrows show the preindustrial fluxes (Pg C yr^{-1}) and red arrows the anthropogenic fluxes from 1980 to 1999. The numbers in brackets denote the preindustrial reservoir sizes (Pg C) in black and the reservoir changes from 1800–1994 in red (Sarmiento and Gruber, 2006).

1.2 Tropical ecosystems and land-use change

Tropical ecosystems play an important role for the global carbon and water cycle, as they account for 60% of the global terrestrial gross primary production (Beer et al., 2010), contain 40% of the carbon stored in the terrestrial biosphere (Grace et al., 2001) and are a major source of global land surface evapotranspiration (Fisher et al., 2009). Given the importance of tropical ecosystems it is crucial to understand how these respond to changing environmental conditions and anthropogenic interference.

Land-use change and fossil fuel emissions have caused increases in atmospheric carbon dioxide (CO_2) concentrations by more than 35% since preindustrial times and thus, substantially influenced the carbon and water cycle (Houghton, 2007). This increase would have been even larger without the biosphere sequestering carbon dioxide: About 46% of the total anthropogenic emissions remain in the atmosphere, while the rest is taken up by oceans and terrestrial ecosystems (Sarmiento and Gruber, 2006; Fig. 1.1). Besides fossil fuel emissions, land-use change (mainly deforestation) in the tropics is the main terrestrial source of CO_2 to the atmosphere (Sarmiento et al., 2010) and is primarily driven by the demand for timber, arable land and livestock production (IPCC, 2007b). Ongoing deforestation strongly reduces the area of rainforest and alternative land-use types such as cropland, pasture and afforestation are becoming more prevalent in the tropics (Alves et al., 2009; Fearnside, 2005). However, only very few studies have been conducted in these managed ecosystems so far and thus, our understanding of their role in the carbon and water cycling of the tropics is still limited.

Continuous eddy covariance measurements of CO_2 and water vapour (H_2O) fluxes (see section 1.5) provide a valuable tool to investigate the regulating mechanisms of the biosphere-atmosphere exchange and the response of ecosystems to changing environmental conditions. Such measurements are generally scarce in the tropics and represent only 10% of all sites within global measurement networks such as FLUXNET (www.fluxnet.ornl.gov). Moreover, tropical forests dominate these sites and only few studies were conducted in managed ecosystems such as tropical grasslands (4 FLUXNET sites; Priante-Filho et al., 2004; Sakai et al., 2004; Santos et al., 2004; von Randow et al., 2004). These studies reported that land-use change from tropical forest to pasture increased inter and intra-annual variations in ecosystem CO_2 fluxes, the sensitivity to seasonal drought and affected ecosystem carbon budgets (Saleska et al., 2009b). However, it is largely unknown how the reverse land-use change – from pasture to afforestation – affects ecosystem CO_2 and H_2O fluxes, and the response to a changing climate in the tropics.

To counteract the anthropogenically induced carbon losses from the biosphere, forest regrowth with reforestation (directly after timber harvest) and afforestation (of nonforested land) is considered as an effective measure to prevent further carbon losses and to increase the carbon stocks of terrestrial ecosystems (Jackson et al., 2007). On a global scale, the mitigation potential of afforestation is estimated in the order of 15% of global CO_2 emissions and the humid tropics are the region with the largest potential (IPCC,

2007a; Malhi et al., 2002) as they have (1) the highest gross primary productivity (Beer et al., 2010), (2) large areas of available land from deforestation (Fearnside and Laurance, 2004), and (3) a positive climate forcing effect (cooling) of afforestation due to dominating moisture *versus* albedo feedbacks (Bonan, 2008; Chapin et al., 2008).

Latin America is one of the regions with the highest deforestation rates in the tropics, with land predominantly converted to pasture (Wassenaar et al., 2007), and thus has a large potential for afforestation of pasture land. Afforestations may in general become more relevant for tropical countries in the future within the international carbon accounting of the Kyoto protocol, but this requires accurate information on the carbon sequestration potential involved.

1.3 Terrestrial carbon sequestration

Carbon sequestration is the process of increasing the carbon content of a reservoir other than the atmosphere, leading to a reduction of the atmospheric CO₂ concentration. The sequestration term implies that atmospheric CO₂ is transferred into long-lived carbon pools that are not immediately re-emitted (IPCC, 2001; Lal, 2004). The main terrestrial carbon reservoirs in the short-term carbon cycle are vegetation biomass and soil organic matter (Lorenz and Lal, 2010). The overall aim of biological carbon sequestration measures is to increase the carbon stocks in biomass and the soil by managing carbon fluxes in a way that results in carbon sinks (Nieder and Benbi, 2008). The potential of biological carbon sequestration largely depends on environmental conditions, such as water, temperature, light and nutrients, but also on the area of available land, on management and on carbon stocks prior and after land-use changes (Canadell et al., 2007; Houghton, 2007; Lorenz and Lal, 2010)

Changes in terrestrial carbon stocks can be estimated by repeated measurements of the stocks (e.g. forest and soil inventories) or direct measurements of the fluxes that are changing the stocks (Houghton, 2007), such as the net ecosystem CO₂ exchange. The increase in carbon stocks or the respective net flux from the atmosphere to the ecosystem yields the carbon sequestration, which is generally assessed on an annual base. However, carbon sequestration also largely depends on the residence time of the carbon sequestered in a terrestrial pool and therefore long-term dynamics such as disturbance need to be considered (Koerner, 2003). Furthermore, annual increases in carbon stocks are declining with forest age and there is still ongoing controversy whether old growth forests are acting as carbon sinks or sources (Luyssaert et al., 2008; Saleska et al., 2003). Evidently, carbon stocks grow but the fluxes become relatively minor compared to the stocks and the risk of disturbances such as fires and windfall increases with forest age (Koerner, 2003; Koerner, 2009). Carbon sequestration assessments of terrestrial ecosystems are thus estimates that assume persistent growth increments in carbon stocks in the future and typically neglect disturbances. However, terrestrial carbon sequestration is considered as an effective measure to establish at least short-term carbon sinks to complement the mitigation of increasing CO₂ concentrations (Jackson et al., 2007) until

more effective measures of sequestration and reductions in fossil fuel emissions are developed (Houghton, 2007; Watson et al., 2000).

1.4 The Sardinilla research site

The Sardinilla site is an international and inter-institutional research facility in Central Panama that is administered by the Smithsonian Tropical Research Institute (STRI). The Sardinilla site is located about 40 km north of Panama City and 30 km north-east of Barro Colorado Island (BCI), at 9°19' N, 79°38' W and about 70 m a.s.l. (Fig. 1.2 and 1.3). The research site consists of several native tree species afforestations with different levels of biodiversity and an adjacent pasture (Fig. 1.3). The primary vegetation (tropical forest) was logged in 1952/1953 and the site was used for agriculture for two years, before it was converted to pasture (Wilsey et al., 2002). In 2001, the so-called 'main experiment' with 24 plots of 45x45 m was established, containing six native tree species in different mixtures. Further trees were planted surrounding these plots to avoid edge effects (see Appendix D). The main afforestation consists of six native species: *Luehea seemanii*, *Cordia alliodora*, *Anacardium excelsum*, *Hura crepitans*, *Cedrela odorata*, *Tabebuia rosea*, with moderately dense understory vegetation (shrubs, grasses and sedges). Another experiment with 24 plots of 15x15 m that are grouped in blocks of three plots each was established in 2003, consisting of up to 18 native tree species (see Appendix D). Grazing was continued on the adjacent pasture since 2001 and the pasture vegetation is dominated by C₄ grasses, consisting of (most abundant first): *Paspalum dilatatum* (C₄), *Rhynchospora nervosa* (sedge, C₃), *Panicum dichotomiflorum* (C₄) and *Sporobolus indicus* (C₄).

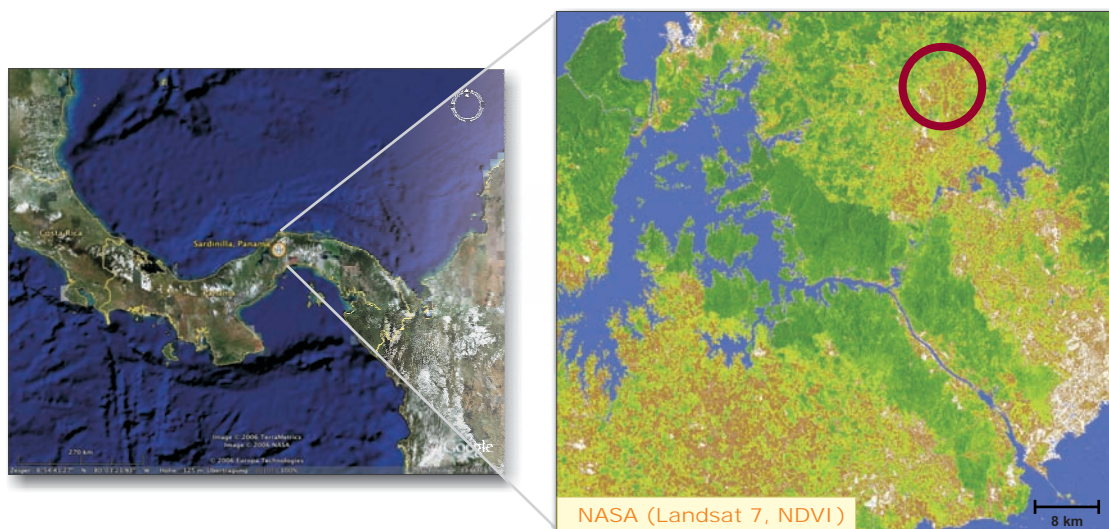


Figure 1.2. Location of the Sardinilla site in Central Panama. The map on the left-hand side is derived from Google Maps. The satellite image was taken by Landsat 7 (NASA) in March 2000 and displays the Normalized Differenced Vegetation Index (NDVI). High values (dark green) represent tropical rainforest, medium values (green) represent shrub and grassland, low values (brown and white) represent bare soil, arable land and infrastructure.

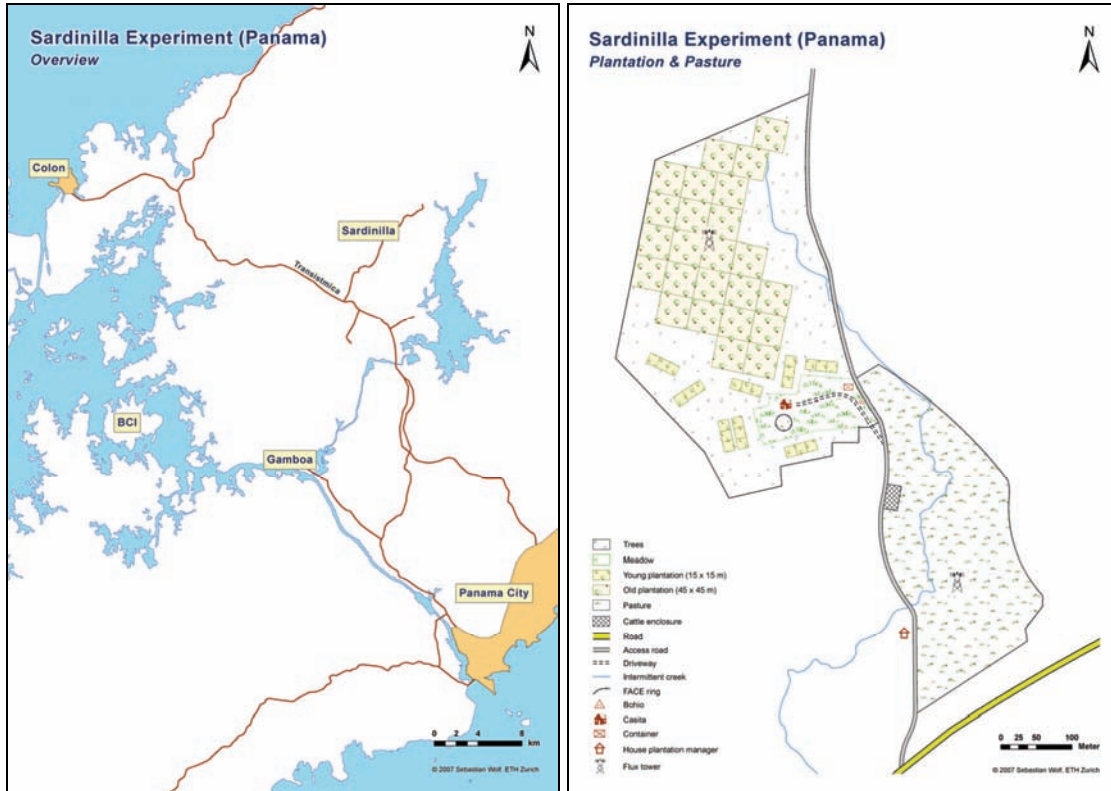


Figure 1.3. Maps of the Sardinilla site (enlarged and additional maps can be found in Appendix D)

1.5 Eddy covariance technique

Two eddy covariance flux towers were deployed in Sardinilla, Central Panama to continuously measure the CO_2 and H_2O exchange between biosphere and atmosphere in a tropical pasture and nearby afforestation.

The eddy covariance technique (EC) is the established method to directly measure turbulent fluxes of trace gases between the biosphere and the atmosphere (Aubinet et al., 2000; Baldocchi, 2008). Micrometeorological measurements that employ the EC technique sample turbulent motions of upward and downward moving air parcels that transport trace gases such as CO_2 , H_2O , CH_4 and N_2O across the biosphere-atmosphere interface (Baldocchi, 2003; Fig. 1.4). The net ecosystem flux (F_N) is calculated from high frequency measurements as the covariance between fluctuations in vertical wind velocity (w) and the mixing ratio of a trace gas (c), using:

$$F_N = \bar{p}_a \cdot \overline{w'c'} \quad (\text{Eq. 1.1}),$$

where p_a is the air density, overbars denote time averaging (typically 30 or 60 min) and primes represent variations from the mean. Negative covariance denotes fluxes from the atmosphere to the biosphere (e.g. uptake of CO_2) while positive covariance denotes the reverse flux (e.g. release of CO_2). The net ecosystem flux of CO_2 is the small difference between the two large flux components – assimilation and respiration (Fig. 1.5).

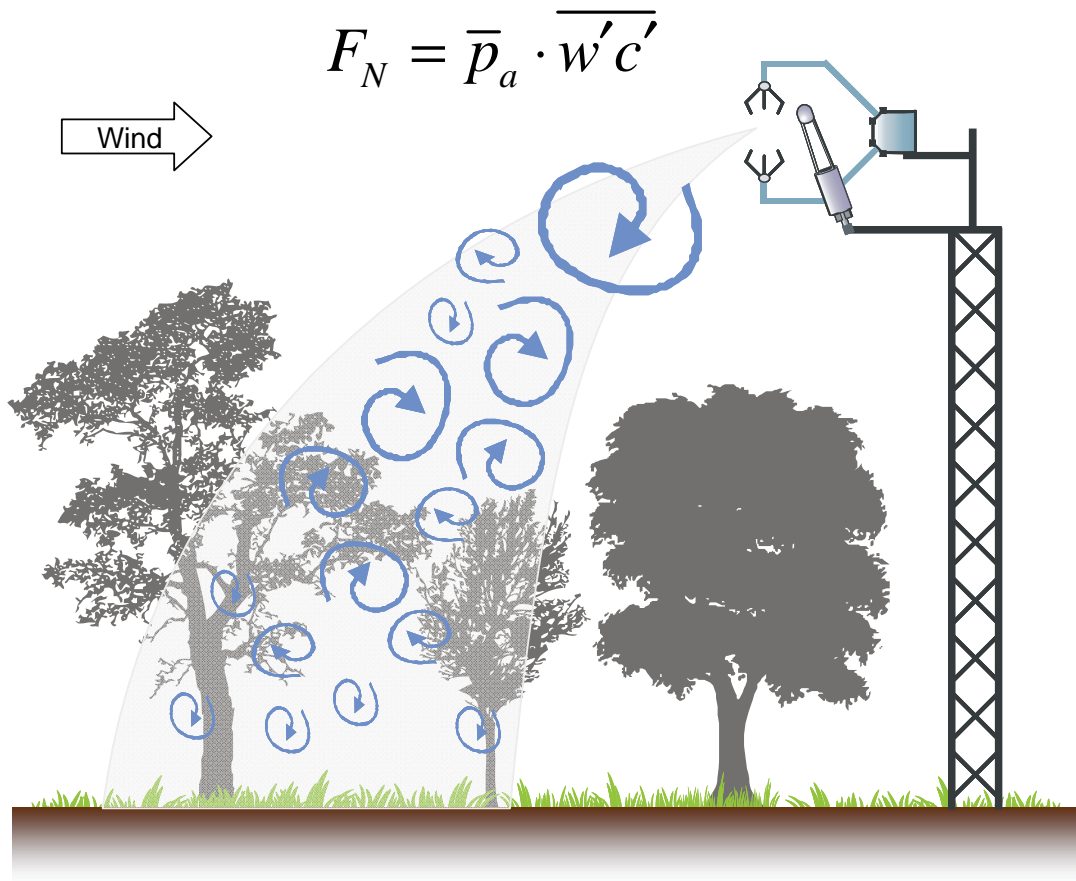


Figure 1.4. Ecosystem flux measurements using the eddy covariance technique. The shaded area denotes the footprint.

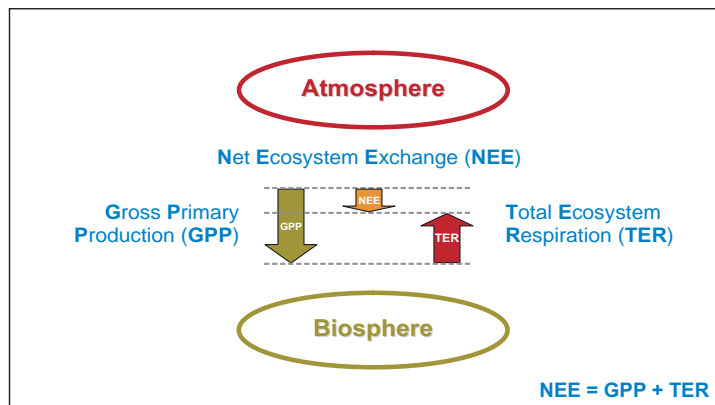


Figure 1.5. Biosphere-atmosphere net ecosystem CO_2 exchange. This schematic example denotes the biosphere as a carbon sink (assimilation exceeding respiration).

1.6 Objectives

This thesis aims to improve our understanding of the biosphere-atmosphere interactions between land use and the carbon and water cycle of managed tropical ecosystems. The overall research objectives are to:

- (1) Quantify and compare the net ecosystem CO₂ exchange (NEE) and ecosystem evapotranspiration (ET) of pasture and native tree species afforestation in Sardinilla, Panama.
- (2) Assess seasonal variations in NEE and ET, and estimate the carbon sequestration potential of tropical pasture compared to afforestation.
- (3) Investigate the environmental controls of NEE and ET, and the impact of management on ecosystem carbon and water fluxes.

1.7 Thesis outline

This thesis is composed of five chapters covering the following contents:

Subsequent to the introductory **first chapter**, the detailed measurement setup in Sardinilla is described in the **second chapter** along with the approach for the separation of seasons used in this thesis. Seasonal and inter-annual variations in net ecosystem CO₂ exchange (NEE) are assessed and the environmental controls of NEE for pasture and afforestation are identified. Chamber based measurements of soil respiration are used to constrain eddy covariance derived total ecosystem respiration (TER) during nighttime. The **third chapter** estimates the carbon sequestration potential of tropical afforestation compared to pasture and elucidates the environmental controls and the impact of management on gross primary production (GPP), TER and NEE. In addition, eddy covariance derived carbon budgets are compared with biomass and soil inventory data that are used to quantify the carbon stocks in Sardinilla.

The **fourth chapter** investigates seasonal and diurnal patterns of evapotranspiration (ET), quantifies ET budgets and assesses the environmental controls of ET for tropical pasture and afforestation. Furthermore, changes in soil infiltrability due to the land conversion from pasture to afforestation are evaluated and discussed.

The main results of this thesis are summarised in the **fifth chapter**. The synthesis reveals implications for land management and suggests considerations for future research in managed tropical ecosystems.

Appendixes A and B present the results of a joint project with the University of Bern to quantify canopy intercepted rain using ground based microwave radiometry in combination with EC measurements in the Sardinilla afforestation.

Appendix C presents a synthesis of the biodiversity effects on above and belowground carbon stocks in the native tree species afforestation in Sardinilla from 2001 to 2009.

Appendix D contains maps of a Geographic Information System (GIS) that were compiled by the author of this thesis for the Sardinilla research site to investigate spatial effects of topographic and environmental parameters.

Chapter 2

2 Seasonal variations in net ecosystem carbon dioxide exchange

Chapter 2 was accepted for publication in the peer-reviewed journal Agricultural and Forest Meteorology as:

Strong seasonal variations in net ecosystem CO₂ exchange of a tropical pasture and afforestation in Panama

Sebastian Wolf¹, Werner Eugster¹, Catherine Potvin^{2,3} and Nina Buchmann¹

¹ Institute of Agricultural Sciences, ETH Zurich, Universitaetsstrasse 2, 8092 Zurich, Switzerland

² Department of Biology, McGill University, 1205 Dr Penfield Avenue, Montréal H3A1B1, Québec, Canada

³ Smithsonian Tropical Research Institute, Apartado 0843-03092, Balboa, Ancón, Panama

Abstract

Pasture and afforestation are land-use types of major importance in the tropics, yet, most flux tower studies have been conducted in mature tropical forests. As deforestation in the tropics is expected to continue, it is critical to improve our understanding of alternative land-use types, and the impact of interactions between land use and climate on ecosystem carbon dynamics. Thus, we measured net ecosystem CO₂ fluxes of a pasture and an adjacent tropical afforestation (native tree species plantation) in Sardinilla, Panama from 2007–2009. The objectives of our paired site study were: (1) to assess seasonal and inter-annual variations in net ecosystem CO₂ exchange (NEE) of pasture and afforestation, (2) to identify the environmental controls of net ecosystem CO₂ fluxes, and (3) to constrain eddy covariance derived total ecosystem respiration (TER) with chamber-based soil respiration (R_{Soil}) measurements. We observed distinct seasonal variations in NEE that were more pronounced in the pasture compared to the afforestation, reflecting changes in plant and microbial activities. The land conversion from pasture to afforestation increased the potential for carbon uptake by trees *versus* grasses throughout most of the year. R_{Soil} contributed about 50% to TER, with only small differences between ecosystems or seasons. Radiation and soil moisture were the main environmental controls of CO₂ fluxes while temperature had no effect on NEE. The pasture ecosystem was more strongly affected by soil water limitations during the dry season, probably due to the shallower root system of grasses compared to trees. Thus, it seems likely that predicted increases in precipitation variability will impact seasonal variations of CO₂ fluxes in Central Panama, in particular of pasture ecosystems.

2.1 Introduction

Tropical ecosystems play an important role in the global carbon cycle. They store 40% of the carbon in the terrestrial biosphere and are responsible for half of the global terrestrial gross primary production (Fisher et al., 2009; Grace et al., 2001). Climate model projections for tropical areas like Amazonia and Central America suggest rising temperatures, a reduction in the total amount of precipitation, and an increase in precipitation variability with more frequent extreme dry seasons by the end of this century (Bates, 2008; IPCC, 2007b). A recent study by Phillips et al. (2009) suggests a large sensitivity of Amazonian ecosystems to drought, which is contrary to findings of Schwalm et al. (2010) who found only a minimal drought sensitivity of CO₂ fluxes in tropical regions. On the other hand, it is well known that variations of precipitation patterns are strongly associated with ENSO (El Niño Southern Oscillation) events, e.g. in Central Panama (Graham et al., 2006; Lachniet, 2009), but little is known on the impacts of these variations on ecosystem carbon fluxes.

Thus, an improved understanding of tropical ecosystem responses to changing environmental conditions such as more severe seasonal droughts and increased precipitation variability is needed.

The eddy covariance technique (EC) is the established method to directly measure turbulent fluxes of trace gases between the biosphere and the atmosphere (Aubinet et al., 2000; Baldocchi, 2003; Baldocchi, 2008). As of March 2010, 502 sites were listed in FLUXNET, the global network of eddy covariance flux tower measurements (www.fluxnet.ornl.gov), which includes a broad range of vegetation types, climates and disturbance regimes (Baldocchi, 2008). However, the distribution of these sites is still largely dominated by temperate climates on the Northern hemisphere, especially within Europe and North America, which was already noted a decade ago (Buchmann and Schulze, 1999). Tropical sites represent only 10% of all sites, and about half of these are located in Brazil. While mature forests dominate these tropical sites in the Amazon region (23 FLUXNET sites; e.g. Chambers et al., 2004; da Rocha et al., 2004; Goulden et al., 2004; Hutyyra et al., 2007; Malhi et al., 1998; Priante-Filho et al., 2004; Saleska et al., 2003; Vourlitis et al., 2001), only a few tropical grasslands were studied using the eddy covariance method (4 FLUXNET sites; Sakai et al., 2004; Santos et al., 2004; von Randow et al., 2004). This is surprising since in Central America and the Caribbean, grasslands (including savanna and shrubland) cover approximately 41% of the total land area, making grasslands the most important land-cover along with forests (34%; EarthTrends, 2003).

With ongoing deforestation and related land-use changes, the tropics are increasingly influenced by agroecosystems and pastures. Land-use change is one of the most important contributors to globally increasing CO₂ concentrations, particularly in developing countries (IPCC, 2007b) where deforestation is primarily driven by the demand for timber, arable land and livestock production. Following deforestation of native primary forest, the land is typically used to cultivate agricultural crops for a few years, before being converted into grasslands used for grazing (Amézquita et al., 2008). However, only few of these often extensively used grasslands (Malmer et al., 2010) are later considered for afforestation. So far, afforestations (forest plantations), typically with non-native, fast growing or high value timber monocultures like Eucalyptus, Pinus or Tectona (Kanowski, 1997), cover only a minimal area in the tropics. Only 3% are reported for Brazil (FAO, 2001) and 1.6% for Central America and the Caribbean (EarthTrends, 2003), although afforestations are considered an effective measure to sequester carbon and mitigate the anthropogenic induced increasing CO₂ concentrations (FAO, 2009), with a mitigation potential in the order of 15% of global CO₂ emissions (Malhi et al., 2002). However, our knowledge about the carbon cycling of tropical pastures and afforestations including the land-use change in between is very limited. Large uncertainties exist in particular about the sensitivity of newly established ecosystems to changes in environmental conditions (Gilmanov et al., 2010).

Thus, we quantified and compared the net ecosystem CO₂ exchange (NEE) of a traditionally grazed pasture and an adjacent afforestation planted with native tree species. The objectives of our paired-sites study were: (1) to assess seasonal and inter-annual variations in NEE of a pasture and an afforestation in Panama, (2) to identify the environmental controls of net ecosystem CO₂ fluxes, and (3) to constrain eddy covariance derived total ecosystem respiration (TER) with chamber based soil respiration (R_{Soil}) measurements.

We hypothesised that the afforestation with native tree species would be more adapted to the pronounced seasonal climate and therefore be less sensitive to variations in climate. We expected soil moisture (dry season limitations) and radiation (wet season limitations) to be the main environmental controls for NEE. Nighttime ecosystem and soil respiration were expected to be controlled by soil moisture and temperature.

2 Material and Methods

2.2.1 Site description

The Sardinilla site is located in Central Panama (9°19' N, 79°38' W), about 40 km north of Panama City and 30 km north-east of Barro Colorado Island (BCI), at about 70 m a.s.l. The site has a semi-humid tropical climate with a mean annual temperature of 25.2 °C, 2289 mm mean annual precipitation (2007–2009) and a pronounced dry season from January to April characterized by strong North-easterly trade winds (Tab. 2.1). Dry season length in Central Panama varies among years (134 ± 19 days for 1954–2009; ACP, 2010) and is influenced by ENSO (Graham et al., 2006; Lachniet, 2009). Geologically, the site belongs to the Gatuncillo formation and the bedrock is classified as tertiary limestone containing clayey schist and quartz sandstone (ANAM, 2010). Soils are classified as Ultisols, with isolated Vertisols at the afforestation and Alfisols at the pasture site (Ben Turner, personal communication), characterised by high clay contents (clay 65%, silt 30%, sand 4%; Abraham, 2004). Consequently, strong soil contractions occur and desiccation cracks developed during the dry season (up to 1 m depth, particularly in the afforestation), enhancing bioturbation of organic material (litter) to deeper soil layers. The afforestation had higher topsoil (0–10 cm) organic carbon and nitrogen concentrations compared to the pasture (4.24% vs. 1.72% and 0.36% vs. 0.17%, respectively). C:N ratios of 10 were found in the pasture and of about 12 in the afforestation site (Tab. 2.1).

The Sardinilla site was logged in 1952/1953 and used for agriculture for two years, before it was converted into a pasture (Wilsey et al., 2002). In 2001, an afforestation using native tree species only was established at parts of the site (7.5 ha), while traditional grazing continued on the remaining pasture (6.5 ha). Pasture vegetation is dominated by C₄ grasses, consisting of: *Paspalum dilatatum* (C₄, 50–75%), *Rhynchospora nervosa* (sedge, C₃, 25–50%), *Panicum dichotomiflorum* (C₄, 5–25%) and *Sporobolus indicus* (C₄, 1–5%; listed in the order of abundance according to Braun-Blanquet method). The

afforestation consists of six native deciduous and semi-deciduous tree species (*Luehea seemanii*, *Cordia alliodora*, *Anacardium excelsum*, *Hura crepitans*, *Cedrela odorata*, *Tabebuia rosea*), with moderately dense understory vegetation (shrubs, grasses and sedges). Trees that are semi-deciduous are losing either part of their foliage or their foliage only for a very short period. In 2008, estimated mean canopy height was about 10 m in the afforestation and 0.09 m in the pasture (Tab. 2.1). The afforestation site has an undulating topography with an elevation range of less than 10 m. In contrast, the adjacent pasture is homogeneously flat with an overall slope of less than two degrees.

Table 2.1. Flux tower site characteristics for the pasture and the afforestation sites at Sardinilla. Values indicate mean \pm standard error for vegetation height and LAI; mean \pm standard deviation for all soil data. LAI data for the wet season are averages for June and July in 2008 and 2009, for the dry season for March to April 2009. LAI data during the phenological transition month in May 2009 were excluded from averaging.

Site	Pasture	Afforestation
Location	9°18'50" N, 79°37'53" W	9°19'5" N, 79°38'5" W
Elevation a.s.l. (m)	68	78
Tower height (m)	3	15
Measurement period	21.03.2007 – 26.01.2010	05.02.2007 – 01.07.2009
Canopy height (m)	0.09 \pm 0.07	8–12 (2007–2009)
Vegetation	dominated by C ₄ grasses	six native tree species
LAI of canopy		
Dry season	1.2 \pm 0.14	3.0 \pm 0.28
Wet season	2.9 \pm 0.15	5.4 \pm 0.24
Management	grazing, herbicide treatment (annually in May)	selective understory thinning (Dec. 2007 & 2008)
Prevailing wind direction during daytime (°)		
Dry season	41	87
Wet season	38	69
Wet season	193	165
Mean horizontal wind speed during daytime (m s ⁻¹)		
Dry season	0.97 \pm 0.85	1.73 \pm 1.45
Wet season	2.36 \pm 0.87	3.14 \pm 1.42
Wet season	0.88 \pm 0.64	1.38 \pm 1.06
Soil (0–10 cm)		
Type	Alfisol ^b	Ultisols, Vertisols ^a
Texture	Clay	Clay
Clay (%)	58, 36, 6	65, 30, 4 ^a
pH	5.58 \pm 0.29 ^a	5.76 \pm 0.35 ^a
C (%)	1.72 \pm 0.33	4.24 \pm 0.92
N (%)	0.17 \pm 0.04	0.36 \pm 0.08
C:N	10.11 \pm 0.16	11.86 \pm 1.32
d _B (g cm ⁻³)	0.86 \pm 0.07 ^a	0.58 \pm 0.09 ^a

^a Abraham (2004), ^b Ben Turner (personal communication)

2.2.2 Instrumentation and data acquisition

Two flux towers using the eddy covariance method were installed in February 2007: one tower in the afforestation, and the second one in the adjacent, grazed pasture. The micrometeorological measurement systems consisted of an open path infrared gas analyzer (IRGA, Li-7500, LI-COR, Lincoln, USA) and a three-dimensional sonic anemometer (CSAT3, Campbell Scientific, Logan, USA). Instruments were installed at a height of 15 m in the afforestation and at 3 m in the pasture site (Tab. 2.1). Micrometeorological data acquisition was carried out with an industry grade embedded box computer (Advantech ARK-3381, Taipei, Taiwan), running a Debian based Linux operating system (Knoppix 4.0.2, Knopper.Net, Schmalenberg, Germany). Measurements of environmental variables included air temperature and relative humidity (MP100A, Rotronic, Bassersdorf, Switzerland), incoming shortwave radiation (R_G , CM3, Kipp & Zonen, Delft, The Netherlands), net radiation (R_N ; afforestation: CN1, Middleton Solar, Brunswick, Australia; pasture: Q*7.1, REBS - Radiation and Energy Balance Systems, Seattle, USA), photosynthetic photon flux density (PPFD, PAR Lite, Kipp & Zonen, Delft, The Netherlands), precipitation (10116 rain gauge, TOSS, Potsdam, Germany), soil heat flux at 5 cm depth (HFP01, Hukseflux, Delft, The Netherlands), soil temperature at 5 cm depth (TB107, Markasub, Olten, Switzerland) and volumetric soil water content (SWC) at 5 and 30 cm depth (EC-5, Decagon, Pullman, USA). Flux measurements were conducted at 20 Hz, meteorological measurements at 10 s and stored as half-hourly averages (sums for precipitation) using data loggers: CR23X at the afforestation and CR10X at the pasture site (both Campbell Scientific, Logan, USA). Precipitation and incoming shortwave radiation were measured at one tower location only. With a distance of 600 m between both flux towers, meteorological conditions can be assumed to be very similar. Regular cleaning of sensors and monthly IRGA calibration checks were performed to assure high data quality. Automated remote connections to Switzerland were established using a GSM modem (GPRS GSM Quadband Modem, ConiuGo, Hohen Neuendorf, Germany) to provide daily information on system status and data quality. Although GSM reception proved to be weak at Sardinilla, it was sufficient to transfer small quantities of status information. Both towers had landline power supply although short power outages occurred frequently. However, data acquisition was normally not affected by short interruptions as all instrumentation, except the GSM modem, were powered by 12 V batteries (90 Ah, 105D31L, Solite Batteries, Seoul, Korea). Batteries were charged using automatic battery chargers (J512A/0145-37, Schauer, Cincinnati, USA). All data were stored on the box computer's hard disk with daily backups to an external flash card device (ImageMate CF Reader with 8 GB Ultra II Compact Flash card, SanDisk, Milpitas, USA). For security reasons, a fenced enclosure of 8 x 8 m (about 2 m high) was installed around the afforestation tower and a barbwire fence of 3 x 3 m around the pasture tower to prevent access by grazing livestock.

2.2.3 Data processing and corrections

Flux data

Data acquisition of flux measurements was done with the in-house software *sonicreadHS*, following the concept by Eugster and Plüss (2010). Raw data were processed to half-hourly averages with the in-house eddy covariance software *eth-flux* (Mauder et al., 2008; source code for Unix/Linux systems can be obtained from the authors). *Eth-flux* uses a 2D coordinate rotation with 30 min block averaging. Corrections for damping losses (Eugster and Senn, 1995) and density fluctuations (Webb et al., 1980) were applied during post-processing to the half-hourly averaged data. Subsequently, quality filtering was applied to the flux data using the following rejection criteria: (1) Optical sensor contamination (spider eggs, rain) resulting in high window dirtiness of the IRGAs (AGC value). We used a 10% threshold above the mean AGC background values of the respective IRGA, which were 62.5% for the pasture and 68.75% for the afforestation site. (2) Filtering for stationarity following Foken and Wichura (1996). We excluded fluxes whenever the 30 min average deviated by more than 100% from the corresponding mean of 5 min averages. (3) CO₂ Fluxes outside the range of -50 to $50 \mu\text{mol m}^{-2} \text{s}^{-1}$ were excluded. (4) Statistical outliers outside the ± 3 SD range of a 14 day running mean window were removed. (5) Periods with low turbulence conditions were excluded based on friction velocity (u^*). We determined seasonal and site-dependent u^* -thresholds according to the method by Gu et al. (2005) and Moureaux et al. (2006), which yielded $u^* < 0.04 \text{ m s}^{-1}$ (dry season), $u^* < 0.03 \text{ m s}^{-1}$ (dry-wet transition) and none during the wet season and wet-dry transition periods for the pasture site. For the afforestation site, u^* -thresholds were $u^* < 0.02 \text{ m s}^{-1}$ (dry season), $u^* < 0.01 \text{ m s}^{-1}$ (wet season), $u^* < 0.05 \text{ m s}^{-1}$ (dry-wet transition) and none during the wet-dry transition period. After quality filtering, 54.6% of good to excellent quality data remained for the pasture (64.7% daytime, 43.6% nighttime data) and 47.6% (65.4% daytime, 28.3% nighttime data) for the afforestation site. For all further data analyses only filtered, high quality flagged data were used. In general, no gap filling was applied to the data. The only exception is Tab. 2.4, which shows seasonal sums using the gap filling method by Moffat et al. (unpublished) for daytime and a 10-day running mean approach for nighttime data.

Footprint analysis was done using the model by Kljun et al. (2004), which employs a parameterisation based on a scaling procedure over a range of stratifications and which accounts for the influence of roughness length. To aggregate the 30 min footprint information, we generated probability density functions in a polar coordinate grid with 3° degrees per wind direction sector and 5 m distance intervals. All data of the specific seasons were used for footprint analysis.

Meteorological data

Raw meteorological data were quality filtered to eliminate unrealistic measurements and outliers. For periods of instrument failure, air temperature was derived from virtual

temperature measurements of the sonic anemometer based on regression analysis. Due to several instrument failures of PPFD measurements at both tower sites, a joint PPFD variable was derived by regression analysis with incoming shortwave radiation. For times of instrument failure of the rain gauge at the pasture site, data were substituted by those from the nearby (about 5 km to the northeast) Salamanca station of the Panama Canal Authority (ACP; STRI, 2010). When SWC data at 5 cm depth in the pasture were not available, we used SWC data from the afforestation site instead.

2.2.4 Separation of seasons

Separation of seasons in the semi-humid tropics is generally done based on monthly precipitation sums using a threshold of 100 mm (Hutyra et al., 2007; Loescher et al., 2003; Malhi et al., 2002; Saleska et al., 2003). More sophisticated approaches include variables like sea surface temperatures, wind velocity and position of the Inter-Tropical Convergence Zone, ITCZ (e.g. method used by Panama Canal Authority, STRI 2010). However, these data are usually not available for flux tower sites. We aimed at a detailed separation of seasons, including transition periods, based on precipitation and thus applied an approach based on daily precipitation sums: (1) Wet season is defined as the time span with periods of less than four consecutive days without rain. If three to four consecutive days without rain occurred, the precipitation in the seven days before this period must have exceeded 20 mm (cumulated sum). The start/end of the first/last period of such consecutive days marked the end/start of the wet season. (2) Dry season is defined as the time of the year with consecutive periods of more than four days without any rain. (3) The dry-wet transition period starts with the first heavy rainfall event (>1 mm) after a period of at least seven days without any rain. It ends with the onset of the wet season. (4) The wet-dry transition starts at the end of the wet season, before the first period of at least three consecutive days without rain and after a period of at least six days of rain within one week. It ends with the start of the first period with more than four consecutive days without rain and less than 5 mm of rain within two weeks. When using only a two season separation (dry vs. wet), the transition periods can be added to the dry season. Our procedure based on daily precipitation sums yielded similar results as the monthly 100 mm threshold but with a much better temporal resolution needed for detailed flux data comparisons. It also agreed well with related environmental variables like SWC using visual diagnostics.

2.2.5 Auxiliary measurements

Auxiliary measurements included measurements of leaf area index (LAI), soil respiration (R_{Soil}) fluxes as well as soil sampling. Leaf area index (LAI) was measured in campaigns with an LAI-2000 (LI-COR, Lincoln, USA) in July 2008 and weekly to bi-weekly from March to July 2009. At the afforestation, LAI was measured separately for the tree canopy (measured at 1 m above ground) and the total canopy including the understory (measured at ground level). We corrected our LAI measurements at the

afforestation for the shading effect of tree stems and branches by subtracting the minimum dry-season value of the tree canopy LAI (DOY 107, 2009; LAI = 0.42). No correction for the shading by stalks was applied to the LAI measurements at the pasture. Data from the phenological transition month of May 2009 was excluded for averaging seasonal LAI.

In addition, nighttime R_{Soil} fluxes were measured between sunset and sunrise on a campaign basis weekly to bi-weekly in February/March and May to July 2009. We used a self-made closed static chamber system, consisting of a 52.5 x 19.5 cm (14.9 l) cylindrical shaped chamber connected to a closed path infrared gas analyzer (Li-6262, LI-COR, Lincoln, USA). Air was pulled through a 1.2 m Bev-A-Line tubing (6 mm in diameter) at 0.5 l min⁻¹ using a diaphragm pump (NMP 830 KNDC B, KNF Neuberger, Balterswil, Switzerland). Chamber measurements were conducted over a period of 5 min with data being recorded every 2 s using a data logger (Pace XR440, Pace Scientific, Mooresville, USA). PVC collars (pasture: n=10; afforestation: n=12) with 5 cm height and 20 cm diameter were installed 2.5 cm deep into the soil. Vegetation cover was manually removed at least 24 hours prior to measurements.

Topsoil (0–10 cm) sampling at the afforestation was done in March 2009 using a cylindrical corer (10 cm long, diameter of 6.8 cm; n=22). At the pasture site, three soil profiles from 0 to 100 cm depth were sampled in January 2010, with 10 cm increments, and additional in 5 cm depth. Topsoil values were derived by averaging the samples from 5 and 10 cm depth. Samples were dried for at least 72 h in a drying room at 60° C, then ground and analyzed for C and N with an elemental analyzer (Thermo Flash 1112 Soil Analyzer, Thermo Fisher Scientific, Waltham, USA) at the Smithsonian Tropical Research Institute (STRI) in Panama.

2.2.6 Energy Balance Closure

Based on the first law of thermodynamics, the energy budget at the earth's surface is calculated as the sum of available energy, i.e., the sum of net radiation (R_N) and ground heat flux (Q_G) or the sum of turbulent fluxes of sensible (Q_H) and latent heat (Q_E). Theoretically, both sums should yield equal results. In reality, however, a residual energy balance closure (EBC) term is found if all four components are measured separately:

$$EBC = \frac{(Q_H + Q_E)}{(R_N - Q_G)} \quad (\text{Eq. 2.1}).$$

The EBC is used as an independent measure to evaluate the performance of eddy covariance flux measurements (Aubinet et al., 2000; Wilson et al., 2002). We derived Q_G from the mean of two soil heat flux plates and corrected for heat storage in the soil layer above according to Monteith and Unsworth (1990). Turbulent fluxes were quality filtered to be within the range of -200 to 800 W m^{-2} and EBC was only calculated for periods when data for all components were available.

2.2.7 Statistical analyses and general conventions

All statistical analyses were carried out using the statistics software package R, version 2.10.0 (R Development Core Team 2009, www.r-project.org). Daytime data were defined as $PPFD > 5 \mu\text{mol m}^{-2} \text{s}^{-1}$. The terms ‘midday’ and ‘nighttime’ were defined as 11:00–13:00 and 0:00–4:00 (UTC), respectively. Negative CO_2 fluxes denote assimilation (carbon uptake) by the ecosystem; positive fluxes indicate respiration (carbon loss). In general, only seasons with full data coverage were used for data analysis. When writing ‘seasonal drought’, we refer to the plant physiological effects of soil moisture deficiency during the dry season. If not denoted otherwise, a two-sided, unpaired t-test was used to test for statistical differences of means between and within study sites and seasons. Differences in seasonal and diurnal variations were tested using a two-sided F-test.

To assess the normalized relation between seasonal mean midday assimilation (NEE_{Midday}) and mean nighttime respiration fluxes (NEE_{Night}), we defined a Midday-Night ratio (MNR)

$$MNR = \left| \frac{NEE_{\text{Midday}}}{NEE_{\text{Night}}} \right| \quad (\text{Eq. 2.2}).$$

The larger the MNR, the less CO_2 is respired during nighttime in relation to CO_2 being assimilated during midday. An MNR below 1 indicates more CO_2 being respired during nighttime than assimilated during midday, while a MNR of 1 denotes an equal magnitude of these opposing CO_2 fluxes.

2.3 Results

2.3.1 Seasonality in climate

We found a pronounced seasonal climate influenced by precipitation in Sardinilla, with a long wet season from May until December, a dry season from January until April, and transition periods with varying and limited amounts of precipitation. Most of the annual precipitation (>98%) was received from April to December (Fig. 2.1, Tab. 2.2). During an average wet season, most precipitation occurred in November (>300 mm), least precipitation in September (about 200 mm). Compared to the long-term annual precipitation mean of the nearby ACP station Salamanca of 2267 mm (1972–2009, derived from STRI 2010), Sardinilla received above average rainfall in 2007 (2553 mm, +13%), below average rainfall in 2008 (2074 mm, –9%) and about average rainfall in 2009 (2233 mm, –1%). Based on the daily sum of precipitation (seasonal average), less rainfall was observed in the wet season and dry-wet transition period in 2008 compared to 2007 and 2009 (Tab. 2.2), while above average rainfall occurred during the wet-dry transition period in 2008. In 2009, the dry season was notably longer (104 days) compared to 2008 (77 days).

Mean soil water content (SWC) at 5 cm depth was closely related to monthly precipitation ($R^2=0.40$, $p<0.001$) and increased swiftly with onset of the wet season (Fig. 2.1, Tab. 2.2). SWC decreased rapidly after the end of the wet season and was lowest during the dry-wet transition period (22%). In 2009, SWC declined less during the dry season compared to 2008. Mean photosynthetic photon flux density (PPFD) varied between $319 \mu\text{mol m}^{-2} \text{s}^{-1}$ during the wet season (max. $1161 \mu\text{mol m}^{-2} \text{s}^{-1}$) and $488 \mu\text{mol m}^{-2} \text{s}^{-1}$ during the dry season, with maximum PPFD of $1636 \mu\text{mol m}^{-2} \text{s}^{-1}$ around noon during the dry season, and $1161 \mu\text{mol m}^{-2} \text{s}^{-1}$ during the wet season (Tab. 2.2, Fig. 2.2). Also the vapour pressure deficit (VPD) showed a pronounced seasonal course with maximum values of up to 1.2 kPa in the dry season (February/March) and minimum values of 0.24 kPa in the wet season. VPD closely followed the diurnal patterns of PPFD (Figs. 2.2 and 2.3). Midday VPD was significantly higher at the pasture compared to the afforestation site during the dry and wet season (both $p<0.01$). Maximum VPD in the dry season 2009 was about 20% higher than in 2008.

Seasonal temperature variations were within $\pm 1^\circ\text{C}$ of the annual mean of 25.2°C at Sardinilla (2007–2009), with a minimum of 24.9°C during the dry season and a maximum of 26.1°C during the dry-wet transition period (Tab. 2.2).

Table 2.2. Season lengths and climatic conditions at Sardinilla, Panama from 2007 to 2009. Season length (d), seasonal precipitation sum (P), daily precipitation sum (Daily P), mean air temperature (T_{Air}), mean photosynthetic photon flux density (PPFD), mean volumetric soil water content at 5 cm depth (SWC). Meteorological variables reported were measured at the pasture site, except for SWC (afforestation).

		Dates	Length (d)	P (mm)	Daily P (mm d ⁻¹)	Mean T_{Air} (°C)	Mean PPFD ($\mu\text{mol m}^{-2} \text{s}^{-1}$)	SWC (%)
2007	Dry season	until 29.03.*	20*	–	–	25.4*	455*	–
	Dry-wet trans.	30.03.–22.04.	24	82	3.4	26.2	410	24
	Wet season	23.04.–28.12.	250	2471	9.9	25.2	319	45
	Wet-dry trans.	29.12.–17.01.	20	17	0.9	24.9	472	33
2008	Dry season	18.01.–03.04.	77	17	0.2	24.7	488	24
	Dry-wet trans.	04.04.–28.04.	25	51	2.0	25.6	484	22
	Wet season	29.04.–05.12.	221	1964	8.9	25.0	327	46
	Wet-dry trans.	06.12.–05.01.	31	34	1.1	25.1	431	43
2009	Dry season	06.01.–19.04.	104	42	0.4	25.1	481	27
	Dry-wet trans.	20.04.–29.04.	10	37	3.7	26.5	403	24
	Wet season	30.04.–30.11.	215	2122	9.9	25.6	336	35*
	Wet-dry trans.	01.12.–03.01.	34	32	0.9	25.4	423	–

* Incomplete, only partial temporal coverage

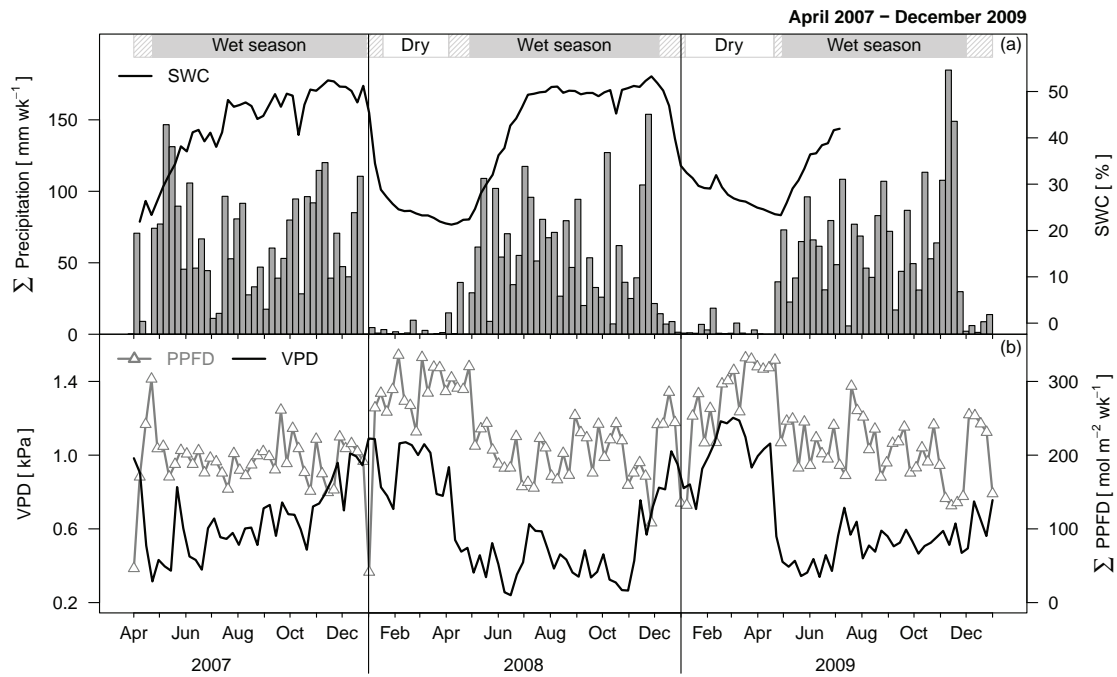


Figure 2.1. Weekly precipitation (grey bars) at the Sardinilla pasture and weekly mean volumetric soil water content (SWC; at 5 cm depth) at the Sardinilla afforestation (a). No SWC data were available after June 2009. Weekly mean vapour pressure deficit (VPD) and weekly total photosynthetic photon flux density (PPFD; b). The inserts at the top indicate the different seasons (wet, dry) including transition periods (shaded areas).

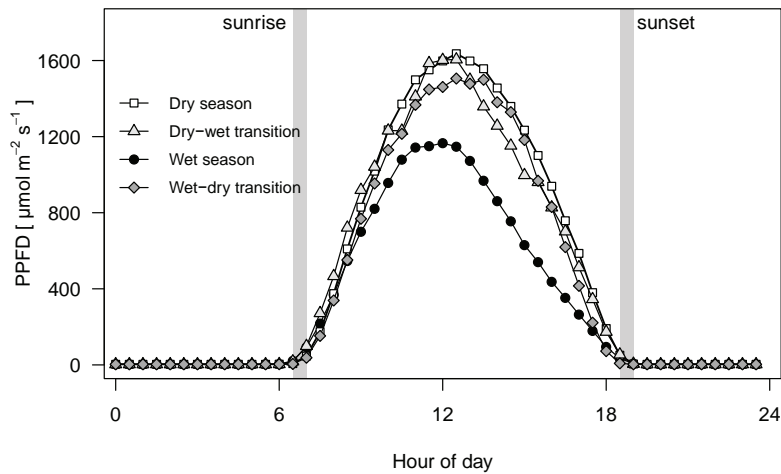


Figure 2.2. Diurnal cycles of seasonally averaged photosynthetic photon flux density (PPFD) at Sardinilla from 2007 to 2009. Grey bars denote the seasonally varying times of sunrise and sunset.

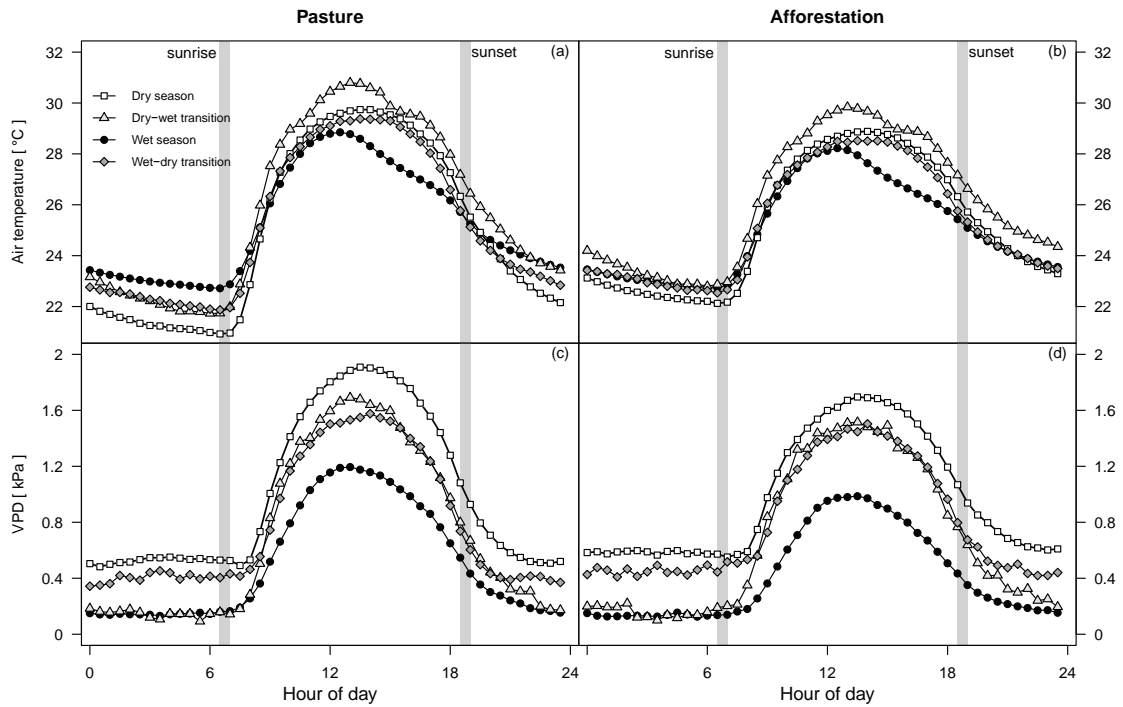


Figure 2.3. Diurnal cycles of seasonally averaged air temperature (a, b) and vapour pressure deficit (VPD; c, d) at the Sardinilla pasture and afforestation sites from 2007 to 2009. Grey bars denote the seasonally varying times of sunrise and sunset.

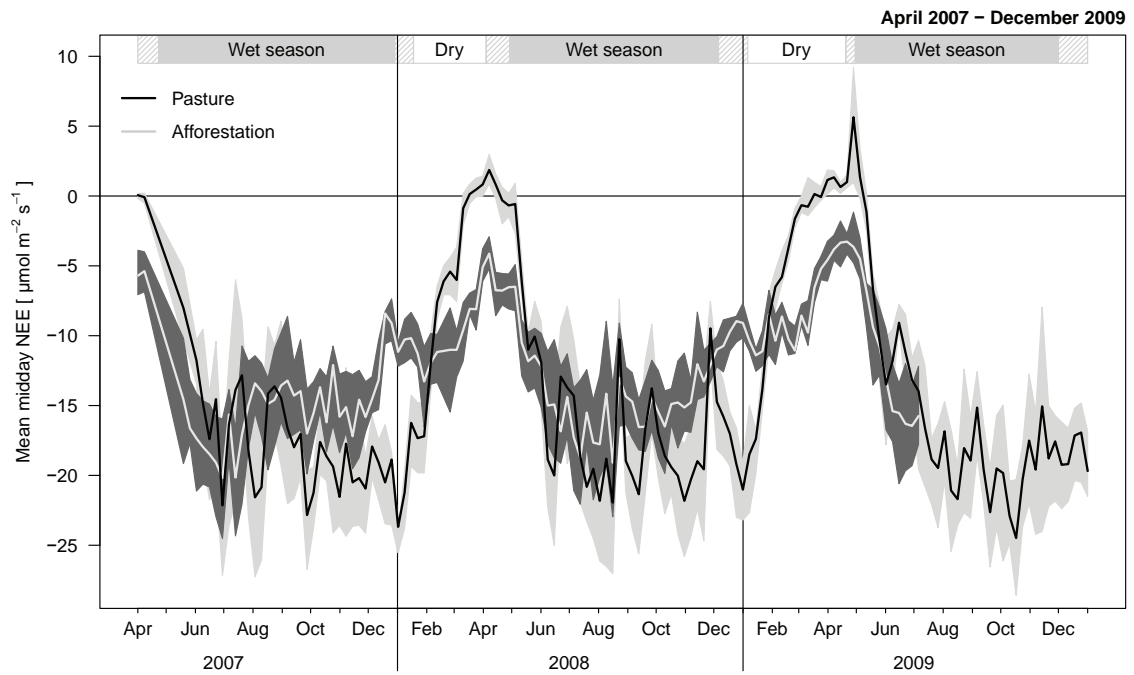


Figure 2.4. Inter-annual and seasonal variations of weekly mean midday (11:00–13:00) net ecosystem CO₂ exchange (NEE) at the Sardinilla pasture and afforestation sites. The shaded areas denote the inter-quartile ranges. The inserts at the top indicate the different seasons (wet, dry) including transition periods (shaded areas). Measurements at the afforestation were discontinued after June 2009.

2.3.2 Seasonal variations of NEE

Large seasonal variations of weekly mean midday NEE were observed in Sardinilla that were more prominent in the pasture than in the afforestation (Fig. 2.4; F-test, $p < 0.001$). We found significantly stronger midday carbon uptake during the wet compared to the dry season at both sites (F-test; pasture $p < 0.001$, afforestation $p < 0.05$). At the pasture site, NEE became positive (respiration dominated) at the end of the dry season and during the dry-wet transition period (up to $5.6 \mu\text{mol m}^{-2} \text{s}^{-1}$). Maximum midday carbon uptake was observed during the middle and at the end of the wet season ($-24.5 \mu\text{mol m}^{-2} \text{s}^{-1}$). The afforestation site maintained carbon uptake throughout all seasons and the highest NEE was found during the dry-wet transition period ($-3.3 \mu\text{mol m}^{-2} \text{s}^{-1}$). During the wet season, similar carbon uptake to the pasture was observed at the afforestation site.

Mean cumulative seasonal NEE indicates carbon losses at the pasture while carbon is sequestered by the afforestation ecosystem throughout most of the year (Tab. 2.4).

2.3.3 Diurnal variations of NEE

Pasture

The pasture ecosystem showed the smallest diurnal variations of NEE during the dry-wet transition period (mean diurnal range of $1.5 \mu\text{mol m}^{-2} \text{s}^{-1}$), with a midday NEE of $0.8 \pm 0.5 \mu\text{mol m}^{-2} \text{s}^{-1}$ and $2.3 \pm 1.1 \mu\text{mol m}^{-2} \text{s}^{-1}$ during nighttime (Tab. 2.3, Fig. 2.5). These CO_2 losses throughout the day were caused by the mostly senescent pasture vegetation. During the dry season, variations in the diurnal cycle of NEE were still small ($8.6 \mu\text{mol m}^{-2} \text{s}^{-1}$). The largest diurnal variations of NEE were observed during the wet-dry transition period ($27.5 \mu\text{mol m}^{-2} \text{s}^{-1}$), with midday NEE of $-18.4 \pm 1.0 \mu\text{mol m}^{-2} \text{s}^{-1}$ and $8.7 \pm 1.1 \mu\text{mol m}^{-2} \text{s}^{-1}$ during nighttime.

Afforestation

Similar to the pasture, the afforestation ecosystem also had strongly reduced diurnal variations of NEE during the dry-wet transition period (mean diurnal range of $9.7 \mu\text{mol m}^{-2} \text{s}^{-1}$), with midday NEE of $-5.7 \pm 0.8 \mu\text{mol m}^{-2} \text{s}^{-1}$ and $4.0 \pm 1.4 \mu\text{mol m}^{-2} \text{s}^{-1}$ during nighttime (Tab. 2.3, Fig. 2.5). During the dry season, NEE was significantly lower during midday ($-8.5 \pm 0.3 \mu\text{mol m}^{-2} \text{s}^{-1}$) and nighttime ($2.8 \pm 0.3 \mu\text{mol m}^{-2} \text{s}^{-1}$) compared to the dry-wet transition period (both $p < 0.001$). During the wet-dry transition period, we observed a midday NEE of $-10.1 \pm 0.1 \mu\text{mol m}^{-2} \text{s}^{-1}$ while NEE at nighttime was comparable to the dry-wet transition period (range of $14.8 \mu\text{mol m}^{-2} \text{s}^{-1}$). The largest diurnal variations of NEE in the afforestation occurred during the wet season ($20.9 \mu\text{mol m}^{-2} \text{s}^{-1}$). Significant differences in diurnal variations of NEE between pasture and afforestation were found during the transition periods only (F-test, both $p < 0.001$).

Midday versus nighttime

The ratio of midday assimilation to nighttime respiration (MNR) was constantly larger than 2 in the pasture ecosystem during the wet season and wet-dry transition period (Tab. 2.3). However, the MNR was much lower during periods with water limitations: During the dry season, NEE during midday and nighttime were in the same order of magnitude in the pasture ecosystem (MNR = 1), while respiration exceeded assimilation even at daytime during the dry-wet transition period (MNR = 0.3). At the afforestation site, similar ratios to the pasture were found during the wet season and wet-dry transition period (Tab. 2.3). Opposing patterns were found during the dry season and dry-wet transition period: NEE at midday exceeded NEE during nighttime significantly in the dry season (MNR = 3.0) and NEE at midday was still higher than at nighttime during the dry-wet transition period (MNR = 1.4).

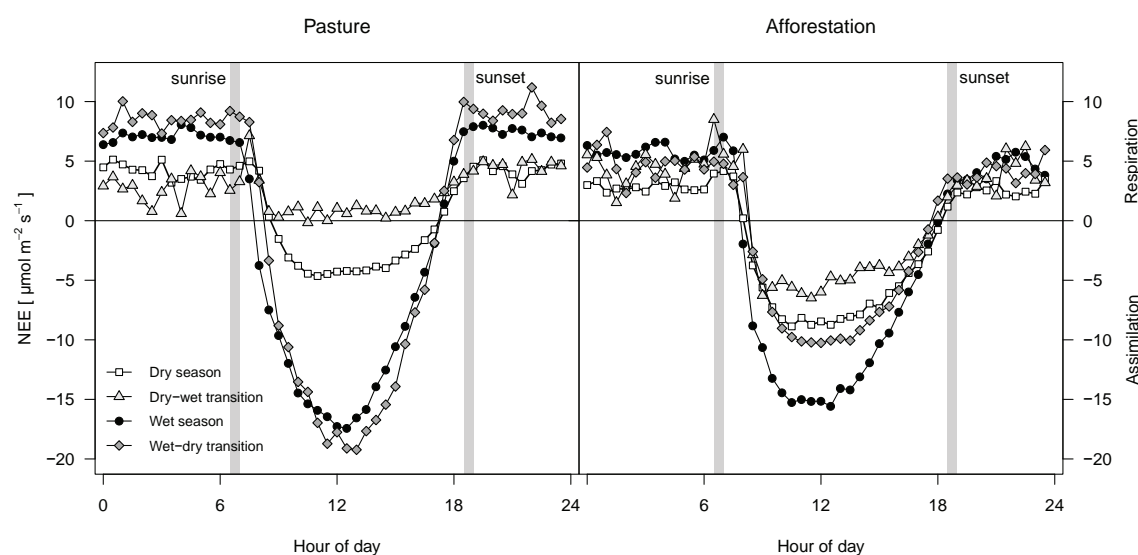


Figure 2.5. Diurnal cycles of seasonally averaged net ecosystem CO₂ exchange (NEE) at the Sardinilla pasture and afforestation sites from 2007 to 2009. Grey bars denote the seasonally varying times of sunrise and sunset.

Table 2.3. Seasonal averages of midday (11:00–13:00) and nighttime (0:00–4:00) net ecosystem CO₂ exchange (NEE; $\mu\text{mol m}^{-2} \text{s}^{-1}$) as well as Midday-Night ratio (MNR) measured over pasture and afforestation in Panama from 2007 to 2009.

	Dry season	Dry-wet transition	Wet season	Wet-dry transition	Total
Pasture					
Midday	-4.4 ± 0.2	0.8 ± 0.5	-16.7 ± 0.6	-18.4 ± 1.0	-13.0 ± 0.4
Nighttime	4.2 ± 0.7	2.3 ± 1.1	7.1 ± 0.5	8.7 ± 1.1	6.5 ± 0.4
MNR	1.0	0.3	2.4	2.1	2.0
Afforestation					
Midday	-8.5 ± 0.3	-5.7 ± 0.8	-15.0 ± 0.6	-10.1 ± 0.1	-12.0 ± 0.4
Nighttime	2.8 ± 0.3	4.0 ± 1.4	5.9 ± 0.5	4.7 ± 1.5	4.7 ± 0.4
MNR	3.0	1.4	2.5	2.1	2.6

Table 2.4. Mean cumulative seasonal net ecosystems exchange (NEE) from gap filled data at the Sardinilla pasture and afforestation sites from 2007 to 2009. Mean annual NEE estimates from all seasons were $253 \text{ g C m}^{-2} \text{ yr}^{-1}$ and $-422 \text{ g C m}^{-2} \text{ yr}^{-1}$ and gap filling accounted for 45.4% and 52.4% of all data for pasture and afforestation, respectively.

	Pasture (g C m^{-2})	Afforestation (g C m^{-2})
Dry season	172	-83
Dry-wet transition	64	11
Wet season	10	-337
Wet-dry transition	7	-13

2.3.4 Nighttime soil and ecosystem respiration

Mean nighttime R_{soil} at the pasture site was $1.4 \pm 0.6 \mu\text{mol m}^{-2} \text{ s}^{-1}$ during the dry season and decreased to a minimum of $0.6 \mu\text{mol m}^{-2} \text{ s}^{-1}$ in March 2009 (Fig. 2.6). During the wet season, mean R_{soil} at the pasture was significantly higher ($3.7 \pm 0.8 \mu\text{mol m}^{-2} \text{ s}^{-1}$; $p < 0.001$) compared to the dry season and increased to a maximum of $4.9 \mu\text{mol m}^{-2} \text{ s}^{-1}$ in June 2009. EC measured nighttime TER was consistently higher than R_{soil} , with $3.5 \pm 1.5 \mu\text{mol m}^{-2} \text{ s}^{-1}$ and $7.0 \pm 1.2 \mu\text{mol m}^{-2} \text{ s}^{-1}$ for dry and wet season, respectively (both $p < 0.001$). At the afforestation site, we observed similar R_{soil} to the pasture during the dry season ($1.4 \pm 0.2 \mu\text{mol m}^{-2} \text{ s}^{-1}$), except for a higher minimum rate (Fig. 2.6, $1.1 \mu\text{mol m}^{-2} \text{ s}^{-1}$). During the wet season, R_{soil} at the afforestation was lower ($3.2 \pm 0.7 \mu\text{mol m}^{-2} \text{ s}^{-1}$; maximum $4.2 \mu\text{mol m}^{-2} \text{ s}^{-1}$) but not statistically different from that of the pasture site. Mean TER at the afforestation was also lower during the dry ($3.3 \pm 1.1 \mu\text{mol m}^{-2} \text{ s}^{-1}$) compared to the wet season ($5.9 \pm 1.5 \mu\text{mol m}^{-2} \text{ s}^{-1}$; $p < 0.001$). No significant differences in R_{soil} and TER were found between both sites in Sardinilla. Similar seasonal patterns were observed with only small differences between the sites: the fraction of R_{soil} contributing to TER was smaller during the dry (40 and 42%) than during the wet season (52 and 54%) for pasture and afforestation, respectively.

2.3.5 Environmental controls of CO_2 fluxes

Daytime NEE

Radiation and soil moisture were the main environmental controls of daytime NEE in Sardinilla. Half-hourly NEE was well correlated with PPFD at the pasture ($r = -0.58$) and afforestation site ($r = -0.53$), and explained 34% and 28% of the variance in NEE, respectively (regression analysis, both $p < 0.001$; not shown). SWC was the strongest residual predictor for NEE at both sites but with differences in depth: 5 cm depth at the pasture (31%) and 30 cm depth at the afforestation (16%; both $p < 0.001$). VPD was only a minor controlling factor of NEE in Sardinilla and explained 3% of the residuals at the pasture and 4% at the afforestation (both $p < 0.001$). Altogether, the factors PPFD, SWC and VPD explained 66% and 50% of the variations in NEE (forward multiple regression analysis) for pasture and afforestation, respectively (both $p < 0.001$). However, when

considering seasonal variations, SWC in 5 cm depth was the dominating environmental control of NEE in Sardinilla, with $R^2=0.65$ at the pasture and $R^2=0.51$ (both $p<0.001$) at the afforestation site (Fig. 2.1, weekly means).

Respiratory fluxes (nighttime)

Variations in R_{Soil} were largely associated with seasonal variations in SWC (Fig. 2.6). For the pasture site, the functional relationship of R_{Soil} to SWC was strongest at 5 cm depth ($R^2=0.27$, $p<0.001$) while it was strongest at 30 cm depth for the afforestation site ($R^2=0.39$; $p<0.001$). At very high, almost water saturated SWC values, R_{Soil} decreased, probably due to anoxic conditions in the water filled pore space. We found no significant relationship of R_{Soil} with soil temperature (T_{Soil}) at both sites. Similar environmental controls as for R_{Soil} were found for TER, although notably weaker for SWC at both sites ($R^2=0.03$, $p<0.001$). We found only a weak temperature sensitivity of TER to soil and air temperature ($R^2<0.02$, $p<0.001$).

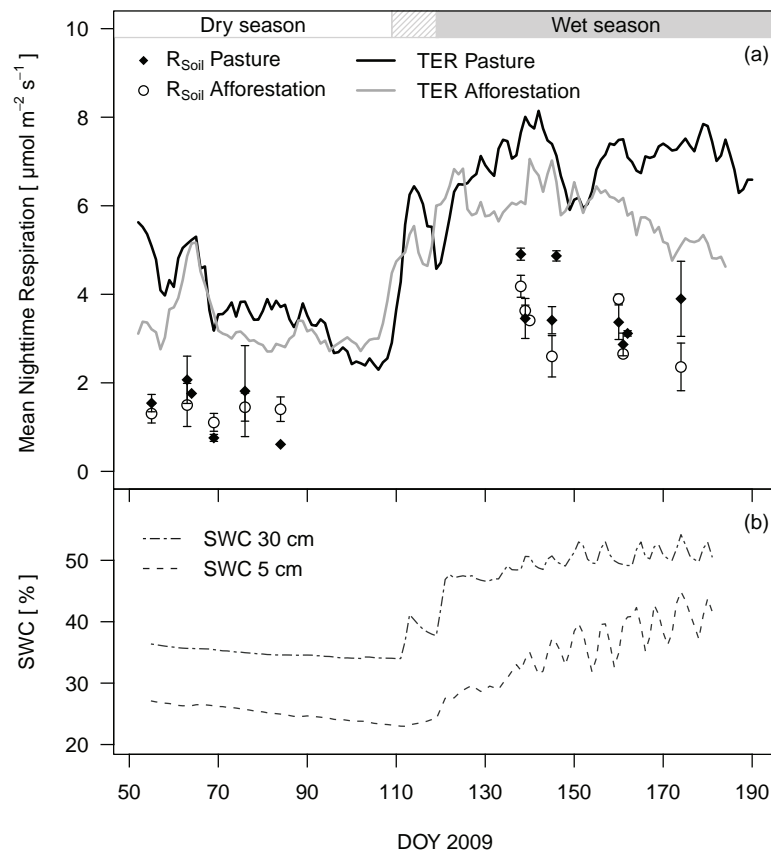


Figure 2.6. Mean nighttime soil respiration (R_{Soil} , based on chamber measurements) and total ecosystem respiration (TER, based on eddy covariance measurements) for the Sardinilla pasture and afforestation sites during February to July 2009 (a). Soil respiration is given as means \pm standard errors. TER is displayed as \pm 3 days running mean. Volumetric soil water content (SWC) at 5 and 30 cm depth was measured at the Sardinilla afforestation site (b).

2.3.6 Quality assessment of flux data

Energy Balance Closure

Assessing energy balance closure (EBC), we found a regression slope of 0.84 and an intercept of 10.8 at the pasture site ($R^2=0.92$, $p<0.001$). Furthermore, pronounced seasonal differences were observed and EBC was better during the dry compared to the wet season (Fig. 2.7). At the afforestation site, the regression slope of the EBC was 0.81, the intercept 19.73 ($R^2=0.87$, $p<0.001$), and only minor seasonal differences were found. The EBC at the Sardinilla sites are comparable to other flux tower sites globally (Wilson et al., 2002) and underlines the quality of our EC measurements.

Footprint modelling

Footprint estimates at the pasture site extended 70 m into the prevailing wind direction (north-east) and measured CO_2 fluxes were constrained to the pasture area all-season (Fig. 2.8). At the afforestation site, footprint estimates extended 150–200 m to easterly directions and additionally, to southerly and westerly directions during the wet season. Consequently, measured CO_2 fluxes predominantly originated from within the afforestation area: only a small percentage was contributed from adjacent pasture land during the wet season ($\leq 10\%$) and a slightly higher percentage during the dry season ($\leq 25\%$). Overall, the footprint estimates confirmed that the measured CO_2 fluxes in Sardinilla are representative for the respective land-use type's pasture and afforestation.

2.3.7 Phenology

At the pasture site, vegetation became senescent during the progressing dry season (mean LAI = 1.2) and LAI declined to a minimum of 0.6 in April 2009 (Tab. 2.1, Fig. 2.9). With the onset of the wet season LAI increased again, reaching a maximum of 3.3 in July (mean LAI = 2.9). The drop of LAI in the pasture in mid June (DOY 168) was caused by an herbicide application in the beginning of June and hence the death of weeds. The afforestation site was characterised by reduced canopy cover during the dry season (mean LAI = 3.0) as most tree species defoliate and understory vegetation became senescent (Tab. 2.1, Fig. 2.9). Bud break occurred within the first weeks of the wet season for most species. Subsequently, canopy cover was increasing rapidly and understory vegetation recovered faster than tree canopy LAI. During the wet season 2009, the afforestation had a fully closed canopy (mean LAI = 5.4) and reached a maximum LAI of 6.0 in July. Overall, LAI was significantly higher at the afforestation compared to the pasture during the dry and wet season (both $p>0.001$).

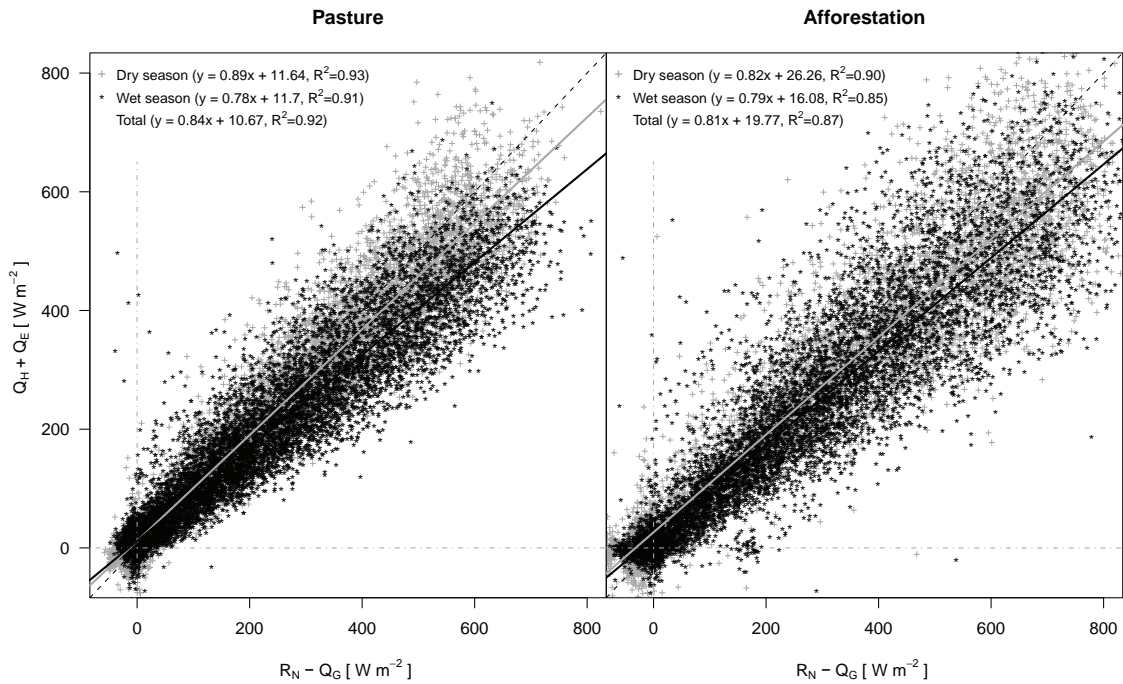


Figure 2.7. Seasonal energy balance closure for the Sardinilla pasture and afforestation sites. The grey dashed line denotes the ideal closure (1:1), the grey line is the best fit for the dry season and the black line is the best fit for the wet season. Linear regressions for all seasons are highly significant ($p < 0.001$) for both sites.

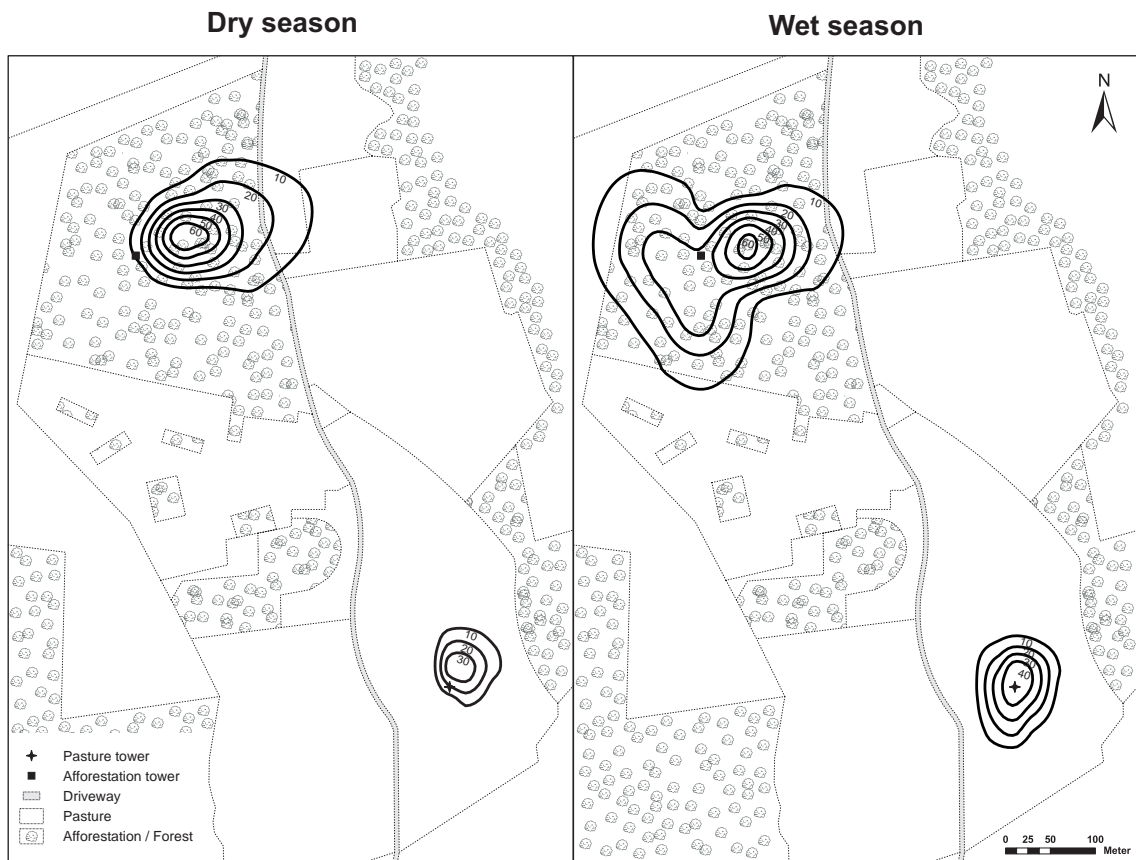


Figure 2.8. Footprint estimates of the two Sardinilla sites for dry and wet season using the model by Kljun et al. (2004). Footprint contours (10% intervals) show lines of equal contribution to the statistical mean flux with respect to the grid cell with maximum (100%) contribution.

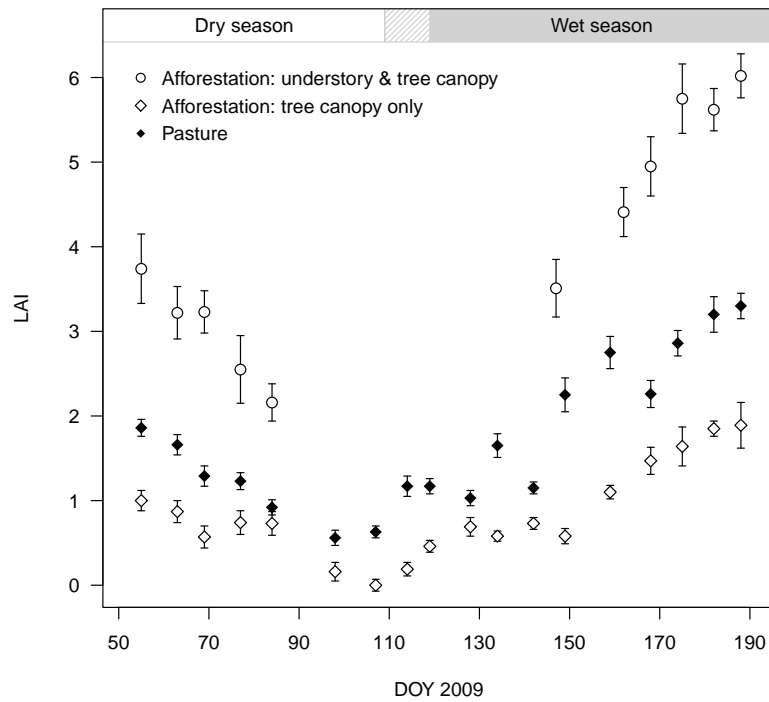


Figure 2.9. Leaf area index (LAI) for the Sardinilla pasture and afforestation sites during February to July 2009. Means \pm standard errors are given. No measurements of afforestation sites understory LAI were taken between DOY 85 and 146.

2.4 Discussion

The results support our initial hypothesis that afforestation with native tree species is more adapted to a pronounced seasonal climate in the tropics. This indicates that afforestation compared to pasture will be less affected by projected changes in precipitation patterns (reduction and increased variability) for Central America (Bates, 2008). The larger seasonal variations of NEE in pasture compared to afforestation in Sardinilla agree with the results reported by Priante-Filho et al. (2004), while von Randow et al. (2004) reported smaller variations of NEE for pasture compared to forest in Amazonia. As dry season length is similar, non-climatic factors such as species composition or land management could be responsible for such differences.

Inter-annual precipitation patterns

Our results indicate that it seems likely that ENSO events and associated increases in precipitation variability impacted CO₂ fluxes in Sardinilla during our observations from 2007 to 2009, particularly in the pasture. ENSO events regularly evolve during the period of April to June and reach their maximum strength during December to February (IRI, 2010). During the cold phase of ENSO (La Niña), Central Panama regularly receives higher precipitation, with the months June to August being wet and cool (Graham et al., 2006; IRI, 2010; Lachniet, 2009; NOAA, 2010). Recent La Niña events occurred in 2007 (strong; Trenberth & Fasullo, 2010) and 2008 (weak). Sardinilla re-

ceived above average rainfall in 2007 and, succeeding this strong La Niña year, experienced a shorter than average dry season in 2008 (Tab. 2.2). This pattern is also observed in long-term datasets (ACP, 2010) and reported in the literature (Lachniet, 2009). On the other hand, during the warm phase of ENSO (El Niño), Central Panama regularly receives below average rainfall, with the months June to August being dry and warm. A moderate El Niño occurred in 2009 (fully developed by June 2009), persisting into the beginning of 2010 (IRI, 2010; Trenberth and Fasullo, 2010). Subsequently, the dry season of 2010 started notably early (end of November 2009), which is a pattern frequently observed following El Niño events in Panama (Lachniet, 2009). ENSO events not only affect the amount of precipitation, but also its variability: the El Niño in 2009 resulted in a longer dry season but at the same time, more precipitation occurred (Tab. 2.2). As a consequence, soil moisture levels were higher compared to 2008 and we observed increased CO₂ release from the Sardinilla pasture during the dry season in 2009.

Daytime NEE

Compared to other tropical pastures, daytime NEE in the Sardinilla pasture (mean $-13 \mu\text{mol m}^{-2} \text{s}^{-1}$) was higher than reported by Santos et al. (2004) from Fazenda Rio de Janeiro (Brazil) during the dry ($-15 \mu\text{mol m}^{-2} \text{s}^{-1}$) and wet season ($-40 \mu\text{mol m}^{-2} \text{s}^{-1}$). In contrast, NEE was lower in Sardinilla compared to a study by Priante-Filho et al. (2004) that observed $-9 \mu\text{mol m}^{-2} \text{s}^{-1}$ in Cotriguacú (Brazil) during the wet season. Overall, these differences to other tropical pastures seem largely related to management factors, like grazing intensity, herbicide application and fertilization (Gilmanov et al., 2010; Wang and Fang, 2009; White et al., 2000). Compared to Sardinilla, the pasture reported by Priante-Filho et al. (2004) was intensively managed (regular burnings and grass cuts, 2nd year of afforestation) and the pasture reported by Santos et al. (2004) was ungrazed. When comparing our young afforestation with mature tropical forest, daytime NEE in the Sardinilla afforestation ($-12 \mu\text{mol m}^{-2} \text{s}^{-1}$) is in the lower range of tropical forests (-8.3 to $-19 \mu\text{mol m}^{-2} \text{s}^{-1}$): Hutyra et al. (2007) reported a higher mean daytime NEE of $-8.3 \mu\text{mol m}^{-2} \text{s}^{-1}$ and von Randow et al. (2004) observed about similar daytime NEE ($-12.5 \mu\text{mol m}^{-2} \text{s}^{-1}$, mean of dry and wet season) in Amazonia. Contrary to Sardinilla, lower daytime NEE were observed at other tropical forest sites, e.g. as reported by Loescher et al. (2003) from Costa Rica ($-18 \mu\text{mol m}^{-2} \text{s}^{-1}$) or Goulden et al. (2004; $-17.5 \mu\text{mol m}^{-2} \text{s}^{-1}$, derived mean of reported range) and Saleska et al. (2003) from Amazonia ($-15 \mu\text{mol m}^{-2} \text{s}^{-1}$). Overall, the differences in daytime NEE compared to mature tropical forest seem to be related to the young age of the Sardinilla afforestation and likely become smaller with the aging of the trees.

Controls of CO₂ fluxes

Radiation was the main environmental control of daytime CO₂ fluxes in Sardinilla, supporting our initial expectations. In addition, soil moisture showed a pronounced seasonality and the pasture ecosystem was more affected by seasonal drought than the

afforestation. This is probably related to differences in soil water access due to the larger rooting depth of trees (tap roots, access to deeper water sources) *versus* the shallow roots of grasses (Jackson et al., 1996). Von Randow et al. (2004) also reported deep water access and hence, reduced drought sensitivity of forest compared to pasture in South West Amazonia during the dry season. As long as trees still have access to ground water – which is normally the case for native tree vegetation under typical seasonal dryness, explaining their competitive advantage over other non-native vegetation types – trees will remain more productive than pasture at this site. How pasture vegetation will respond to a serious drought is unclear, however, this situation seems not very likely in the near future, given recent IPCC scenarios for Panama.

Besides environmental controls, plant physiological differences between C₃ and C₄ plants affected CO₂ fluxes in Sardinilla: with the more efficient photosynthetic pathway of the dominating C₄ grasses at the pasture (Ehleringer and Monson, 1993), this ecosystem achieved higher midday assimilation rates during the wet season than the afforestation (dominated by C₃ trees).

Nighttime respiratory fluxes

Our results confirm the expectation that soil moisture is an important environmental control for respiratory fluxes in Sardinilla, similar to observations at other tropical sites (Adachi et al., 2006; Davidson et al., 2000) and for plants with similar ecophysiological characteristics (Vargas et al., 2010). On the other hand, our results contradict the effect of temperature, which is surprising as microbial activity, i.e. heterotrophic soil respiration, typically has a strong temperature dependency. However, temperature variations in Sardinilla were small during nighttime (on average only about 2°C) which seems to explain the relatively low power to find such temperature sensitivity. Similar weak sensitivity was reported from Hytyra et al. (2007) from the Amazon and Davidson and Hanssens (2006) for tropical soils in general.

Compared to other tropical sites, R_{Soil} in the Sardinilla pasture and afforestation were within the range reported for tropical forests (Buchmann et al., 2004). However, the R_{Soil} values in the afforestation were in the lower range compared to other tropical forest sites, probably due to the young age of the afforestation (planted in 2001). At the afforestation site, R_{Soil} during the dry season 2009 was similar to R_{Soil} measured at the same site by Murphy et al. (2008) in 2004 ($1.0 \pm 0.7 \mu\text{mol m}^{-2} \text{s}^{-1}$). In contrast, R_{Soil} during the wet season 2009 was much lower than the values reported by Murphy et al. (2008), although the variability of the 2004 measurements was an order of magnitude larger ($7.2 \pm 3.5 \mu\text{mol m}^{-2} \text{s}^{-1}$). These differences are supposedly related to the small size of the trees in 2004 and the associated larger ground cover with C₄ understory vegetation (grasses).

Compared to other tropical pastures, TER observed in the Sardinilla pasture was higher than reported by von Randow et al. (2004) and lower than TER reported by Santos et al. (2004). These differences seem related to grazing, particularly as the latter study was

conducted at an ungrazed site with exceptionally high NEE in general (Santos et al., 2004). Priante-Filho et al. (2004) observed comparable TER during the wet season with only small differences between a pasture and forest site. Strong increases in TER at both sites during the dry-wet transition period were closely related to increasing soil moisture and stimulated microbial activity. Large amounts of leaf litter (afforestation) and manure (pasture) accumulated during the dry season, when decomposition was inhibited by moisture limitations (Scherer-Lorenzen et al., 2007). Eventually, the accumulated organic material started to decompose rapidly following the first rainfalls during the dry-wet transition period ('Birch effect') and caused the strong increases in TER.

2.5 Conclusions

Land-use change has a strong impact on net ecosystem CO₂ fluxes in Central Panama. The pasture studied in Sardinilla is more strongly affected by soil water limitations during the dry season than the afforestation, most likely due to the shallow roots of grasses. Consequently, land-use change from pasture to afforestation can reduce seasonal variations in CO₂ fluxes and the sensitivity to seasonal drought under present day climate conditions. Midday assimilation fluxes are persistently larger than nighttime respiratory fluxes in the afforestation ecosystem, indicating a potential for carbon uptake by the ecosystem throughout most of the year (c.f. Tab. 2.4). Future research should focus on the effects of land management on tropical afforestation (e.g. thinning, pruning, harvest) and the effects of grazing intensity on pasture ecosystem CO₂ fluxes. Our results suggest that ENSO events and associated increases in precipitation variability impact ecosystem fluxes and seasonal variations of CO₂ fluxes in Central Panama, particularly for pasture. However, long-term measurements are needed to constrain these patterns more comprehensively. With projected changes in precipitation patterns for Central America (reduction and increased variability), it can be expected that the variations of CO₂ fluxes in pasture ecosystems will increase. As long as serious droughts are not lowering the ground water table below the reach of tree roots, it can be expected that the afforestation remains more productive than the pasture in Sardinilla, Panama.

Acknowledgements

Funding for this project was provided by the North-South Centre (former Swiss Centre for International Agriculture) of ETH Zurich. We thank the Meteorology and Hydrology Branch of the Panama Canal Authority (ACP), Republic of Panama, for providing meteorological data. We are grateful to Timothy Seipel for identifying grass species of the pasture and for valuable comments on the manuscript. Many thanks also to Nicolas Gruber for inspiring discussions. We particularly thank José Monteza for assistance in the field.

Chapter 3

3 Carbon sequestration potential of pasture compared to afforestation

Chapter 3 was accepted for publication in the peer-reviewed journal
Global Change Biology as:

Carbon sequestration potentials of tropical pasture compared to afforestation in Panama

Sebastian Wolf¹, Werner Eugster¹, Catherine Potvin^{2,3}, Benjamin L. Turner³
and Nina Buchmann¹

¹ *Institute of Agricultural Sciences, ETH Zurich, Universitaetsstrasse 2, 8092 Zurich, Switzerland*

² *McGill University, Department of Biology, 1205 Dr Penfield Avenue, Montréal H3A1B1, Québec, Canada*

³ *Smithsonian Tropical Research Institute, Apartado 0843-03092, Balboa, Ancon, Panama*

Abstract

Tropical forest ecosystems play an important role in regulating the global climate, yet deforestation and land-use change mean that the tropical carbon sink is increasingly influenced by agroecosystems and pastures. Despite this, it is not yet fully understood how carbon cycling in the tropics responds to land-use change, particularly for pasture and afforestation. Thus, the objectives of our study were: (1) to elucidate the environmental controls and the impact of management on gross primary production (GPP), total ecosystem respiration (TER) and net ecosystem CO₂ exchange (NEE); (2) to estimate the carbon sequestration potential of tropical afforestation compared to pasture; and (3) to compare eddy covariance-derived carbon budgets with biomass and soil inventory data. We performed comparative measurements of NEE in a tropical C₄ pasture and an adjacent afforestation with native tree species in Sardinilla (Panama) from 2007 to 2009. Pronounced seasonal variation in GPP, TER and NEE were closely related to radiation, soil moisture and C₃ *versus* C₄ plant physiology. The shallow rooting depth of grasses compared to trees resulted in a higher sensitivity of the pasture ecosystem to water limitation and seasonal drought. During 2008, substantial amounts of carbon were sequestered by the afforestation (-442 g C m^{-2} , negative values denote ecosystem carbon uptake), which was in agreement with biometric observations (-450 g C m^{-2}). In contrast, the pasture ecosystem was a strong carbon source in 2008 and 2009 (261 g C m^{-2}), associated with seasonal drought and overgrazing. In addition, soil carbon isotope data indicated rapid carbon turnover after conversion from C₄ pasture to C₃ afforestation. Our results clearly show the potential for considerable carbon sequestration of tropical afforestation and highlight the risk of carbon losses from pasture ecosystems in a seasonal tropical climate.

3.1 Introduction

Tropical ecosystems account for more than half of the global terrestrial gross primary production (Beer et al., 2010), contain 40% of the carbon stored in the terrestrial biosphere, and are considered to sequester large amounts of carbon dioxide from the atmosphere (Grace et al., 2001). However, the current role of tropical ecosystems in terrestrial carbon sequestration remains uncertain as ongoing deforestation and associated land-use changes strongly reduce the area of tropical forests, with cropland and pasture becoming more prevalent (Alves et al., 2009; Fearnside, 2005). Land-use change from tropical forest to pasture has been reported to affect ecosystem carbon budgets in the short-term through increased inter and intra-annual variations in ecosystem CO₂ fluxes and the sensitivity to seasonal drought (Priante-Filho et al., 2004; Saleska et al., 2009a; von Randow et al., 2004). Moreover, one of the major long-term effects of such land-use changes is the reduced carbon sink strength of pasture ecosystems (IPCC, 2007a).

Despite the general importance of tropical ecosystems for global climate and carbon cycling, eddy covariance (EC) flux measurements in the tropics remain scarce and thus are globally under-represented. Tropical sites represent only 10% of the global FLUXNET measurement network, with most sites located in neotropical forests and only a few in tropical pastures or other land-use types (www.fluxnet.ornl.gov). A recent FLUXNET synthesis highlighted the importance of C₄ vegetation for terrestrial gross primary production (GPP), accounting for 20% of global terrestrial GPP, and emphasized the need for an expansion of observations in these scarcely covered ecosystems (Beer et al., 2010).

Eddy covariance flux measurements indicate that many tropical forests act as carbon sinks, which is consistent with carbon uptake inferred from long-term biometric data at some of these sites (Bonal et al., 2008; Loescher et al., 2003; Luysaert et al., 2007; Malhi et al., 1999). A few tropical forests were reported to act as carbon sources, although this might have been related to severe drought or disturbance recovery (Hutyra et al., 2007; Saleska et al., 2003). In Brazil, a transitional forest was found to have an annual carbon budget close to equilibrium (Vourlitis et al., 2001) while a tropical savanna appeared to be a sink of carbon (Miranda et al., 1997). Published results of carbon fluxes for other land-use types in the neotropics are limited: again in Brazil, Grace et al. (1998) and von Randow et al. (2004) found indications that a tropical pasture sequestered carbon, as did Priante-Filho et al. (2004) for a pasture under conversion to afforestation. In contrast, chamber measurements by Wilsey et al. (2002) showed carbon losses from tropical pastures in Panama. It therefore remains unclear whether tropical pastures are carbon sinks or sources.

Latin America has one of the highest deforestation rates in the tropics, with land predominantly converted to pasture for extensive grazing (Wassenaar et al., 2007). Few of these pastures are later used for afforestation, although this is considered an effective measure to sequester carbon and mitigate increasing CO₂ concentrations in the atmosphere (FAO, 2009). Malhi et al. (2002) estimated the mitigation potential of tropical afforestation at 15% of global CO₂ emissions. Afforestation of pasture may become more relevant for tropical countries in the future within the international carbon accounting of the Kyoto protocol, but this requires accurate information on the carbon sequestration potential involved.

A comparative measurement design is needed to quantify carbon dynamics involved in the land-use change from pasture to afforestation, to account for confounding factors of spatial divergence and variations in meteorology (Don et al., 2009). In this study, we determined the carbon budgets of tropical pasture and native tree species afforestation at a site in Central Panama from 2007 to 2009 based on continuous measurements using two eddy covariance flux towers. The objectives of our study were: (1) to elucidate the environmental controls and the impact of management on gross primary production (GPP), total ecosystem respiration (TER) and net ecosystem CO₂ exchange (NEE); (2) to estimate the carbon sequestration potential of tropical afforestation compared to pas-

ture; and (3) to compare eddy covariance-derived carbon budgets with biomass and soil inventory data.

3.2 Material and Methods

3.2.1 Site description

The Sardinilla site (Panama) is located at 9°19' N, 79°38' W and 70 m a.s.l., about 30 km north-east of Barro Colorado Island (BCI). Sardinilla has a semi-humid tropical climate with a mean annual temperature of 25.2 °C, 2289 mm annual precipitation (2007–2009; long-term mean of nearby Salamanca 1972–2009 is 2267 mm) and a pronounced dry season from January to April. Dry season length in Central Panama varies among years (134 ± 19 days for 1954–2009; ACP, 2010) and is – along with precipitation patterns – influenced by ENSO, the El Niño Southern Oscillation (Graham et al., 2006; Lachniet, 2009). Geologically, the site belongs to the Gatuncillo formation and the bedrock is classified as tertiary limestone containing clayey schist and quartz sandstone (ANAM, 2010). Soils in the pasture are Alfisols, based on their high base status and clay translocation in the profile. Soils in the afforestation are similar and include as well large areas with cracking clays that exhibit vertic properties. The Sardinilla site was logged in 1952/1953 and shortly used as arable land, before it was converted to pasture (Wilsey et al., 2002). An improved afforestation (i.e., plantation using native tree species only) was established at parts of the site (7.5 ha) in 2001 with an average of 1141 stems per ha and without any particular soil preparation (ploughing). The six native tree species used for the afforestation site were: *Luehea seemanii*, *Cordia alliodora*, *Anacardium excelsum*, *Hura crepitans*, *Cedrela odorata*, *Tabebuia rosea*. A moderately dense understory vegetation (shrubs, grasses and sedges) was present, which was cut once a year (typically in December) by manual thinning and the residues left on-site. Traditional grazing continued on an adjacent pasture (6.5 ha), where vegetation is dominated by C₄ grasses, and consists of (most abundant first): *Paspalum dilatatum* (C₄), *Rhynchospora nervosa* (sedge, C₃), *Panicum dichotomiflorum* (C₄) and *Sporobolus indicus* (C₄). Mean canopy height was about 10 m in the afforestation and 0.09 m in the pasture (in 2008). While the afforestation site has an undulating topography (elevation range <10 m), the adjacent pasture is homogeneously flat with an overall slope of less than 2°. Detailed footprint analyses indicated that fluxes measured at both sites indeed originate predominantly from the respective land-use type (see Chapter 2).

3.2.2 Instrumentation and data acquisition

Two flux towers were established in Sardinilla over a grazed pasture (March 2007 to January 2010), and an adjacent afforestation (February 2007 to June 2009). Our micro-meteorological measurement systems consisted of an open path infrared gas analyzer (IRGA, Li-7500, LI-COR, Lincoln, USA) and a three-dimensional sonic anemometer

(CSAT3, Campbell Scientific, Logan, USA). Instruments were installed at a height of 3 m at the pasture and 15 m at the afforestation site. Data acquisition was performed using an industry grade embedded box computer (Advantech ARK-3381, Taipei, Taiwan), running a Debian based Linux operating system (Knoppix 4.0.2, Knopper.Net, Schmalenberg, Germany). Ancillary meteorological measurements included air temperature and relative humidity (MP100A, Rotronic, Bassersdorf, Switzerland), incoming shortwave radiation (R_G , CM3, Kipp & Zonen, Delft, The Netherlands), photosynthetic photon flux density (PPFD, PAR Lite, Kipp & Zonen, Delft, The Netherlands), precipitation (10116 rain gauge, TOSS, Potsdam, Germany), soil temperature at 5 cm depth (TB107, Markasub, Olten, Switzerland) and volumetric soil water content (SWC) at 5 and 30 cm depth (EC-5, Decagon, Pullman, USA). Flux measurements were conducted at 20 Hz, meteorological measurements at 10 s and stored as half-hourly averages (sums for precipitation) using data loggers: CR23X at the afforestation and CR10X at the pasture site (both Campbell Scientific, Logan, USA). Precipitation and incoming shortwave radiation were measured at one tower location only. Regular cleaning of sensors and IRGA calibration checks were carried out to assure data quality. A fenced enclosure of 8 x 8 m (about 2 m high) was installed around the afforestation tower (for security reasons) and a barbwire fence of 3 x 3 m around the pasture tower to prevent access by grazing livestock. Further details on the measurement setup at the Sardinilla site are reported in Chapter 2.

3.2.3 Flux data processing

Data acquisition and quality filtering

Flux measurements were recorded using the in-house software *sonicreadHS* and raw data were processed to half-hourly averages using the in-house EC software *eth-flux* (Mauder et al., 2008; source code for Unix/Linux systems can be obtained from the authors). During post-processing, fluxes were corrected for damping losses (Eugster and Senn, 1995) and density fluctuations (Webb et al., 1980). Data screening was done using the following rejection criteria: (1) Optical sensor contamination (spider eggs, rain) resulting in high window dirtiness of the IRGAs. We used a 10% threshold above the mean background value of the respective IRGA. (2) Filtering for stationarity following Foken and Wichura (1996). We excluded fluxes whenever the 30 min average deviated by more than 100% from the corresponding mean of 5 min averages. (3) CO₂ fluxes outside the range of -50 to $50 \mu\text{mol m}^{-2} \text{s}^{-1}$ were excluded. (4) Statistical outliers outside the ± 3 SD range of a 14 day running mean window were removed. (5) Periods with low turbulence conditions were excluded based on friction velocity (u^*). Seasonal and site-dependent u^* -thresholds were determined according to the method by Gu et al. (2005) and Moureaux et al. (2006). These thresholds yielded $u^* < 0.04 \text{ m s}^{-1}$ during the dry season, $u^* < 0.03 \text{ m s}^{-1}$ during the dry-wet transition, while no thresholds were found during the wet season and wet-dry transition periods for the pasture site. At the afforestation site, the thresholds determined were $u^* < 0.02 \text{ m s}^{-1}$ during the dry season,

$u^* < 0.01 \text{ m s}^{-1}$ during the wet season, $u^* < 0.05 \text{ m s}^{-1}$ during the dry-wet transition, while no threshold was found during the wet-dry transition period. (6) Negative nighttime fluxes and a respective amount of positive nighttime data were removed using a trimmed mean approach.

Gap Filling

Filling of data gaps was required to obtain a continuous time series of flux data for budget assessments. At the pasture site, data were available for 97.7% of the time between June 2007 and January 2010. After quality filtering, 54.6% of good to excellent quality data remained (64.7% daytime, 43.6% nighttime data). At the afforestation site, data availability was 94.5% between June 2007 and June 2009, with 47.6% of good to excellent quality data remaining after quality filtering (65.4% daytime, 28.3% nighttime data).

Gap filling of NEE_{daytime} was based on non-linear light response curves (LRC), i.e., the functional relationship between daytime CO_2 fluxes and photosynthetic photon flux density (PPFD). We used a logistic sigmoid function as suggested by Moffat (unpublished) that has been used by Eugster et al. (2010) to determine light-response parameters for each single day:

$$NEE_{\text{daytime}} = 2A_{\text{max}} \left(0.5 - \frac{1}{1 + e^{\frac{-2\alpha \text{PPFD}}{A_{\text{max}}}}} \right) + TER_{\text{daytime}} \quad (\text{Eq. 3.1}).$$

A_{max} denotes the maximum photosynthetic capacity of the ecosystem ($\mu\text{mol CO}_2 \text{ m}^{-2} \text{ s}^{-1}$), α the apparent quantum yield ($\mu\text{mol CO}_2$ per $\mu\text{mol photons}$), PPFD the photosynthetic photon flux density ($\mu\text{mol photons m}^{-2} \text{ s}^{-1}$, 90% quantile used to exclude outliers) and TER_{daytime} the daytime total ecosystem respiration ($\mu\text{mol CO}_2 \text{ m}^{-2} \text{ s}^{-1}$). The initial value of α was set to 0.03 and the initial value of TER_{daytime} was determined using a linear least-squares regression. The applied sigmoid fit overcomes some of the limitations of the widely used rectangular (Michaelis-Menten equation) and non-rectangular hyperbolic fits (Gilmanov et al., 2003). In particular, it was found to yield the best light response approximation of all semi-empirical functions by properly describing the different phases of the light response of NEE_{daytime} (Eugster et al., 2010; Moffat, unpublished). For days, when the logistic sigmoid function did not converge or the curvature in the relationship between NEE_{daytime} and PPFD was not significant, a linear least-squares regression was used. Remaining daytime gaps (e.g. due to few or no measurements) were filled using a gap model with parameters estimated from the LRC of the days prior and subsequent to the gaps, or using linear interpolation. During nighttime, we found only a weak temperature sensitivity of ecosystem respiration to soil and air temperatures ($R^2 < 0.02$), irrespective of the choice of non-linear (Lloyd and Taylor model, Q_{10}) or linear functions. Therefore, we gap filled nighttime data using a

10-day running mean approach. Few nighttime gaps that still remained (<1%) at the afforestation site were filled using linear interpolation.

Partitioning

To partition the comparably small flux of daytime NEE into its much larger gross components, we used:

$$GPP = -NEE_{\text{daytime}} + TER \quad (\text{Eq. 3.2}),$$

with gross primary production (GPP, positive value) inferred from the difference of daytime net ecosystem exchange (NEE_{daytime}) and total ecosystem respiration (TER). TER was inferred from mean nighttime data (as no temperature sensitivity was observed, c.f. Gap Filling section), when photosynthesis is zero (and thus GPP is zero). In cases when NEE_{daytime} exceeded TER (resulting in negative GPP values), e.g. with onset of turbulent mixing in the morning or after rainfall, we replaced TER derived from nighttime data with NEE_{daytime} and set GPP to zero. Since our daytime TER is inferred from mean nighttime data without a temperature dependency observed in Sardinilla, no diurnal variations in TER are assumed. In general, daytime TER inferred from nighttime data should be considered as best estimate, since it neglects photorespiration occurring during the day. While this is a valid assumption for our pasture site which is dominated by C_4 vegetation, this assumption is more critical for our afforestation site which is dominated by C_3 vegetation, although TER during the day is typically dominated by soil respiration.

3.2.4 LAI, biomass, grazing and soil measurements

Auxiliary variables included leaf area index (LAI) and standing biomass measurements, stocking densities and soil sampling. Leaf area index (LAI) was measured in campaigns with a LAI-2000 (LI-COR, Lincoln, USA) in July 2008 and weekly till bi-weekly from March to July 2009. At the afforestation site, LAI was measured separately for the tree canopy (measured at 1 m above ground) and the total canopy including the understory (measured at ground level). In the pasture, aboveground standing biomass was sampled bi-weekly ($n=10$) from June 2008 to January 2010 using a 50x50 cm aluminium frame with subsequent drying for at least 3 days at 60° C. Since February 2009, photosynthetic active (green) biomass was separated from senescent biomass. Based on the measurements from 2009 and 2010, we estimated the percentage of living biomass prior to March 2009. Total aboveground biomass carbon at the pasture was calculated by assuming that 50% of the dry weight green biomass is carbon.

Grazing (i.e., stocking density) at the pasture was monitored between June 2008 and January 2010 by counting the number of grazing livestock (dominantly cattle with a few horses) on a daily basis. We used coefficients reported by Chilonda and Otte (2006) to calculate standardized livestock units (LU) per hectare, with cattle accounting for 0.7 LU and horses for 0.5 LU in Central America. Overgrazing was defined as

$>4 \text{ LU ha}^{-1} \text{ d}^{-1}$, which is rather conservative with respect to generally accepted values of the carrying capacity of 1–2 LU ha^{-1} in Europe.

At the afforestation site, standing biomass was assessed using annually measured biometric data for trees (calculated based on allometric equations; on 22 plots of 45x45 m size), herbaceous plants, litter and coarse woody debris (CWD). Details on the assessment of biometric data can be found in Appendix C. As herbaceous biomass data were not available for 2009, we assumed no change from 2008. Data on CWD were not available for the years 2007 and 2009, and thus, we estimated CWD by averaging the data from available years.

Since the year 2008 was the only calendar year with full data coverage by EC measurements at the afforestation, our direct comparison with inventory data was initially constrained to that specific year. However, we used our EC measurements from 2008 to estimate fluxes from January to May of the year 2007, and July to December 2009. This extrapolation made it possible to compare three years of EC fluxes with the biomass inventory at the afforestation.

Topsoil (0–10 cm) sampling at the afforestation was done in March 2009 ($n=22$) using a cylindrical corer 10 cm long with a diameter of 6.8 cm. At the pasture site, three soil profiles from 0 to 100 cm depth were sampled horizontally in January 2010, in 10 cm increments, and additional samples in 5 cm depth. Topsoil values at the pasture were derived by averaging the samples from 5 and 10 cm depth. All samples were dried at 60° C for at least 72 h before they were ground and analyzed for C, N and $\delta^{13}\text{C}$ with an elemental analyzer (Thermo Flash HT Soil Analyzer, Thermo Fisher Scientific, Waltham, USA) coupled through a ConFlo III interface to an isotope ratio mass spectrometer (Delta V Advantage, Thermo Fisher Scientific, Waltham, USA). To assess changes in soil parameters since afforestation establishment, we compared our measurements with samplings from June 2001 and 2002 by Abraham (2004). We used bulk density (d_B) values reported by Abraham (2004) to calculate topsoil (0–10 cm) carbon and nitrogen pools, by assuming no changes in d_B since 2001/2002. This is supported by a study of Seitlinger (2008) that found no changes of topsoil d_B in the afforestation between 2001 and June 2007. Data on carbon pools below 10 cm at the afforestation site was extracted from Abraham (2004), assuming changes in carbon pools since 2001 occurred predominantly in the topsoil, as deeper soil carbon pools are considered relatively stable (Malhi and Davidson, 2009). At the pasture site, we used the mean of the three soil profiles sampled in 2010 and the topsoil d_B reported by Abraham (2004) to estimate soil carbon pools from 0–100 cm. A mixing model was used to assess the carbon isotopic source contribution of organic matter in the soil, with litter values reported by Abraham (2004) as -14.4‰ for pasture and -29.5‰ for tree litter.

3.2.5 Statistical analyses and general conventions

All statistical analyses were carried out using the R statistics software package, version 2.10.0 (R Development Core Team 2009, www.r-project.org). Daytime was defined as

the period when PPFD exceeded $5 \mu\text{mol m}^{-2} \text{s}^{-1}$. Fluxes from the atmosphere to the biosphere are marked with a negative sign denoting carbon uptake by the ecosystem; positive fluxes indicate carbon loss. In general, only seasons with full data coverage were used for seasonal averaging. Separation of dry from wet seasons and transition periods was done based on daily precipitation sums using the methodology described in Chapter 2: wet season was defined as the time span with no periods of more than four consecutive days without rain, and the dry season *vice versa*. Transition periods mark the time span between both main seasons. When writing ‘seasonal drought’, we refer to the plant physiological effects of soil moisture deficiency during the dry season.

3.3 Results

3.3.1 Intra- and inter-annual variations in precipitation

We found a pronounced seasonality in the climate in Sardinilla where most of the precipitation (>98%) occurred during the wet season from April to December (Tab. 3.1, Fig. 3.1d). On average, November was the wettest (>300 mm) and September was the driest month (about 200 mm) during the wet season. The dry season lasted from about January to April. The two transition periods were characterized by highly variable but limited amounts of precipitation ($<4 \text{ mm d}^{-1}$). Compared to the long-term annual mean from nearby Salamanca (2267 mm, 1972–2009; derived from STRI 2010), Sardinilla received above average rainfall in 2007 (2553 mm, +13%), below average rainfall in 2008 (2074 mm, –9%) and about average rainfall in 2009 (2233 mm, 1%).

In contrast to the predicted reductions in precipitation in Central America for the future (IPCC, 2007b), the long-term data from Salamanca indicated a positive trend in the annual sum of precipitation from 1972 to 2009 (+17 mm per year; $R^2=0.14$, $p<0.05$). On a monthly basis, we observed significantly positive trends in precipitation for the months February (+1.1 mm; $R^2=0.19$, $p<0.01$), July (+3.8 mm; $R^2=0.10$, $p<0.05$) and November (+4.9 mm; $R^2=0.14$, $p<0.05$).

Soil water content (SWC) at 5 cm depth exceeded 40% during most of the wet season (mean 46%, maximum of 52% in November) and rapidly declined to below 30% after the onset of the dry season (mean 26%, minimum of 22% in April; Tab. 3.1, Fig. 3.1d). Following the first rainfalls during the dry-wet transition period in April, SWC started to increase swiftly and exceeded 40% by June. During the dry season in 2009, SWC declined less compared to 2008, which was related to moderate precipitation events in February. SWC in deeper soil layers (30 cm, not shown) was higher compared to SWC in 5 cm depth during the dry season and about similar during the wet season. Daily total photosynthetic photon flux density (PPFD) ranged from a minimum of $5.2 \text{ mol m}^{-2} \text{ d}^{-1}$ in November (wet season) to a maximum of $58.5 \text{ mol m}^{-2} \text{ d}^{-1}$ in March (dry season; Fig. 3.1c). PPFD exceeded $40 \text{ mol m}^{-2} \text{ d}^{-1}$ during most of the dry season (mean $41.8 \text{ mol m}^{-2} \text{ d}^{-1}$) and was reduced during the wet season (mean $28.6 \text{ mol m}^{-2} \text{ d}^{-1}$). Seasonal temperature variations at Sardinilla were small and within $\pm 1^\circ\text{C}$ of the annual

mean of 25.2°C (2007–2009), with the lowest values generally occurring during November to March (Tab. 3.1). The diurnal temperature range in Sardinilla was larger than seasonal variations and ranged from 22.2°C (nighttime) to 27.4°C (daytime) during the dry season and 23.5°C to 26.8°C during the wet season, respectively.

Table 3.1. Monthly values of, precipitation sum (P), mean soil water content (SWC, Sardinilla afforestation, at 5 cm depth), total photosynthetic photon flux density (PPFD), mean air temperature (T_{Air}), total net ecosystem exchange (NEE), total gross primary production (|GPP|) and total ecosystem respiration (TER) at Sardinilla, Panama from 2007 to 2009. Measurements at the afforestation were discontinued after June 2009.

Year	Month	P (mm)	SWC (%)	PPFD (mol m ⁻²)	T_{Air} (°C)	Pasture			Afforestation		
						NEE (g C m ⁻²)	GPP (g C m ⁻²)	TER (g C m ⁻²)	NEE (g C m ⁻²)	GPP (g C m ⁻²)	TER (g C m ⁻²)
2007	Jun	278	40.5	802	25.5	9.3	216	225	-41.4	211	170
	Jul	197	43.7	815	25.3	3.8	225	229	-26.7	200	174
	Aug	223	45.9	814	25.0	6.9	215	222	-23.4	188	164
	Sep	206	48.2	901	25.1	-13.5	239	226	-36.2	196	160
	Oct	380	47.2	867	25.1	-13.8	240	226	-39.9	201	161
	Nov	351	51.6	751	24.9	-19.5	219	199	-31.1	184	153
	Dec	288	49.8	942	24.7	-23.9	253	229	-1.5	150	148
2008	Jan	11	28.3	1290	24.6	16.6	270	287	-27.6	168	140
	Feb	11	24.0	1152	24.6	54.5	144	199	-42.2	155	112
	Mar	4	22.3	1350	24.9	69.0	72	141	-27.0	135	108
	Apr	72	22.1	1249	25.5	98.4	68	166	8.7	119	127
	May	289	30.7	985	25.5	62.8	173	236	-3.4	183	180
	Jun	230	42.8	781	25.1	8.6	210	219	-43.7	199	155
	Jul	356	49.9	825	24.6	-19.5	239	220	-58.1	206	148
	Aug	263	50.3	874	24.9	-9.8	225	215	-59.4	207	148
	Sep	203	49.5	934	25.5	-7.9	225	218	-44.7	189	145
	Oct	241	49.1	945	25.2	-16.0	260	245	-61.2	199	138
	Nov	338	51.9	680	24.3	-9.2	202	193	-57.2	169	112
	Dec	53	45.9	1149	25.1	13.4	257	270	-26.0	154	128
2009	Jan	13	30.2	1125	24.7	31.7	211	242	-30.7	153	122
	Feb	20	29.1	1121	25.3	71.6	94	166	-40.7	133	93
	Mar	12	25.8	1373	25.2	75.9	51	127	-11.2	114	103
	Apr	94	23.9	1235	25.8	87.2	25	112	22.1	86	108
	May	239	32.0	958	25.7	73.4	145	219	13.3	148	162
	Jun	238	39.1	953	25.5	33.2	177	210	-60.8	212	151
	Jul	309	-	982	26.1	-3.3	226	223	-	-	-
	Aug	286	-	923	25.7	-22.1	233	210	-	-	-
	Sep	211	-	913	26.0	-36.5	231	194	-	-	-
	Oct	296	-	894	25.3	-40.7	251	211	-	-	-
	Nov	486	-	595	24.7	-10.5	202	192	-	-	-
	Dec	30	-	1112	25.5	-0.2	246	245	-	-	-

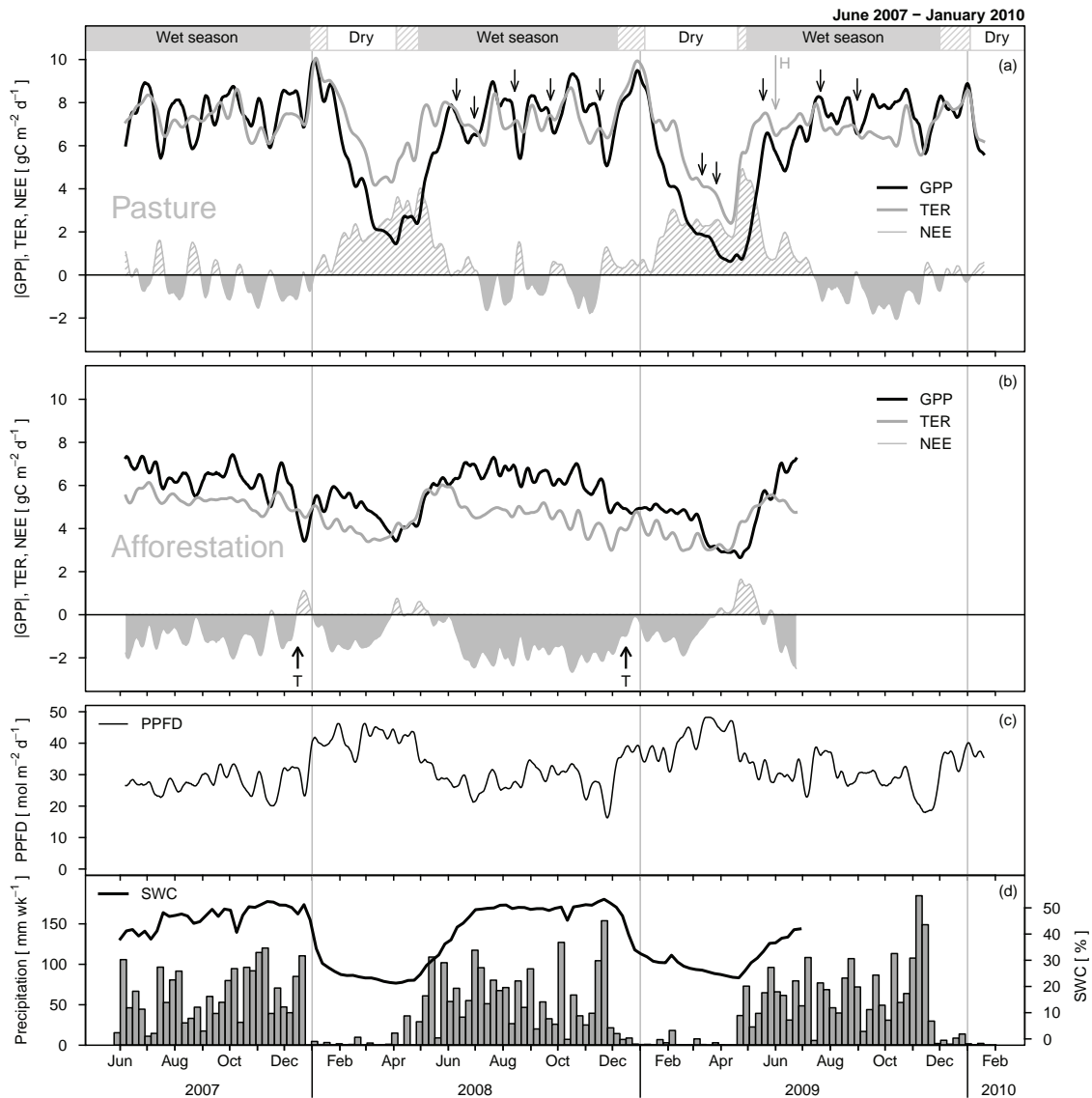


Figure 3.1. Daily total gross primary production ($|GPP|$, absolute value), total ecosystem respiration (TER) and net ecosystem exchange (NEE; full shading indicates periods of carbon sinks, striped periods of carbon sources) of the Sardinilla pasture (a) and afforestation (b) sites. Daily total of photosynthetic photon flux density (PPFD) is shown from June 2007 to January 2010 (c). $|GPP|$, TER, NEE and PPFD are displayed as 14-days running means. Black arrows denote first day of periods with overgrazing ($>4 \text{ LU ha}^{-1} \text{ d}^{-1}$) and “H” combined with grey arrow marks the day of herbicide application by the farmer at the pasture. “T” combined with the black arrow indicates periods of understory thinning at the afforestation. Weekly precipitation (grey bars) and weekly mean volumetric soil water content (SWC; Sardinilla afforestation, at 5 cm depth) are given (d). Measurements at the afforestation were discontinued after June 2009. The inserts at the top indicate the different seasons (wet, dry) including transition periods (shaded areas).

3.3.2 Seasonal patterns in GPP, TER and NEE

We observed strong seasonal variations of gross primary production (GPP), total ecosystem respiration (TER) and net ecosystem exchange (NEE) in both pasture and afforestation ecosystems. Seasonal variations at both sites were larger during the year 2009 than in 2008 (Figs. 3.1 and 3.2).

At the pasture site, daily NEE ranged from a minimum of $-4.6 \text{ g C m}^{-2} \text{ d}^{-1}$ during the wet season to a maximum of $8.3 \text{ g C m}^{-2} \text{ d}^{-1}$ during the dry-wet transition period (mean of $0.5 \text{ g C m}^{-2} \text{ d}^{-1}$). During the wet season, average GPP and TER were on the same order of magnitude with seasonal means of $7.0 \text{ g C m}^{-2} \text{ d}^{-1}$. GPP dropped several times by up to 30% during the wet seasons 2007 and 2008 (Fig. 3.1). We observed maximum values for GPP and TER during the wet-dry transition period, with $8.5 \text{ g C m}^{-2} \text{ d}^{-1}$ and $8.7 \text{ g C m}^{-2} \text{ d}^{-1}$ respectively (seasonal means). During the dry season, GPP was limited by water availability and declined to a minimum of $2.0 \text{ g C m}^{-2} \text{ d}^{-1}$ (seasonal mean) during the dry-wet transition period with predominantly senescent pasture vegetation (LAI = 0.6). TER was reduced during the dry season as well (mean $5.6 \text{ g C m}^{-2} \text{ d}^{-1}$) but exceeded GPP (mean $3.7 \text{ g C m}^{-2} \text{ d}^{-1}$), resulting in positive NEE and thus, carbon release from the ecosystem (Fig. 3.2). With the first rainfalls during the dry-wet transition period, TER increased rapidly and reached the level of the mean seasonal TER within about one month (Fig. 3.1). However, with most of the pasture grasses senescent, GPP did not increase for another 1–2 weeks. Maximum carbon losses occurred during the dry-wet transition period. Overall, mean daily TER ($6.89 \pm 1.38 \text{ g C m}^{-2} \text{ d}^{-1}$) was similar to GPP ($6.39 \pm 2.59 \text{ g C m}^{-2} \text{ d}^{-1}$).

At the afforestation site, we observed smaller seasonal variations of NEE, GPP and TER compared to the pasture, along with lower absolute values in general. Daily NEE ranged from $-5.4 \text{ g C m}^{-2} \text{ d}^{-1}$ during the wet season to $3.7 \text{ g C m}^{-2} \text{ d}^{-1}$ during the dry-wet transition period (mean of $-1.0 \text{ g C m}^{-2} \text{ d}^{-1}$). During the wet season, GPP consistently exceeded TER with $6.3 \text{ g C m}^{-2} \text{ d}^{-1}$ vs. $4.7 \text{ g C m}^{-2} \text{ d}^{-1}$, except during December 2007 (Fig. 3.1). Accordingly, NEE was negative and the afforestation acted as a carbon sink throughout the wet season. GPP and TER peaked during the early wet season in June and July, after the leaves of all tree species had fully developed (LAI of 6.0 in 2009). Besides a second wet season maximum of GPP during October, GPP and TER declined gradually during the wet season. During the wet-dry transition, TER increased while GPP remained stable. This increase was particularly strong in December 2008 and reduced NEE to $-0.6 \text{ g C m}^{-2} \text{ d}^{-1}$ (seasonal mean). During the dry season, GPP initially increased (in 2007) or remained relatively constant (in 2009) during the early dry season, while TER was declining. From February on, GPP also declined, in 2008 rather gradually and in 2009 slowly at first and subsequently rapidly in March. However, as GPP exceeded TER, the afforestation maintained carbon uptake during most of the dry season, with a mean NEE of $-0.9 \text{ g C m}^{-2} \text{ d}^{-1}$. During the dry-wet transition, TER increased strongly following the first rainfall while GPP did not increase for another 1–2 weeks. During the dry-wet transition period the afforestation was a carbon source (mean NEE of $0.6 \text{ g C m}^{-2} \text{ d}^{-1}$). In contrast to the pasture, mean daily GPP ($5.59 \pm 1.57 \text{ g C m}^{-2} \text{ d}^{-1}$) exceeded TER ($4.61 \pm 0.87 \text{ g C m}^{-2} \text{ d}^{-1}$) at the afforestation site, resulting in a negative mean NEE of $-0.98 \pm 1.43 \text{ g C m}^{-2} \text{ d}^{-1}$.

Overall, we observed a strong coupling of daily TER with GPP during the dry season. This coupling was stronger at the pasture ($R^2=0.85$, $p<0.001$) compared to the afforesta-

tion ($R^2=0.26$, $p<0.001$). During the wet season, however, daily variations in TER were only weakly correlated with GPP at both sites.

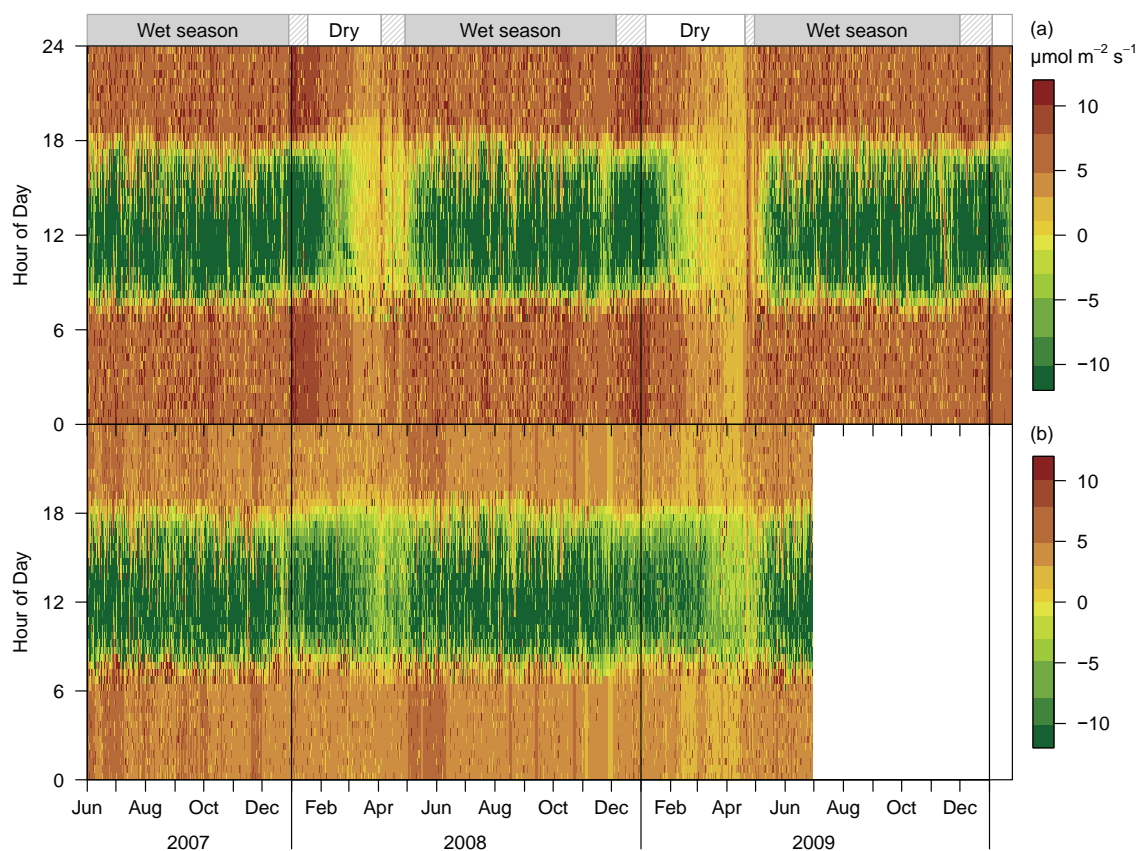


Figure 3.2. Flux fingerprints of gap filled net ecosystem exchange (NEE) of Sardinilla pasture (a) and afforestation (b) sites. Measurements at the afforestation were discontinued after June 2009. The inserts at the top indicate the different seasons (wet, dry) including transition periods (shaded areas).

Table 3.2. Season length (d), precipitation sum (P), mean of total daily photosynthetic photon flux density (PPFD) and seasonal total net ecosystem exchange at the pasture (NEE.Pa) and afforestation site (NEE.Aff).

		Dates	Length (d)	P (mm)	PPFD ($\text{mol m}^{-2} \text{d}^{-1}$)	NEE.Pa (g C m^{-2})	NEE.Aff (g C m^{-2})
2007	Wet season	23.04.–28.12.	250	2471	27.3*	-43.3*	-198.8*
	Wet-dry transition	29.12.–17.01.	20	17	40.8	3.5	-8.2
2008	Dry season	18.01.–03.04.	77	17	42.1	135.3	-89.6
	Dry-wet transition	04.04.–28.04.	25	51	41.8	81.3	7.3
	Wet season	29.04.–05.12.	221	1964	28.2	22.0	-337.2
	Wet-dry transition	06.12.–05.01.	31	34	37.2	17.6	-18.4
2009	Dry season	06.01.–19.04.	104	42	41.6	208.9	-75.4
	Dry-wet transition	20.04.–29.04.	10	37	34.8	46.5	15.2
	Wet season	30.04.–30.11.	215	2122	29.0	-1.7	-44.8*
	Wet-dry transition	01.12.–03.01.	34	32	36.6	-1.4	-

* Incomplete, only partial temporal coverage

3.3.3 Carbon budgets

The pasture ecosystem was a substantial carbon source and lost 470 g C m^{-2} from June 2007 to December 2009. Inter-annual variation in the carbon budget was small, with $261 \text{ g C m}^{-2} \text{ yr}^{-1}$ in 2008 and $260 \text{ g C m}^{-2} \text{ yr}^{-1}$ in 2009 (Fig. 3.3). Using the mean NEE from January to May 2008 and 2009, we estimated an annual carbon budget of $251 \text{ g C m}^{-2} \text{ yr}^{-1}$ for 2007. The pasture ecosystem lost carbon during most of the year except during the late wet season. Seasonal carbon budgets indicated that more carbon was lost during the dry season 2009 compared to 2008 but losses were in reverse order during the wet season 2008 compared to 2009 (Tab. 3.2). Total monthly NEE ranged from $-2.3 \text{ g C m}^{-2} \text{ mo}^{-1}$ during the wet season to $92.8 \text{ g C m}^{-2} \text{ mo}^{-1}$ during the dry-wet transition period (overall mean $15.2 \text{ g C m}^{-2} \text{ mo}^{-1}$, Tab. 3.1).

The afforestation ecosystem was a strong carbon sink from June 2007 to June 2009 (-750 g C m^{-2}). Total annual NEE was -442 g C m^{-2} in 2008 and we estimated the annual budgets (see pasture) for 2007 and 2009 to -292 g C m^{-2} and -419 g C m^{-2} , respectively (Fig. 3.3). The afforestation was a continuous carbon sink during most of the year, except the end of the dry season, the dry-wet transition period and in December 2007. Seasonal budgets indicated higher carbon losses during the dry-wet transition and onset of the wet season in 2009 compared to 2008 (Tab. 3.2). Carbon uptake increased from 2007 to 2009 due to reductions in TER, primarily during the wet season. Monthly NEE ranged from $-36.0 \text{ g C m}^{-2} \text{ mo}^{-1}$ during the wet season to $15.4 \text{ g C m}^{-2} \text{ mo}^{-1}$ during the dry-wet transition period (overall mean $-30.0 \text{ g C m}^{-2} \text{ mo}^{-1}$, Tab. 3.1).

During the entire dry season and the beginning of the wet season, the pasture was a persistent and strong source of CO_2 . In contrast, the afforestation was a net carbon sink that was only occasionally interrupted during this period (Fig. 3.1).

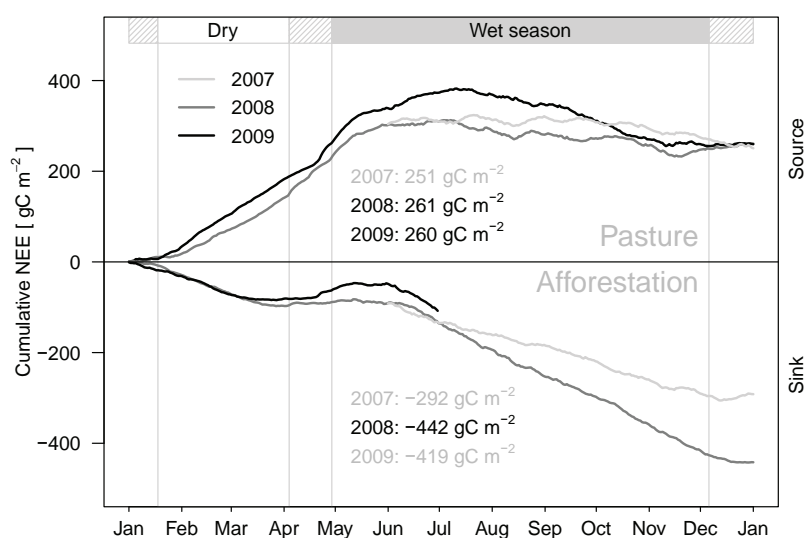


Figure 3.3. Cumulative annual net ecosystem exchange (NEE) of the Sardinilla pasture and afforestation sites from 2007 until 2009. Numbers displayed denote annual total budgets with grey indicating years only partly measured. Annual budgets for those years have been estimated using the respective periods from prior and following and years. Annual budget uncertainties are estimated to be below $\pm 100 \text{ g C m}^{-2} \text{ yr}^{-1}$.

3.3.4 Environmental controls of GPP, TER and NEE

SWC and VPD

A strong correlation between monthly mean SWC at 5 cm depth and monthly total NEE was found at the pasture site ($R^2=0.84$, $p<0.001$; not shown). Below a threshold of about 47% in monthly mean SWC at 5 cm depth, the pasture ecosystem became a source of carbon. The ecosystem response of NEE to SWC at 30 cm depth was weaker ($R^2=0.64$, $p<0.001$) compared to 5 cm depth at the pasture site. SWC at 5 cm depth explained less variation in monthly total GPP ($R^2=0.59$, $p<0.001$) and TER ($R^2=0.20$, $p<0.05$) compared to NEE. In addition, we found vapour pressure deficit (VPD) weakly related to NEE ($R^2=0.24$, $p<0.01$) and GPP ($R^2=0.23$, $p<0.01$). Similar but weaker relationships were found on weekly but not on shorter timescales (daily and half-hourly).

At the afforestation site, monthly mean SWC at 30 cm depth showed a stronger relationship to monthly total NEE ($R^2=0.39$, $p<0.01$) compared to SWC at 5 cm depth ($R^2=0.26$, $p<0.01$). GPP was associated even stronger with monthly variations in SWC at 30 cm depth ($R^2=0.57$, $p<0.001$). TER was weakly related to SWC at 5 cm depth only ($R^2=0.21$, $p<0.05$). Unlike at the pasture site, no significant relationship of VPD with NEE was observed, but with GPP ($R^2=0.48$, $p<0.001$) and TER ($R^2=0.49$, $p<0.001$).

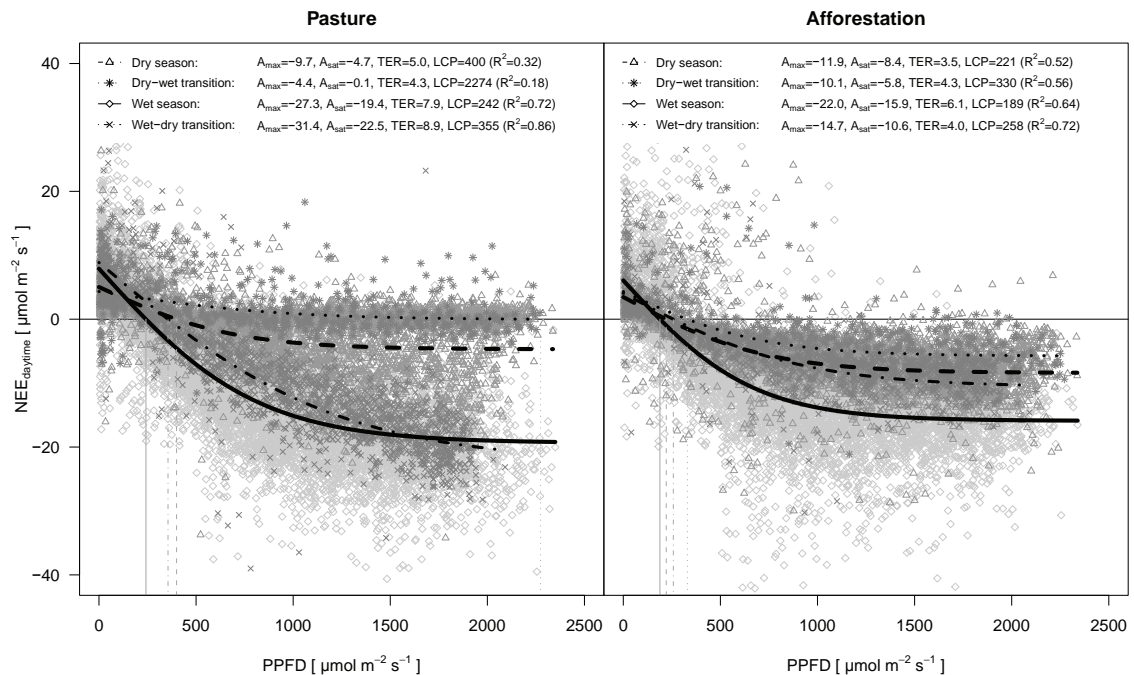


Figure 3.4. Seasonally averaged light response curves (LRC) for Sardinilla pasture and afforestation sites from 2007 to 2009. Daytime net ecosystem exchange (NEE_{daytime}) is displayed as a function of photosynthetic photon flux density (PPFD, $\mu\text{mol m}^{-2} \text{s}^{-1}$). Symbols denote half-hourly measurements. LRC were estimated using a nonlinear logistic sigmoid function with seasonal fitting parameters: maximum photosynthetic capacity (A_{max}), saturated photosynthetic capacity (A_{sat}), daytime total ecosystem respiration (TER) and light compensation point (LCP, all in $\mu\text{mol m}^{-2} \text{s}^{-1}$). In addition, seasonal LCPs are represented by the dotted grey lines.

PPFD, Ecosystem light response of NEE

We observed a strong seasonality in ecosystem light response to photosynthetic photon flux density (PPFD) with differences between the two sites (Fig. 3.4). The pasture ecosystem showed a relatively weak light response during the dry season with a high light compensation point (LCP) of $400 \mu\text{mol m}^{-2} \text{s}^{-1}$ and light saturation (due to limited carboxylation rate) at about $1500 \mu\text{mol m}^{-2} \text{s}^{-1}$. This was even more pronounced during the dry-wet transition, light compensation was actually never achieved and total ecosystem respiration constantly exceeded photosynthesis. During the wet season, the photosynthetic efficiency was most pronounced with a low LCP of $242 \mu\text{mol m}^{-2} \text{s}^{-1}$ and high values of A_{sat} ($-19.4 \mu\text{mol m}^{-2} \text{s}^{-1}$) and $\text{TER}_{\text{daytime}}$ ($7.9 \mu\text{mol m}^{-2} \text{s}^{-1}$). Basically light saturation was not reached during the wet-dry transition period, which exhibited the highest rates of A_{max} ($-31.4 \mu\text{mol m}^{-2} \text{s}^{-1}$) and A_{sat} ($-22.5 \mu\text{mol m}^{-2} \text{s}^{-1}$) along with $\text{TER}_{\text{daytime}}$ ($8.9 \mu\text{mol m}^{-2} \text{s}^{-1}$).

The afforestation ecosystem exhibited less seasonal variation in light response and we observed overall lower LCPs compared to the pasture (Fig. 3.4). During the dry season, A_{sat} ($-8.4 \mu\text{mol m}^{-2} \text{s}^{-1}$) exceeded $\text{TER}_{\text{daytime}}$ ($3.5 \mu\text{mol m}^{-2} \text{s}^{-1}$) and light saturation was reached at approximately $1500 \mu\text{mol m}^{-2} \text{s}^{-1}$, similar to the pasture. The highest LCP at the afforestation was observed during the dry-wet transition ($330 \mu\text{mol m}^{-2} \text{s}^{-1}$) and light saturation was reached at about $1200 \mu\text{mol m}^{-2} \text{s}^{-1}$. During the wet season, the light response of NEE at the afforestation ecosystem was most pronounced with a low LCP ($189 \mu\text{mol m}^{-2} \text{s}^{-1}$) and the highest seasonal values of A_{max} ($-22.0 \mu\text{mol m}^{-2} \text{s}^{-1}$), A_{sat} ($-15.9 \mu\text{mol m}^{-2} \text{s}^{-1}$) and $\text{TER}_{\text{daytime}}$ ($6.1 \mu\text{mol m}^{-2} \text{s}^{-1}$). However, the light response during the wet-dry transition period was very limited and similar to the light response during the dry season.

3.3.5 Management controls of GPP and TER

Grazing

Grazing was the main management factor that influenced GPP and TER at the pasture site. Grazing varied substantially from June 2008 to January 2010, from zero to 75 live-stock per day (median: 18.1) on the 6.5 ha pasture. This corresponds to a median and maximum of 1.6 and $8.0 \text{ LU ha}^{-1} \text{ d}^{-1}$, respectively (Fig. 3.5b). Periods of average grazing were constrained by isolated periods of overgrazing ($>4 \text{ LU ha}^{-1} \text{ d}^{-1}$). Lower stocking densities were observed in 2008 (median: $1.2 \text{ LU ha}^{-1} \text{ d}^{-1}$) compared to 2009 ($2.0 \text{ LU ha}^{-1} \text{ d}^{-1}$). On the other hand, periods of overgrazing persisted longer in 2008 (up to 9 days) compared to 2009 (up to 3 days).

Overgrazing strongly reduced GPP of the pasture ecosystem, particularly during the wet season 2008 (Fig. 3.1a). We observed a strong correlation between GPP and grazing intensity during the major part of the wet season 2008, with GPP being significantly reduced when the pasture was overgrazed. The significant reduction in GPP started immediately, reached a maximum after 4 days ($R^2=0.42$) of the start of overgrazing, and

lasted for an average for 6 days. TER was reduced as well but was delayed with respect to the beginning of overgrazing. A significant reduction in TER started after 2 days, had its maximum after 6 days ($R^2=0.23$) and lasted on average for 9 days. Along with GPP, NEE showed less net uptake, which was most pronounced after 1 day ($R^2=0.37$) and lasted for 5 days. No significant time lag of GPP *versus* grazing was observed during the wet season 2009. Furthermore, we observed an apparent reduction in ecosystem light response during and shortly after overgrazing: When excluding overgrazing periods with confounding limitations by environmental controls (namely PPF), the pasture exhibited a reduction in daily photosynthetic capacity (A_{\max}), increased total ecosystem respiration (TER_{daytime}) and increased the LCP. For instance, during overgrazing in September 2008 (DOY 267–270, 7.7 LU ha⁻¹), A_{\max} was reduced from 31.5 to 26.9 $\mu\text{mol m}^{-2} \text{s}^{-1}$, TER increased from 10.7 to 14.5 $\mu\text{mol m}^{-2} \text{s}^{-1}$ and the LCP increased from 311 to a maximum of 597 $\mu\text{mol m}^{-2} \text{s}^{-1}$. We used this period of overgrazing combined with the reduction in aboveground biomass (DOY 259–274) and estimated an average forage consumption of 0.81 g C m⁻² d⁻¹ (for 1 LU) or 475 g C m⁻² yr⁻¹, when using the median stocking density of 1.6 LU ha⁻¹ for Sardinilla.

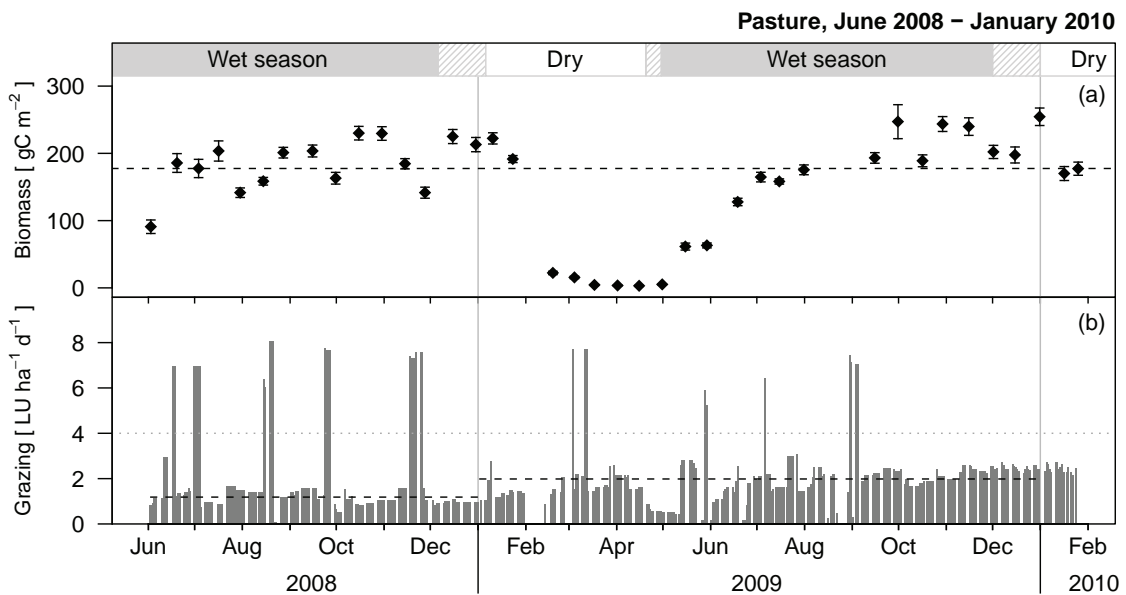


Figure 3.5. Aboveground green biomass (a) and grazing (in livestock units, LU; b) at the Sardinilla Pasture from June 2008 to January 2010. The dashed black lines denote the overall median for biomass (a) and the annual median for grazing (b). The dotted grey line shows the overgrazing threshold of 4 LU.

Herbicide application

Another management factor at the pasture site was herbicide application by the farmer. The recovery of the vegetation after the dry season was dominated by the fast growing pioneering weed *Croton hirtus*, which inhibits the recovery of other grasses. In 2009, herbicide was applied by the farmer on June 1st and within about 2–3 weeks, the weed died off. Following the herbicide application, we observed a reduction in GPP by about

15%, an increase in TER by about 10% and a reduction in LAI from 2.75 ± 0.19 (June 8th) to 2.26 ± 0.15 (June 18th). No exact dates for herbicide application in 2007 and 2008 could be obtained.

Understory thinning

Thinning of the understory (i.e., weed removal) at the end of the year was the only management intervention at the afforestation site. No carbon was exported, and all clipped biomass was left on site. A major thinning (full afforestation area) was carried out in December 2007. This reduced GPP substantially by about 50% and turned the afforestation site into a carbon source (Fig. 3.1) for a period of 17 days. Understory thinning in December 2008 was minor and included only parts of the afforestation site. We observed an accompanying reduction in GPP as well but less strong than in 2007. This difference was largely due to lower TER in December 2008. However, TER increased strongly following the thinning in 2008, indicating enhanced microbial activity due to decomposing litter.

3.3.6 Inventory data

Biomass

Significant seasonal variations in aboveground green biomass were observed at the pasture site, ranging from zero during the dry season and dry-wet transition period (senescent vegetation) to a maximum of 254 g C m^{-2} during the wet-dry transition period, with an overall median of $178 \pm 77 \text{ g C m}^{-2}$ (Fig. 3.5a). With re-growing vegetation after onset of the wet season, average aboveground biomass was reached during July and lasted until January, except for periods with pronounced overgrazing during the wet season 2008. Substantial reductions in aboveground biomass by up to 20% were observed following periods of overgrazing, e.g. in September 2008 from $204 \pm 8.9 \text{ g C m}^{-2}$ (DOY 259) to $163 \pm 8.7 \text{ g C m}^{-2}$ (DOY 274), when overgrazing occurred from DOY 267–270. Aboveground biomass and LAI were strongly correlated at the pasture site ($R^2=0.84$, $p<0.001$). Belowground biomass was determined once in March 2009 ($n=1$) and was with 176 g C m^{-2} similar to average aboveground biomass. At the afforestation, total aboveground biomass more than tripled from $772 \pm 136 \text{ g C m}^{-2}$ in 2005 to $2449 \pm 891 \text{ g C m}^{-2}$ in 2009 (Tab. 3.3). Belowground biomass (coarse roots) increased from $112 \pm 63 \text{ g C m}^{-2}$ in 2005 to $693 \pm 306 \text{ g C m}^{-2}$ in 2009. In 2008, tree biomass (above and belowground) was the largest component of ecosystem biomass with $1533 \pm 705 \text{ g C m}^{-2}$ (72.3%), followed by understory vegetation with $546 \pm 89 \text{ g C m}^{-2}$ (25.7%), coarse woody debris (CWD) with $14.8 \pm 12.6 \text{ g C m}^{-2}$ (0.7%) and litter with $27.9 \pm 20.0 \text{ g C m}^{-2}$ (1.3%). The annual increase in tree biomass was highest in 2006 (+69.4%) and 2009 (+66.6%), while it was smaller in 2007 (+55.9%) and lowest in 2008 (41.2%). The relative contribution of understory vegetation to the total aboveground biomass was reduced considerably from 50.1% in 2005 to 17.4% in 2009. However, total herbaceous biomass increased strongly

from 2006 to 2007 (+34.5%), due to the invasion of *Saccharum spontaneum* (Canal grass) in parts of the afforestation site. Overall, annual ecosystem biomass increments varied strongly from $263 \pm 225 \text{ g C m}^{-2}$ in 2006, to a maximum of $1021 \pm 556 \text{ g C m}^{-2}$ in 2009. The large increment in 2007 was primarily associated with the strong increase in herbaceous biomass.

Table 3.3. Above and belowground standing biomass at the Sardinilla afforestation from 2005 to 2009. Values indicate mean \pm standard deviation. No data on herbaceous biomass and coarse woody debris were available for 2009 and thus, data from 2008 were used to estimate total biomass (*).

	2005	2006	2007	2008	2009
			(g C m ⁻²)		
Trees	299 \pm 168	506 \pm 269	792 \pm 419	1116 \pm 522	1861 \pm 879
Herbaceous biomass	443 \pm 109	401 \pm 65	539 \pm 82	546 \pm 89	546 \pm 89 *
Coarse woody debris	2.1	21.8	18.3	14.8	14.8 *
Litter			27.9 \pm 20.0		
Total aboveground biomass	772 \pm 136	957 \pm 285	1377 \pm 448	1705 \pm 537	2449 \pm 891
Roots	112 \pm 63	190 \pm 98	294 \pm 144	417 \pm 188	693 \pm 306
Total biomass	884 \pm 63	1147 \pm 377	1671 \pm 524	2122 \pm 719	3143 \pm 1189
Total biomass increment (g C m ⁻² yr ⁻¹)	–	263 \pm 225	524 \pm 275	450 \pm 324	1021 \pm 556

Table 3.4. Topsoil (0–10 cm) characteristics at the Sardinilla pasture (2002 to 2010) and afforestation sites (2001 to 2009). Values indicate mean \pm standard deviation. Bulk density (d_B), carbon concentration (C), carbon pool (C), nitrogen concentration (N), nitrogen pool (N), C:N ratio (C:N) and carbon isotope ratio ($\delta^{13}\text{C}$). Data from 2001/2002 are derived from Abraham (2004). Soil sampling at the pasture was done in January 2010 and at the afforestation in March 2009. No bulk density data were available for 2009/2010; hence, values from 2001/2002 were used to calculate soil pools.

	d_B (g cm ⁻³)	C (%)	C (kg m ⁻²)	N (%)	N (kg m ⁻²)	C:N	$\delta^{13}\text{C}$ (‰)
Pasture							
2002	0.86 \pm 0.07	3.21 \pm 0.45	2.73 \pm 0.35	0.31 \pm 0.05	0.27 \pm 0.03	10.44 \pm 0.70	-17.80 \pm 1.86
2010	–	1.72 \pm 0.33	1.48 \pm 0.14	0.17 \pm 0.04	0.15 \pm 0.02	10.11 \pm 0.16	-18.93 \pm 0.56
Afforestation							
2001	0.59 \pm 0.05	5.85 \pm 0.52	3.45 \pm 0.24	0.49 \pm 0.03	0.29 \pm 0.02	11.93 \pm 0.68	-17.01 \pm 0.78
2009	–	4.24 \pm 0.92	2.52 \pm 0.57	0.36 \pm 0.08	0.21 \pm 0.05	11.86 \pm 1.32	-20.86 \pm 1.23

Soil

A strong reduction in topsoil (0–10 cm) carbon pools was found over a period of 8 years since 2001/2002 at both sites. This reduction was stronger at the pasture site (reduction of 1250 g C m^{-2} or -46%) as compared to the afforestation (930 g C m^{-2} or -28%, Tab. 3.4). Correspondingly, nitrogen pools decreased more strongly at the pasture compared to the afforestation by 120 gN m^{-2} (-44%) and 80 gN m^{-2} (-30%), respectively. At the afforestation, the stable carbon isotope ratio ($\delta^{13}\text{C}$) became significantly more depleted from 2001 ($-17.0 \pm 0.8\text{‰}$) to 2009 ($-20.9 \pm 1.2\text{‰}$). This change in $\delta^{13}\text{C}$ indicated that in 2001 about 83% of the organic matter in the topsoil was derived from C₄

pasture vegetation, whereas this contribution had decreased to 57% by 2009. As expected, no significant change in $\delta^{13}\text{C}$ was observed at the pasture site. The total soil carbon pool from 0–100 cm depth was clearly lower at the pasture ($5.36 \pm 0.18 \text{ kg m}^{-2}$) than at the afforestation site ($7.64 \pm 1.63 \text{ kg m}^{-2}$). At both sites, roughly one third of the carbon pool was concentrated in the top 10 cm of soil (27.6% and 33.0% for pasture and afforestation, respectively).

3.4 Discussion

The pasture under investigation was heavily grazed at an intensity which cannot be considered sustainable under current conditions. In addition, water limitations led to strong and persistent carbon losses during the dry season that continued into the first weeks of the wet season. Due to overgrazing, carbon uptake of the pasture during the wet season was not sufficient to compensate carbon losses during the dry season. In contrast, the afforestation site persistently sequestered large amounts of carbon as measured with the eddy-covariance method and supported by biometric observations.

Environmental Controls

The main environmental controls of ecosystem CO_2 fluxes in Sardinilla were PPFD and SWC. Considerable differences in the ecosystem response of pasture and afforestation to seasonal limitations in soil moisture were found, with the pasture ecosystem being more susceptible to seasonal drought than the afforestation. During the dry season, GPP at the pasture was strongly reduced whereas the afforestation maintained a GPP that exceeded TER well into the dry season (for about 75 days in 2008 and 81 days in 2009). This seems strongly related to the rooting depth of grasses versus trees as we observed a mean rooting depth of only about 10–20 cm at the pasture. In comparison, mean rooting depth at the afforestation was 1.4 m in 2009 (Jefferson Hall, personal communication, unpublished data).

Light reduction due to cloudiness during periods of intense precipitation (e.g. in November) strongly reduced GPP at both ecosystems. Similar reductions in GPP were observed at tropical forest sites in Amazonia (Malhi et al., 1998) and Costa Rica (Loescher et al., 2003) during the wet season. However, the ecosystem response to varying light and soil moisture conditions was very different between pasture and afforestation (Fig. 3.4). This seems predominantly related to the different photosynthetic pathways of C_4 grasses and C_3 trees. C_3 species are generally most active during the early growing season while C_4 species increase photosynthetic activity at warmer and drier conditions (Lambers et al., 2008). An additional explanation for the limited light response of the afforestation during the wet-dry transition period could be the age of the foliage, as the chlorophyll concentration per unit leaf area decreases with age (Lambers et al., 2008). It is likely that this is also the case with grasses but the grazed pasture vegetation has higher turnover rates and thus persistent re-growth of plant tissues.

Considerable differences and seasonal shifts in LCP between pasture and afforestation were found that do not agree with the typical patterns of C_3 versus C_4 vegetation: The C_4 dominated pasture in Sardinilla had consistently higher LCPs compared to the C_3 dominated afforestation ecosystem (except during the dry-wet transition when the pasture vegetation was senescent). This is surprising as C_4 vegetation generally exhibits lower LCP compared to C_3 vegetation due to absent photorespiration and higher light use efficiency (Lambers et al., 2008). This indicates that another factor is relevant, most likely independent from irradiance and soil moisture at the pasture ecosystem. Nutrient deficiency might be one possible explanation as soil nitrogen concentrations are generally low in the Sardinilla pasture (Tab. 3.4). Enhanced decomposition induced by grazing might be another potential reason. At the afforestation, seasonal patterns of LCPs observed in Sardinilla compare well with results for tropical forest by Andreae et al. (2002) and Carswell et al. (2002), having higher LCPs during the dry ($275\text{--}322 \mu\text{mol m}^{-2} \text{s}^{-1}$) compared to the wet season ($195\text{--}254 \mu\text{mol m}^{-2} \text{s}^{-1}$). However, LCPs in Sardinilla are somewhat lower (about 20%).

GPP and TER patterns

Total annual GPP at the Sardinilla pasture was higher compared to the afforestation (Tab. 3.5) but lower than a tropical pasture in Brazil reported by Gilmanov et al. (2010) and Grace et al. (1998). Annual GPP at the afforestation was consistent with results reported by Vourlitis et al. (2001) for a transitional tropical forest in Brazil but lower than the range reported from tropical forests (Tab. 3.5). This is likely due to the young age of the afforestation, which is still in its establishment phase.

Overall higher TER in the pasture compared to afforestation seems to be caused by enhanced biomass turnover including decomposition rates due to grazing. The observed strong increases of TER during the dry-wet transition period are likely a combination of physical and physiological effects: Firstly, highly concentrated CO_2 is pushed out of the soil pore space (macro-pores and desiccation cracks; Birch effect). Secondly, large amounts of organic material that accumulated during the dry season start to decompose rapidly with the suddenly increasing soil moisture. The stronger increase in TER at the pasture compared to the afforestation seems related to additional accumulated organic material (manure) by grazing livestock.

Carbon budget synthesis

The pasture ecosystem was a large carbon source from 2007 to 2009. As far as we are aware, the average annual loss of $261 \text{ g C m}^{-2} \text{ yr}^{-1}$ is the first quantitative estimate for tropical pasture that covers more than one year (Tab. 3.5). Only three other studies reported total NEE, but on a daily base. All found carbon uptake for pastures: Grace et al. (1998) observed $-1.9 \text{ g C m}^{-2} \text{ d}^{-1}$ in Amazonia during 11 days in May 1993, and von Randow et al. (2004) found similar uptake of $-1.8 \text{ g C m}^{-2} \text{ d}^{-1}$ at the same pasture dur-

ing 1999–2002. Priante-Filho et al. (2004) found an even larger carbon uptake of $-4.6 \text{ g C m}^{-2} \text{ d}^{-1}$ in a pasture in conversion to afforestation.

The large carbon losses at the Sardinilla pasture could be either associated with soil carbon, dissolved organic carbon (DOC) or hidden abiotic factors like weathering of calcareous bedrock as suggested by Serrano-Ortiz et al. (2010). The substantial reduction in topsoil carbon seems to be the main source for the strong carbon losses. Potential causes for the discrepancy to the EC measured carbon losses are measurement uncertainties or carbon export, such as by livestock or DOC. However, Waterloo et al. (2006) found that export of DOC played only a minor role in the carbon budget of a tropical forest with similar annual rainfall in Amazonia.

The seven-year-old Sardinilla afforestation was a larger net carbon sink in 2008 than reported for most tropical forests (Tab. 3.5). On the other hand, Carswell et al. (2002) and Malhi et al. (1999; 1998) found larger carbon sequestration while Saleska et al. (2003) and Hutyra et al. (2007) found carbon losses in tropical forests in Amazonia (Tab. 3.5). Consequently, the young afforestation is sequestering substantial amounts of carbon following its establishment phase that exceeds other, mature tropical forests. It can be expected that the carbon sink strength of the afforestation will continue and might even increase until the trees reach maturity (Canadell et al., 2007), provided that there are no disturbances like fires, storms or harvesting. A long-term (55–61 years) inventory-based study of Silver et al. (2004) reported that carbon sequestration in a tropical afforestation did not slow down with aging trees, indicating significant carbon uptake ($140 \text{ g C m}^{-2} \text{ yr}^{-1}$) even after the establishment phase.

Only few studies assessed comparative EC and biometric carbon budgets in the tropics (Tab. 3.5). In general, EC derived carbon budgets were lower than biometric field estimates as observed by, for example, Malhi et al. (1999; 1998) in Manaus (Amazonia), Saleska et al. (2003) and Hutyra et al. (2007) in Santarem (Amazonia), and Tan et al. (2010) in China (Tab. 3.5). The only tropical study that reported a larger carbon uptake with the EC method compared to biometric data was Bonal et al. (2006; 2008) in French Guinea. Including the topsoil carbon losses with the biometric carbon uptake yields a similar result in Sardinilla, with a larger carbon uptake measured by EC compared to inventory data in 2008 ($-335 \text{ g C m}^{-2} \text{ yr}^{-1}$). Only the study by San José et al. (2008) reported close agreement of eddy covariance and biometric-derived carbon budgets for a tall-grass *Andropogon* site and a savanna–woodland continuum in the Orinoco lowlands. However, and as emphasized by Saleska et al. (2003), large uncertainties are associated with both methods.

The change in topsoil $\delta^{13}\text{C}$ from 2001 to 2009 at the afforestation clearly indicates the increased inputs of organic matter (litter) by the dominating C_3 -vegetation in combination with the rapid carbon turnover in this tropical ecosystem. Besides the considerable reductions in topsoil carbon pools at both sites, it should be noted that topsoil generally constitutes only a small amount of the total soil carbon pool in the tropics. In Sardinilla, the topsoil carbon pool represents about 30% of the total carbon pool down to one meter

depth, which is more or less consistent with about 25% found for tropical forest at Barro Colorado Island (B. Turner, unpublished data).

Measurement uncertainties in the EC carbon budgets are largely related to ecosystem respiration and its consideration in data quality filtering and gap filling. We observed only a weak temperature sensitivity of nighttime ecosystem respiration, which is consistent with other tropical studies (Hutyra et al., 2007) and the relatively low temperature sensitivity of tropical forest soils as reported by Davidson and Janssens (2006). Our results indicate that using weak temperature sensitivities to gap-fill nighttime ecosystem respiration could result in large biases of carbon budgets in tropical ecosystems. Hence, alternative running mean approaches should be considered more comprehensively. Further bias in carbon budgets can originate from advection (see e.g. Kruijt et al. 2004). However, nighttime advection is probably only small at our Sardinilla. The u^* -filter and stationarity criterion used in data quality filtering are assumed to account for advection effects already (Aubinet, 2008; Etzold et al., 2010). Further evidence for this is given by the energy balance closure, which was found to be comparable to other flux tower sites globally, with 84% and 81% for pasture and afforestation, respectively (see Chapter 2), and the close agreement with independently measured inventories.

Overall, the reported uncertainties in annual EC budgets range from less than $\pm 50 \text{ g C m}^{-2} \text{ yr}^{-1}$ for nearly ideal sites (relatively flat terrain) to $\pm 130\text{--}180 \text{ g C m}^{-2} \text{ yr}^{-1}$ for non-ideal sites with hilly topography (Baldocchi, 2003). Considering that both sites in Sardinilla are nearly ideal from a topographic perspective, we conservatively estimate that our annual budget uncertainties should be below $\pm 100 \text{ g C m}^{-2} \text{ yr}^{-1}$.

Management impact on carbon cycling

Both ecosystems exhibited strong responses to management, with understory thinning at the afforestation and grazing at the pasture site. Understory thinning considerably reduced GPP and gave evidence that understory vegetation accounts for a significant amount of GPP at the young afforestation 6–7 years after establishment. At the pasture site, periodical overgrazing during 2008 and persistently high stocking densities in 2009 were the major cause for carbon losses. Vegetation recovery was swift after periods of overgrazing during the wet season but was inhibited by soil moisture during the dry season. Hence, overgrazing during the dry season reduced aboveground biomass without the potential of recovery before the beginning of the wet season.

Similar rates of forage consumption by livestock like at the Sardinilla pasture were found by Dias-Filho et al. (2000) in the Amazon basin ($0.74 \text{ g C m}^{-2} \text{ d}^{-1}$). Wilsey et al. (2002) reported lower forage consumption at adjacent pastures in Sardinilla ($0.61 \text{ g C m}^{-2} \text{ d}^{-1}$) and found that grazing significantly reduced ecosystem respiration, but not carbon uptake. However, they also emphasized that grazing does not necessarily increase carbon losses from tropical pastures as the reduction in aboveground biomass lowers ecosystem respiration whereas grazing enhances aboveground productivity. Kirkman et al. (2002) reported a decrease in carrying capacity of about 50% from a cat-

the ranch in Brazil from 1992 to 2000, indicating a strong impact of grazing on carbon and nutrient cycling of tropical pastures. If the current losses in soil carbon and nitrogen continue, the pasture in Sardinilla seems at high risk of irreversible degradation. Consequently, a reduction of stocking densities to a maximum of 1 LU ha⁻¹ appears crucial for mitigation efforts to decrease carbon losses in this highly seasonal climate.

3.5 Conclusions

We conclude that tropical afforestation can sequester large amounts of carbon, reduce the intra-annual variability of gross primary production, and enhance the ecosystem resilience to seasonal drought. High stocking densities in combination with seasonal drought can result in reduced productivity and carbon losses from tropical pasture. Projected changes in precipitation (reduction and increased variability) for Central America might affect the carbon balance of these tropical ecosystems in different ways, i.e., the carbon source strength of pastures might increase while the sink strength of afforestations might be reduced. Furthermore, the conversion from pasture to afforestation may become more relevant for Panama and other

Acknowledgements

Funding for this project was provided by the North-South Centre (former Swiss Centre for International Agriculture) of ETH Zurich. Catherine Potvin acknowledges the support from a Discovery grant of the Natural Sciences and Engineering Council of Canada. We are grateful to the Smithsonian Tropical Research Institute (STRI) for support with the Sardinilla site and the Meteorology and Hydrology Branch of the Panama Canal Authority (ACP), Republic of Panama, for providing meteorological data. We thank Timothy Seipel for identifying grass species of the pasture, Jefferson Hall and his project funded by SENACYT for providing information on rooting depth at the afforestation site, Dayana Agudo and Tania Romero (STRI) for laboratory support, Nicolas Gruber for inspiring discussions, Rodrigo Vargas for valuable comments on the manuscript, and José Monteza for tower maintenance and assistance in the field.

Table 3.5. Summary of ecosystem CO₂ flux studies in the tropics. All studies except the one from Xishuangbanna (China) were located in the neotropics. The vegetation types are tropical rainforest (TRF), Young forest (YF, <10 years), Transitional tropical forest (TF), Tropical forest with monsoonal climate (TMF), Pasture (P), Pasture with starting afforestation (P-A) and Savanna (S). Further listed are leaf area index (LAI), mean of nighttime total ecosystem respiration (TER_{night}), daily mean net ecosystem exchange (NEE_{day}), annual total gross primary production (GPP_{annual}), annual total net ecosystem exchange (NEE_{annual}) and total above and belowground biomass increment; except Guyaflux: only aboveground biomass increment. Missing information on location and climate was supplemented from the FLUXNET database (www.fluxnet.ornl.gov).

Site (Country)	Location (Lat., Long.)	Rainfall (mm yr ⁻¹)	Vegetation type	Time	LAI	TER _{night} (μmol m ⁻² s ⁻¹)	NEE _{day} (g C m ⁻² d ⁻¹)	GPP _{annual} (g C m ⁻² yr ⁻¹)	NEE _{annual} (g C m ⁻² yr ⁻¹)	Biomass (g C m ⁻² yr ⁻¹)	References
Xishuangbanna (China)	21°55' N, 101°16' E	1487	TMF	2003–2006	–	–	–	2594	–119	–359	Tan et al. (2010)
La Selva (Costa Rica)	10°26' N, 84°99' W	4000	TRF	1998–2000	2.7–4.9	7.05	–	3097	–242 ^a	–	Loescher et al. (2003)
Sardinilla Afforestation (Panama)	9°18' N, 79°38' W	2267	P	2007–2009	1.2–2.9	6.5	0.5	2345 ^b	261 ^b	–	This study
Sardinilla Pasture (Panama)	9°19' N, 79°38' W	2267	YF	2007–2009	3.0–5.4	4.7	–1.0	2082 ^b	–442 ^b	–450 ^b	This study
Guyaflux (French Guiana)	5°17' N, 52°54' W	3041	TRF	2004–2005	6.9	10.0–15.0	–0.4	3911 ^c	–150	–102 ^d	Bonal et al. (2006; 2008)
Caxiuanã (Brazil)	1°43' S, 51°28' W	2500	TRF	1999 (108 d)	5–6	7.6	–	3630	–560	–	Carswell et al. (2002)
Cuiteras, C14 (Brazil)	2°35' S, 60°07' W	2200	TRF	1995–1996	5–6	6.5	–	3040	–590	–230	Malthi et al. (1999; 1998)
Tapajos km67, Santarém (Brazil)	2°51' S, 54°58' W	1920	TRF	2002–2005	6–7	9.2	0.8	3157	94	200 ^e	Huyra et al. (2007)
Ducke (Brazil)	2°57' S, 59°57' W	2431	TRF	1987 (12 d)	5–6	5.95	–2.2	–	–220 ^f	–	Fan et al. (1990)
Tapajos km83, Santarém (Brazil)	3°3' S, 54°56' W	1920	TRF ^g	2000–2001	6–7	6.0–7.0	–	3000	130	200	Saleska et al. (2003)
Cotruaguacú (Brazil)	9°52' S, 58°14' W	2000	P-A	2002 (10 mo)	1.0–2.7	5.9	–4.6	–	–	–	Priante-Filho et al. (2004)
Jaru, Rondonia (Brazil)	10°05' S, 61°57' W	2170	TRF	1992–1993 (55 d)	4	6.6	–0.8	2440	–102	–	Grace et al. (1995; 1998; 1996)
FNS-A, Rondonia (Brazil)	10°46' S, 62°21' W	2170	P	1993 (11 d)	1.1–3.9	6.0	–1.9	4000	–	–	Grace et al. (1998)
				1999–2002	–	3.8	–1.8	–	–	–	von Randow et al. (2004)
Sirop (Brazil)	11°25' S, 55°20' W	2037	TF	1999–2002	2.5–5.0	5.0	1.2	2062	–5	–	Vourilis et al. (2005; 2001; 2004)
Emendadas (Brazil)	15°33' S, 47°36' W	1556	S	2002 (10 mo)	2.5–5.0	3.9	3.1	–	–	–	Priante-Filho et al. (2004)
				1993–1994	0.4–1.0	4.8	–	–	–250	–	Miranda et al. (1996; 1997)
				1999–2000	–	7.6	–1.3	–	–	–	von Randow et al. (2004)

^a mean of 1998–2000

^b values reported from 2008

^c reported by Gilmanov *et al.* (2010)

^d aboveground biomass of 70 g C m⁻² yr⁻¹ reported only; adding belowground estimate (45% of aboveground, (Malhi and Grace, 2000) yields 102 g C m⁻² yr⁻¹

^e reported by Saleska *et al.* (2003)

^f derived from Tab. 1 in Mahli *et al.* (1998); modelled annual budget

^g selectively logged in Sept. 2001 (reported measurements were done before)

^h estimated from Fig. 7F in Gilmanov *et al.* (2010)

Chapter 4

4 Evapotranspiration of tropical pasture and afforestation

Chapter 4 was submitted to the peer-reviewed journal *Ecosystems* as:

Afforestation of tropical pasture only marginally affects ecosystem-scale evapotranspiration

Sebastian Wolf¹, Werner Eugster¹, Sonja Majorek¹ and Nina Buchmann¹

¹ *Institute of Agricultural Sciences, ETH Zurich, Universitaetsstrasse 2, 8092 Zurich, Switzerland*

Abstract

Evapotranspiration (ET) from tropical ecosystems is a major constituent of the global land-atmosphere water flux and strongly influences the global hydrological cycle. Previous studies have been predominantly conducted in tropical forests with only few observations covering tropical land-use types such as pastures, croplands and savannas. Thus, the objectives of our study were: (1) to estimate daily, monthly and annual budgets of ET for tropical pasture compared to afforestation, (2) to assess seasonal and diurnal patterns of ET, (3) to investigate environmental controls of ET, and (4) to evaluate soil infiltrability in these ecosystems. We performed comparative eddy covariance measurements of ET in a tropical pasture and an adjacent afforestation native tree species in Sardinilla (Panama) from 2007 to 2009. Daily ET at the pasture ranged from 2.1 mm d^{-1} during the dry-wet transition period to 3.8 mm d^{-1} during the wet-dry transition period, while daily ET ranged from 2.7 to 4.1 mm d^{-1} at the afforestation. Only minor differences were found in the diurnal patterns and the total annual ET between the two ecosystems. In 2008, total annual ET was 1034 mm yr^{-1} at the pasture and 1114 mm yr^{-1} at the afforestation. Radiation was the main environmental control of ET. However, we observed considerable seasonal variations in the strength of this control. Our results suggest that the land conversion from tropical pasture to afforestation only has a minor effect on annual ET rates (less than 100 mm yr^{-1}), mainly due to increases in soil infiltrability.

4.1 Introduction

Evapotranspiration (ET) from tropical ecosystems is a major constituent of the global land-atmosphere water flux and strongly influences the global hydrological cycle (Werth and Avissar, 2004). Given the importance of tropical ecosystems it is indispensable to understand how these respond to anthropogenic interference and changing environmental conditions. Up to date, seasonal and spatial variations of terrestrial water fluxes in the tropics are not yet fully understood (Hasler and Avissar, 2007). Moreover, the area of tropical forest is declining with ongoing deforestation and managed ecosystems like afforestations, croplands and particularly pastures become more prevalent (Alves et al., 2009; Fearnside, 2005), altering the patterns and variability of ET. In addition to this anthropogenic induced land-use change, it is critical to understand the response of tropical ET to a changing climate (Fisher et al., 2009). The feedbacks of the hydrological cycle to a changing climate are not well understood (Bates, 2008; Jung et al., 2010), but there is evidence that climate change causes an intensification of the water cycle (Huntington, 2006). Besides rising temperatures, climate model projections for Amazonia and Latin America indicate a reduction in the total amount of precipitation and an increase in precipitation variability with more frequent extreme dry seasons by the end of this century (Bates, 2008; IPCC, 2007b).

Eddy covariance (EC) measurements of turbulent trace gas fluxes (such as CO₂ and H₂O) between vegetation and atmosphere are widely established within the global measurement network FLUXNET (www.fluxnet.ornl.gov). Despite the importance of tropical ecosystems for the global water cycle, EC measurements in the tropics are still scarce and globally under-represented within FLUXNET (only 10%). Tropical ET has been predominantly investigated within the Large Scale Biosphere-Atmosphere Experiment (LBA) in Amazonia, covering primarily tropical forests and savanna ecosystems (da Rocha et al., 2009a; da Rocha et al., 2009b; Hasler and Avissar, 2007). Studies covering other parts of the tropics are still very limited and have been focused largely on carbon fluxes (e.g., Loescher et al., 2003; Merbold et al., 2009; Tan et al., 2010). Only very few tropical studies have been conducted in non forested land-use types such as croplands (Sakai et al., 2004) and pastures (von Randow et al., 2004). However, as recently emphasized by global synthesis activities, particularly ecosystems dominated by C₄ vegetation (i.e. tropical pastures) play a major role for terrestrial gross primary production (Beer et al., 2010) and therefore also for ET. Consequently, an expansion of observations for tropical C₄ ecosystems is needed to understand their role in the global carbon and water cycle. Furthermore, afforestations are becoming more prevalent in the tropics as these are considered an effective measure to sequester carbon and mitigate anthropogenic induced increases of CO₂ concentrations (FAO, 2009). The knowledge about changes in water cycling due to land conversion from tropical pasture to afforestation is still very limited, especially as most studies so far focused on carbon sequestration of afforestations (Farley et al., 2005). The ‘sponge theory’ considers forests to enhance soil infiltration and thus, ground water recharge with gradual releases

during dry periods (Malmer et al., 2010). On the other hand, the increased water use of trees in afforestations (Scott et al., 2005) compared to the former land use, e.g. grasses, could also compensate these benefits and result in relatively minor changes of the water balance due to afforestation. However, comparative measurements to test these considerations are scarce in the tropics.

Our study measured land-atmosphere water fluxes (evapotranspiration) of tropical pasture and native tree species afforestation in Sardinilla (Panama) from 2007 to 2009 using the eddy covariance technique. The objectives of our study were: (1) to estimate daily, monthly and annual budgets of ET for tropical pasture compared to afforestation, (2) to assess seasonal and diurnal patterns of ecosystem ET, (3) to investigate environmental controls of ET in these ecosystems, and (4) to evaluate potential changes in soil infiltrability due to the land conversion from pasture to afforestation.

4.2 Material and Methods

4.2.1 Site description

Our study was conducted at the Sardinilla research site (Central Panama), located at 9°19' N, 79°38'W (70 m a.s.l.) and about 40 km north of Panama City. The site has a semi-humid tropical climate with a pronounced dry season lasting from about January to April (Fig. 4.1) and 2289 mm annual precipitation. The length of the dry season varies among years (134 ± 19 days for 1954–2009; ACP, 2010) and is influenced by the El Niño Southern Oscillation (Lachniet, 2009). The Sardinilla site was logged in 1952/1953 and used two years for agriculture, before it was converted to pasture (Wilsey et al., 2002). In 2001, an afforestation using native tree species was established at parts of the site (7.5 ha), while grazing continued on the remaining pasture (6.5 ha). Pasture vegetation is dominated by C_4 grasses, consisting of (listed in the order of abundance): *Paspalum dilatatum* (C_4), *Rhynchospora nervosa* (sedge, C_3), *Panicum dichotomiflorum* (C_4) and *Sporobolus indicus* (C_4). The afforestation consists of six native species: *Luehea seemanii*, *Cordia alliodora*, *Anacardium excelsum*, *Hura crepitans*, *Cedrela odorata*, *Tabebuia rosea*, with moderately dense understory vegetation (shrubs, grasses and sedges). In 2008, mean canopy height was 10 m in the afforestation and 0.09 m in the pasture. The afforestation site has an undulating topography (elevation range <10 m) and the pasture is homogeneously flat with an overall slope of less than 2 degrees. For further details on the Sardinilla site see Chapter 2.

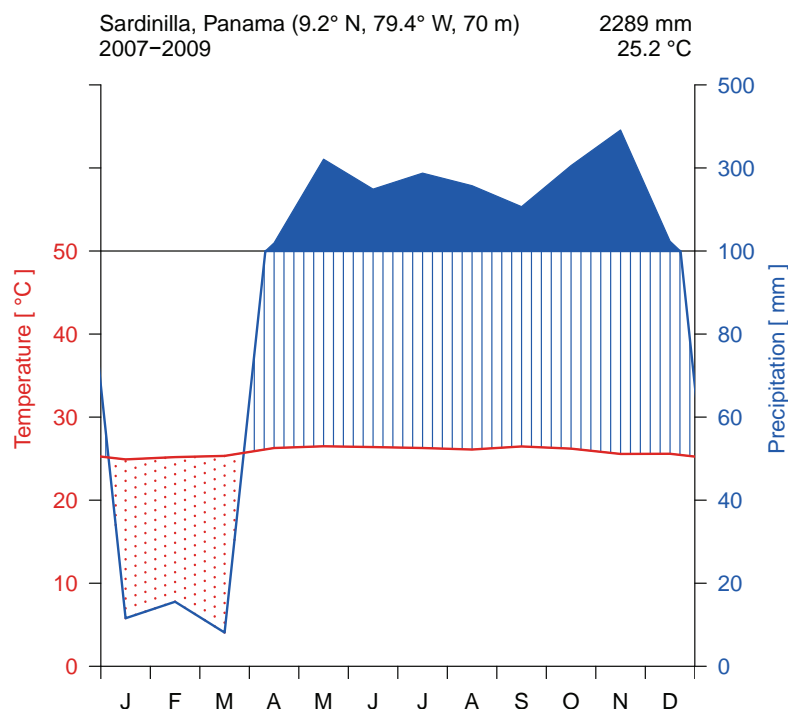


Figure 4.1. Climate diagram of Sardinilla, based on measurements from April 2007 to December 2010. The red line indicates the mean monthly temperature, the red dotted area denotes periods with arid and the vertical blue lines periods with humid climate. In addition, the blue shading indicates periods with monthly precipitation exceeding 100 mm. Note the change in scale on the precipitation axis that complies with Walter and Lieth (1960).

4.2.2 Instrumentation

Two EC flux towers (Tab. 4.1) were used in Sardinilla at a grazed pasture (March 2007 to January 2010) and an adjacent afforestation (February 2007 to June 2009). Our flux measurement systems consisted of open path infrared gas analyzers (IRGA, Li-7500, LI-COR, Lincoln, USA) and three-dimensional sonic anemometers (CSAT3, Campbell Scientific, Logan, USA). Flux measurements were conducted at 20 Hz and data acquisition was performed by an industry grade embedded box computer (Advantech ARK-3381, Taipei, Taiwan), running a Debian based Linux operating system (Knoppix 4.0.2, Knopper.Net, Schmalenberg, Germany) and the in-house software *sonicreadHS*. Additional meteorological measurements included air temperature and relative humidity (MP100A, Rotronic, Bassersdorf, Switzerland), incoming shortwave radiation (R_G , CM3, Kipp & Zonen, Delft, The Netherlands), net radiation (R_N ; afforestation: CN1, Middleton Solar, Brunswick, Australia; pasture: Q*7.1, REBS - Radiation and Energy Balance Systems, Seattle, USA), photosynthetic photon flux density (PPFD, PAR Lite, Kipp & Zonen, Delft, The Netherlands), precipitation (10116 rain gauge, TOSS, Potsdam, Germany), soil heat flux at 5 cm depth (HFP01, Hukseflux, Delft, The Netherlands), soil temperature at 5 cm depth (TB107, Markasub, Olten, Switzerland) and volumetric soil water content (SWC) at 5 and 30 cm depth (EC-5, Decagon, Pullman, USA). All meteorological measurements were recorded at 10 s and stored as half-

hourly averages (sums for precipitation) using data loggers: CR23X at the afforestation and CR10X at the pasture site (both Campbell Scientific, Logan, USA). Precipitation and incoming shortwave radiation were measured at one tower location only (600 m distance between both towers). Daily cleaning of sensors and monthly IRGA calibration checks were carried out to assure data quality. Further details on the measurement setup at the Sardinilla site are reported in Chapter 2.

Table 4.1. Site characteristics for the pasture and afforestation flux towers at Sardinilla. Values of leaf area index (LAI) denote mean \pm standard error.

Site	Pasture	Afforestation
Location	9°18'50" N, 79°37'53" W	9°19'5" N, 79°38'5" W
Elevation a.s.l. (m)	68	78
Tower height (m)	3	15
Canopy height (m)	0.09	8–12 (2007–2009)
Vegetation	dominated by C ₄ grasses	six native tree species
LAI of canopy		
Dry season	1.2 \pm 0.14	3.0 \pm 0.28
Wet season	2.9 \pm 0.15	5.4 \pm 0.24
Management	grazing, herbicide treatment (annually in May)	selective understory thinning (Dec. 2007 & 2008)

4.2.3 Data processing

Raw flux data were processed to half-hourly averages using the in-house eddy covariance software *eth-flux* (Mauder et al. 2008, source code for Unix/Linux systems can be obtained from the authors). Subsequently, half-hourly fluxes were corrected for damping losses (Eugster and Senn, 1995) and density fluctuations (Webb et al., 1980). We applied a rigorous data screening and excluded data using the following rejection criteria: (1) Fluxes during optical sensor contamination resulting in increased window dirtiness of the IRGA, using a 10% threshold above the mean background value of the respective IRGA; (2) Fluxes deviating by more than 100% between the 30 min and 5 min averages using stationarity following Foken and Wichura (1996); (3) Statistical outliers exceeding the ± 3 SD range of a 14 days running mean window; (4) Negative fluxes of H₂O were excluded during daytime and set to zero during nighttime; (5) Fluxes during periods with low turbulent conditions based on friction velocity (u^*). We determined seasonal and site-dependent u^* -thresholds according to the method by Gu et al. (2005) and Moureaux et al. (2006). At the pasture site, this algorithm yielded $u^* < 0.04 \text{ m s}^{-1}$ (dry season), $u^* < 0.03 \text{ m s}^{-1}$ (dry-wet transition) and none during the wet season and wet-dry transition. At the afforestation, u^* -thresholds were $u^* < 0.02 \text{ m s}^{-1}$ (dry season), $u^* < 0.01 \text{ m s}^{-1}$ (wet season), $u^* < 0.05 \text{ m s}^{-1}$ (dry-wet transition) and none during the wet-dry transition.

We quality filtered raw meteorological data to eliminate unrealistic measurements and outliers. During periods of instrument failure, we derived air temperature from virtual

temperature measurements of the sonic anemometer (regression analysis). Missing precipitation data were supplemented from the nearby (about 5 km to the northeast) Salamanca station of the Panama Canal Authority (ACP; STRI, 2010). SWC data from the afforestation site was used for periods when SWC data in the pasture were not available.

4.2.4 Gap filling

Continuous data of water vapour fluxes were available since June 2006 for both sites. Budget assessments required a gap filling of the quality filtered data. Gap filling of daytime net ecosystem H₂O exchange was based on a significant functional relationship to PPFD (both sites $p < 0.001$) using linear least-squares regression with parameters fitted separately for each day. Few remaining gaps in daytime data were filled using a gap model with parameters estimated from the days prior and subsequent to the gaps. All nighttime H₂O fluxes (measured and missing) were set to zero, assuming no significant nocturnal evapotranspiration due to closed plant stomata and absent radiation (zero approach, see e.g. Novick et al., 2009).

4.2.5 Supplementary measurements

Supplementary measurements consisted of leaf area index (LAI) and saturated soil infiltrability: Leaf area index (LAI) was measured in campaigns with an LAI-2000 (LI-COR, Lincoln, USA) weekly to bi-weekly from March to July 2009 (10 to 30 replicates). At the afforestation site, LAI was measured separately for the tree canopy (measured at 1 m above ground) and the total canopy including the understory (measured at ground level). LAI measurements at the afforestation were corrected for the shading effect of tree stems and branches by subtracting the minimum dry-season value of tree canopy LAI (DOY 107, 2009; LAI = 0.42). No correction for shading was applied to the LAI measurements at the pasture. We excluded the phenological transition month of May 2009 for seasonal averaging.

Furthermore, we conducted in situ soil infiltrability (i.e. saturated soil hydraulic conductivity) measurements once in June 2009 using a hood infiltrometer (UGT, Münchberg, Germany) according to Schwarz and Punzel (2007), with 10 replicates at each site. The infiltrometer had an acrylic hood with 17.6 cm in diameter and was connected to a conventional Mariotte water supply (12 cm diameter and 71.6 cm height). A u-tube manometer was used to adjust water pressure and prevent overflow. Metal retaining rings were installed at the soil surface and the interface to the hood was sealed using quartz sand.

4.2.6 Statistical analyses and general conventions

We used the statistics software package R, version 2.10.0 (R Development Core Team 2009, www.r-project.org) for data analyses. Daytime data were defined as PPFD $> 5 \mu\text{mol m}^{-2} \text{s}^{-1}$. The term ‘midday’ was defined as 11:00–13:00 (UTC). The

micrometeorological sign convention is used throughout the manuscript, where fluxes from the biosphere to the atmosphere are positive and vice versa. Separation of seasons (Tab. 4.2) was done based on daily precipitation sums using the methodology described in Chapter 2: wet season was defined as the time span with no periods of more than four consecutive days without rain, the dry season vice versa. Transition periods mark the time span between both main seasons. In general, only seasons with full data coverage were used for seasonal averaging. When not stated otherwise, reported values denote mean \pm standard deviation. When writing ‘seasonal drought’, we refer to the plant physiological effects of soil moisture deficiency during the dry season.

4.3 Results

4.3.1 Ecosystem water budgets

We found only small differences in annual ET between pasture and afforestation (Tab. 4.2). In 2008, the pasture ecosystem returned 1034 mm or 50% of the annual rainfall (2074 mm) via ET to the atmosphere, while this percentage was somewhat lower in 2009 (40%). At the afforestation, 1114 mm or 54% of the annual rainfall were returned to the atmosphere via ET in 2008. Moreover, we found large seasonal differences in the amount of water transferred to the atmosphere via ET: During the wet season, only 27% (pasture) and 28% (afforestation) of the seasonal rainfall was lost from the ecosystems via ET and thus, the deficiency (rainfall minus ET) was attributed to surface runoff and infiltration. Both ecosystems were close to water balance (rainfall input equals ET loss) during the dry-wet transition period, while large water deficits between rainfall and ET were observed during the dry season and wet-dry transition period (Tab. 4.2).

Table 4.2. Seasonal overview of meteorological variables at Sardinilla, Panama from 2007 to 2009: Season length (d), seasonal sum of precipitation (P), mean volumetric soil water content at 5 cm depth (SWC; afforestation), seasonal mean of daytime incoming shortwave radiation (R_G), and seasonal sum of ecosystem evapotranspiration (ET) at the pasture (ET.Pa) and afforestation (ET.Aff) site. Continuous data of ET was available since June 2007. Measurements at the afforestation were discontinued after June 2009.

		Dates	Length (d)	P (mm)	SWC (%)	R_G ($W m^{-2}$)	ET.Pa (mm)	ET.Aff (mm)
2007	Dry-wet transition	30.03.–22.04.	24	82	24	370	–	–
	Wet season	23.04.–28.12.	250	2471	45	286	484*	605*
	Wet-dry transition	29.12.–17.01.	20	17	33	436	75	78
	Annual sum	–	–	2553	–	–	495*	617*
2008	Dry season	18.01.–03.04.	77	17	24	444	224	274
	Dry-wet transition	04.04.–28.04.	25	51	22	425	61	72
	Wet season	29.04.–05.12.	221	1964	46	291	572	590
	Wet-dry transition	06.12.–05.01.	31	34	43	398	132	132
	Annual sum	–	–	2074	–	–	1034	1114
2009	Dry season	06.01.–19.04.	104	42	27	439	238	342
	Dry-wet transition	20.04.–29.04.	10	37	24	361	14	22
	Wet season	30.04.–30.11.	215	2122	35*	316	529	187*
	Wet-dry transition	01.12.–03.01.	34	32	–	402	112	–
	Annual sum	–	–	2233	–	–	900	570*

* Incomplete, only partial temporal coverage

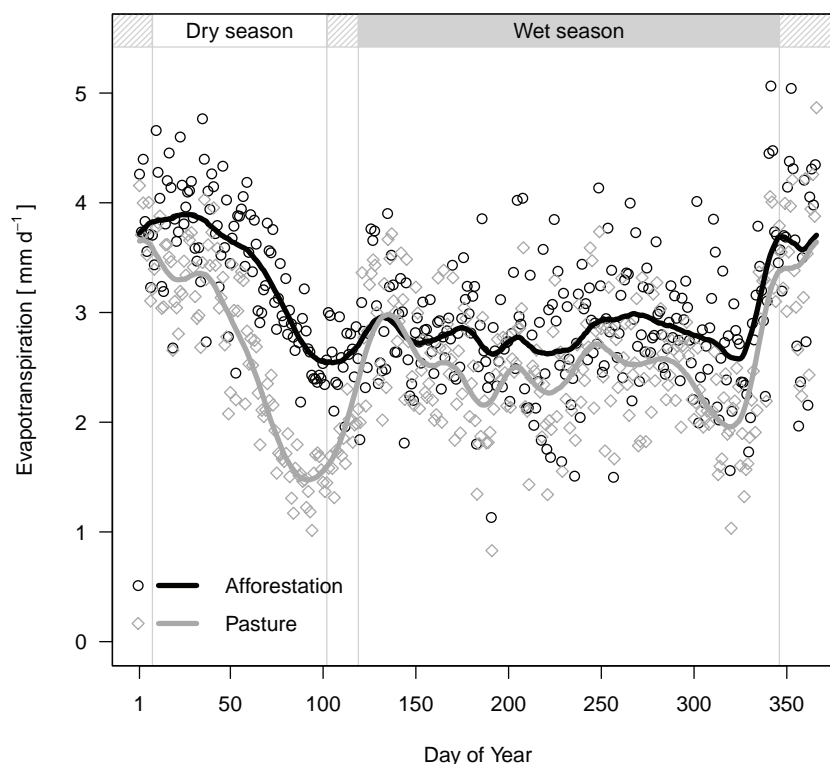


Figure 4.2. Mean annual course of daily total evapotranspiration (ET) for pasture and afforestation in Sardinilla from 2007 to 2009. Lines denote the monthly running mean. The inserts at the top indicate the mean period of different seasons (wet, dry) including transition periods (shaded areas).

4.3.2 Seasonal and inter-annual variations in ET

Pronounced seasonal variations in ET were observed for pasture and afforestation in Sardinilla that were predominantly related to the seasonal patterns of precipitation and associated radiation due to cloud cover (Tab. 4.2).

Variations in monthly water budgets were more pronounced at the pasture compared to the afforestation (Fig. 4.2). We observed a slightly higher monthly ET at the afforestation ($92 \pm 15 \text{ mm mo}^{-1}$) compared to the pasture ($78 \pm 19 \text{ mm mo}^{-1}$). Maximum monthly ET was reached during January, with $114 \pm 1 \text{ mm mo}^{-1}$ and $120 \pm 2 \text{ mm mo}^{-1}$ in the pasture and in the afforestation, respectively. April and November were the months with the lowest rates of ET at both sites (pasture 51 ± 9 and $60 \pm 9 \text{ mm mo}^{-1}$, afforestation 60 ± 6 and $79 \pm 8 \text{ mm mo}^{-1}$).

Daily ET ranged from 0.4 to 5.2 mm d^{-1} (mean $2.6 \pm 1.0 \text{ mm d}^{-1}$) in the pasture and from 0.6 to 6.0 mm d^{-1} (mean $3.0 \pm 0.9 \text{ mm d}^{-1}$) in the afforestation (Tab. 4.3, Figs. 4.2 and 4.3). The differences between both ecosystems were particularly large during the dry season, when ET at the pasture declined more ($2.5 \pm 1.1 \text{ mm d}^{-1}$) compared to the afforestation ($3.4 \pm 0.8 \text{ mm d}^{-1}$). Besides the dry season, ET was lowest during the dry-wet transition period when ET was persistently lower in the pasture than in the afforestation (Fig. 4.4). Large reductions in ET also occurred in both ecosystems at the end of the wet season, which was the wettest period of the year and thus accompanied by strong reductions in radiation. However, the highest rates of ET were achieved subsequently during the wet-dry transition when neither moisture nor radiation were limiting. We also found considerable inter-annual variations in ET between 2007 and 2009 (Fig. 4.3): During the wet seasons 2007 and 2009, ET was on average 23% higher at the afforestation compared to the pasture, while both ecosystems exhibited similar ET during the wet season 2008 with 2.6 and 2.7 mm d^{-1} for pasture and afforestation, respectively. Furthermore, ET in both ecosystems declined to a substantially lower minimum during the prolonged dry season 2009 compared to the previous year.

4.3.3 Diurnal cycles of ET

We observed similar patterns in the diurnal cycles of ET between pasture and afforestation with strong increases in the morning and radiation induced maxima around noon. During the wet season, the midday ET of 0.44 mm h^{-1} was higher at the afforestation than the 0.39 mm h^{-1} measured at the pasture (Fig. 4.5). The highest rates of midday ET were observed during the wet-dry transition period with similar rates in both ecosystems (0.55 and 0.54 mm h^{-1}), but the afforestation maintained high ET rates for a longer period over the day than the pasture. Midday ET during the dry season was lower compared to the wet season at the pasture site only (0.35 mm h^{-1}). The lowest rates of midday ET were found during the dry-wet transition period with 0.28 mm h^{-1} in the pasture and 0.36 mm h^{-1} in the afforestation. In addition, we observed a pronounced midday reduction ('midday depression') in ET during the dry-wet transition period in

the afforestation. During nighttime, ET was generally very small but higher at the afforestation (mean 0.03 mm h^{-1}) compared to the pasture ecosystem (mean 0.02 mm h^{-1}).

Table 4.3. Seasonal averages of daily total evapotranspiration (mm d^{-1}) over pasture and afforestation in Panama from 2007 to 2009. Values indicate mean \pm standard deviation. The percentage denotes ET of the pasture compared to the afforestation.

	Dry season	Dry-wet transition	Wet season	Wet-dry transition	Total
Pasture	2.5 ± 1.1	2.1 ± 0.6	2.5 ± 1.0	3.8 ± 0.8	2.6 ± 1.0
Afforestation	3.4 ± 0.8	2.7 ± 0.5	2.7 ± 0.8	4.1 ± 0.7	3.0 ± 0.9
<i>Pasture / Afforestation</i>	<i>73.5%</i>	<i>77.8%</i>	<i>92.6%</i>	<i>92.7%</i>	<i>86.7%</i>

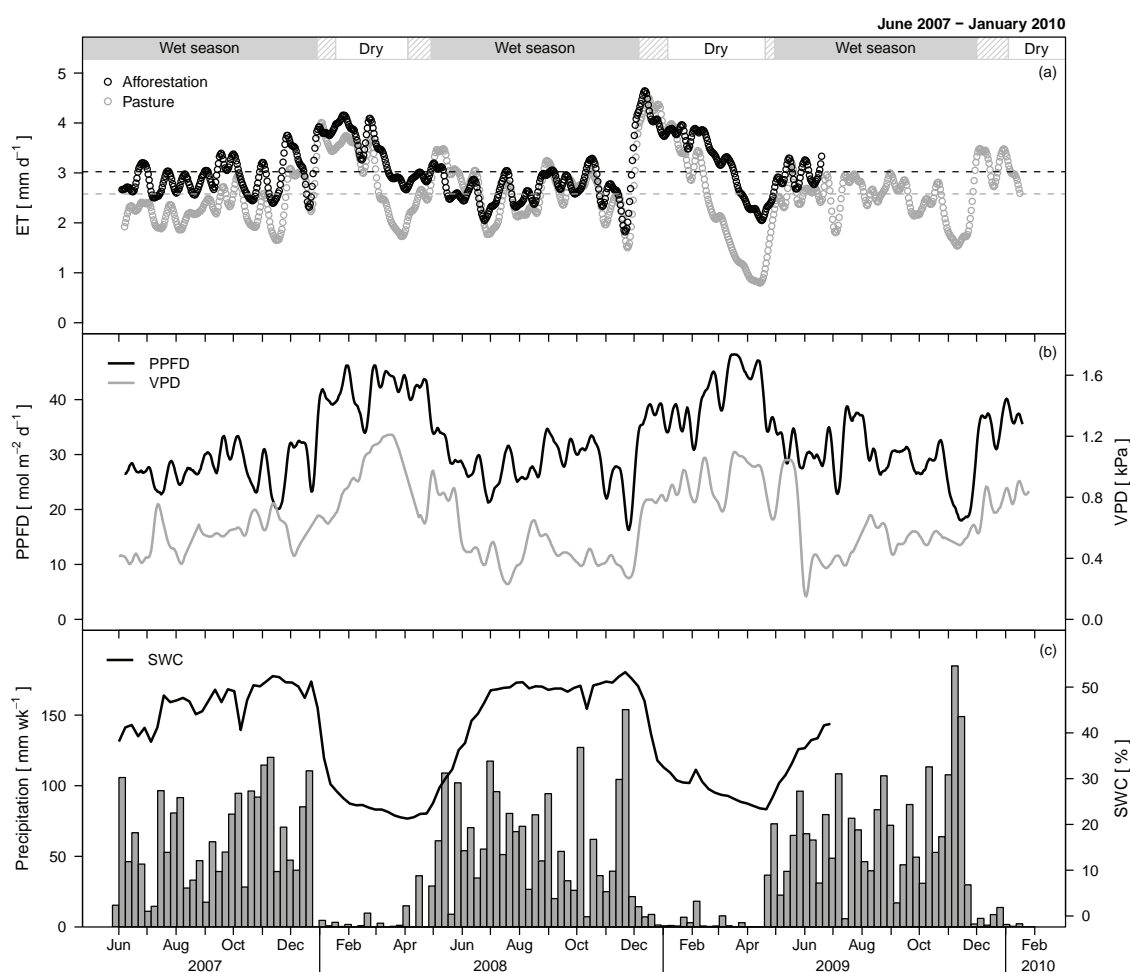


Figure 4.3. Daily total evapotranspiration (ET) at the Sardinilla pasture and afforestation from June 2007 to January 2010 (a). The dashed grey lines denote the daily means. Daily total of photosynthetic photon flux density (PPFD) and vapour pressure deficit (VPD) at the Sardinilla pasture (b). ET, PPFD and VPD are displayed as 14-days running means. Weekly precipitation (grey bars) and weekly mean volumetric soil water content (SWC; afforestation, at 5 cm depth) at Sardinilla (c). Measurements at the afforestation were discontinued after June 2009. The inserts at the top indicate the different seasons (wet, dry) including transition periods (shaded areas).

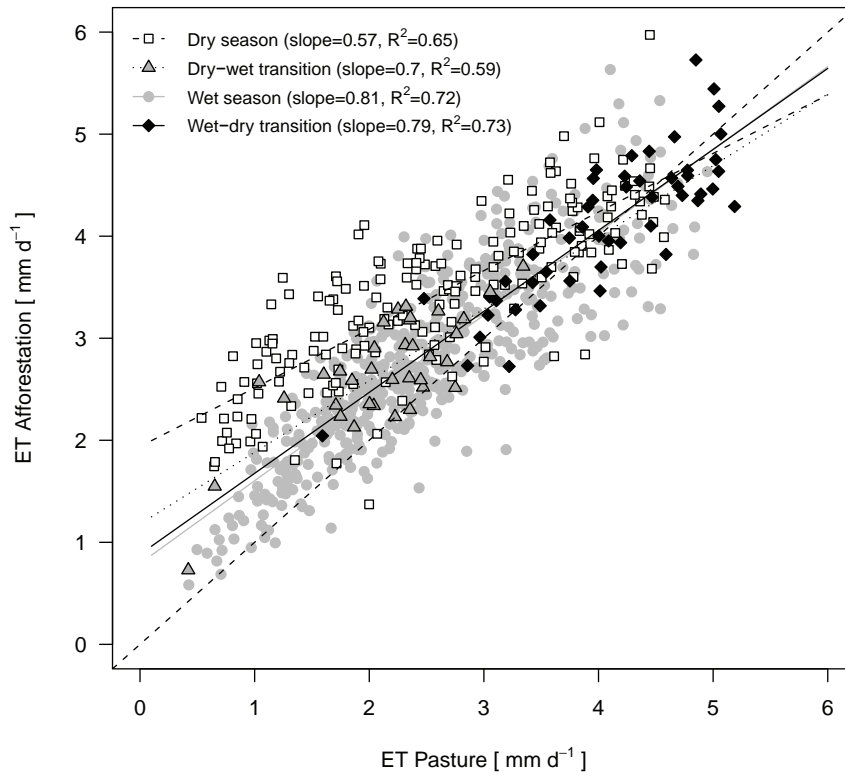


Figure 4.4. Relationship between daily total evapotranspiration (ET) of pasture and afforestation in Sardinilla, Panama. The dashed line denotes the 1:1 relationship.

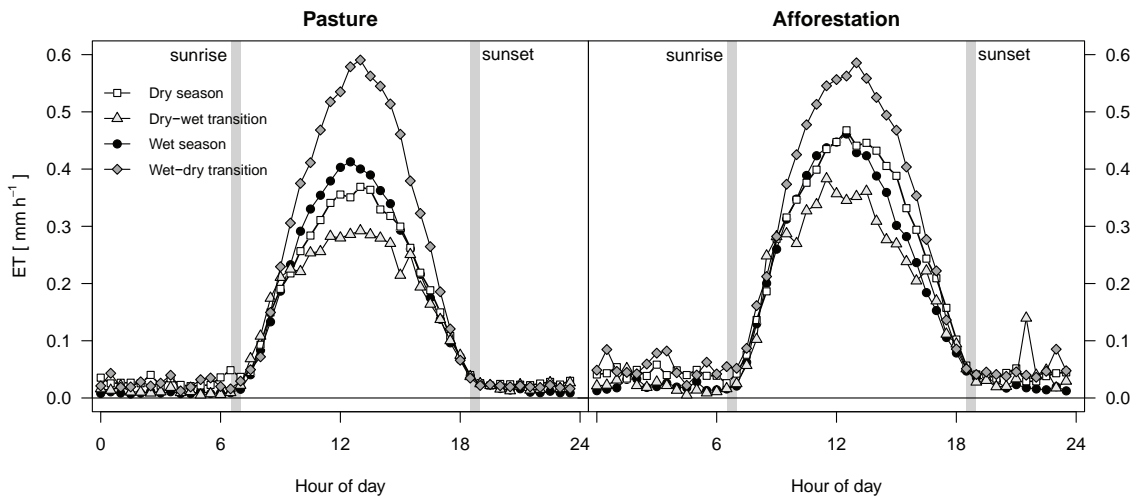


Figure 4.5. Diurnal cycles of seasonally averaged, non gap filled evapotranspiration (ET) at the Sardinilla pasture and afforestation sites from 2007 to 2009. Grey bars denote the seasonally varying times of sunrise and sunset.

4.3.4 Environmental controls of ET

Radiation was the main environmental control of ET in Sardinilla, followed by soil moisture, which played an important role during the dry season (Fig. 4.3). At the pasture, net radiation (R_N) was overall the strongest determinant of ET and explained 77% of the variance in half-hourly ET (regression analysis, $p < 0.001$; PPF explained 75%, Fig. 4.6). Soil water content (SWC) in 5 cm depth was the strongest residual predictor (3.5%), followed by soil temperature (1.5%) and wind speed (0.9%). However, we observed considerable seasonal differences in the environmental controls: during the dry season, R_N explained only 58% of the variance in ET and the residual predictors were stronger, with SWC (13.5%) and soil temperature (21.1%). The contrary was observed during the wet season, when R_N explained 89% of the variance in ET and, air temperature (9.6%) and VPD (6.5%) were the strongest residual predictors.

At the afforestation, PPF was overall the main environmental control and explained 72% of the variance in ET (R_N explained 71%). The strongest residual predictor was soil water content (SWC) in 30 cm depth (5.4%), followed by soil temperature (3.1%) and precipitation (0.8%). Seasonal variations in environmental controls were smaller at the afforestation compared to the pasture (Fig. 4.6). During the dry season, PPF explained 68% of the variance in ET at the afforestation, with SWC at 30 cm depth as the strongest residual predictor (15%), followed by soil temperature (7.1%). During the wet season, PPF explained 77% of ET and, soil temperature (7.1%) and VPD (2.3%) were the strongest residual predictors.

When considering the phenological state of the canopies, we found only weak linear relationships of weekly total ET with LAI from February to June 2009: at the pasture, ET increased with LAI ($R^2 = 0.17$, $p < 0.05$) while ET decreased with LAI at the afforestation ($R^2 = 0.22$, $p < 0.1$).

4.3.5 Soil infiltrability

We observed distinct differences in the soil infiltrability (infiltration potential) between pasture and afforestation. Less water infiltrated into the soil to recharge soil water at the pasture compared to the afforestation as indicated by measurements of SWC in 30 cm depth, which were persistently lower at the pasture (mean 34.9%) compared to the afforestation (mean 44.8%). The land conversion from pasture to afforestation strongly increased the saturated infiltrability by a factor of 12. The soil infiltrability was with $114 \pm 65 \text{ mm h}^{-1}$ significantly lower at the pasture compared to $1313 \pm 169 \text{ mm h}^{-1}$ at the afforestation site. To test the hypothesis of soil compaction as the main cause for these differences, four measurements were taken on walking trails at the afforestation site. Infiltrability at these disturbed locations was with $466 \pm 145 \text{ mm h}^{-1}$ significantly lower compared to the undisturbed soil in the afforestation.

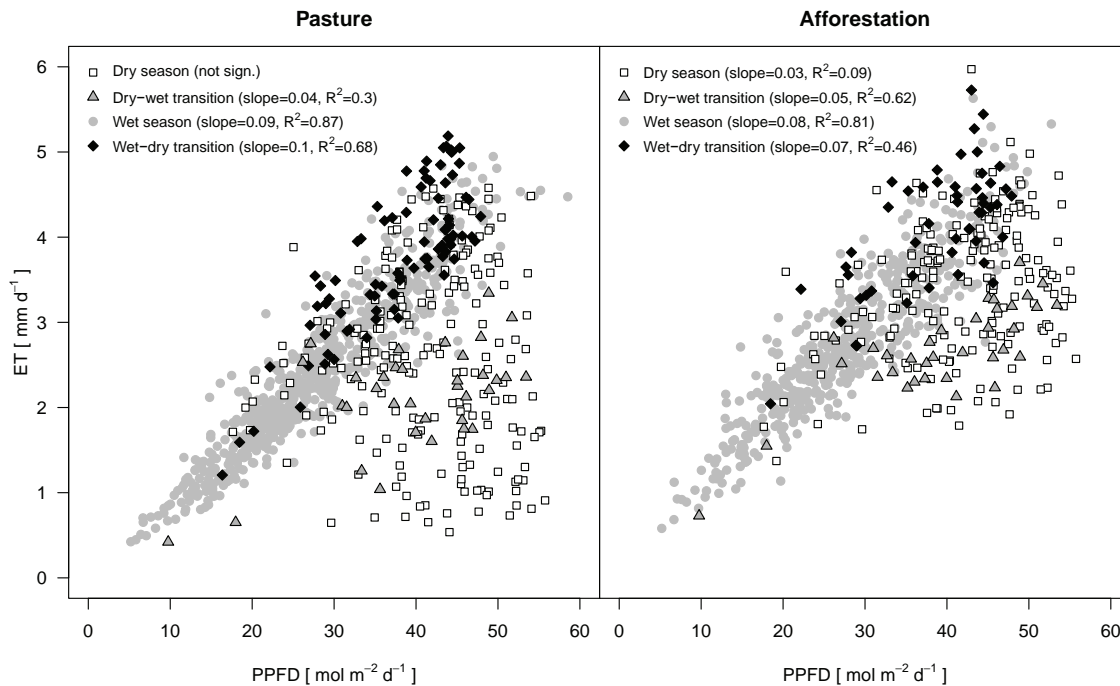


Figure 4.6. Seasonal variability in the functional relationship of daily total evapotranspiration (ET) and photosynthetic photon flux density (PPFD) at the Sardinilla pasture and afforestation from 2007 to 2009. Measurements at the afforestation were discontinued after June 2009.

4.4 Discussion

Against our expectation, the land conversion from pasture to afforestation did not significantly increase total annual ET in Sardinilla. Annual ET at the Sardinilla afforestation (2008: 1114 mm yr⁻¹) was comparable to the 1135 mm yr⁻¹ reported from an old-growth tropical forest in Brazil (Hutyra et al., 2007), and the absolute ET mean of 1096 mm yr⁻¹ from Amazonia as reported by Fisher et al. (2009). Da Rocha et al. (2004) found a higher annual ET in a tropical forest in Tapajos, Brazil (1300 mm yr⁻¹) but a similar ET-precipitation ratio (60%). To our knowledge, no annual ET using the eddy covariance technique was reported for other tropical pastures. However, modelled values of annual pasture ET are reported by Kabat et al. (1999) in the range of 915–1024 mm yr⁻¹ from Amazonia that are comparable to the Sardinilla pasture.

Seasonal variations in ET

The land conversion from pasture to afforestation reduced seasonal variations in ET. Rooting depth and the access to water from deeper soil layers are the likely cause for these differences in ET between different tropical land-use types (Jackson et al., 1996). Further evidence for that theory is given by root measurements in the Sardinilla afforestation done by Jefferson Hall et al. (personal communication, unpublished data), who found a mean rooting depth of 144 cm at the afforestation, compared to 10–20 cm as observed by ourselves at the pasture.

Compared to other tropical pastures, ET observed in the Sardinilla pasture was similar as reported by Grace et al. (1998) for a pasture in Brazil (2.7 mm d^{-1}). During the dry season, however, ET at the Sardinilla pasture was higher than the 1.9 to 2.2 mm d^{-1} as reported from Amazonia by da Rocha et al. (2009a). During the wet season, similar to Sardinilla rates of daily ET were found in Amazonia, with 2.2 to 2.9 mm d^{-1} (da Rocha et al., 2009a; von Randow et al., 2004). Grazing seems to reduce ET as Santos et al. (2004) reported a higher daily mean of 3.4 mm d^{-1} (dry and wet season) for a pasture without grazing in Brazil. When considering alternative tropical land-use types, the lowest values of daily ET in Amazonia were reported with 1.2 mm d^{-1} from bare soil during the dry season (Sakai et al., 2004).

Mean ET observed in the Sardinilla afforestation was similar compared to the 3 to 3.5 mm d^{-1} reported as average from tropical forests (Nobre et al., 2009), along with seasonal differences ranging from 2.8 to 3.6 mm d^{-1} during the wet season to ET rates of 3.3 to 3.9 mm d^{-1} during the dry season. In general, the highest rates of ET in tropical forests were measured during the dry season when radiation was not inhibited by cloud cover (da Rocha et al., 2009b).

Diurnal cycles

Surprisingly, we found no differences in the diurnal cycle of ET between dry and wet season at the afforestation and only small differences at the pasture. This is contrary to our observations in carbon fluxes (see Chapter 2) and suggests a decoupling between transpiration and evaporation during the dry season. As grasses at the pasture became fully senescent at the end of the dry season, ET can be largely attributed to be plant independent, notably evaporation from the soil and from limited dew formation that occurred in the mornings. An additional source could have been water import by grazing livestock (urine, transpiration) from a creek located outside the perimeter of the pasture (not within flux tower footprint). However, when estimating the potential water import by using observed stocking densities (up to 72 livestock per day on the 6.5 ha pasture) and regular consumption rates of cattle (50 – 100 l), this would yield even with severe overgrazing at the maximum to about 0.1 mm d^{-1} . Consequently, water import by grazing livestock is negligible in Sardinilla.

Environmental controls of ET

Radiation was by far the main driver of ecosystem ET in Sardinilla. Similar environmental controls were found by da Rocha et al. (2004) with R_N as the main driver of ET in a tropical forest in Tapajos, Brazil and seasonal patterns of ET closely following radiation. In addition, a synthesis by Fisher et al. (2009) found that R_N explained 87% of the variance in monthly ET of Amazonia, with VPD as the strongest residual predictor. Another study from Amazonia by da Rocha et al. (2009a) reported similar controls. In contrast, VPD was of minor relevance in Sardinilla and its relevance was clearly restricted to the wet season, while SWC was the strongest residual predictor. The variable

length of the dry season throughout Amazonia along with predominantly old-growth tropical forest sites and divergence in the edaphic characteristics could potentially explain these differences. Furthermore, we found a stronger decoupling of environmental controls during the dry season at the pasture compared to the afforestation in Sardinilla. The prevalence of surface SWC and soil temperature as residual predictors indicate that evaporation comprised a larger fraction of pasture ET during the dry season. The senescence of grasses with the progressing dry season, as observed with LAI and aboveground biomass data, gives further evidence for that theory.

Soil infiltrability

Our observations of soil infiltrability in Sardinilla are consistent with values reported by Zimmermann et al. (2006) from Rondonia (Brazil) with 122 mm h^{-1} for pasture, $834\text{--}1155 \text{ mm h}^{-1}$ for plantations and 1533 mm h^{-1} reported for primary rainforest. Malmer et al. (2010) also reported improved soil infiltrability associated with tree planting at other tropical sites across a wide range of rainfall conditions. Soil compaction due to grazing livestock is the main cause of reduced infiltrability in pastures (Vanclay, 2009). In addition to the removal of grazing, the conversion from pasture to afforestation results in the development of coarse and fine roots that increase soil porosity and thus infiltrability. Overall, our results support the ‘sponge theory’ of enhanced infiltrability of forest compared to non-forested land cover, c.f. Malmer et al. (2010).

With infiltrability at the pasture being less than one twelfth of the infiltrability at the afforestation, a much larger percentage of the excess water at the pasture is available for surface runoff and evaporation from the surface. As we found only small differences in annual ET between both ecosystems, we can deduce that the fraction of evaporation from the soil is higher in the pasture compared to the afforestation. This is supported by two facts: (1) Less shading by vegetation provides more available energy reaching the soil surface in the pasture. (2) The terrain at the pasture is homogeneously flat (compare to an undulating topography at the afforestation), which in combination with less infiltrability provides less surface runoff and thus larger amounts of water that potentially evaporate directly from the soil surface. Further evidence for that was found in a Meta analysis by Farley et al. (2005), who found that the afforestation of grasslands reduced annual surface runoff by 44% and thus, increased the water yield of ecosystems. Consequently, ET is not necessarily increased with the land conversion from pasture to afforestation as more water infiltrates into the soil and less water is lost from the ecosystem via surface runoff or evaporates from the soil surface.

4.5 Conclusions

Based on our measurements from Sardinilla, ET of tropical pasture and afforestation are astonishingly similar during the wet season. Deduced from a strongly reduced infiltration potential, this effect is supposedly caused by a higher fraction of evaporation from the pasture compared to the afforestation site. Due to the shallow roots of grasses compared to trees, pasture vegetation is much more sensitive to water limitations during the dry season and becomes fully senescent. Hence, the reduction in ET during the dry season is stronger at the pasture compared to the afforestation, and differences in annual ET are largely based on the dry season reduction. The conversion from pasture to afforestation reduces the seasonal variability in ET but results in only minor differences of total annual ET. Consequently, tropical afforestation can stabilize variations in ET but does not necessarily increase total ecosystem ET. Environmental controls such as radiation, soil water content and vapour pressure deficit are by far more important factors than the respective land use. However, the land conversion from pasture to afforestation largely increases soil infiltrability and properties during the establishment phase already.

Acknowledgements

Funding for this project was provided by the North-South Centre (former Swiss Centre for International Agriculture) of ETH Zurich. We are grateful to the Smithsonian Tropical Research Institute (STRI) for support with the Sardinilla site, the Meteorology and Hydrology Branch of the Panama Canal Authority (ACP) for providing meteorological data, Jefferson Hall and his project funded by SENACYT for information on rooting depth at the afforestation site, Beate Zimmermann for support with the measurements of soil infiltrability, José Monteza for tower maintenance, and Rebecca Hiller, Matthias Barthel and Lutz Merbold for their internal reviews of the manuscript.

Chapter 5

5 Synthesis

The aim of this thesis was to improve our understanding of the interactions between land use and climate on ecosystem CO₂ and H₂O fluxes of tropical pasture and afforestation, with the main focus on seasonal variations and carbon sequestration potentials. For this purpose, comparative eddy covariance measurements were performed in a tropical C₄ pasture and adjacent afforestation with native tree species in Sardinilla (Panama) from 2007 to 2009. The net ecosystem CO₂ exchange (NEE) and ecosystem evapotranspiration (ET) of these two tropical ecosystems were quantified, seasonal variations between pasture and afforestation were assessed and environmental controls of NEE and ET were identified. Measurements of NEE were used to estimate the carbon sequestration potential of tropical pasture compared to afforestation and to elucidate the impact of management on the ecosystem carbon budgets. This thesis presents the first continuous multi-year measurements of ecosystem carbon and water fluxes for tropical pasture and afforestation.

5.1 Main results

The main results of this thesis are summarized as follows:

- Afforestation of tropical pasture can sequester large amounts of carbon, reduce seasonal variations of CO₂ fluxes, and enhance the ecosystem resilience to seasonal drought (Chapters 2 and 3).
- The afforestation was a substantial carbon sink in 2008 and estimates for 2007 and 2009 also indicate strong carbon uptake. Good agreement of EC and biometric derived carbon uptake was found in 2008 (Chapter 3).
- The pasture was a strong and persistent carbon source in 2008 and 2009. Carbon losses of the pasture were predominantly associated with high stocking densities and overgrazing. The carbon losses originated primarily from soil organic matter (Chapter 3).
- The pasture ecosystem was more susceptible to water limitations during the dry season, due to the shallower root system of grasses compared to trees (Chapters 2 to 4).
- Soil respiration contributed about half of TER during nighttime, with only small differences between ecosystems or seasons (Chapter 2).

- Afforestation of tropical pasture only marginally affected ecosystem-scale annual ET but reduced the seasonal variations in ET and largely increased the soil infiltrability. About half of the annual precipitation was returned by ET to the atmosphere (Chapter 4).
- Radiation and soil moisture were the main environmental controls of CO₂ fluxes and ET in Sardinilla. Temperature was found to have no effect on ecosystem and soil respiration in Sardinilla (Chapters 2 to 4).
- ENSO events and associated increases in precipitation variability had a strong impact on seasonal variations of CO₂ fluxes in Central Panama, particularly in the pasture ecosystem (Chapters 2 and 3).

5.2 Carbon stocks and fluxes

The carbon stocks and fluxes assessed in Sardinilla are a comparative case study for the tropics that elucidates the effect of land-use change from pasture to afforestation on the ecosystem carbon cycle (Fig. 5.1). While persistent carbon losses were observed in the pasture, the seven-year-old afforestation sequestered substantial amounts of carbon in 2008. The strength of the carbon sink in the afforestation was confirmed by biometric inventory data and measurements from 2009, suggesting continuous carbon uptake for this ecosystem. Soil data showed that carbon is lost from soil organic matter in both ecosystems and that carbon stocks are much smaller in the pasture than the afforestation (Fig. 5.1, Chapter 3). When assuming that the soil carbon stocks were similar at both sites following the deforestation of the area in 1952/1953 and the short agricultural use afterwards, the large divergence in soil carbon stocks suggests management differences (i.e., grazing) between the pastures until the establishment of the afforestation in 2001. Further evidence for this hypothesis is given by bulk density data that were sampled before the establishment of the afforestation: the pasture site was found to have a 46% higher bulk density compared to the afforestation (Abraham, 2004), likely caused by more intense and persistent grazing of livestock, which results in soil compaction. Additional indicators for more intense grazing could be the closer proximity to the village (easier access), the more homogenous and flat topography, and the size of the pasture site compared to the afforestation. Aerial photographs from 1987 and 2000 (see Appendix D5 and D7 for 2000) show that the continuous area of pasture land-use was substantially larger at the afforestation site. Consequently, differences in the history of land-use management seem to explain the substantial lower soil carbon stocks at the pasture site. If the carbon losses measured in 2008 and 2009 are continuing at this site, the soil carbon pool will be further depleted. Thus, the Sardinilla pasture is at high risk of degradation. Therefore, reduced stocking densities not exceeding 1 LU ha⁻¹ appear crucial for mitigation. However, further research is needed to assure the development in topsoil carbon stocks as the sample size was very limited at the pasture site.

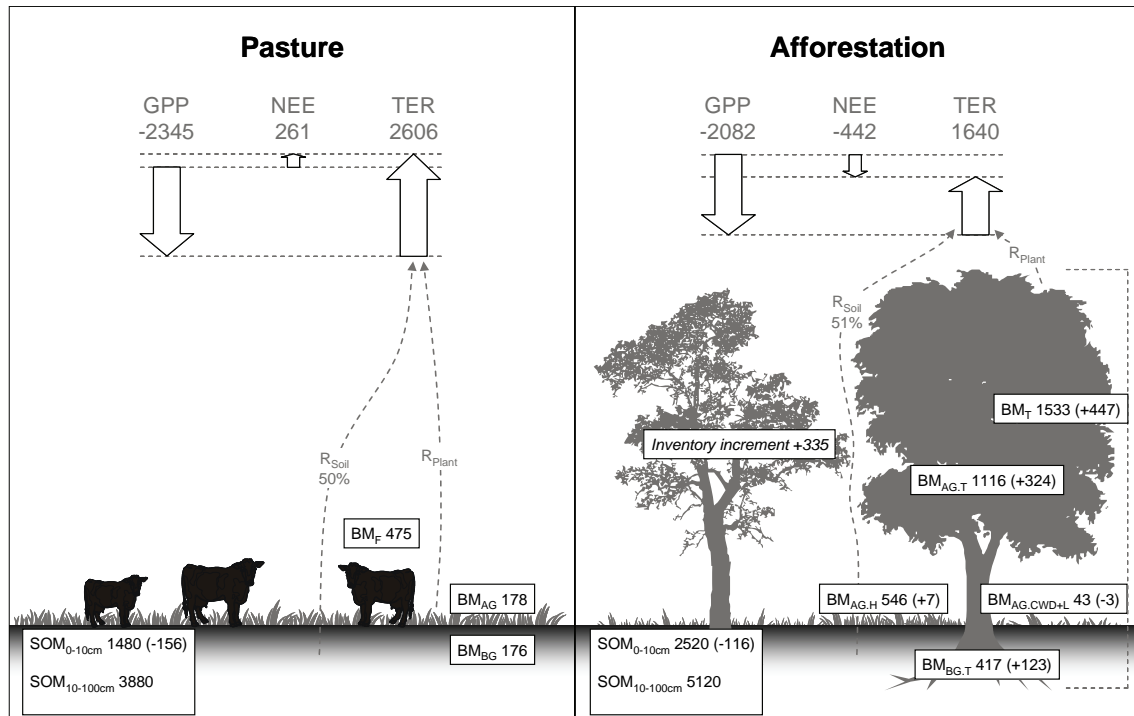


Figure 5.1. Carbon stocks (g C m^{-2}) and fluxes ($\text{g C m}^{-2} \text{ yr}^{-1}$) in the Sardinilla pasture and afforestation in 2008. Grey numbers denote carbon fluxes with net ecosystem exchange (NEE) and its components gross primary production (GPP), and total ecosystem respiration (TER). Wide arrows indicate the size and direction of the fluxes, slim arrows the origin of the TER components soil (R_{Soil}) and plant respiration (R_{Plant}); the percentage denotes the measured source contribution of soil respiration. Numbers in boxes denote carbon stocks with annual increments ($\text{g C m}^{-2} \text{ yr}^{-1}$) given in brackets. Soil organic matter (SOM) is reported for topsoil (0–10 cm) and 10–100 cm depth. Aboveground biomass (BM_{AG}) in the afforestation is separated in tree biomass (BM_{T}), herbaceous biomass (BM_{H}), coarse woody debris (BM_{CWD}) and litter (BM_{L}). Belowground biomass (BM_{BG}) is reported for trees only in the afforestation ($\text{BM}_{\text{AG,T}}$). In the pasture, foraged biomass (BM_{F}) by grazing livestock was estimated using the biomass reduction during periods of overgrazing. The ‘Inventory increment’ incorporates biometric uptake minus soil carbon losses.

5.3 Implications for the tropics

Pasture

The persistent carbon losses observed in the Sardinilla pasture were to a large extent related to management (grazing) and it remains unknown how the carbon budget would develop without grazing. Foraging estimates suggest (Fig. 5.1, Chapter 3.3.5) that the pasture could be a carbon sink or close to equilibrium when considering that about half of the foraged carbon is returned as waste to the pasture (Conant et al., 2001). Previous studies from various biomes have reported that pastures (i.e. grazed grasslands) can be carbon sinks, close to equilibrium or even carbon sources, depending on climatic factors and management (Gilmanov et al., 2010; Xu and Baldocchi, 2004; Zhang et al., 2010). Overall, managed grasslands do not provide a considerable carbon sequestration potential as the accumulated carbon in form of biomass is mostly exported by forage and harvest (Gilmanov et al., 2010). However, as grasslands contain 34% of the global ter-

restrial carbon stock with two-thirds in the form of soil organic carbon (White et al., 2000), it is essential to conserve the carbon stocks of these ecosystems. The prevention of high stocking densities and overgrazing appears crucial for grazed grasslands to avoid soil carbon losses and degradation (Conant et al., 2001; Reid et al., 2004). The results from Sardinilla demonstrated the strong influence of grazing on the carbon cycling of a pasture and the importance of sustainable grazing management especially in the tropics. As the area of pasture land is increasing due to ongoing tropical deforestation (Alves et al., 2009), grazing management has large implications on the tropical carbon budget and has the potential to increase the tropical carbon source.

Afforestation

The afforestation was a substantial carbon sink from 2007 to 2009 and sequestered most of the carbon in the biomass of trees (Fig. 5.1, Chapter 3.3.6). This biomass carbon uptake exceeded by far carbon losses from the topsoil that originated predominantly from former pasture vegetation (as indicated by carbon stable isotope data). In 2008, the total carbon stock in biomass at the Sardinilla afforestation was about 21 Mg C ha⁻¹ and increased by about 4.5 Mg C ha⁻¹ yr⁻¹. The annual increase is higher than the average rate of carbon sequestration reported with 3.6 Mg C ha⁻¹ yr⁻¹ for afforestations in general (Jackson et al., 2007). When conservatively assuming continued carbon uptake like in 2008 for another 30 years without disturbance in the Sardinilla afforestation, the total biomass carbon stock would exceed 150 Mg C ha⁻¹. This estimate is conservative because biometric data from 2009 indicate a strong increase in the sink strength in Sardinilla and forest stands typically maintain increases in sink strength for more than 30 years (Canadell et al., 2007). Further evidence is given by Silver et al. (2004), who found in a long-term inventory based study that the sink strength was not reduced with tree ages up to 55–61 years. Extrapolating the results from Sardinilla to the tropics – assuming that Sardinilla is representative – to estimate the potential of carbon sequestration requires knowledge of the area available for afforestation. Area estimates for the humid tropics range from 300 to 1000 million hectares (Van Noordwijk et al., 2005). Taking the lower value of this estimate would result in 1.35 Pg C yr⁻¹ or about the amount of carbon lost annually from tropical deforestation. Consequently, tropical afforestations have the potential to mitigate further carbon losses of anthropogenic land-use change. Moreover, terrestrial ecosystems evidently affect climate and thus, tropical afforestations are not only a powerful tool to sequester carbon, but can also mitigate climate warming (Foley et al., 2003). The tropics are the only area where afforestation counteracts climate warming due to a positive climate forcing effect (Bonan, 2008; Chapin et al., 2008).

Water fluxes

The observed changes in annual ecosystem ET with the land conversion from pasture to afforestation in Sardinilla were relatively small (+80 mm) seven years after establish-

ment of the afforestation. The differences in the annual water balance of pasture and afforestation will potentially increase with the age of the trees. This assumption is supported by measurements from 2009. More soil water from larger depth is transpired by the increasing canopy area, a larger fraction of precipitation is intercepted by the canopy, surface runoff is further decreasing and thus also streamflow (Farley et al., 2005). Besides the small changes in annual ET, the land-use change from pasture to afforestation reduced the seasonal variations of ET already during the establishment phase already, which is largely related to rooting depth and dormant pasture vegetation during the dry season. However, while deforestation causes large changes in the water balance of ecosystems by reducing evapotranspiration, research has shown that these changes are not fully reversible with afforestation (Jackson et al., 2007), at least not within the first years.

Along with ET, canopy interception of precipitation is generally increasing with afforestation while interception is relatively small in grasslands (Jackson et al., 2007). The average of canopy intercepted rain in the Sardinilla afforestation was 15% (Appendix B) and is close to the 12% reported recently from a rainforest in Amazonia (Czikowsky and Fitzjarrald, 2009). Dew evaporation from the canopy contributed 5% of the total ecosystem evapotranspiration in the Sardinilla afforestation (Appendix B). Consequently, canopy intercepted rain and dew evaporation contribute a substantial amount of total evapotranspiration in the Sardinilla afforestation.

Temperature sensitivity of respiration

Consistent with the observations in Sardinilla, only a weak temperature sensitivity of respiration was found for other tropical ecosystems in Amazonia (Davidson and Janssens, 2006; Hutryra et al., 2007). This has large implications on the gap filling of EC derived tropical carbon budgets as uncertainties are largely related to ecosystem respiration during nighttime. The data from Sardinilla indicate that using weak temperature sensitivities to gap fill nighttime ecosystem respiration could result in large biases of carbon budgets. Running mean approaches and lookup tables are alternatives that should be considered more comprehensively for tropical ecosystems. However, more research at other tropical sites including comparative measurements of soil respiration is needed to further elucidate the temperature sensitivity of respiration in the tropics. This seems particularly important, as a recent synthesis study based on 60 FLUXNET sites reported a global convergence in the temperature sensitivity of ecosystem respiration, independent of mean annual temperature and with no differences among biomes (Mahecha et al., 2010). This study, however, was predominantly based on data from non-tropical sites in the Northern Hemisphere (only 5 tropical sites) and thus might overestimate the temperature sensitivity in the tropics.

5.4 Outlook

Continuous measurements of CO₂ and H₂O fluxes provide a valuable tool to investigate the process understanding of the biosphere-atmosphere exchange in managed tropical ecosystems. This thesis presents the first multi-year measurements for tropical pasture and afforestation and provides detailed insights into the carbon and water cycle of two managed tropical ecosystems. The results can be used to improve ecosystem models for the tropics, to enhance estimates of the tropical carbon budget, and to understand the impact of non-forested ecosystems on the tropical water cycle. Following considerations for further research can be derived from the results in Sardinilla:

- Detailed assessments of the management impact on CO₂ fluxes are essential to estimate and understand the carbon budget of tropical pastures. Measurements of carbon export by grazing livestock and other carbon fluxes, such as methane (CH₄) and nitrous oxide (N₂O), will help to quantify the full greenhouse gas budget of these managed ecosystems.
- Future studies should address the question of the role of pasture management under varying climatic conditions and its impact on the tropical carbon budget in more detail, for instance by using comparative measurements of differing grazing intensities and along gradients of environmental conditions throughout the tropics.
- The investigation of soil carbon pools will provide additional information on the source of ecosystem carbon losses. It appears to be essential to sample only during the wet season and at about the same time of the year, as soil contractions in clay rich soils can substantially bias bulk density measurements.
- It remains uncertain if the carbon sequestration potential of native tree species afforestation in mixture exceeds the one of non-native monocultures, such as *Eucalyptus*, *Pinus* or *Tectona*, as quantitative data on tropical afforestations are limited in general. The respective understanding will have large implications on the promotion of afforestation projects within the carbon accounting of the Kyoto protocol.
- Open questions remain regarding the components of ecosystem evapotranspiration and associated changes with the land conversion from pasture to afforestation, particularly concerning plant transpiration. Measurements of transpiration, soil evaporation and surface runoff will provide further insights in afforestation related changes of the ecosystem water balance that will assist in decisions on land management.
- The investigation of interactions between the carbon and water cycle in the tropics will improve the understanding of the ecosystem response to climate change.
- The role of tropical C₄ ecosystems in the global carbon and water cycling remains poorly understood, particularly in terms of the carbon budget (sink or source potential) and ecosystem response to changing environmental conditions.

References

- Abraham, M., 2004. Spatial variation in soil organic carbon and stable carbon isotope signature in a pasture and a primary forest in Central Panama. Master Thesis, McGill University, Montreal, 91 pp.
- ACP, 2010. Meteorological Data. Panama Canal Authority (ACP), Meteorology and Hydrology Branch (Republic of Panama), Data provided by Mike Hart.
- Adachi, M., Bekku, Y.S., Rashidah, W., Okuda, T. and Koizumi, H., 2006. Differences in soil respiration between different tropical ecosystems. *Applied Soil Ecology*, 34(2-3): 258-265.
- Alves, D.S., Morton, D.C., Batistella, M., Roberts, D.A. and Souza JR, C., 2009. The changing rates and patterns of deforestation and land use in Brazilian Amazonia. In: M. Keller, M. Bustamante, J. Gash and P.S. Dias (Editors), *Amazonia and Global Change. Geophysical Monograph*. American Geophysical Union, Washington, DC, pp. 11-23.
- Amézquita, M.C., Murgeitio, E., Ramirez, B.L. and Inrahim, M.A., 2008. Tropical America: land use, land use change, economic and environmental importance of pasture and silvopastoral production systems. In: L. t' Mannetje, M.C. Amézquita, B. P. and M.A. Ibrahim (Editors), *Carbon sequestration in tropical grassland ecosystems*. Wageningen Academic Publishers, Wageningen, The Netherlands, pp. 221.
- ANAM, 2010. Geological map of Panama. Autoridad Nacional del Ambiente of Panama (ANAM). <http://mapserver.anam.gob.pa>, 15.01.2010.
- Andreae, M.O., Artaxo, P., Brandao, C., Carswell, F.E., Ciccioli, P., da Costa, A.L., Culf, A.D., Esteves, J.L., Gash, J.H.C., Grace, J., Kabat, P., Lelieveld, J., Malhi, Y., Manzi, A.O., Meixner, F.X., Nobre, A.D., Nobre, C., Ruivo, M., Silva-Dias, M.A., Stefani, P., Valentini, R., von Jouanne, J. and Waterloo, M.J., 2002. Biogeochemical cycling of carbon, water, energy, trace gases, and aerosols in Amazonia: The LBA-EUSTACH experiments. *Journal of Geophysical Research-Atmospheres*, 107(D20).
- Arneth, A., Harrison, S.P., Zaehle, S., Tsigaridis, K., Menon, S., Bartlein, P.J., Feichter, J., Korhola, A., Kulmala, M., O'Donnell, D., Schurgers, G., Sorvari, S. and Vesala, T., 2010. Terrestrial biogeochemical feedbacks in the climate system. *Nature Geoscience*, 3(8): 525-532.
- Aubinet, M., 2008. Eddy covariance CO₂ flux measurements in nocturnal conditions: An analysis of the problem. *Ecological Applications*, 18(6): 1368-1378.
- Aubinet, M., Grelle, A., Ibrom, A., Rannik, U., Moncrieff, J., Foken, T., Kowalski, A.S., Martin, P.H., Berbigier, P., Bernhofer, C., Clement, R., Elbers, J., Granier, A., Grunwald, T., Morgenstern, K., Pilegaard, K., Rebmann, C., Snijders, W., Valentini, R. and Vesala, T., 2000. Estimates of the annual net carbon and water exchange of forests: The EUROFLUX methodology, *Advances in Ecological Research*, Vol 30. *Advances in Ecological Research*. Academic Press Inc, San Diego, pp. 113-175.
- Baldocchi, D.D., 2003. Assessing the eddy covariance technique for evaluating carbon dioxide exchange rates of ecosystems: past, present and future. *Global Change Biology*, 9(4): 479-492.

- Baldocchi, D.D., 2008. Breathing of the terrestrial biosphere: lessons learned from a global network of carbon dioxide flux measurement systems. *Australian Journal of Botany*, 56(1): 1-26.
- Bates, B.C., Z.W. Kundzewicz, S. Wu, J.P. Palutikof (Eds.), 2008. *Climate Change and Water*. Technical Paper of the Intergovernmental Panel on Climate Change, IPCC Secretariat, Geneva, 210 pp.
- Beer, C., Reichstein, M., Tomelleri, E., Ciais, P., Jung, M., Carvalhais, N., Rodenbeck, C., Arain, M.A., Baldocchi, D., Bonan, G.B., Bondeau, A., Cescatti, A., Lasslop, G., Lindroth, A., Lomas, M., Luysaert, S., Margolis, H., Oleson, K.W., Rouspard, O., Veenendaal, E., Viovy, N., Williams, C., Woodward, F.I. and Papale, D., 2010. Terrestrial Gross Carbon Dioxide Uptake: Global Distribution and Covariation with Climate. *Science*, 329(5993): 834-838.
- Bonal, D., Bosc, A., Ponton, S., Goret, J.Y., Burban, B., Gross, P., Bonnefond, J.M., Elbers, J., Longdoz, B., Epron, D., Guehl, J.M. and Granier, A., 2006. The influence of severe seasonal soil drought on ecosystem functioning in the tropical rainforest of French Guiana. Poster at Guyaflux Summer School.
- Bonal, D., Bosc, A., Ponton, S., Goret, J.Y., Burban, B., Gross, P., Bonnefond, J.M., Elbers, J., Longdoz, B., Epron, D., Guehl, J.M. and Granier, A., 2008. Impact of severe dry season on net ecosystem exchange in the Neotropical rainforest of French Guiana. *Global Change Biology*, 14(8): 1917-1933.
- Bonan, G.B., 2008. Forests and climate change: Forcings, feedbacks, and the climate benefits of forests. *Science*, 320(5882): 1444-1449.
- Buchmann, N., Bonal, D., Barigah, T.S., Guehl, J.M. and Ehleringer, J.R., 2004. Insights in the carbon dynamics of tropical primary rainforests using stable carbon isotope analyses. In: S. Gourlet-Fleury, J.M. Guehl and O. Laroussinie (Editors), *Ecology and management of a neotropical rainforest*. Elsevier, Applied Science, London, NY.
- Buchmann, N. and Schulze, E.D., 1999. Net CO₂ and H₂O fluxes of terrestrial ecosystems. *Global Biogeochemical Cycles*, 13(3): 751-760.
- Canadell, J., Pataki, D., Gifford, R., Houghton, R., Luo, Y., Raupach, M., Smith, P. and Steffen, W., 2007. Saturation of the Terrestrial Carbon Sink. In: J.G. Canadell, D.E. Pataki and L.F. Pitelka (Editors), *Terrestrial Ecosystems in a Changing World*. Global Change - The IGBP Series. Springer Berlin Heidelberg, pp. 59-78.
- Carswell, F.E., Costa, A.L., Palheta, M., Malhi, Y., Meir, P., Costa, J.D.R., Ruivo, M.D., Leal, L.D.M., Costa, J.M.N., Clement, R.J. and Grace, J., 2002. Seasonality in CO₂ and H₂O flux at an eastern Amazonian rain forest. *Journal of Geophysical Research-Atmospheres*, 107(D20).
- Chambers, J.Q., Tribuzy, E.S., Toledo, L.C., Crispim, B.F., Higuchi, N., dos Santos, J., Araujo, A.C., Kruijt, B., Nobre, A.D. and Trumbore, S.E., 2004. Respiration from a tropical forest ecosystem: Partitioning of sources and low carbon use efficiency. *Ecological Applications*, 14(4): 72-88.
- Chapin, F.S., Randerson, J.T., McGuire, A.D., Foley, J.A. and Field, C.B., 2008. Changing feedbacks in the climate-biosphere system. *Frontiers in Ecology and the Environment*, 6(6): 313-320.
- Chilonda, P. and Otte, J., 2006. Indicators to monitor trends in livestock production at national, regional and international levels. *Livestock Research for Rural Development*, 18: Article #117.

- Conant, R.T., Paustian, K. and Elliott, E.T., 2001. Grassland management and conversion into grassland: Effects on soil carbon. *Ecological Applications*, 11(2): 343-355.
- Czikowsky, M.J. and Fitzjarrald, D.R., 2009. Detecting rainfall interception in an Amazonian rain forest with eddy flux measurements. *Journal of Hydrology*, 377(1-2): 92-105.
- da Rocha, H., Manzi, A.O. and Shuttleworth, J., 2009a. Evapotranspiration. In: M. Keller, M. Bustamante, J. Gash and P.S. Dias (Editors), *Amazonia and Global Change*. American Geophysical Union, Washington, DC, pp. 261-272.
- da Rocha, H.R., Goulden, M.L., Miller, S.D., Menton, M.C., Pinto, L., de Freitas, H.C. and Figueira, A., 2004. Seasonality of water and heat fluxes over a tropical forest in eastern Amazonia. *Ecological Applications*, 14(4): 22-32.
- da Rocha, H.R., Manzi, A.O., Cabral, O.M., Miller, S.D., Goulden, M.L., Saleska, S.R., Coupe, N.R., Wofsy, S.C., Borma, L.S., Artaxo, P., Vourlitis, G., Nogueira, J.S., Cardoso, F.L., Nobre, A.D., Kruijt, B., Freitas, H.C., von Randow, C., Aguiar, R.G. and Maia, J.F., 2009b. Patterns of water and heat flux across a biome gradient from tropical forest to savanna in Brazil. *Journal of Geophysical Research-Biogeosciences*, 114.
- Davidson, E.A. and Janssens, I.A., 2006. Temperature sensitivity of soil carbon decomposition and feedbacks to climate change. *Nature*, 440(7081): 165-173.
- Davidson, E.A., Janssens, I.A. and Luo, Y.Q., 2006. On the variability of respiration in terrestrial ecosystems: moving beyond Q(10). *Global Change Biology*, 12(2): 154-164.
- Davidson, E.A., Verchot, L.V., Cattanio, J.H., Ackerman, I.L. and Carvalho, J.E.M., 2000. Effects of soil water content on soil respiration in forests and cattle pastures of eastern Amazonia. *Biogeochemistry*, 48(1): 53-69.
- Dias-Filho, M.B., Davidson, E.A. and de Carvalho, C.J.R., 2000. Linking Biogeochemical cycles to cattle pasture management and sustainability in the Amazon basin. In: M.E. McClain, R.L. Victoria and J.E. Richey (Editors), *The biogeochemistry of the Amazon Basin*. Oxford University Press, New York, pp. 84-105.
- Don, A., Rebmann, C., Kolle, O., Scherer-Lorenzen, M. and Schulze, E.D., 2009. Impact of afforestation-associated management changes on the carbon balance of grassland. *Global Change Biology*, 15(8): 1990-2002.
- EarthTrends, 2003. Forests, Grasslands, and Drylands - Country Profile Panama. World Resource Institute. http://earthtrends.wri.org/country_profiles/fetch_profile.php?theme=9&filename=for_cou_591.PDF, 11.05.2010.
- Ehleringer, J.R. and Monson, R.K., 1993. Evolutionary and ecological aspects of photosynthetic pathway variation. *Annual Review of Ecology and Systematics*, 24: 411-439.
- Etzold, S., Buchmann, N. and Eugster, W., 2010. Contribution of advection to the carbon budget measured by eddy covariance at a steep mountain slope forest in Switzerland. *Biogeosciences*, 7(8): 2461-2475.
- Eugster, W., Moffat, A.M., Ceschia, E., Aubinet, M., Ammann, C., Osborne, B., Davis, P.A., Smith, P., Jacobs, C., Moors, E., Le Dantec, V., Béziat, P., Saunders, M., Jans, W., Grünwald, T., Rebmann, C., Kutsch, W.L., Czerný, R., Janous, D., Moureaux, C., Dufranne, D., Carrara, A., Magliulo, V., Di Tommasi, P., Olesen, J.E., Schelde, K., Olioso, A., Bernhofer, C., Cellier, P., Larmanou, E., Loubet,

- B., Wattenbach, M., Marloie, O., Sanz, M.-J., Søgaard, H. and Buchmann, N., 2010. Management effects on European cropland respiration. *Agriculture, Ecosystems & Environment*, 139(3): 346-362.
- Eugster, W. and Plüss, P., 2010. A fault-tolerant eddy covariance system for measuring CH₄ fluxes. *Agricultural and Forest Meteorology*, 150(6): 841-851.
- Eugster, W. and Senn, W., 1995. A cospectral correction model for measurement of turbulent NO₂ flux. *Boundary-Layer Meteorology*, 74(4): 321-340.
- Fan, S.M., Wofsy, S.C., Bakwin, P.S., Jacob, D.J. and Fitzjarrald, D.R., 1990. Atmosphere-biosphere exchange of CO₂ and O₃ in the Central Amazon forest. *Journal of Geophysical Research-Atmospheres*, 95(D10): 16851-16864.
- FAO, 2001. Global data on forest plantations resources, Food and Agriculture Organization of the United Nations (FAO), Rome.
- FAO, 2009. State of the World's Forests 2009, Food and Agriculture Organization of the United Nations (FAO), Rome.
- Farley, K.A., Jobbagy, E.G. and Jackson, R.B., 2005. Effects of afforestation on water yield: a global synthesis with implications for policy. *Global Change Biology*, 11(10): 1565-1576.
- Fearnside, P.M., 2005. Deforestation in Brazilian Amazonia: History, rates, and consequences. *Conservation Biology*, 19(3): 680-688.
- Fearnside, P.M. and Laurance, W.F., 2004. Tropical deforestation and greenhouse-gas emissions. *Ecological Applications*, 14(4): 982-986.
- Fisher, J.B., Malhi, Y., Bonal, D., Da Rocha, H.R., De Araujo, A.C., Gamo, M., Goulden, M.L., Hirano, T., Huete, A.R., Kondo, H., Kumagai, T., Loescher, H.W., Miller, S., Nobre, A.D., Nouvellon, Y., Oberbauer, S.F., Panuthai, S., Roupsard, O., Saleska, S., Tanaka, K., Tanaka, N., Tu, K.P. and Von Randow, C., 2009. The land-atmosphere water flux in the tropics. *Global Change Biology*, 15(11): 2694-2714.
- Foken, T. and Wichura, B., 1996. Tools for quality assessment of surface-based flux measurements. *Agricultural and Forest Meteorology*, 78(1-2): 83-105.
- Foley, J.A., Costa, M.H., Delire, C., Ramankutty, N. and Snyder, P., 2003. Green surprise? How terrestrial ecosystems could affect earth's climate. *Frontiers in Ecology and the Environment*, 1(1): 38-44.
- Freeman, T.G., 1991. Calculating catchment-area with divergent flow based on a regular grid. *Computers & Geosciences*, 17(3): 413-422.
- Gilmanov, T.G., Aires, L., Barcza, Z., Baron, V.S., Belelli, L., Beringer, J., Billesbach, D., Bonal, D., Bradford, J., Ceschia, E., Cook, D., Corradi, C., Frank, A., Gianelle, D., Gimeno, C., Gruenwald, T., Guo, H.Q., Hanan, N., Haszpra, L., Heilman, J., Jacobs, A., Jones, M.B., Johnson, D.A., Kiely, G., Li, S.G., Magliulo, V., Moors, E., Nagy, Z., Nasyrov, M., Owensby, C., Pinter, K., Pio, C., Reichstein, M., Sanz, M.J., Scott, R., Soussana, J.F., Stoy, P.C., Svejcar, T., Tuba, Z. and Zhou, G.S., 2010. Productivity, Respiration, and Light-Response Parameters of World Grassland and Agroecosystems Derived From Flux-Tower Measurements. *Rangeland Ecology & Management*, 63(1): 16-39.
- Gilmanov, T.G., Johnson, D.A. and Saliendra, N.Z., 2003. Growing season CO₂ fluxes in a sagebrush-steppe ecosystem in Idaho: bowen ratio/energy balance measurements and modeling. *Basic and Applied Ecology*, 4(2): 167-183.
- Goulden, M.L., Miller, S.D., da Rocha, H.R., Menton, M.C., de Freitas, H.C., Figueira, A. and de Sousa, C.A.D., 2004. Diel and seasonal patterns of tropical forest CO₂ exchange. *Ecological Applications*, 14(4): 42-54.

- Grace, J., Lloyd, J., McIntyre, J., Miranda, A.C., Meir, P., Miranda, H.S., Nobre, C., Moncrieff, J., Massheder, J., Malhi, Y., Wright, I. and Gash, J., 1995. Carbon dioxide uptake by an undisturbed tropical rain-forest in Southwest Amazonia, 1992 to 1993. *Science*, 270(5237): 778-780.
- Grace, J., Lloyd, J., Miranda, A.C., Miranda, H. and Gash, J.H.C., 1998. Fluxes of carbon dioxide and water vapour over a C₄ pasture in south-western Amazonia (Brazil). *Australian Journal of Plant Physiology*, 25(5): 519-530.
- Grace, J., Malhi, Y., Higuchi, N. and Meir, P., 2001. Productivity of tropical forests. In: J. Roy, B. Saugier and H. Mooney (Editors), *Terrestrial Global Productivity*. Academic Press, San Diego, CA, USA, pp. 401-426.
- Grace, J., Malhi, Y., Lloyd, J., McIntyre, J., Miranda, A.C., Meir, P. and Miranda, H.S., 1996. The use of eddy covariance to infer the net carbon dioxide uptake of Brazilian rain forest. *Global Change Biology*, 2(3): 209-217.
- Graham, N.E., Georgakakos, K.P., Vargas, C. and Echevers, M., 2006. Simulating the value of El Niño forecasts for the Panama Canal. *Advances in Water Resources*, 29(11): 1665-1677.
- Gu, L.H., Falge, E.M., Boden, T., Baldocchi, D.D., Black, T.A., Saleska, S.R., Suni, T., Verma, S.B., Vesala, T., Wofsy, S.C. and Xu, L.K., 2005. Objective threshold determination for nighttime eddy flux filtering. *Agricultural and Forest Meteorology*, 128(3-4): 179-197.
- Hasler, N. and Avissar, R., 2007. What controls evapotranspiration in the Amazon basin? *Journal of Hydrometeorology*, 8(3): 380-395.
- Houghton, R.A., 2007. Balancing the global carbon budget. *Annual Review of Earth and Planetary Sciences*, 35: 313-347.
- Huntington, T.G., 2006. Evidence for intensification of the global water cycle: Review and synthesis. *Journal of Hydrology*, 319(1-4): 83-95.
- Hutyra, L.R., Munger, J.W., Saleska, S.R., Gottlieb, E., Daube, B.C., Dunn, A.L., Amaral, D.F., de Camargo, P.B. and Wofsy, S.C., 2007. Seasonal controls on the exchange of carbon and water in an Amazonian rain forest. *Journal of Geophysical Research-Biogeosciences*, 112(3).
- IPCC, 2001. *Climate Change 2001: Synthesis Report*. A Contribution of Working Groups I, II, and III to the Third Assessment Report of the Intergovernmental Panel on Climate Change. Cambridge University Press, Cambridge, United Kingdom, 398 pp.
- IPCC, 2007a. *Climate Change 2007: Mitigation*. Contribution of Working Group III to the Fourth Assessment Report of the Intergovernmental Panel on Climate Change. Cambridge University Press, Cambridge, United Kingdom.
- IPCC, 2007b. *Climate Change 2007: The Physical Science Basis*. Contribution of Working Group I to the Fourth Assessment Report of the Intergovernmental Panel on Climate Change. Cambridge University Press, Cambridge, United Kingdom, 1028 pp.
- IRI, 2010. ENSO Quick Look – A monthly summary of the status of El Niño, La Niña and the Southern Oscillation. The International Research Institute for Climate and Society (IRI). <http://iri.columbia.edu/climate/ENSO/currentinfo/QuickLook.html>, 15.01.2010.
- Jackson, R., Farley, K., Hoffmann, W., Jobbágy, E. and McCulley, R., 2007. Carbon and Water Tradeoffs in Conversions to Forests and Shrublands. In: J.G. Canadell, D.E. Pataki and L.F. Pitelka (Editors), *Terrestrial Ecosystems in a*

- Changing World. Global Change - The IGBP Series. Springer Berlin Heidelberg, pp. 237-246.
- Jackson, R.B., Canadell, J., Ehleringer, J.R., Mooney, H.A., Sala, O.E. and Schulze, E.D., 1996. A global analysis of root distributions for terrestrial biomes. *Oecologia*, 108(3): 389-411.
- Jung, M., Reichstein, M., Ciais, P., Seneviratne, S.I., Sheffield, J., Goulden, M.L., Bonan, G., Cescatti, A., Chen, J., de Jeu, R., Dolman, A.J., Eugster, W., Gerten, D., Gianelle, D., Gobron, N., Heinke, J., Kimball, J., Law, B.E., Montagnani, L., Mu, Q., Mueller, B., Oleson, K., Papale, D., Richardson, A.D., Rouspard, O., Running, S., Tomelleri, E., Viovy, N., Weber, U., Williams, C., Wood, E., Zaehle, S. and Zhang, K., 2010. Recent decline in the global land evapotranspiration trend due to limited moisture supply. *Nature*, 467(7318): 951-954.
- Kabat, P., Dolman, A.J., Ashby, M., Gash, J.C., Wright, I., Culf, A., Calvet, J.C., Delire, C., Noilhan, J., Jochum, A., Silva Dias, M.A., Fisch, G.A., Santos Alvala, R.C., Nobre, C.A., Prince, S.D. and Steininger, M., 1999. Use of integrated modelling for experimental design; final report, pp. 210.
- Kanowski, P., 1997. Plantation forestry for the 21st century. Afforestation and plantation forestry, XI World Forestry Congress, Antalya, Turkey, pp. 23-34.
- Kirkman, G.A., Gut, A., Ammann, C., Gatti, L.V., Cordova, A.M., Moura, M.A.L., Andreae, M.O. and Meixner, F.X., 2002. Surface exchange of nitric oxide, nitrogen dioxide, and ozone at a cattle pasture in Rondonia, Brazil. *Journal of Geophysical Research-Atmospheres*, 107(D20).
- Kljun, N., Calanca, P., Rotachhi, M.W. and Schmid, H.P., 2004. A simple parameterisation for flux footprint predictions. *Boundary-Layer Meteorology*, 112(3): 503-523.
- Koerner, C., 2003. Slow in, Rapid out—Carbon Flux Studies and Kyoto Targets. *Science*, 300(5623): 1242-1243.
- Koerner, C., 2009. Biological Carbon Sinks: Turnover Must Not Be Confused with Capital! *Gaia-Ecological Perspectives for Science and Society*, 18(4): 288-293.
- Kruijt, B., Elbers, J.A., von Randow, C., Araujo, A.C., Oliveira, P.J., Culf, A., Manzi, A.O., Nobre, A.D., Kabat, P. and Moors, E.J., 2004. The robustness of eddy correlation fluxes for Amazon rain forest conditions. *Ecological Applications*, 14(4): 101-113.
- Lachniet, M.S., 2009. Sea surface temperature control on the stable isotopic composition of rainfall in Panama. *Geophysical Research Letters*, 36.
- Lal, R., 2004. Soil carbon sequestration impacts on global climate change and food security. *Science*, 304(5677): 1623-1627.
- Lambers, H., Chapin, F.S., III and Pons, T.L., 2008. *Plant Physiological Ecology*. Plant Physiological Ecology. Springer-Verlag New York, Inc.; Springer-Verlag, 610 pp.
- Le Quere, C., Raupach, M.R., Canadell, J.G., Marland, G., Bopp, L., Ciais, P., Conway, T.J., Doney, S.C., Feely, R.A., Foster, P., Friedlingstein, P., Gurney, K., Houghton, R.A., House, J.I., Huntingford, C., Levy, P.E., Lomas, M.R., Majkut, J., Metzl, N., Ometto, J.P., Peters, G.P., Prentice, I.C., Randerson, J.T., Running, S.W., Sarmiento, J.L., Schuster, U., Sitch, S., Takahashi, T., Viovy, N., van der Werf, G.R. and Woodward, F.I., 2009. Trends in the sources and sinks of carbon dioxide. *Nature Geoscience*, 2(12): 831-836.

- Loescher, H.W., Oberbauer, S.F., Gholz, H.L. and Clark, D.B., 2003. Environmental controls on net ecosystem-level carbon exchange and productivity in a Central American tropical wet forest. *Global Change Biology*, 9(3): 396-412.
- Lorenz, K. and Lal, R., 2010. *Carbon Sequestration in Forest Ecosystems*. Springer, 277 pp.
- Luysaert, S., Inglima, I., Jung, M., Richardson, A.D., Reichsteins, M., Papale, D., Piao, S.L., Schulzes, E.D., Wingate, L., Matteucci, G., Aragao, L., Aubinet, M., Beers, C., Bernhoffer, C., Black, K.G., Bonal, D., Bonnefond, J.M., Chambers, J., Ciais, P., Cook, B., Davis, K.J., Dolman, A.J., Gielen, B., Goulden, M., Grace, J., Granier, A., Grelle, A., Griffis, T., Grunwald, T., Guidolotti, G., Hanson, P.J., Harding, R., Hollinger, D.Y., Hutya, L.R., Kolar, P., Kruijt, B., Kutsch, W., Lagergren, F., Laurila, T., Law, B.E., Le Maire, G., Lindroth, A., Loustau, D., Malhi, Y., Mateus, J., Migliavacca, M., Misson, L., Montagnani, L., Moncrieff, J., Moors, E., Munger, J.W., Nikinmaa, E., Ollinger, S.V., Pita, G., Rebmann, C., Roupsard, O., Saigusa, N., Sanz, M.J., Seufert, G., Sierra, C., Smith, M.L., Tang, J., Valentini, R., Vesala, T. and Janssens, I.A., 2007. CO₂ balance of boreal, temperate, and tropical forests derived from a global database. *Global Change Biology*, 13(12): 2509-2537.
- Luysaert, S., Schulze, E.D., Borner, A., Knohl, A., Hessenmoller, D., Law, B.E., Ciais, P. and Grace, J., 2008. Old-growth forests as global carbon sinks. *Nature*, 455(7210): 213-215.
- Mahecha, M.D., Reichstein, M., Carvalhais, N., Lasslop, G., Lange, H., Seneviratne, S.I., Vargas, R., Ammann, C., Arain, M.A., Cescatti, A., Janssens, I.A., Migliavacca, M., Montagnani, L. and Richardson, A.D., 2010. Global Convergence in the Temperature Sensitivity of Respiration at Ecosystem Level. *Science*, 329(5993): 838-840.
- Malhi, Y., Baldocchi, D.D. and Jarvis, P.G., 1999. The carbon balance of tropical, temperate and boreal forests. *Plant Cell and Environment*, 22(6): 715-740.
- Malhi, Y. and Davidson, E.A., 2009. Biogeochemistry and ecology of terrestrial ecosystems in Amazonia. In: M. Keller, M. Bustamante, J. Gash and P.S. Dias (Editors), *Amazonia and global change*. American Geophysical Union, Washington, DC, pp. 293-298.
- Malhi, Y. and Grace, J., 2000. Tropical forests and atmospheric carbon dioxide. *Trends in Ecology & Evolution*, 15(8): 332-337.
- Malhi, Y., Meir, P. and Brown, S., 2002. Forests, carbon and global climate. *Philosophical Transactions of the Royal Society of London Series A - Mathematical Physical and Engineering Sciences*, 360(1797): 1567-1591.
- Malhi, Y., Nobre, A.D., Grace, J., Kruijt, B., Pereira, M.G.P., Culf, A. and Scott, S., 1998. Carbon dioxide transfer over a Central Amazonian rain forest. *Journal of Geophysical Research-Atmospheres*, 103(D24): 31593-31612.
- Malmer, A., Murdiyarso, D., Bruijnzeel, L.A. and Ilstedt, U., 2010. Carbon sequestration in tropical forests and water: a critical look at the basis for commonly used generalizations. *Global Change Biology*, 16(2): 599-604.
- Mauder, M., Foken, T., Clement, R., Elbers, J.A., Eugster, W., Grunwald, T., Heusinkveld, B. and Kolle, O., 2008. Quality control of CarboEurope flux data - Part 2: Inter-comparison of eddy-covariance software. *Biogeosciences*, 5(2): 451-462.
- Merbold, L., Ardo, J., Arneth, A., Scholes, R.J., Nouvellon, Y., de Grandcourt, A., Archibald, S., Bonnefond, J.M., Boulain, N., Brueggemann, N., Bruemmer, C.,

- Cappelaere, B., Ceschia, E., El-Khidir, H.A.M., El-Tahir, B.A., Falk, U., Lloyd, J., Kergoat, L., Le Dantec, V., Mouglin, E., Muchinda, M., Mukelabai, M.M., Ramier, D., Rouspard, O., Timouk, F., Veenendaal, E.M. and Kutsch, W.L., 2009. Precipitation as driver of carbon fluxes in 11 African ecosystems. *Biogeosciences*, 6(6): 1027-1041.
- Miranda, A.C., Miranda, H.S., Lloyd, J., Grace, J., Francey, R.J., McIntyre, J.A., Meir, P., Riggan, P. and Lockwood, R., 1996. Carbon dioxide fluxes over a cerrado *sensu stricto* in central Brazil. In: J.H.C. Gash, C.A. Nobre, J.M. Roberts and R.L. Victoria (Editors), *Amazonian deforestation and climate*. Wiley, Chichester, pp. 353-362.
- Miranda, A.C., Miranda, H.S., Lloyd, J., Grace, J., Francey, R.J., McIntyre, J.A., Meir, P., Riggan, P., Lockwood, R. and Brass, J., 1997. Fluxes of carbon, water and energy over Brazilian cerrado: An analysis using eddy covariance and stable isotopes. *Plant Cell and Environment*, 20(3): 315-328.
- Moffat, A.M., unpublished. A new methodology to interpret high resolution measurements of net carbon fluxes between terrestrial ecosystems and the atmosphere. PhD thesis, Friedrich Schiller University, Jena.
- Monteith, J.L. and Unsworth, M.H., 1990. *Principles of Environmental Physics*. Principles of Environmental Physics. Edward Arnold, London, 291 pp.
- Moorcroft, P.R., 2003. Recent advances in ecosystem-atmosphere interactions: an ecological perspective. *Proceedings of the Royal Society B-Biological Sciences*, 270(1521): 1215-1227.
- Moureaux, C., Debacq, A., Bodson, B., Heinesch, B. and Aubinet, M., 2006. Annual net ecosystem carbon exchange by a sugar beet crop. *Agricultural and Forest Meteorology*, 139(1-2): 25-39.
- Murphy, M., Balsler, T., Buchmann, N., Hahn, V. and Potvin, C., 2008. Linking tree biodiversity to belowground process in a young tropical plantation: Impacts on soil CO₂ flux. *Forest Ecology and Management*, 255(7): 2577-2588.
- Nieder, R. and Benbi, D.K., 2008. *Carbon and Nitrogen in the Terrestrial Environment*. Carbon and Nitrogen in the Terrestrial Environment. Springer, 415 pp.
- NOAA, 2010. National Weather Service, JetStream - Online School for Weather. National Oceanic and Atmospheric Administration (NOAA). http://www.srh.noaa.gov/jetstream/tropics/enso_impacts.htm, 15.01.2010.
- Nobre, C.A., Marengo, J.A. and Artaxo, P., 2009. Understanding the climate of Amazonia: Progress from LBA. In: M. Keller, M. Bustamante, J. Gash and P.S. Dias (Editors), *Amazonia and global change*. American Geophysical Union, Washington, DC, pp. 145-147.
- Novick, K.A., Oren, R., Stoy, P.C., Siqueira, M.B.S. and Katul, G.G., 2009. Nocturnal evapotranspiration in eddy-covariance records from three co-located ecosystems in the Southeastern US: Implications for annual fluxes. *Agricultural and Forest Meteorology*, 149(9): 1491-1504.
- Oki, T. and Kanae, S., 2006. Global Hydrological Cycles and World Water Resources. *Science*, 313(5790): 1068-1072.
- Phillips, O.L., Aragao, L., Lewis, S.L., Fisher, J.B., Lloyd, J., Lopez-Gonzalez, G., Malhi, Y., Monteagudo, A., Peacock, J., Quesada, C.A., van der Heijden, G., Almeida, S., Amaral, I., Arroyo, L., Aymard, G., Baker, T.R., Banki, O., Blanc, L., Bonal, D., Brando, P., Chave, J., de Oliveira, A.C.A., Cardozo, N.D., Czimczik, C.I., Feldpausch, T.R., Freitas, M.A., Gloor, E., Higuchi, N., Jimenez, E., Lloyd, G., Meir, P., Mendoza, C., Morel, A., Neill, D.A., Nepstad, D.,

- Patino, S., Penuela, M.C., Prieto, A., Ramirez, F., Schwarz, M., Silva, J., Silveira, M., Thomas, A.S., ter Steege, H., Stropp, J., Vasquez, R., Zelazowski, P., Davila, E.A., Andelman, S., Andrade, A., Chao, K.J., Erwin, T., Di Fiore, A., Honorio, E., Keeling, H., Killeen, T.J., Laurance, W.F., Cruz, A.P., Pitman, N.C.A., Vargas, P.N., Ramirez-Angulo, H., Rudas, A., Salamao, R., Silva, N., Terborgh, J. and Torres-Lezama, A., 2009. Drought Sensitivity of the Amazon Rainforest. *Science*, 323(5919): 1344-1347.
- Priante-Filho, N., Vourlitis, G.L., Hayashi, M.M.S., Nogueira, J.D., Campelo, J.H., Nunes, P.C., Souza, L.S.E., Couto, E.G., Hoeger, W., Raiter, F., Trienweiler, J.L., Miranda, E.J., Priante, P.C., Fritzen, C.L., Lacerda, M., Pereira, L.C., Biudes, M.S., Suli, G.S., Shiraiwa, S., Do Paulo, S.R. and Silveira, M., 2004. Comparison of the mass and energy exchange of a pasture and a mature transitional tropical forest of the southern Amazon Basin during a seasonal transition. *Global Change Biology*, 10(5): 863-876.
- Reid, R., Thornton, P., McCrabb, G., Kruska, R., Atieno, F. and Jones, P., 2004. Is it possible to mitigate greenhouse gas emissions in pastoral ecosystems of the tropics? *Environment, Development and Sustainability*, 6(1): 91-109.
- Sakai, R.K., Fitzjarrald, D.R., Moraes, O.L.L., Staebler, R.M., Acevedo, O.C., Czikowsky, M.J., Da Silva, R., Brait, E. and Miranda, V., 2004. Land-use change effects on local energy, water, and carbon balances in an Amazonian agricultural field. *Global Change Biology*, 10(5): 895-907.
- Saleska, S., da Rocha, H., Kruijt, B. and Nobre, A.D., 2009a. The changing rates and patterns of deforestation and land use in Brazilian Amazonia. In: M. Keller, M. Bustamante, J. Gash and P.S. Dias (Editors), *Amazonia and Global Change*. American Geophysical Union, Washington, DC, pp. 389-408.
- Saleska, S., da Rocha, H., Kruijt, B. and Nobre, A.D., 2009b. Ecosystem carbon fluxes and Amazonian forest metabolism. In: M. Keller, M. Bustamante, J. Gash and P.S. Dias (Editors), *Amazonia and Global Change*. American Geophysical Union, Washington, DC, pp. 389-408.
- Saleska, S.R., Miller, S.D., Matross, D.M., Goulden, M.L., Wofsy, S.C., da Rocha, H.R., de Camargo, P.B., Crill, P., Daube, B.C., de Freitas, H.C., Hutyyra, L., Keller, M., Kirchhoff, V., Menton, M., Munger, J.W., Pyle, E.H., Rice, A.H. and Silva, H., 2003. Carbon in Amazon forests: Unexpected seasonal fluxes and disturbance-induced losses. *Science*, 302(5650): 1554-1557.
- San José, J., Montes, R., Grace, J. and Nikonova, N., 2008. Land-use changes alter CO₂ flux patterns of a tall-grass *Andropogon* field and a savanna-woodland continuum in the Orinoco lowlands. *Tree Physiology*, 28(3): 437-450.
- Santos, A.J.B., Quesada, C.A., Da Silva, G.T., Maia, J.F., Miranda, H.S., Miranda, A.C. and Lloyd, J., 2004. High rates of net ecosystem carbon assimilation by *Brachiara* pasture in the Brazilian Cerrado. *Global Change Biology*, 10(5): 877-885.
- Sarmiento, J.L., Gloor, M., Gruber, N., Beaulieu, C., Jacobson, A.R., Fletcher, S.E.M., Pacala, S. and Rodgers, K., 2010. Trends and regional distributions of land and ocean carbon sinks. *Biogeosciences*, 7(8): 2351-2367.
- Sarmiento, J.L. and Gruber, N., 2006. *Ocean Biogeochemical Dynamics*. Princeton University Press.
- Scherer-Lorenzen, M., Bonilla, J.L. and Potvin, C., 2007. Tree species richness affects litter production and decomposition rates in a tropical biodiversity experiment. *Oikos*, 116(12): 2108-2124.

- Schwalm, C.R., Williams, C.A., Schaefer, K., Arneth, A., Bonal, D., Buchmann, N., Chen, J.Q., Law, B.E., Lindroth, A., Luysaert, S., Reichstein, M. and Richardson, A.D., 2010. Assimilation exceeds respiration sensitivity to drought: A FLUXNET synthesis. *Global Change Biology*, 16(2): 657-670.
- Schwarzl, K. and Punzel, J., 2007. Hood infiltrometer - A new type of tension infiltrometer. *Soil Science Society of America Journal*, 71(5): 1438-1447.
- Scott, D.F., Bruijnzeel, L.A. and Mackensen, J., 2005. The hydrological and soil impacts of forestation in the tropics, *Forests, Water and People in the Humid Tropics*. International Hydrology Series. Cambridge Univ Press, New York, pp. 622-651.
- Seitlinger, T., 2008. Einfluss der Artenzahl auf die Phosphorgehalte der oberirdischen Biomasse und auf die Phosphorverfügbarkeit im Boden, University of Zurich, Zurich, 58 pp.
- Serrano-Ortiz, P., Roland, M., Sanchez-Moral, S., Janssens, I.A., Domingo, F., Godderis, Y. and Kowalski, A.S., 2010. Hidden, abiotic CO₂ flows and gaseous reservoirs in the terrestrial carbon cycle: Review and perspectives. *Agricultural and Forest Meteorology*, 150(3): 321-329.
- Silver, W.L., Kueppers, L.M., Lugo, A.E., Ostertag, R. and Matzek, V., 2004. Carbon sequestration and plant community dynamics following reforestation of tropical pasture. *Ecological Applications*, 14(4): 1115-1127.
- STRI, 2010. Physical Monitoring Program. Smithsonian Tropical Research Institute (STRI). http://striweb.si.edu/esp/physical_monitoring/index_phy_mon.htm, 15.01.2010.
- Tan, Z.H., Zhang, Y.P., Yu, G.R., Sha, L.Q., Tang, J.W., Deng, X.B. and Song, Q.H., 2010. Carbon balance of a primary tropical seasonal rain forest. *Journal of Geophysical Research-Atmospheres*, 115.
- Trenberth, K.E. and Fasullo, J.T., 2010. Climate Change, Tracking Earth's Energy. *Science*, 328(5976): 316-317.
- Van Noordwijk, M., Woomer, P.L., Algre, J.C., Arévalo, L., Castilla, C.E., Cordeiro, D.C., Hairiah, K., Kotto-Same, J., Moukam, A., Parton, W.J., Ricse, A., Rodrigues, V. and Sitompu, I.S.M., 2005. Carbon losses and sequestration after land use change in the humid tropics. In: C.A. Palm, S.A. Vosti, P.A. Sanchez and P.J. Ericksen (Editors), *Palm Slash-and-Burn Agriculture: the Search for Alternatives*. Columbia University Press, New York, pp. 41-63.
- Vanclay, J.K., 2009. Managing water use from forest plantations. *Forest Ecology and Management*, 257(2): 385-389.
- Vargas, R., Baldocchi, D.D., Querejeta, J.I., Curtis, P.S., Hasselquist, N.J., Janssens, I.A., Allen, M.F. and Montagnani, L., 2010. Ecosystem CO₂ fluxes of arbuscular and ectomycorrhizal dominated vegetation types are differentially influenced by precipitation and temperature. *New Phytologist*, 185(1): 226-236.
- von Randow, C., Manzi, A.O., Kruijt, B., de Oliveira, P.J., Zanchi, F.B., Silva, R.L., Hodnett, M.G., Gash, J.H.C., Elbers, J.A., Waterloo, M.J., Cardoso, F.L. and Kabat, P., 2004. Comparative measurements and seasonal variations in energy and carbon exchange over forest and pasture in South West Amazonia. *Theoretical and Applied Climatology*, 78(1-3): 5-26.
- Vourlitis, G.L., Nogueira, J.D.S., Priante, N., Hoeger, W., Raiter, F., Biudes, M.S., Arruda, J.C., Capistrano, V.B., de Faria, J.L.B. and Lobo, F.D.A., 2005. The sensitivity of Diel CO₂ and H₂O vapor exchange of a tropical transitional forest to seasonal variation in meteorology and water availability. *Earth Interactions*, 9.

- Vourlitis, G.L., Priante, N., Hayashi, M.M.S., Nogueira, J.D., Caseiro, F.T. and Campelo, J.H., 2001. Seasonal variations in the net ecosystem CO₂ exchange of a mature Amazonian transitional tropical forest (cerradao). *Functional Ecology*, 15(3): 388-395.
- Vourlitis, G.L., Priante, N., Hayashi, M.M.S., Nogueira, J.D., Raiter, F., Hoegel, W. and Campelo, J.H., 2004. Effects of meteorological variations on the CO₂ exchange of a Brazilian transitional tropical forest. *Ecological Applications*, 14(4): 89-100.
- Walter, H. and Lieth, H., 1960. *Klimadiagramm Weltatlas*. Fischer Verlag, Jena.
- Wang, W. and Fang, J.Y., 2009. Soil respiration and human effects on global grasslands. *Global and Planetary Change*, 67(1-2): 20-28.
- Wassenaar, T., Gerber, P., Verburg, P.H., Rosales, M., Ibrahim, M. and Steinfeld, H., 2007. Projecting land use changes in the Neotropics: The geography of pasture expansion into forest. *Global Environmental Change*, 17(1): 86-104.
- Waterloo, M.J., Oliveira, S.M., Drucker, D.P., Nobre, A.D., Cuartas, L.A., Hodnett, M.G., Langedijk, I., Jans, W.W.P., Tomasella, J., de Araujo, A.C., Pimentel, T.P. and Estrada, J.C.M., 2006. Export of organic carbon in run-off from an Amazonian rainforest blackwater catchment. *Hydrological Processes*, 20(12): 2581-2597.
- Watson, R.T., Noble, I.R., Bolin, B., Ravindranath, N.H., Verardo, D.J., Dokken, D.J. and eds, 2000. *Land use, Land-use change, and Forestry. A Special Report of the Intergovernmental Panel on Climate Change (IPCC)*. Cambridge University Press, New York.
- Webb, E.K., Pearman, G.I. and Leuning, R., 1980. Correction of flux measurements for density effects due to heat and water-vapor transfer. *Quarterly Journal of the Royal Meteorological Society*, 106(447): 85-100.
- Werth, D. and Avissar, R., 2004. The regional evapotranspiration of the Amazon. *Journal of Hydrometeorology*, 5(1): 100-109.
- White, R., Murray, S. and Rohweder, M., 2000. *Pilot Analysis of Global Ecosystems (PAGE), Grassland Ecosystems*. World Resources Institute, Washington, DC, 81 pp.
- Wilsey, B.J., Parent, G., Roulet, N.T., Moore, T.R. and Potvin, C., 2002. Tropical pasture carbon cycling: relationships between C source/sink strength, above-ground biomass and grazing. *Ecology Letters*, 5(3): 367-376.
- Wilson, K., Goldstein, A., Falge, E., Aubinet, M., Baldocchi, D., Berbigier, P., Bernhofer, C., Ceulemans, R., Dolman, H., Field, C., Grelle, A., Ibrom, A., Law, B.E., Kowalski, A., Meyers, T., Moncrieff, J., Monson, R., Oechel, W., Tenhunen, J., Valentini, R. and Verma, S., 2002. Energy balance closure at FLUXNET sites. *Agricultural and Forest Meteorology*, 113(1-4): 223-243.
- Xu, L.K. and Baldocchi, D.D., 2004. Seasonal variation in carbon dioxide exchange over a Mediterranean annual grassland in California. *Agricultural and Forest Meteorology*, 123(1-2): 79-96.
- Zhang, L., Wylie, B.K., Ji, L., Gilmanov, T.G. and Tieszen, L.L., 2010. Climate-Driven Interannual Variability in Net Ecosystem Exchange in the Northern Great Plains Grasslands. *Rangeland Ecology & Management*, 63(1): 40-50.
- Zimmermann, B., Elsenbeer, H. and De Moraes, J.M., 2006. The influence of land-use changes on soil hydraulic properties: Implications for runoff generation. *Forest Ecology and Management*, 222(1-3): 29-38.

Appendixes

Appendix A:

Schneebeli M, Mätzler C, **Wolf S**, Eugster W (2008) X-band opacity of a tropical tree canopy and its relation to intercepted rain, eddy fluxes and other meteorological variables. *Microwave Radiometry and Remote Sensing of the Environment, MICRORAD 2008*. doi: 10.1109/MICRAD.2008.4579514. pp 223-235

Appendix B:

Schneebeli M, **Wolf S**, Kunert N, Eugster W, Mätzler C (accepted) Relating the X-Band opacity of a tropical tree canopy to sapflow, rain interception and dew formation. *Remote Sensing of Environment*

Appendix C:

Potvin C, Manzilla L, Buchmann N, Monteza J, Moore T, Murphy M, Oelmann Y, Scherer-Lorenzen M, Turner, B.L., Wilcke W, Zeugin F, **Wolf S** (in press) An ecosystem approach to biodiversity effects: carbon pools in a tropical tree plantation. *Forest Ecology and Management*. doi: 10.1016/j.foreco.2010.11.015

Appendix D:

GIS Maps

X-Band Opacity of a Tropical Tree Canopy and its Relation to Intercepted Rain, Eddy Fluxes and other Meteorological Variables

Marc Schneebeli
and Christian Mätzler
Institute of Applied Physics
University of Bern
Bern, Switzerland
Email: schnee@iap.unibe.ch

Sebastian Wolf
and Werner Eugster
Institute of Plant Sciences
Federal Institute of Technology
Zurich, Switzerland
Email: sebastian.wolf@ipw.agrl.ethz.ch

Abstract—During Summer and Autumn 2007, we deployed a 11 GHz microwave radiometer in an experimental tree plantation in Sardinilla, Panama, in the vicinity of the Panama Canal. With this instrument, we determined the opacity of the tree canopy. A collocated eddy-covariance flux tower measured water vapor and carbon dioxide fluxes as well as other meteorological variables such as photosynthetically active radiation (PAR), vapor pressure deficit (VPD) and rain. We observed a pronounced diurnal cycle of the opacity during dry periods and a close relation of the opacity to canopy intercepted rain during rainy periods. The diurnal opacity cycle shows a strong correlation with PAR, VPD and the water vapor flux.

I. INTRODUCTION

Tropical rain forests play a dominant role in the earth's water cycle. Direct evaporation of rain and evapotranspiration are major sources of lower tropospheric humidity. A promising tool to monitor these processes is microwave radiometry.

Microwave properties of tree canopies have been investigated for many years and a good overview over this research topic is given in [1]. In contrast to the wealth of available information, reports on measurements of diurnal variations in tree opacities as well as observations of tree opacities focusing on intercepted water are rather sparse. In [2] the authors reported diurnal variations in the dielectric constant of the xylem and hypothesize a relation to the ascent of sap in the xylem. In [3] diurnal changes of the radar backscatter of tropical trees with the Ku-Band Radar of the TRMM satellite were studied and it was concluded that the signal has a relation to dew deposition. A large experiment on diurnal changes in the optical and microwave frequency range was reported in [4], although not very clear conclusions on diurnal behaviour could be drawn from their X-Band measurements. The measurement of the attenuation of a 10 GHz signal over a horizontal path through a Douglas fir stand was reported in [5] and a nice linear relation to intercepted rain was found. The authors then proposed this attenuation method as a tool to monitor rain water interception.

Recently, because of the launch of the SMOS satellite in the near future, L-Band attenuation through tree canopies becomes more and more interesting and therefore several studies are being performed with L-Band radiometers. A very recent study measured the L-Band and X-Band transmissivities of a deciduous forest site during 4 months with a method similar to ours but the focus of this work was not put on diurnal changes [6].

In our experiment to be presented here, we measured the brightness temperature of a tropical tree canopy, consisting of *Anacardium excelsum*, *Tabebuia rosea* and *Hura crepitans*. These trees are part of an experimental biodiversity plantation, have an age of about seven years and an average height of 8 m. We modeled the incoming sky radiation with a radiative transfer model which allowed us to calculate the canopy opacity. We accounted for the effect of temperature on the opacity with a simple canopy opacity model. Finally we state that the difference between the opacity model and the measured opacity originates from unaccounted dielectric changes in the tree, probably induced by sap flow, dew deposition and intercepted rain.

II. EXPERIMENTAL SETUP

Our microwave radiometer was placed on the ground, looking upwards through the canopy under an elevation angle of 40°, measuring in horizontal polarization. The radiometer was placed below a tarp, which allowed us also to measure during rain. Data were gathered from July to October 2007. Figure 1 shows the instrument as it was deployed in the field.

A. Microwave radiometer

For this experiment, a simple single polarization 11.4 GHz microwave radiometer has been developed. For our purpose and in order to be deployed in a tropical environment, the instrument had to fulfill several requirements. First of all, we required an instrument with automated internal calibration, since tipping-calibration is not possible below the canopy and manual calibration with hot/cold loads not desirable. To



Fig. 1. The radiometer deployed in the field

achieve this, the instrument was equipped with a waveguide switch, switching every 5 s to an ambient load (internal termination load enclosed in a copper block). Every minute, additional 80 K noise from a solid state noise source was coupled in over a 20 dB cross coupler.

Second, the instrument required protection against tropical heat, high relative humidity, rain and insects. This was achieved with installing the radiometer together with the horn antenna in a sealed solid aluminum box. The radiation entered through a microwave transparent Styrofoam window in the box. The Schottky diode detectors and the noise source, being the most temperature critical components, were enclosed in a solid aluminum block and attached to a Peltier element, capable of heating and cooling. The temperature of this block was stabilized to 26° C such that the Peltier element had to cool during the day and to heat during the night, when we had high relative humidity.

Finally our system had built-in data acquisition and storage and was capable of unattended operation over several days. Data were taken every 100 ms and averaged over one full calibration cycle, which took 1 min.

The radiometer has two channels, both measuring at the same center frequency but one with 50 MHz and the other with 500 MHz bandwidth. The antenna we used is a rectangular horn with a beamwidth of about 15°. In addition to the microwave part, we installed a thermal infrared radiometer (Everest 4000.5 GL) into the box. A schematic drawing of the instrument can be found in Figure 2.

B. Other measurements

Collocated to the microwave radiometer, an eddy-covariance flux tower measured CO₂ and water vapor fluxes over the canopy. In addition, other variables like temperature, soil moisture, wind, photosynthetically active radiation (PAR) and relative humidity were also measured. Rain measurements were performed with two tipping buckets, of which one was placed below the canopy and another in the open field. The leaf area index (LAI) of the canopy was determined

with hemispherical photography and the software 'Gap Light Analyzer' (© Simon Fraser University, Institute of Ecosystem Studies, BC).

III. METHOD AND MEASUREMENTS

A. Canopy opacity measurement

According to [7], the canopy transmissivity t_c can be expressed with the following equation:

$$t_c = \frac{T_c - T_{b,in}}{T_c - T_{b,sky}} \quad (1)$$

T_c is hereby the physical canopy temperature measured with our infrared radiometer, $T_{b,in}$ is the brightness temperature measured with the microwave radiometer and $T_{b,sky}$ is the brightness temperature emitted from the sky. This formula is valid if the emissivity of the ground is high and if the temperature difference between the ground and the canopy as well as the canopy reflectivity are low. The opacity is then calculated with the Beer-Lambert law, yielding the expression $\tau = -\log(t)$. What we can not measure with our configuration is the sky radiation $T_{b,sky}$, and therefore this contribution needs to be modeled. To do so, we used ECMWF profiles of water vapor volume mixing ratio, pressure and temperature. Those profiles were interpolated on a quarter hour time grid and scaled with the measured ground values. Cloud water was added to the profile with an algorithm described in [8]. With the so derived atmospheric profiles, we calculated absorption coefficients with an atmospheric propagation model [9]. Radiative transfer calculations led then to the T_{b1} under rain free conditions, with typical values of 20 K at an elevation angle of 40°. In order to account for the rain contribution on the incoming sky radiation, we measured the sky brightness temperature during rain events and set the measured increase in brightness temperature in relation to the rain rate. We were then able to account for the rain contribution on the incoming sky radiation. It is clear that we cannot calculate the brightness temperature T_{b1} very accurately with the described technique, but the impact of T_{b1} on the canopy opacity is rather weak. An underestimation of T_{b1} of 20 K results in an opacity error of about 4%.

B. Canopy opacity model

For the interpretation of our measurements we incorporate an effective medium canopy opacity model of leaves, that treats scattering with a geometrical optics approach. It is described in [10] and reads:

$$\tau_c = A_p \cdot \text{LAI} \cdot k d \epsilon'' \frac{1}{\cos \theta} t_l \quad (2)$$

with A_p being a geometrical factor we set to 1, the leaf area index LAI with a value of 3.5, the wave number k , leaf thickness d , the complex part of the leaf dielectric constant ϵ'' , observation angle θ and the single leaf transmissivity t_l . t_l can be computed with the coherent model for layered media, discussed for example in [11]. As input parameters the model requires the frequency, incidence angle, leaf thickness and

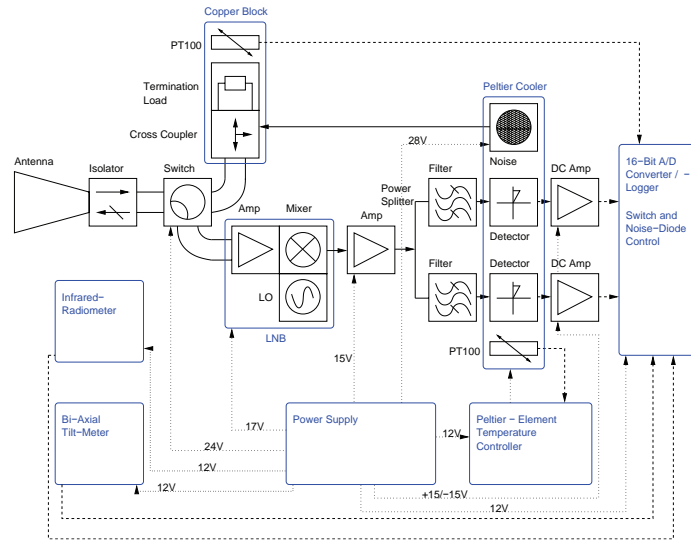


Fig. 2. Schematic drawing of the microwave radiometer

leaf dielectric constant ϵ . The leaf thickness distribution was measured and a mean value of approx. 0.2 mm was found. We determined the leaf dielectric constant with the semi-empirical model developed in [12]. It reads:

$$\epsilon = 0.522(1 - 1.32m_d)\epsilon_{sw} + 0.51 + 3.84m_d \quad (3)$$

with the leaf dry matter fraction m_d and the temperature dependent saline water dielectric constant ϵ_{sw} . This constant was determined with a dielectric model of sea water [13]. For the salinity, we used a constant value of 0.5 ‰. The quotient of the dried leaf mass and the fresh leaf mass m_d was determined to a value of approx. 0.4. For our model opacity τ_{mod} , we keep all of the above inputs fixed with the exception of the canopy temperature T_c .

C. Measurement and modeling examples

Time series of the measured canopy opacity τ_{me} and τ_{mod} as well as of the canopy infrared temperature are shown in Figure 3 during an almost rainless period of 4 days.

IV. RESULTS AND DISCUSSION

In the upper panel of Figure 3 we see that our opacity measurements and the modeled opacities are anti-correlated. Therefore we conclude that the measured opacity τ_{me} must be expressed as a sum of different opacity contributions:

$$\tau_{me} = \tau_{diu} + \tau_{wet} + \tau_{mod} \quad (4)$$

with τ_{diu} being the diurnal contribution and τ_{wet} being the contribution coming from water on the leaves. In this equation, τ_{mod} only accounts for opacity changes due to the change in temperature of the canopy. The difference $\tau_{me} - \tau_{mod}$ during a rain- and dewfree period ($\tau_{wet} = 0$) leads to the diurnal

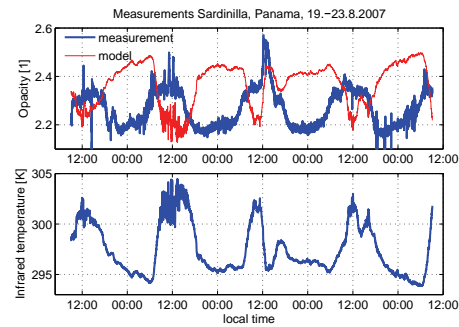


Fig. 3. Time series of modeled and measured opacity (upper panel) and the canopy infrared temperature (lower panel). The shown period was dry with the exception of a weak rain shower (5 mm of rain) around 12 o'clock at the third day.

contribution, which is plotted in in Figure 4 together with PAR, VPD and the CO_2 and water vapor fluxes for the same period as in Figure 3. It is obvious that there is a strong correlation between the diurnal opacity τ_{diu} and the other plotted variables.

VPD and PAR are proxies for the flow of sap in the tree. Since τ_{diu} has to originate from one or several of the input parameters of the opacity model that were held constant (d , m_d , salinity), we conclude that sap flow induces changes in one or several of these parameters.

If we want to study τ_{wet} , we have to model τ_{diu} with one of the variables of Figure 4. We achieve the best fit with the

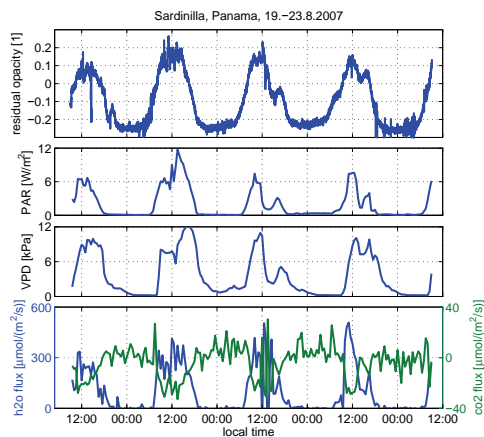


Fig. 4. Time series of the diurnal opacity contribution τ_{diu} , VPD, PAR and the eddy fluxes for the same time period as in Figure 3

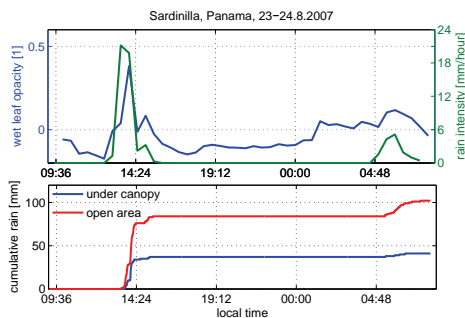


Fig. 5. Upper panel: τ_{wet} (blue curve) and the difference between the open area rain intensity and the rain intensity under the canopy with a time resolution of 30 min (green curve). Lower panel: The cumulative rain sum from the two tipping buckets with a one minute time resolution.

following expression:

$$\tau_{\text{diu}} = 0.055 + 0.4 \cdot \text{PAR} \cdot e^{(-0.7 \cdot \text{PAR} + 0.002)} - 0.3 \quad (5)$$

This Equation together with Eq. 4 allows us to calculate τ_{wet} as a function of PAR, τ_{me} and τ_{mod} . In the upper panel of Figure 5, τ_{wet} is plotted together with the difference between the cumulative rain sum of the two tipping buckets divided by the 30 min time bin for a period with two rain events. We see a strong resemblance between the two curves, but the increase of the microwave signal during the night is not reflected in the green curve. We assume that this increase is induced by dew deposition on the leaves during the night.

V. CONCLUSION

We have shown some evidence that the observed diurnal cycle in the residual opacity can be explained with dielectric

changes in the leaves induced by sap flow. We have also shown that water deposited on the leaves has a strong influence on the canopy opacity. If we are able to accurately model the diurnal opacity cycle, we can calculate the opacity change due to leaf wetness. This method can possibly be used for dew deposition, evapotranspiration and rain interception studies.

ACKNOWLEDGMENT

Since this project was based on a private initiative, I am very grateful for the financial support I received from the following Swiss institutions: Prof. Heinrich Greinacher Foundation; Travel grants commission and the Remote sensing commission of the Swiss Academy of Sciences SCNAT; Institute of Plant Sciences, Federal Institute of Technology; Institute of Applied Physics, University of Bern.

Further, I am also very appreciative to logistics support provided by the Smithsonian Tropical Research Institute, Panama and to Prof. Catherine Potvin from the McGill University, Canada, who allowed me to conduct this project on her research plantation. I would like to thank the Institute of Geography of the University of Bern that lent me the hemispherical camera and last but not least José and Iliana Monteza-Cabrera with family who shared their home with me and made my stay very comfortable.

REFERENCES

- [1] A. A. Chukhlantsev, *Microwave Radiometry of Vegetation Canopies*. 3300 AA Dordrecht, The Netherlands: Springer, 2006.
- [2] K. C. McDonald, R. Zimmermann, and J. S. Kimball, "Diurnal and spatial variation of xylem dielectric constant in norway spruce (*Picea abies* [L.] karst.) as related to microclimate, xylem sap flow, and xylem chemistry," *IEEE Trans. Geosci. Remote Sens.*, vol. 40, no. 9, pp. 2063–2082, 2002.
- [3] M. Satake and H. Hanado, "Diurnal change of amazon rain forest σ^0 observed by Ku-band spaceborne radar," *IEEE Trans. Geosci. Remote Sens.*, vol. 42, no. 6, pp. 1127–1134, 2004.
- [4] J. Way, J. Paris, M. Dobson, K. McDonald, F. T. Ulaby, and V. Vanderbilt, "Diurnal change in trees as observed by optical and microwave sensors: The Eos synergism study," *IEEE Trans. Geosci. Remote Sens.*, vol. 29, no. 6, pp. 817–820, 2004.
- [5] W. Bouten, P. Swart, and E. D. Water, "Microwave transmission, a new tool in forest and hydrological research," *J. of Hydrology*, vol. 124, no. 1-2, pp. 119–130, 1991.
- [6] M. Guglielmetti, M. Schwank, C. Mätzler, C. Oberdörster, J. Vanderborght, and H. Flübler, "Measured microwave radiative transfer properties of a deciduous forest canopy," *Remote Sens. Environ.*, vol. 109, no. 4, pp. 523–532, 2007.
- [7] C. Mätzler, "Microwave transmissivity of a forest canopy: Experiments made with a beech," *Remote Sens. Environ.*, vol. 48, pp. 172–180, 1994.
- [8] P. W. Rosenkranz, "Retrieval of temperature and moisture profiles from AMSU-A and AMSU-B measurements," *IEEE Trans. Geosci. Remote Sens.*, vol. 39, no. 11, pp. 2429–2435, 2001.
- [9] —, "Water vapor microwave continuum absorption: A comparison of measurements and models," *Radio Sci.*, vol. 33, pp. 919–928, 1998.
- [10] U. Wegmüller, C. Mätzler, and E. G. Njoku, "Canopy opacity models," in *Passive Microwave Remote Sensing of Land-Atmosphere Interactions*, E. G. Njoku, P. Pampaloni, B. J. Choudhury, and Y. H. Kerr, Eds. Utrecht, The Netherlands: VSP, 1995, pp. 375–387.
- [11] J. A. Kong, *The Theory of Electromagnetic Waves*. New York: J. Wiley & Sons, 1975.
- [12] C. Mätzler, "Microwave (1–100 GHz) dielectric model of leaves," *IEEE Trans. Geosci. Remote Sens.*, vol. 32, no. 5, pp. 947–949, 1994.
- [13] T. Meissner and F. J. Wentz, "The complex dielectric constant of pure and sea water from microwave satellite observations," *IEEE Trans. Geosci. Remote Sens.*, vol. 42, no. 9, pp. 1836–1849, 2004.

Relating the X-band Opacity of a Tropical Tree Canopy to Sapflow, Rain Interception and Dew Formation

Marc Schneebeli^{a,c,e}, Sebastian Wolf^b, Norbert Kunert^d, Werner Eugster^b, Christian Mätzler^c

^aEPFL, Environmental Remote Sensing Laboratory, Lausanne, Switzerland

^bETH Zurich, Institute of Plant, Animal and Agroecosystem Sciences, Zurich, Switzerland

^cUniversity of Bern, Institute of Applied Physics, Bern, Switzerland

^dMax-Planck-Institute for Biogeochemistry, Department of Biogeochemical Processes, Jena, Germany

^enow at: National Institute for Space Research (INPE), Center for Weather Forecast and Climate Studies (CPTEC), Cachoeira Paulista/SP, Brazil

Abstract

During summer and autumn 2007, a 11 GHz microwave radiometer was deployed in an experimental tree plantation in Sardinilla, Panama. The opacity of the tree canopy was derived from incoming brightness temperatures received on the ground. A collocated eddy-covariance flux tower measured water vapor fluxes and meteorological variables above the canopy. In addition, xylem sapflow of trees was measured within the flux tower footprint. We observed considerable diurnal differences between measured canopy opacities and modeled theoretical opacities, that were closely linked to xylem sapflow. It is speculated that dielectric changes in the leaves induced by the sapflow are causing the observed diurnal changes. In addition, canopy intercepted rain and dew formation also modulated the diurnal opacity cycle. With an enhanced canopy opacity model accounting for water deposited on the leaves, we quantified the influence of canopy stored water (i.e. intercepted water and dew) on the opacity. A time series of dew formation and rain interception was directly monitored during a period of two weeks. We found that during light rainfall up to 60% of the rain amount is intercepted by the canopy whereas during periods of intense rainfall, only 4% were intercepted. On average, 0.17 mm of dew was formed during the night. Dew evaporation contributed 5% to the total water vapor flux measured above the canopy.

Keywords: X-band, Tropics, Rain interception, Dew, Sapflow, Radiometry, Microwave techniques, Eddy Covariance

1. Introduction

1.1. Rain interception and dew formation

Tropical rain forests play a dominant role in the earth's water balance. An important fraction of the hydrological cycle amounts to rain water interception and its subsequent re-evaporation. According to Lawrence et al. (2007), transpiration is the dominant process of evapotranspiration with a contribution of 58%, followed by interception evaporation (33%) and soil evaporation (9%).

Rain interception is rather difficult to measure accurately. The most frequently used technique is the measurement of throughfall by setting up several rain-gauges below the canopy and one or more above the canopy. The difference of the collected water is assumed to be withheld by the canopy. There are some major drawbacks to this method: Due to the complex structure of a forest canopy, the spatial variability of the throughfall is very large, hence numerous rain gauges are needed in order to achieve representative and accurate sampling (Kimmins, 1973). Direct evaporation of intercepted rain water is another effect that cannot be tackled with the throughfall method, wherefore reliable measurements can only be conducted during night time.

A promising technique is the attenuation measurement of a 10 GHz signal over a horizontal path through a Douglas fir stand as reported in Bouten et al. (1991). They observed a

distinct linear relation of the attenuated signal to intercepted rain. The authors then employed this attenuation method in several upcoming studies as a monitoring tool for water interception in forest canopies (Bouten et al., 1996; Vrugt et al., 2003). Czikowsky and Fitzjarrald (2009) reported on a new interception estimation technique that estimates the excess evaporation following rain events with eddy covariance flux measurements.

Recently, a global assessment of canopy interception from satellite data was published in Miralles et al. (2010). The authors used an analytical interception model (Valente et al., 1997) and fed it with satellite data of precipitation, lightning frequency and canopy fraction. It was found that the interception loss is sensitive to the rainfall volume, rain intensity and the forest cover. Some of these findings will be confirmed in the article at hand.

Compared to intercepted rain, very little is known about the importance of dew formation and dew evaporation, most likely because no established measurement technique is available so far to measure the dew amount in a forest canopy. It is although known that dew not only promotes diseases of plant crops and is therefore an important parameter in agriculture (for tropical conditions see e.g. Holliday, 1980), according to Kabela et al. (2009), dew "also may contaminate remotely sensed measurements of important ecosystem variables such as soil moisture, land surface temperature, and vegetation biomass". Dew duration is relatively easy to measure by using electrical devices

Schneebeli M, Wolf S, Kunert N, Eugster W, Mätzler C (accepted) Relating the X-Band opacity of a tropical tree canopy to sapflow, rain interception and dew formation. *Remote Sensing of Environment*

that change their resistance or capacity when becoming wet (Noffsinger, 1965; Kidron et al., 1965). However, methods for measuring dew amounts (e.g. weighing dew gauges, weighing lysimeters) are limited and solely used for measurements close to the ground (Agam and Berliner, 2006).

1.2. Microwave properties of forest canopies

Microwave properties of tree canopies have been investigated for many years and good overviews over this research topic are given in Chukhlantsev (2006) and Pampaloni (2004). In contrast to the wealth of available information on radiometric forest properties like the emissivity of forests (e.g., Ferrazoli and Guerriero, 1996; Della Vecchia et al., 2007; Santi et al., 2009), canopy scattering (e.g., Karam et al., 1995) and canopy attenuation (e.g., Kurum et al., 2009), reports on measurements of diurnal variations in tree opacities as well as observations of tree opacities focusing on intercepted water are sparse. McDonald et al. (2002) reported on diurnal variations in the dielectric constant of the xylem and hypothesized a relation to the ascent of sap in the xylem. Satake and Hanado (2004) studied diurnal changes of the radar backscatter of tropical trees with the Ku-band Radar of the TRMM satellite and concluded that the signal has a relation to dew formation. A large experiment on diurnal changes in the optical and microwave frequency range was reported in Way et al. (2004), although no evident conclusions on diurnal variations could be derived from their measurements at X-band frequencies.

With the launch of the SMOS satellite in November 2009, L-band attenuation through tree canopies is recently attracting interest and therefore several studies are being performed with L-band radiometers. A recent study by Guglielmetti et al. (2007) measured the L-band and X-band transmissivities of a deciduous forest site during a 4 months defoliation period. The main focus of this work was not on diurnal changes but they found out that leaves contribute more to the transmissivity at X-band than at L-band frequencies, leading to a stronger response to the defoliation of the canopy. In addition, it was shown that the transmissivity at both frequencies is related to the rain intensity. A similar experiment was conducted by Mätzler (1994b), who observed an individual beech tree during two years with several microwave radiometers that covered a frequency range from 1 to 100 GHz. A pronounced seasonal cycle caused by the foliation and defoliation of the tree was registered during this experiment.

In our study, the downwelling brightness temperature of a tropical tree canopy was measured with an ground deployed 11.4 GHz microwave radiometer that was looking up through the canopy. The objectives of these measurements were to test if the opacity of the tree canopy underlies a diurnal cycle and to relate the microwave signal to the amount of water deposited on the leaves. In Section 2, the microwave radiometer and the other instruments are described. Section 3 treats the different radiative transfer models that allow 1. to calculate the canopy opacity, 2. to model the effect of the temperature on the opacity and 3. to account for the radiative effect of wet leaves in the canopy. Furthermore, we also relate the sapflow in the tree to opacity of the tree. These findings were then applied to opacity

time series in Section 4 and they allowed us to quantify the water amount of intercepted rain and dew formation in the canopy. Finally, in Section 5 we summarize and conclude on our findings.

2. Instruments and study site

2.1. Microwave radiometer

For this experiment, a single polarization microwave radiometer operating at a frequency of 11.4 GHz has been developed. The frequency selection was based on the availability of high-quality but still inexpensive receivers. From the point of view of the application there is nothing against this selection. For our purpose and in order to be deployed in a tropical environment, the instrument had to fulfill certain requirements. First of all, an instrument with automated internal calibration was needed, since tipping-calibration (Han and Westwater, 2000) is not possible below the canopy and manual calibration with hot/cold black-body loads not desirable. To achieve this, the instrument was equipped with a waveguide switch, switching every 5 s to an ambient load (internal termination load enclosed in a copper block). Every minute, additional 80 K noise from a solid state noise source was coupled in over a 20 dB cross coupler. Second, the instrument needed protection against tropical heat, high relative humidity, rain and insects. This was achieved by installing the radiometer together with the horn antenna in a sealed solid aluminum box. The radiation entered the box through a microwave transparent Styrofoam window. The Schottky diode detectors and the noise source, being the most temperature critical components, were enclosed in a solid aluminum block and attached to a Peltier element, capable of heating and cooling. The temperature of this block was stabilized to 26° C such that the Peltier element had to cool during the day and to heat during the night, when we had high relative humidity. Finally, our system had built-in data acquisition and storage and was capable of unattended operation over several days. Data were taken every 100 ms and averaged over one full calibration cycle of 1 min.

The radiometer has two channels, both measuring at the same center frequency but one with 50 MHz and the other with 500 MHz bandwidth. The 50 MHz channel was built in the radiometer in order to mitigate possible radio frequency interferences (RFI) that are more likely for a wider bandwidth. Since the antenna could be adjusted to a position where no RFI was detected, the wider bandwidth was employed for all the measurements, resulting in an improved signal-to-noise ratio. The antenna we used is a rectangular horn with a beam width of about 15°. In addition to the microwave part, a thermal infrared radiometer (Everest 4000.5 GL) was installed in the box. More technical details on the radiometer system are found in Schneebeli et al. (2008).

The microwave radiometer was placed on the ground, looking upwards through the canopy under an elevation angle of 40°, measuring in horizontal polarization. A tarp, set-up above the instrument without interfering with the radiometer's line-of-sight, protected the antenna from becoming wet and therefore



Figure 1: The microwave radiometer deployed in the field.

enabled us to conduct measurements during rain as well. Data were gathered from July to October 2007. Figure 1 shows the instrument operating at the field site in Sardinilla.

2.2. Sapflow measurements

Continuous measurements of xylem sapflow were performed within the flux tower footprint using the thermal dissipation method by Granier (1985). The sapflow sensors consisted of two cylindrical probes that were embedded into the tree stem (0–20 mm below cambium) with a vertical distance of 10–15 cm between both probes. Two sensors were installed on each of the 5 trees measured, at 130 cm height (DBH) on the southern and northern side of the trees. A Styrofoam box combined with reflective foil and a plastic cover reduced thermal influences and provided rain shelter. Voltage output of the thermocouple were measured every 30 sec and 15 min averages were stored on CR800 and CR1000 data loggers, and AM16/32 and AM416 multiplexer (Campbell Scientific, Logan, USA). Sap flux velocity (m/h) was calculated from differences in voltage using the calibration equation determined by Granier (1987). Further details on the measurements and the calculation of sapflow are given in Kunert et al. (2010).

2.3. Eddy covariance flux measurements

Continuous eddy covariance flux measurements were conducted at 20 Hz atop a 15 m aluminium triangle tower using an open path infrared gas analyzers (IRGA, Li-7500, LI-COR, Lincoln, USA) and a three-dimensional sonic anemometer (CSAT3, Campbell Scientific, Logan, USA). An industry grade embedded box computer (Advantech ARK-3381, Taipei, Taiwan) running a Debian based Linux operating system (Knoppix 4.0.2, Klaus Knopper, Schmalenberg, Germany) was used for the flux data acquisition. Raw data were processed to half-hourly averages using the in-house eddy covariance software eth-flux (ETH Zurich, Grassland Sciences Group) and the equation

$$F = p_a \overline{w'c'} \quad (1)$$

where F denotes the vertical water vapor flux, p_a the air density, w the vertical wind speed, c the water vapor concentration, the overbar the temporal averaging (30 min) and primes the variations from the mean. During post-processing, fluxes were corrected for damping loss (Eugster and Senn, 1995) and density fluctuations (Webb et al., 1980).

2.4. Meteorological and leaf area measurements

Additional meteorological measurements included air temperature and relative humidity (MP100A, Rotronic, Bassersdorf, Switzerland), and precipitation (10116, TOSS, Potsdam, Germany). Meteorological measurements were conducted at 10 sec and stored as half-hourly averages (sums for precipitation) using a CR23X data logger (Campbell Scientific, Logan, USA). The leaf area index (LAI) of the canopy was determined with hemispherical photography and the software ‘Gap Light Analyzer’ (© Simon Fraser University, Institute of Ecosystem Studies, BC).

Specific leaf area (SLA in $\text{cm}^2 \text{g}^{-1}$) was estimated for trees equipped with sap flow sensors. For each tree five sun leaves and five shade leaves were collected and scanned with a commercial USB-scanner. Leaf surface area was determined from the images using Win Folia 5.1 a (Rgent Instruments Inc., Quebec, Canada). Leaves were dried for 3 days at 70°C and weighed. We calculated SLA as the ratio of leaf surface to leaf dry mass.

2.5. Study site

The experiment was conducted near the village Sardinilla, Panama ($9^\circ 19' \text{N}$, $79^\circ 38' \text{W}$), in an experimental biodiversity plantation (Potvin and Dutilleul, 2009). The canopy under observation consisted of *Anacardium excelsum*, *Tabebuia rosea* and *Hura crepitans*. The trees had an age of about 7 years and an average height of 8 m. Mean SLA of the studied species and trees were 88, 96 and $138 \text{ cm}^2 \text{g}^{-1}$, respectively (Kunert, unpublished data). Our experiment took place within the wet season (May to November) that is characterized by about 250 mm rainfall per month. The site receives 2289 mm annual precipitation and the temperature is relatively constant throughout the year with an annual mean of 25.2°C .

The leaves of *Anacardium excelsum* are simple, alternative and relatively large. Leaf length is between 15 and 35 cm, leaf width is between 5 and 15 cm. The leaves have no stipules, are obovate-oblong in outline with a rounded apex. The texture is glabrous and coriaceous. The species has a rounded and dense crown (Fournier, 2003).

The leaves of *Hura crepitans* are simple and have long petioles. The leaves are ovate with cordate-shaped apex and a round base. The margin of the leaves is denticulated and the stipules are lanceolate or triangular. Leaves are between 4 and 16 cm long and equal in width. The texture is glabrous. The crown of *Hura crepitans* is wide and the horizontal spreading branches have hanging twigs (Sandi and Flores, 2003).

The leaves of *Tabebuia rosea* are decussate, compound, digitate and long petiolate. Each leaf consists out of five leaflets that differ in size, with the leaflet in the middle being the largest.

The shape ranges between elliptic-oblong, obovate and oblong-ovate. The apex is acute or acuminate, has an entire margin, and an obtuse base. The leaf surface can be glabrous or rough on both the upper and lower surfaces. The leaflets are between 6 and 20 cm long and between 3 and 10 cm wide. The crown of *Tabebuia rosea* is wide, well stratified with a few thick branches that grow irregular and horizontal (Flores and Marin, 2003).

3. Method

3.1. Canopy opacity from measurements

According to Mätzler (1994b), the canopy transmissivity t_c can be expressed with the following equation:

$$t_c = \frac{T_c - T_{b,in}}{T_c - T_{b,sky}} \quad (2)$$

T_c is hereby the physical canopy temperature measured with the infrared radiometer, $T_{b,in}$ is the brightness temperature measured with the microwave radiometer and $T_{b,sky}$ is the brightness temperature emitted from the sky. This formula is valid if one of two possible conditions is fulfilled: (1) if the reflectivity of the canopy is zero or (2) if the ground temperature is equal to T_c and the emissivity of the ground is 1. For details the reader is referred to Mätzler (1994b). Since our trees are relatively small, it is likely that condition (2) is true and that Equation 2 is therefore valid. The effective opacity is obtained with the Beer-Lambert law,

$$\tau_{meas} = -\ln(t_c). \quad (3)$$

The subscript 'meas' was added to τ to indicate that this opacity is considered as measured quantity. As stated in Mätzler (1994b), this law is only valid for homogeneous media: In a canopy, where the transmissivity within the beam of a radiometer varies due to gaps between branches and leaves, the mean opacity is higher than what is obtained with Equation (3). Since we observed a relatively dense canopy ($LAI \approx 3.5$), where the spatial inhomogeneity is expected to be small, we neglected this effect.

What cannot be measured with this configuration is the sky radiation $T_{b,sky}$, wherefore this contribution needs to be modeled. The solution of the radiative transfer equation for a non-scattering atmosphere (e.g. Janssen, 1993) is used to calculate the incoming brightness temperature on the ground:

$$T_{b,sky} = T_c e^{-\tau(s)} + \int_0^\infty (\gamma_a^{dry}(s') + \gamma_a^{rain}(s')) T(s') e^{-\tau(s')} ds' \quad (4)$$

In the above equation, $T_c \approx 3$ K is the cosmic microwave background, $\tau(s)$ is the opacity along the path through the atmosphere s , $\gamma_a^{dry}(s)$ and $\gamma_a^{rain}(s)$ are the absorption coefficients for the dry atmosphere and the rain respectively and $T(s)$ denotes the temperature profile.

We assume $\gamma_a^{dry}(s)$ to decrease exponentially with height. Therefore, the height profile of $\gamma_a^{dry}(s)$ can be written as

$$\gamma_a^{dry}(z) = \gamma_a^{dry}(0) e^{-z/z_0^{dry}} \quad (5)$$

where z_0^{dry} denotes the scale height and $z = s/\cos(\theta)$ is the height above the ground with the zenith angle θ .

In addition, $T(s)$ is assumed to decrease linearly with height while $\gamma_a^{rain}(s)$ is assumed to be equal to its surface value $\gamma_a^{rain}(0)$ between the rain layer height z_0^{rain} and the surface. Everywhere else we set $\gamma_a^{rain}(s) = 0$. Above z_0^{rain} we therefore have only the cosmic microwave background and the thermal emission from the dry atmosphere that contribute to the downwelling brightness temperature. The analytic model developed in Schneebeli and Mätzler (2011) can be used to calculate the brightness temperature T_b^{dry} intercepted at height z_0^{rain} as a function of the temperature on the ground T_g , the temperature gradient of the troposphere Γ , the height of the tropopause z_p , the scale height z_0^{dry} , the surface value of the absorption coefficient $\gamma_a^{dry}(0)$ and the zenith angle θ . Below z_0^{rain} the total absorption coefficient profile and the temperature profile need to be discretized such that Equation (4) can be solved numerically. The cosmic microwave background T_c is hereby exchanged with the already obtained T_b^{dry} .

For our simulations, the height of the tropopause z_p was set to 15 km and Γ to -6.5 K/km. With T_g , as well as the pressure and RH measured on the ground serving as input to the microwave absorption model of Rosenkranz (1998), $\gamma_a^{air}(0)$ can be determined. Similarly, $\gamma_a^{rain}(0)$ is calculated from the rain intensity measured on the ground by using the model of Liebe et al. (1993). Finally, adequate values for z_0^{rain} and z_0^{dry} had to be found. We found the best agreement between modeled brightness temperatures and measurements made above the canopy during clear-sky conditions with $z_0^{dry} = 4$ km (see Figure 3).

Usually, the rain layer height z_0^{rain} is parameterized with the height of the melting layer h_m , i.e. the 0° C barrier of the atmosphere. In the tropics, this barrier is found around 4000 m, but it was pointed out in Czekala et al. (2001) that for heavy convective situations, as they predominantly occurred in the present study, the true rain layer height is no longer of importance, because of the three-dimensional structure of the rain fields. A simplified model that takes the spatial extent of the rain cells into account was therefore developed: The horizontal length of the rain field l_r was determined from the duration of the individual rain event t_r and the average wind speed of the event v_r with $l_r = v_r t_r$. Figure 2 illustrates the situation of the radiometer being inside of a rain cell that was approaching the radiometer from ahead. From this figure it is seen that the rain layer height can be calculated as

$$z_0^{rain} = \tan(\theta)(l_r - t_e v_r) \quad (6)$$

where t_e is the elapsed time since the beginning of the rain event. If the rain cell is approaching the radiometer from behind, z_0^{rain} is calculated as

$$z_0^{rain} = \tan(\theta)(t_e v_r) \quad (7)$$

The above equations are only true if $t_e v_r$ is smaller than l_r . For the case of a rain cell approaching from the side, we have to assume that both sides of the rain field have length l_r and that the radiometer is located in the middle of the field. This leads

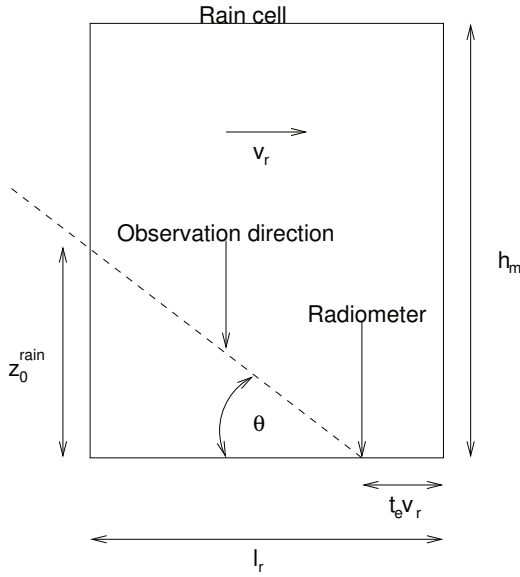


Figure 2: Sketch of the radiometer located within a rain cell of limited vertical extent. The denotations are defined in the text.

to

$$z_0^{\text{rain}} = \tan(\theta) (l_r/2) \quad (8)$$

The melting layer height $h_m = (0^\circ + T_g)/\Gamma$ is used instead of z_0^{rain} where z_0^{rain} exceeds h_m . The three different cases were distinguished with the wind direction measurements. There is also a contribution from the rain when the radiometer is not located within the cell but the radiometer beam captures radiation from the remote rain field. This contribution is not modeled because information on the intensity of the distant rain field is not available. This modeling approach might appear like a strong simplification, but it was found that $T_{b,\text{sky}}$ modeled with this method is consistent with brightness temperature measurements that were made above the canopy during rainfall (see the comparison shown in Figure 3). Without considering the three dimensional structure of the rain fields the modeled radiation would be largely too high.

One must be aware that the estimation of z_0^{rain} introduces ambiguities in the estimation of $T_{b,\text{sky}}$ during rainfall. On the other hand, the impact of $T_{b,\text{sky}}$ on the canopy opacity is relatively small: An underestimation of $T_{b,\text{sky}}$ of 20 K results in an opacity error of about 4% only. Despite the fact that the agreement between the modeled and measured brightness temperature is relatively good in the example shown in Figure 3, one must be aware that a direct measurement with a second radiometer above the canopy would lead to more trustful results. For example, the contribution of clouds cannot be taken into account with our model and it is therefore expected that opacity errors exist during overcast non-rainy situations. Another potential error source is the spatial variability of precipitation (see e.g., Moreau et al., 2009): within a few hundred meters, the rain

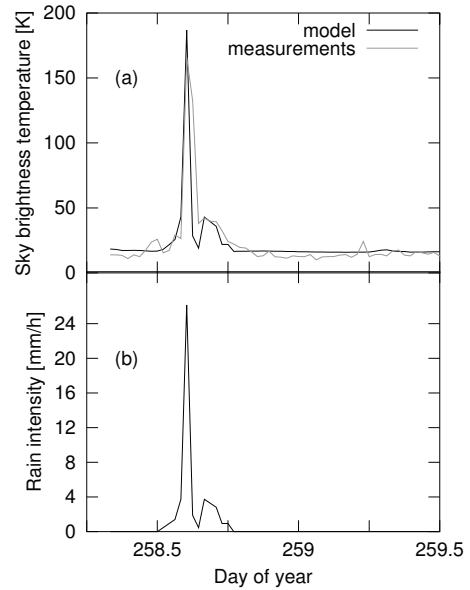


Figure 3: a) Time series of the modeled microwave brightness temperature (11.4 GHz) of the sky at an elevation angle of 40° (black line) together with the measurements made above the canopy (gray line). b) Time series of the rain intensity measured with a tipping bucket rain gauge.

intensity can vary significantly, which also introduces opacity errors since the radiometer is looking into a distant atmosphere. The fact that rain intensity data with a temporal resolution of one minute are averaged onto a half an hour time grid for the calculation of $T_{b,\text{sky}}$ might however mitigate this error source.

3.2. Canopy opacity model

For the interpretation of our measurements we incorporated an effective medium canopy opacity model of leaves, that treats scattering with a geometrical optics approach. It was described in Wegmüller et al. (1995) and is written as

$$\tau_{\text{temp}} = A_p \cdot \text{LAI} \cdot kd\epsilon_l'' \frac{1}{\cos\theta} t_l + \tau_b \quad (9)$$

The subscript ‘temp’ was added to τ in order to emphasize that in the forthcoming treatment all model parameters except the temperature are kept constant. In contrast to the original model, we added a constant opacity τ_b that takes into account the opacity contribution from the branches and the stem. In the above Equation, A_p denotes a geometrical factor we set to 1 (Wegmüller et al., 1995), the leaf area index is set to $\text{LAI} = 3.5$, $k = 2\pi/\lambda$ is the wave number, d the leaf thickness, ϵ_l'' the complex part of the leaf dielectric constant, θ the observation elevation angle and the t_l expresses the single leaf transmissivity. It can be computed with the coherent model for layered media, discussed e.g. in Kong (1975). As input parameters the

model requires the frequency, incidence angle, leaf thickness and ϵ_l . The leaf thickness distribution was manually measured and a mean value of approximately $d = 0.2$ mm was found. The leaf dielectric constant was determined with the semi-empirical model developed in Mätzler (1994a) that reads:

$$\epsilon_l = 0.522(1 - 1.32m_d)\epsilon_{sw} + 0.51 + 3.84m_d \quad (10)$$

with the leaf dry matter fraction m_d and the temperature dependent saline water dielectric constant ϵ_{sw} . This constant was determined with a dielectric model of sea water (Meissner and Wentz, 2004). For the salinity, we used a constant value of 0.5 ‰ which is a reasonable choice considering literature values given in Guglielmetti et al. (2007), McDonald et al. (2002) and El-Rayes and Ulaby (1987). In the latter report it is also seen that at X-band frequencies the influence of the salinity on the imaginary part of the dielectric constant is very low, therefore the assumption of a constant value does not hamper the applicability of the model. The quotient of the dried leaf mass and the fresh leaf mass m_d was determined to a value of about 0.4. In Mätzler (1994b) and Guglielmetti et al. (2007) the X-band opacity of a defoliated tree canopy was determined to values between 0.6 – 1.2. Since the visual impression suggests that our canopy under consideration consists of less branches than the canopies from the two cited articles, we set $\tau_b = 0.5$. This is also supported by the fact that our canopy is much younger wherefore the branches and the stem are less developed. A time series of the raw brightness temperature measurements as well as the results of this modeling and measuring approach are presented in Figure 4.

The most prominent feature between the modeled and measured opacity time series is that they exhibit a strong anti-correlated behavior. Consequently, either the measurement or the opacity modeling were wrong or at least incomplete. Since the literature gives some indication that the dielectric constant of vegetation is related to the sapflow (McDonald et al., 2002), we hypothesized that the difference between the modeled and measured opacities originated from dielectric changes related to the sapflow in the observed trees, that were not accounted for in the model. In order to test this hypothesis, the time series of the difference between the modeled (τ_{temp}) and the measured opacity (τ_{meas}), formally written as

$$\tau_{res} = \tau_{temp} - \tau_{meas} \quad (11)$$

and named ‘residual opacity’, was plotted in Figure 5-a in comparison to the time series of the sapflow.

We found a strong correlation between the two time series, at least during dry periods. Water on the leaves is expected to strongly influence the dielectric characteristics of the canopy, which is an effect that needs to be treated separately from the dielectric changes during dry conditions (see Section 3.3).

The interaction between the sapflow and τ_{res} can be quantified by only correlating the two variables during dry periods. For that, periods without water deposited on the leaves had to be identified. As a first criterion, the relative humidity, RH, had to be lower than 90%. This threshold was suggested by Thompson (1981) based on the common belief that plants remain wet after

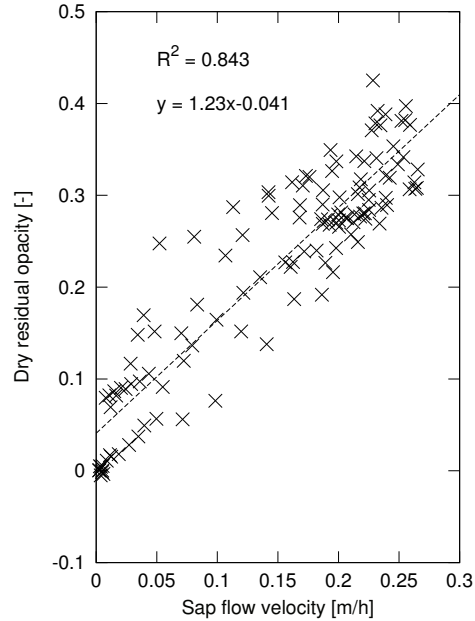


Figure 6: Scatter plot of the sapflow versus τ_{res} during dry periods.

rain or dew as long as the relative humidity remains above 90% (Agam and Berliner, 2006). Although this is not a very sharp threshold visual inspection of our own data did not suggest the need to define a different threshold. The goal in our application was to reject cases where dew formation could potentially affect our interpretation. As a second criterion for dry periods, the delay after the latest detected rainfall had to be larger than 6 hours such that there was enough time to evaporate the rain water intercepted in the tree canopy. In Figure 6, a scatter plot between the dry residual opacity, τ_{res}^{dry} , and the sapflow is shown.

The high correlation coefficient ($R^2 = 0.84$) supports the hypothesis of previously unaccounted dielectric changes induced by the flow of sap in the tree. With a linear model that relates the sapflow S with τ_{res}^{dry} , determined as

$$\tau_{res}^{dry} = 1.29 \cdot S - 0.0367 \quad (12)$$

it was now possible to completely model the time series of the canopy opacity during dry periods. Hence, any deviations of the measured opacity to modeled opacity must originate from water in the canopy. Formally, this can be expressed as

$$\tau_{meas} = \tau_{temp} + \tau_{res}^{dry} + \tau_{res}^{wet} \quad (13)$$

The opacity component that is due to a water film on the leaves, τ_{res}^{wet} , is treated with some radiative transfer considerations that will be presented in more detail below.

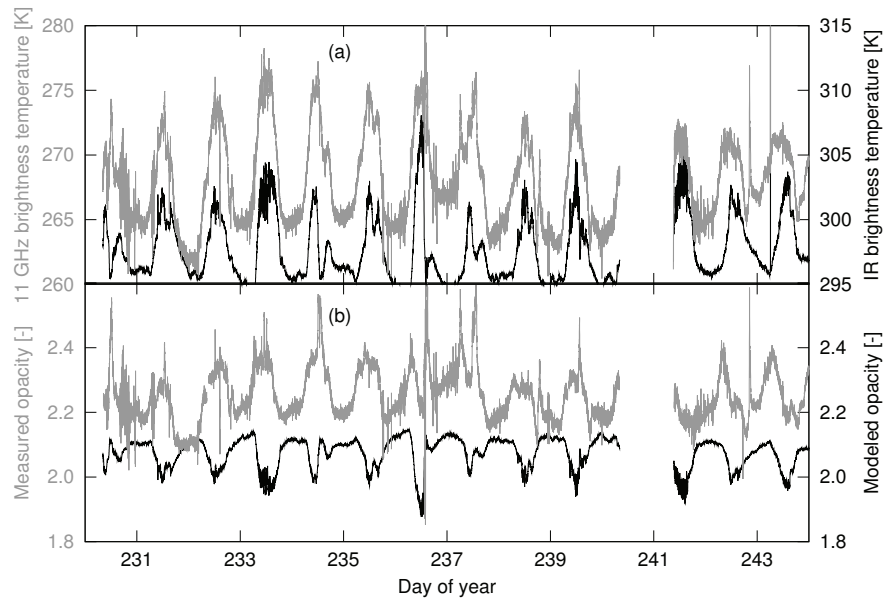


Figure 4: a) Time series of the microwave and infrared brightness temperature measurements. b) Time series of the measured canopy opacity determined with Eqs. (2,3) and the result of the modeled opacity from Eq. (9)

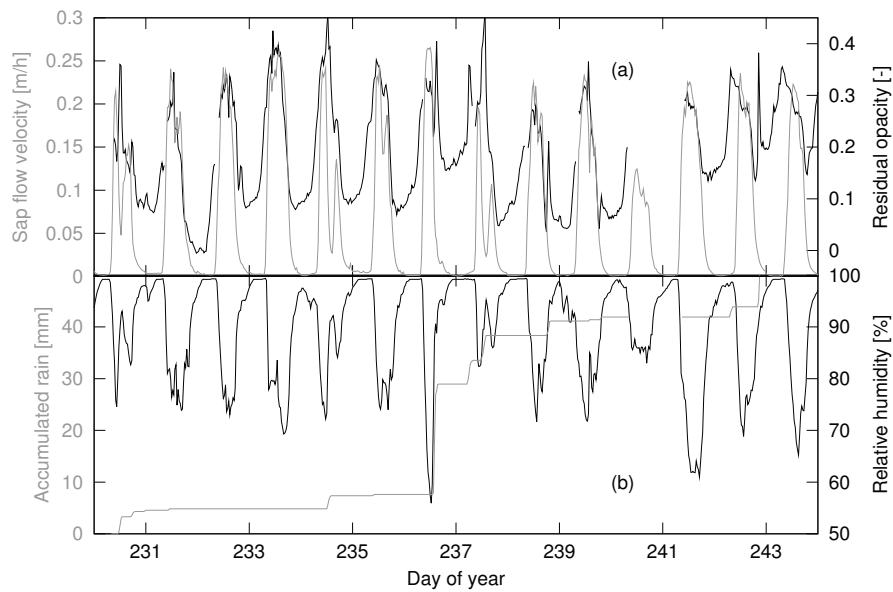


Figure 5: a) Time series of the residual opacity τ_{res} and the sapflow of the trees. b) Time series of the rain accumulation and the relative humidity.

3.3. Effect of wet leaves

In order to quantify the influence of water on the leaves on the canopy opacity, the effective canopy opacity model from Eq. (9) has to be slightly modified. In our model, we considered the water as a homogeneous layer on both sides of the leaves. In the case of dew, this assumption is justified regarding the observations made by Kabela et al. (2009): The authors found that in a soybean and corn canopy, dew forms on top and on the bottom of the leaves, while the fraction between top- and bottom-formed dew depended on the dew amount but also on the time of the observation. For details, the reader is referred to Kabela et al. (2009). In the case of rain interception, we follow the assumption of a homogeneous water layer around the leaf by Schwank et al. (2008). The effect of such water layers on the single leaf transmissivity t_l is calculated with the matrix model of Bass et al. (1995). The second alteration in Eq. (9) concerns the leaf dielectric constant ϵ_l'' , as this is influenced by water-layer induced changes. Since we consider the water-leaf compound as stratified dielectric layers, the problem can be regarded as parallel plate capacitors connected in serial: The capacitance C of such a capacitor is calculated with the well-known formula

$$C = \frac{\epsilon A}{d} \quad (14)$$

with the plate area A , the dielectric constant of the medium between the plates ϵ and the plate distance d . Consequently, we can write the total capacity of serially connected capacitors with the water and leaf material acting as dielectric media as following:

$$\frac{d_w + d_l + d_w}{\epsilon_{\text{eff}} A} = \frac{d_w}{\epsilon_w A} + \frac{d_l}{\epsilon_l A} + \frac{d_w}{\epsilon_w A} \quad (15)$$

Herby, ϵ_w and ϵ_l is the dielectric constant of water and the leaf, respectively and $d_{w,l}$ are the corresponding thicknesses of the layers, i.e. the distance of the capacitor plates. Since A is similar in all the terms the total dielectric constant can be written as:

$$\epsilon_{\text{eff}} = \frac{(2d_w + d_l) \epsilon_l \epsilon_w}{2d_w \epsilon_l + d_l \epsilon_w} \quad (16)$$

By that, the thickness of the water layer can vary and we can observe the change in the opacity. The LAI enables us also to calculate the canopy stored water amount per unit area I :

$$I = 2 \cdot d_w \cdot \text{LAI} \quad (17)$$

Figure 7 depicts the results of opacity calculations with different water layer thicknesses. In addition, the temperature was set to a range from 290 K to 300 K. These results were fitted with a polynomial of 9th degree, such that $\tau_{\text{res}}^{\text{wet}}$ can be directly related to the stored water amount in the canopy.

Separating $\tau_{\text{res}}^{\text{wet}}$ from the total observed opacity and transforming this variable into I by employing the determined relation between I and $\tau_{\text{res}}^{\text{wet}}$ enables us to quantitatively monitor time series of rain interception (I_{rain}) and dew formation I_{dew} . Hereby we assume the stored water amount in the canopy I to be a sum of rain interception and dew formation:

$$I = I_{\text{rain}} + I_{\text{dew}} \quad (18)$$

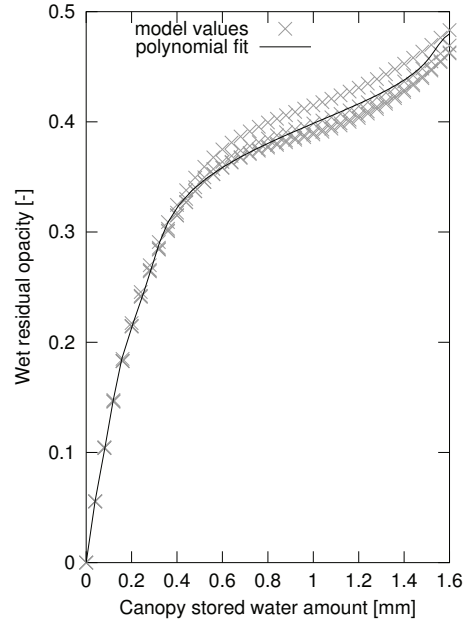


Figure 7: Model result of the effect of water stored in the canopy (as a water film on both sides of the tree leaves) on the canopy opacity. The model was run at four temperatures between 290 and 300 K.

Whether I_{dew} or I_{rain} (or both) contribute to I must be determined by observing the rain gauge and the temperature of the canopy leaves relative to the dew point temperature.

Canopy water I_{rain} and I_{dew} can be quantified with even more accuracy if the knowledge of the occurrence of dry periods is used. During these periods, where I must be zero, an additive correction ΔI_{dry} is introduced which corrects the determined I to a value of zero, i.e., $\Delta I_{\text{dry}} = I$. For the whole time series, dry periods are determined with the criteria defined in Section 3.2 and ΔI_{dry} is calculated for all time points within these periods. The resulting ΔI_{dry} time series contains gaps at times when the conditions were wet. These gaps were finally filled with linear interpolation.

4. Results and Discussion

4.1. Rain interception

With the methods developed in the previous section, the water stored in the canopy was quantified and the result is given in Figure 8, where a time series of I is plotted jointly with the above-canopy water vapor flux. We observe a temporal evolution of intercepted water and a first slight increase of I in the morning hours of day of year (DOY) 236. This increase did not correspond to any detected rain, and hence it is assumed that this signal is induced by dew formation which will be treated in more detail in Section 4.2. At the peak of the dew formation

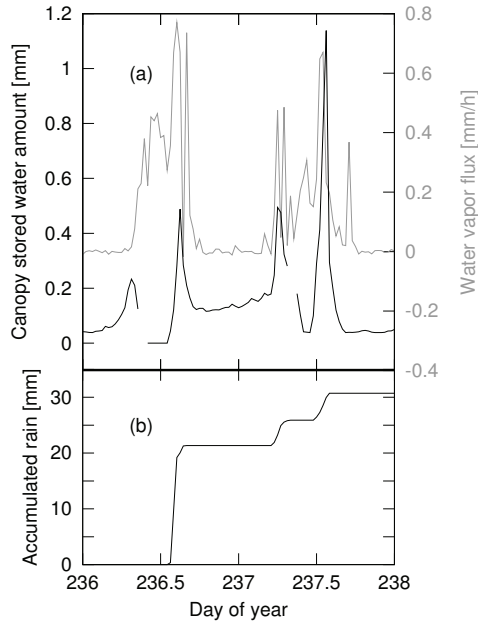


Figure 8: a) 2-day time series of the canopy water storage I together with the above-canopy water vapor flux that was measured with the eddy covariance technique. b) Time series of the cumulative rainfall measured with a tipping bucket rain gauge.

signal, the water vapor flux started simultaneously with sun rise and caused evaporation of dew from the leaves.

Shortly after midday of DOY 236, rainfall of high intensity started, immediately causing I to rise abruptly. At the same time, increasing water vapor fluxes were observed, which is most likely caused by direct evaporation of the intercepted water. After the rain stopped, I decreased quickly during about 2 hours, but since the water vapor flux is more or less terminated after sun set, I does not reach zero causing some water to remain on the leaves during the night. Due to dew formation, I even slightly increases in the night hours until the two upcoming rain showers in the morning and the afternoon of DOY 237 again cause the water vapor flux as well as I to strongly increase. In between and after these rain events, strong evaporation reduces I to zero.

As can be seen in Figure 8, it is not the most intense rain event that leads to the highest value of intercepted rain. The reason of this behavior might be related to possible inaccuracies of the modeled background brightness temperatures $T_{b,sky}$, which is assumed to be more inaccurate during intense rain events. However, heavy precipitation also strongly disturbs the leaves which might facilitate the throughfall of rain through the canopy. In order to test the existence of a relationship between the rain intensity and the percentage of intercepted to total rainfall, all 13 rainfall events that occurred during the two week period from mid- to end of August have been analyzed and the

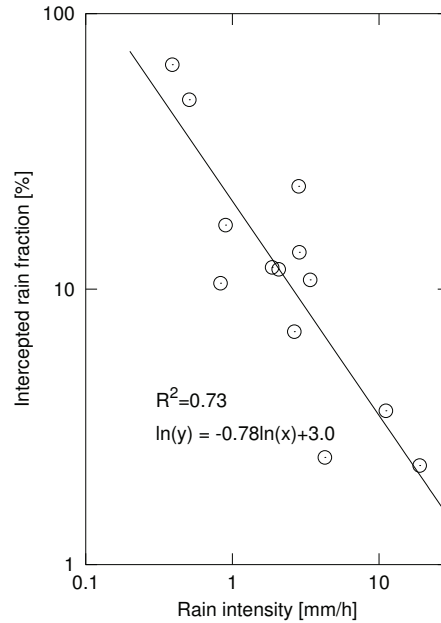


Figure 9: The percentage of rain water intercepted in the canopy to the total rain amount as a function of the rain intensity.

results are plotted in Figure 9. In this graph, the intercepted rain fraction was calculated by dividing the maximum amount of intercepted rain by the accumulated rain measured by the tipping bucket during each rain event, which was plotted as a function of the maximum rain intensity during each rain event.

We observe a strong anti-correlation between both quantities. For light rain events, up to 60% of rain was intercepted by the canopy while during intense precipitation, only about 4% of rain was intercepted by the canopy. During moderate events, i.e. rain intensities between 2 and 16 mm/h, the average interception percentage is 15%, which is in agreement with findings of Czikowsky and Fitzjarrald (2009) and Miralles et al. (2010).

4.2. Dew formation

While rain interception measurements can be performed with various techniques, the formation of dew on a forest canopy is much more difficult to quantify and very few (if any) direct measurements exist. As mentioned in Section 4.1 we believe that the increase of I during non-rainy nocturnal periods is induced by dew formation. A more evident understanding of this condensation process is obtained if several dry midnight to mid-day time series of I are averaged: The mean time series of 8 periods of similar kind is shown in Figure 10 together with the averaged water vapor flux and the relative humidity. Although the standard deviation error bars are relatively large, distinct characteristics were observed: During the night, while the air around the canopy is saturated with water vapor, dew is formed

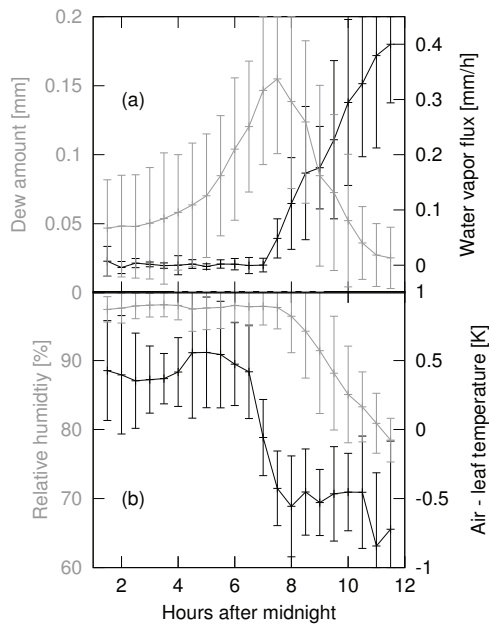


Figure 10: a) Average over 8 time series of I and the water vapor flux that were not affected by rain. b) Relative humidity and the time series of the difference between the leaf temperature and the surrounding air temperature averaged over the same periods considered in panel a). The error bars in both plots show the standard deviation.

on the leaves and reaches a maximum at around 7.30 a.m. After sun rise (6.10 a.m.), the water vapor flux starts to increase at 7.00 a.m. with evolving turbulent mixing that reduces water vapor concentrations in the air surrounding the canopy. As soon as the air becomes unsaturated (between 7.30 a.m. and 8.00 a.m.), dew on the canopy starts to evaporate until the leaves are completely dry at around 11.00 a.m. In Figure 10-b the averaged time series of the difference between the leaf temperature (measured with the infrared radiometer) and the temperature of the surrounding air is depicted. It is emphasized in the review paper by Agam and Berliner (2006) that, being a physical principle, dew only forms if the temperature of the respective surface (i.e. the leaves) is below the dew point. During the night hours of the time series shown in Figure 10, the relative humidity is 100%, meaning that the physical temperature equals the dew point temperature. If then the leaf temperature is below the air temperature, dew can form on the leaf surface. The air-leaf temperature difference remains at a mostly steady and positive state during the night until 6.30 h. After sunrise (6.10 h), this difference starts to drop and reaches a new steady state at 8 h. In the transition phase between these two states, the water vapor flux is about to increase. In addition, dew also continuous to form and reaches its maximum amount shortly before the steady state is reached, which is most likely the time where the air-leaf temperature difference is becoming negative. It must

be kept in mind that the absolute value of the air-leaf temperature difference might be slightly shifted towards higher values, since the leaf temperatures are inferred from IR radiation measurements that are likely to be affected by calibration errors and/or the fact that the tree canopy is not an optimal black body radiator.

Visual observations confirmed the measured duration of dew on the leaves. Due to the fact that this is the first time (to our knowledge) that the dew amount of a tree canopy is directly quantified, we cannot compare our findings with any references in the literature. However, since our rain interception measurements made with the same technique are in agreement with the findings of other authors (e.g. Czikowsky and Fitzjarrald, 2009) and since the averaged time series plotted in Figure 10 seem realistic from the micro meteorological point of view, we are confident that our measurements are reliable.

Furthermore, the ratio of dew amount to the total evaporated water enables some further insights: For the eight day period that was taken into account for the dew quantification, we calculated an average water vapor flux per day (3.24 mm) and related this value to the average maximum dew amount (0.17 mm). These figures show that a considerable fraction of 5.2% of the evaporated water vapor originates from the dew on the leaves.

5. Summary and Conclusion

Diurnal cycles of downwelling microwave brightness temperatures were measured from below a 7 year old tropical tree plantation. The experimental setup was composed of an 11.4 GHz microwave and thermal infrared radiometer, an eddy covariance flux tower as well as xylem sapflow sensors that measured several trees in the close vicinity of the observed canopy. The radiometer was deployed on the ground and pointed at an elevation angle of 40° towards the canopy.

The canopy microwave opacity was calculated from modeled incoming sky brightness temperatures at 11.4 GHz and from thermal infrared temperatures that provided the physical temperature of the canopy. A canopy opacity model that considered the canopy temperature as the only input variable was found to be anti-correlated to the opacities that were inferred from microwave brightness temperature measurements. The difference between the modeled and the measured opacity during dry periods was found to be linearly related to the xylem sapflow of trees. Our study provides the first observation of a close relationship between the two variables. However, the physical cause of this behavior remains subject to speculation: one hand, it is possible that the sapflow somehow modifies the dielectric constant of the plant material. On the other hand, sapflow is also expected to modify the water amount in the leaves: Under ample soil moisture conditions, xylem sapflow is increasing with decreasing leaf water status (Cermak et al., 1980) to compensate stomatal water loss.

The elucidated relation of the canopy opacity to the xylem sapflow made it possible to completely describe the opacity behavior during dry conditions. In addition, this enabled us to account for opacity changes that were caused by water deposited on the leaves of the canopy. The ability of taking into account

a thin water film on both sides of the leaves was added to the canopy opacity model, leading to the possibility to quantitatively relate opacity changes to the amount of water stored in the canopy.

Time series of rain interception and of dew formation were calculated and it was found that between 4% and 60% percent of the rain amount was intercepted in the canopy, depending on the rain intensity. On average, about 15% of the rain amount was intercepted during rainfalls of medium intensities. By comparing the interception with the water vapor flux time series it was found that intercepted water is evaporated rapidly after it is deposited on the leaves, which resulted in an enhanced water vapor flux.

Our study provides the first direct measurements and quantifications of the temporal evolution of dew formation and evaporation in a tree canopy on a diurnal base. Dew accumulated during the night and until about two hours after sunrise, when the water vapor flux began to exceed the dew formation rate. The dew continued to evaporate for another 3.5 h until the surface of the leaves was completely dry. The fact that dew continued to form even after sunrise can be explained with the Priestly-Taylor equilibrium equation (Priestley and Taylor, 1972), which is used to estimate the actual evaporation. In this equation, evaporation is linear to the difference between net radiation and the soil heat flux. Measurements made by Clothier et al. (1986) show that this difference is very small after sunrise and starts to increase significantly 1 hour after sunrise. However, this time delay between sunrise and the beginning of evaporation most probably depends on the location as well as the structure and type of the canopy and is therefore only qualitatively comparable to our findings.

Acknowledgments

Since this project was based on a private initiative, the first author is grateful for the financial support from the following Swiss institutions: Prof. Heinrich Greinacher Foundation, Bern; Travel grants commission and the Remote sensing commission of the Swiss Academy of Sciences SCNAT; Institute of Plant, Animal and Agroecosystem Sciences, ETH Zurich; Institute of Applied Physics, University of Bern. He is also indebted to his wife Fabienne Zeugin for constant support during the time in Panama. We would like to thank Catherine Potvin and the administrative staff of the Smithsonian Tropical Research Institute, Panama, who made this project possible by providing access to the research plantation and by logistics support. Furthermore, thanks go to the Institute of Geography, University of Bern, that lent the hemispherical camera, and last but not least to José and Iliana Monteza-Cabrera with family who shared their home and became essential for the success of the project. S. Wolf and W. Eugster acknowledge financial support from the North-South Centre (former Swiss Centre for International Agriculture) of ETH Zurich. N. Kunert acknowledges financial support from the German Research Foundation (grant Ho-2119/3-1).

References

- Agam, N., Berliner, P., 2006. Dew formation and water vapor adsorption in semi-arid environments - A review. *J. of Arid Env.* 65, 572–590.
- Bass, M., Stryland, E. V., Williams, D., Wolfe, W., 1995. Optical properties of films and coatings, Part 11. In: *Handbook of Optics*. McGraw-Hill, New York, San Francisco, Washington D.C.
- Bouten, W., Schaap, M., Vermetten, A., 1996. Monitoring and modelling canopy water storage amounts in support of atmospheric deposition studies. *J. Hydrol.* 181, 305–321.
- Bouten, W., Swart, P., Water, E. D., 1991. Microwave transmission, a new tool in forest and hydrological research. *J. Hydrol.* 124, 119–130.
- Cermak, J., Huzula, J., Penka, M., 1980. Water potential and sap flow rate in adult trees with moist and dry soil as used for the assessment of root system depth. *Biologia Plantarum* 22, 34–41.
- Chukhlantsev, A. A., 2006. *Microwave Radiometry of Vegetation Canopies*. Springer, 3300 AA Dordrecht, The Netherlands.
- Clothier, B., Clawson, K. JR., P. P., Moran, M., Reginato, R., Jackson, R., 1986. Estimation of soil heat flux from net radiation during the growth of alfalfa. *Agric. For. Meteorol.* 37, 319–329.
- Czekala, H., Crewell, S., Simmer, C., Thiele, A., Hornbostel, A., Schroth, A., 2001. Interpretation of polarization features in ground-based microwave observations as caused by horizontally aligned oblate raindrops. *J. Appl. Met.* 40, 1918–1932.
- Czikowsky, M., Fitzjarrald, D., 2009. Detecting rainfall interception in an amazonian rain forest with eddy flux measurements. *J. Hydrol.* 377, 92–105.
- Della Vecchia, A., Ferrazzoli, P., Wigneron, J.-P., Grant, J. P., 2007. Modeling forest emissivity at L-band and a comparison with multitemporal measurements. *IEEE Geosci. Remote Sens Lett.* 4, 508–512.
- El-Rayes, M., Ulaby, F. T., 1987. Microwave dielectric behavior of vegetation material. Tech. rep., Radiation Laboratory, Department of Electrical Engineering and Computer Science, The University of Michigan.
- Eugster, W., Senn, W., 1995. A cospectral correction model for measurement of turbulent NO₂ flux. *Boundary-Layer Meteorol.* 74 (4), 321–340.
- Ferrazzoli, P., Guerriero, L., 1996. Passive microwave remote sensing of forests: A model investigation. *IEEE Trans. Geosci. Remote Sens.* 34, 433–443.
- Flores, E. M., Marin, W. A., 2003. *Tabebuia rosea* (Bertol.) DC. In: *Vozzo, J. A. (Ed.), Tropical Tree Seed Manual. Part II - Species Descriptions*. Agriculture Handbook 721. United States Department of Agriculture, Forest Service, Washington, DC, pp. 737–739.
- Fournier, L. A., 2003. *Anacardium excelsum* (Bertero & Balb. ex Kunth) Skeels. In: *Vozzo, J. A. (Ed.), Tropical Tree Seed Manual. Part II - Species Descriptions*. Agriculture Handbook 721. United States Department of Agriculture, Forest Service, Washington, DC, pp. 294–296.
- Granier, A., 1985. A new method of sap flow measurement in tree stems. *Ann. For. Sci.* 42, 193–200.
- Granier, A., 1987. Evaluation of transpiration in a douglas-fir stand by means of sap flow measurements. *Tree Physiol.* 3, 309–320.
- Guglielmetti, M., Schwank, M., Mätzler, C., Oberdörster, C., Vanderborcht, J., Flübler, H., 2007. Measured microwave radiative transfer properties of a deciduous forest canopy. *Remote Sens. Environ.* 109 (4), 523–532.
- Han, Y., Westwater, E. R., 2000. Analysis and improvement of tipping calibration for ground-based microwave radiometers. *IEEE Trans. Geosci. Remote Sens.* 38, 1260–1276.
- Holliday, P., 1980. *Fungus diseases of tropical crops*. Cambridge University Press, Cambridge, England.
- Janssen, M. A., 1993. An introduction to the passive microwave remote sensing of atmospheres. In: *Janssen, M. A. (Ed.), Atmospheric Remote Sensing by Microwave Radiometry*. Wiley, New York, pp. 1–35.
- Kabela, E. D., Hornbuckle, B. K., Cosh, M. H., Anderson, M. C., Gleason, M. L., 2009. Dew frequency, duration, amount, and distribution in corn and soybean during SMEX05. *Agric. For. Meteorol.* 149, 11–24.
- Karam, M. A., Amar, F., Fung, A. K., Mougou, E., Lopes, A., Le Vine, D. M., Beaudoin, A., 1995. A microwave polarimetric scattering model for forest canopies based on vector radiative transfer theory. *Remote Sens. Environ.* 53, 16–30.
- Kidron, G., Barzilay, E., Sachs, E., 1965. Microclimate control upon sand microbiotic crusts, western Negev Desert, Israel. *Geomorphology* 36, 1–18.
- Kimmins, J., 1973. Some statistical aspects of sampling throughfall precipitation in nutrient cycling studies in British Columbian coastal forests. *Ecology* 54, 10081019.

- Kong, J. A., 1975. *The Theory of Electromagnetic Waves*. J. Wiley & Sons, New York.
- Kunert, N., unpublished data. Specific leaf area of the trees in the experimental plantation in Sardinilla, Panama.
- Kunert, N., Schwendenmann, L., Holscher, D., 2010. Seasonal dynamics of tree sap flux and water use in nine species in Panamanian forest plantations. *Agric. For. Meteorol.* 150, 411–419.
- Kurum, M., Lang, R. H., O'Neill, P. E., Joseph, A. T., Jackson, T. J., Cosh, M. H., 2009. L-band radar estimation of forest attenuation for active/passive soil moisture inversion. *IEEE Trans Geosci. Remote Sens.* 47, 3026–3040.
- Lawrence, D., Thornton, P., Oleson, K., Bonan, G., 2007. The partitioning of evapotranspiration into transpiration, soil evaporation, and canopy evaporation in a GCM: impacts on land-atmosphere interaction. *J. Hydrometeorol.* 8, 862–880.
- Liebe, H. J., Hufford, G. A., Cotton, M. G., 1993. Propagation modeling of moist air and suspended water/ice particles at frequencies below 1000 GHz. In: *AGARD 52nd Specialists Meeting Electromagn. Wave Propagation Panel*. Palma de Mallorca, Spain.
- Mätzler, C., 1994a. Microwave (1 – 100 GHz) dielectric model of leaves. *IEEE Trans. Geosci. Remote Sens.* 32, 947–949.
- Mätzler, C., 1994b. Microwave transmissivity of a forest canopy: Experiments made with a beech. *Remote Sens. Environ.* 48, 172–180.
- McDonald, K. C., Zimmermann, R., Kimball, J. S., 2002. Diurnal and spatial variation of xylem dielectric constant in Norway spruce (*Picea abies* [L.] Karst.) as related to microclimate, xylem sap flow, and xylem chemistry. *IEEE Trans. Geosci. Remote Sens.* 40, 2063–2082.
- Meissner, T., Wentz, F. J., 2004. The complex dielectric constant of pure and sea water from microwave satellite observations. *IEEE Trans. Geosci. Remote Sens.* 42, 1836–1849.
- Miralles, D. G., Gash, J. H., Holmes, T. R. H., de Jeu, R. A. M., Dolman, A. J., 2010. Global canopy interception from satellite observations. *J. Geophys. Res.* 115, D16122.
- Moreau, M., Testud, J., Le Bouar, E., 2009. Rainfall spatial variability observed by X-band weather radar and its implication for the accuracy of rainfall estimates. *Adv. Water Res.* 32, 1011–1019.
- Noffsinger, T., 1965. Survey of techniques for measuring dew. In: Waxler, A. (Ed.), *Humidity and Moisture*. Reinhold, New York, pp. 523–531.
- Pampaloni, P., 2004. Radiometry of forests. *Waves in random media* 14, 275–298.
- Potvin, C., Dutilleul, P., 2009. Neighborhood effects and size-asymmetric competition in a tree plantation varying in diversity. *Ecology* 90, 321–327.
- Priestley, C., Taylor, R., 1972. On the assessment of surface heat flux and evaporation using large-scale parameters. *Mon. Weather Rev.* 100, 81–92.
- Rosenkranz, P. W., 1998. Water vapor microwave continuum absorption: A comparison of measurements and models. *Radio Sci.* 33, 919–928.
- Sandí, C., Flores, E. M., 2003. Hura crepitans. In: Vozzo, J. A. (Ed.), *Tropical Tree Seed Manual. Part II - Species Descriptions. Agriculture Handbook 721*. United States Department of Agriculture, Forest Service, Washington, DC, pp. 511–513.
- Santi, E., Paloscia, S., Pampaloni, P., Pettinato, S., 2009. Ground-based microwave investigations of forest plots in Italy. *IEEE Trans. Geosci. Remote Sens.* 47, 3016–3025.
- Satake, M., Hanado, H., 2004. Diurnal change of Amazon rain forest σ^0 observed by Ku-band spaceborne radar. *IEEE Trans. Geosci. Remote Sens.* 42, 1127–1134.
- Schneebeil, M., Mätzler, C., 2011. A radiative transfer model for an idealized and non-scattering atmosphere and its application for ground-based remote sensing. *J. Quant. Spec. Rad. Trans.* 112, 883–892.
- Schneebeil, M., Wolf, S., Eugster, W., Mätzler, C., 2008. X-Band opacity of a tropical tree canopy and its relation to intercepted rain, eddy fluxes and other meteorological variables. In: *2008 Microwave Radiometry and Remote Sensing of the Environment*. Florence, Italy.
- Schwank, M., Guglielmetti, M., Mätzler, C., Flüher, H., 2008. Testing a new model for the L-band radiation of moist leaf litter. *IEEE Trans. Geosci. Remote Sens.* 46, 1982–1994.
- Thompson, N., 1981. The duration of leaf wetness. *Meteorological Magazine* 110, 1–12.
- Valente, F., David, J. S., Gash, J. H. C., 1997. Modelling interception loss for two sparse eucalypt and pine forests in central Portugal using reformulated Rutter and Gash analytical models. *J. Hydrol.* 190, 141–162.
- Vrugt, J., Dekker, S., Bouten, W., 2003. Identification of rainfall interception model parameters from measurements of throughfall and forest canopy storage. *Water Res. R.* 39 (9).
- Way, J., Paris, J., Dobson, M., McDonald, K., Ulaby, F. T., Vanderbilt, V., 2004. Diurnal change in trees as observed by optical and microwave sensors: The EOS synergism study. *IEEE Trans. Geosci. Remote Sens.* 29 (6), 817–820.
- Webb, E., Pearman, G., Leuning, R., 1980. Correction of flux measurements for density effects due to heat and water-vapor transfer. *Quart. J. Roy. Meteor. Soc.* 106 (447), 85–100.
- Wegmüller, U., Mätzler, C., Njoku, E. G., 1995. Canopy opacity models. In: Njoku, E. G., Pampaloni, P., Choudhury, B. J., Kerr, Y. H. (Eds.), *Passive Microwave Remote Sensing of Land-Atmosphere Interactions*. VSP, Utrecht, The Netherlands, pp. 375–387.

G Model

FORECO-12439; No. of Pages 11

ARTICLE IN PRESS

Forest Ecology and Management xxx (2010) xxx–xxx



Contents lists available at ScienceDirect

Forest Ecology and Management

journal homepage: www.elsevier.com/locate/foreco

An ecosystem approach to biodiversity effects: Carbon pools in a tropical tree plantation

Catherine Potvin^{a,b,*}, Lady Mancilla^b, Nina Buchmann^c, Jose Monteza^b, Tim Moore^g,
Meaghan Murphy^g, Yvonne Oelmann^d, Michael Scherer-Lorenzen^f, Benjamin L. Turner^b,
Wolfgang Wilcke^e, Fabienne Zeuglin^c, Sebastian Wolf^c

^a Department of Biology, McGill University, 1205 Dr Penfield, Montreal, Canada H3A 1B1

^b Smithsonian Tropical Research Institute, Apartado 0843-03092, Balboa, Ancón, Panama

^c Institute of Plant, Animal and Agroecosystem Sciences, ETH Zurich, Universitätsstrasse 2, 8092 Zurich, Switzerland

^d Institute of Integrated Natural Sciences, Geography, University of Koblenz-Landau, Universitätsstr. 1, 56070 Koblenz, Germany

^e Geographic Institute, University of Berne, Hallerstrasse 12, 3012 Berne, Switzerland

^f Faculty of Biology, Albert-Ludwigs University of Freiburg, Schaenzlestrasse 1, 79104 Freiburg, Germany

^g Department of Geography, McGill University, 805 Sherbrooke Street West, Montreal, Quebec, Canada H3A 2K6

ARTICLE INFO

Article history:

Received 15 July 2010

Received in revised form 4 November 2010

Accepted 15 November 2010

Keywords:

Tropical tree plantation

Carbon pools and fluxes

Diversity effect

Ecosystem carbon storage

ABSTRACT

This paper presents a synthesis of experiments conducted in a tropical tree plantation established in 2001 and consisting of 22 plots of 45 m × 45 m with either one, three or six native tree species. We examined the changes in carbon (C) pools (trees, herbaceous vegetation, litter, coarse woody debris (CWD), and mineral topsoil at 0–10 cm depth) and fluxes (decomposition of CWD and litter, as well as soil respiration) both through time and among diversity levels. Between 2001 and 2009 the aboveground C pools increased, driven by trees. Across diversity levels, the mean observed aboveground C pool was 7.9 ± 2.5 Mg ha⁻¹ in 2006 and 20.4 ± 7.4 Mg ha⁻¹ in 2009, a 158% increase. There was no significant diversity effect on the observed aboveground C pool, but we found a significant decrease in the topsoil C pool, with a mean value of 34.5 ± 2.4 Mg ha⁻¹ in 2001 and of 25.7 ± 5.7 Mg ha⁻¹ in 2009 ($F_{1,36} = 52.12$, $p < 0.001$). Assuming that the biomass C pool in 2001 was negligible (<1 Mg ha⁻¹), then the plantation gained in C, on average, ~20 and lost ~9 Mg ha⁻¹ in biomass and soil respectively, for an overall gain of ~11 Mg ha⁻¹ over 8 years. Across the entire data set, we uncovered significant effects of diversity on CWD decomposition (diversity: $F_{2,393} = 15.93$, $p < 0.001$) and soil respiration (monocultures vs mixtures: $t = 15.35$, $df = 11$, $p < 0.05$) and a marginally significant time × diversity interaction on the loss of total C from the mineral topsoil pool (see above). Monthly CWD decomposition was significantly faster in monocultures (35.0 ± 24.1%) compared with triplets (31.3 ± 21.0%) and six-species mixtures (31.9 ± 26.8%), while soil respiration was higher in monocultures than in mixtures ($t = 15.35$, $df = 11$, $p < 0.001$). Path analyses showed that, as diversity increases, the links among the C pools and fluxes strengthen significantly. Our results demonstrate that tree diversity influences the processes governing the changes in C pools and fluxes following establishment of a tree plantation on a former pasture. We conclude that the choice of tree mixtures for afforestation in the tropics can have a marked influence on C pools and dynamics.

© 2010 Published by Elsevier B.V.

1. Introduction

An important challenge of climate change mitigation is the management of terrestrial carbon (C) either to create new C sinks or to preserve existing ones (Malhi et al., 1999). In this context, a number of studies have recently compared the productivity of mixed-species plantations with monocultures to test

whether diversity would enhance productivity and hence C storage (Caspersen and Pacala, 2001; Vila et al., 2007; Firn et al., 2007; Schlapfer and Schmid, 1999; Piotta et al., 2010; Erskine et al., 2006). Tree plantations and agroforests are widely believed to enhance the terrestrial C pool (Nair et al., 2009b) and reforestation with native species could potentially yield a range of additional benefits, including soil stabilization, reduced erosion, habitat for a variety of species including birds, seed deposition, and increased understory diversity (Wishnie et al., 2007). Nevertheless, there is a growing concern that tree plantations, whether with natives or exotics, might decrease water availability at the ecosystem level (Malmer et al., 2010).

* Corresponding author at: Department of Biology, McGill University, 1205 Dr Penfield, Montreal, Quebec, Canada H3A 1B1.

E-mail address: catherine.potvin@mcgill.ca (C. Potvin).

Potvin C, Manzilla L, Buchmann N, Monteza J, Moore T, Murphy M, Oelmann Y, Scherer-Lorenzen M, Turner, B.L., Wilcke W, Zeuglin F, Wolf S (in press) An ecosystem approach to biodiversity effects: carbon pools in a tropical tree plantation. *Forest Ecology and Management*. doi: 10.1016/j.foreco.2010.11.015

Many studies examining the effect of tree diversity on productivity or C storage used aboveground tree biomass as a surrogate for net primary productivity (NPP: the total production of plant biomass within a given time period) (Catovsky et al., 2002). NPP is a good indicator of ecosystem C storage only if large-scale disturbances during a specific period can be ruled out, because C is lost through heterotrophic respiration, fire and other disturbances such as human harvest (Körner, 2000, 2003; Schlesinger and Lichter, 2001; Schulze et al., 2000). Ecosystem C storage is tightly coupled with changes in the soil that occur in response to alterations in above- and below-ground productivity, rooting depth and root distribution, and changes in the quality and quantity of litter (Catovsky et al., 2002; Nair et al., 2009b; Valverde-Barrantes, 2007). Assessment of ecosystem C storage must therefore include belowground C pools.

We compared several pools of C (standing tree biomass, coarse woody debris (CWD), herbaceous vegetation, litter and soil) and fluxes of C (soil respiration and the decomposition of CWD and litter) in a tropical tree plantation established with one, three or six native species. We hypothesized that tree diversity affects the soil C pool through its effect on inputs, mainly as CWD and litter, and that, therefore, tree diversity affects ecosystem C storage beyond its effect on aboveground NPP.

2. Methods

Measurements took place in a diversity plantation established near the village of Sardinilla in the region of Buena Vista, Panama (9°19'30"N, 79°38'00"W) between 2001 and 2009. In 2001, six native tree species were selected for planting, including two pioneers (*Luehea seemannii* Triana & Planch (Ls) and *Cordia alliodora* (Ruiz & Pavon) Oken (Ca)), two light-intermediate species (*Anacardium excelsum* (Bert. & Balb. Ex Kunth) Skeels (Ae) and *Hura crepitans* L. (Hc)) and two long lived pioneers (*Cedrela odorata* L. (Co) and *Tabebuia rosea* (Bertol.) DC. (Tr)) (Delagrangue et al., 2008). The plantation consisted of 24 plots of approximately the same size (45 × 45 m). Twelve plots (two for each species) are monocultures, six plots contain different combinations of three tree species, and six plots contain all tree species (Scherer-Lorenzen et al., 2005b). The 24 diversity plots were embedded to the north, south and east, in a larger reforestation area using native tree species (~10 ha total reforestation area), which reduced the edge effect in all but one cardinal direction. Undergrowth was cleared annually to eliminate other competing vegetation and facilitate work within the plantation. Each plot was distributed randomly to reduce bias caused by differences in soil conditions. Plots were square-shaped and established with an average of 231 trees planted at 3 m spacing. *Cordia alliodora* suffered significant mortality after planting, so monocultures of this species were excluded from the analyses.

2.1. Carbon pools

2.1.1. Aboveground tree biomass

Every year at the onset of the dry season (December–January), height, basal diameter at 10 cm from the ground, and diameter at breast height (DBH) of every stem were measured on each indi-

vidual tree. These traits were used to compute the above-ground biomass of individual trees based on species-specific allometric regressions developed at the site in 2007 (Table 1). Because biomass production varied with tree age, we restricted our analysis to the years 2006, 2007 and 2009 to ensure the relevance of the allometric equations. The year 2008 was excluded because data on CWD were not available. The area of each plot varied slightly, ranging from 0.2025 to 0.2304 ha. It was therefore necessary to scale up biomass to 1 ha to compare stand-level tree biomass of the different diversity levels (Eq. (1)):

$$T_1 = A \cdot \left(\frac{\sum b_i}{N} \right) \quad (1)$$

where T_1 is aboveground tree biomass at the plot level, b_i is the biomass of each tree in the plot, N is the number of living trees in the plot, and A is the area of each plot.

Since planting, a number of trees have died in the plots and consequently plots have different numbers of trees ranging between 101 trees in plot A2 (one of the six-species plots) and 229 trees in plot Tr1 (monoculture of *Tabebuia rosea*). Potvin and Gotelli (2008) showed that tree mortality in Sardinilla was dependent on species and independent of diversity. To correct for mortality, a second estimate of tree biomass at the plot level was calculated using the following equation:

$$T_2 = 1111 \cdot \left(\frac{\sum b_i}{N} \right) \quad (2)$$

where T_2 is aboveground tree biomass at the plot level corrected for mortality and 1111 is the number of trees planted in a 1 ha reforestation plot with no mortality. Throughout the paper, we maintain the distinction between the estimates of biomass with (observed aboveground C pools) or without mortality (maximum aboveground C pool).

Tree biomass at the plot level was converted to tree C using species-specific trunk C concentration obtained from coring tree trunks in the vicinity (Hc: 45.07 g C kg⁻¹; Ls: 45.76 g C kg⁻¹; Ae: 45.82 g C kg⁻¹; Tr: 47.01 g C kg⁻¹; Co: 47.39 g C kg⁻¹) (Elias and Potvin, 2003). For species mixtures, the mean C concentration of the constituent species was used.

2.1.2. Coarse woody debris

All CWD within each plot was collected and weighed at the height of the dry season in March of 2006, 2007 and 2009. Each plot was searched by a team of people walking in a straight line between the trees and collecting all visible twigs, branches, and trunks belonging to the trees in that plot. Leaf litter and litter from the herbaceous understory were excluded. All materials were weighed on site and values were scaled to a hectare basis in the same way as tree biomass with or without correcting for tree mortality. Coarse woody debris biomass was then converted to C using the species-specific trunk C concentration.

2.1.3. Litter production

Yearly litter production at the plot level was estimated by combining two existing data sets. First, for the dry season, a total of 204 litter traps of 1 m² were positioned randomly in the plantation

Table 1

Best species specific least square linear regression between tree biomass and basal diameter (BD), height (H), the sum of the DBH of all stems (DBH_{all}) and wood.

Species	Allometric equation	Height range	R ²
<i>Anacardium excelsum</i>	$\log(\text{Biom}) = 0.73943 - 7.32969 \text{ BD} - 4.02612 \text{ BD}^2 - 0.49008 \text{ BD}^3$	0.9–8.4 m	0.9693
<i>Cedrela odorata</i>	$\log(\text{Biomass}) = -1.3288 - 10.278 \log \text{BD} - 5.5171 (\log \text{DB})^2 - 0.7624 (\log \text{BD})^3$	0.13–10.8 m	0.7685
<i>Hura crepitans</i>	$\log(\text{Biomass}) = 2.0279 + 1.8733 \log \text{H} + 1.0001 \log \text{DBH}_{\text{all}}$	0.9–10.3 m	0.884
<i>Luehea seemannii</i>	$\log(\text{Biomass}) = 0.2335 + 2.1608 \log \text{H} + 0.6082 \log \text{DBH}_{\text{all}}$	1–8.2 m	0.8826
<i>Tabebuia rosea</i>	$\log(\text{Biomass}) = 6.21017 + 1.1268 \log(\text{BD}^2 \text{HS})$	1.3–7.8 m	0.8646

with 12 traps per plot and three traps per subplot. To establish the subplots, each plot was separated into four equal sections. Randomizing per subplot ensured that litter traps were positioned throughout each plot. Litter collection took place between February and April 2005. Litter was collected on a bi-weekly basis and samples were dried before weighing as described in Scherer-Lorenzen et al. (2007). Litter production at the plot level was estimated for the four month dry season as follows:

$$\text{Litter}_{\text{dry}} = \left(P_j \cdot \frac{A_j}{N_j} \right) \cdot N_j \quad (3)$$

where P_j is litter production per area in plot j (g m^{-2}), A_j the area of plot j (m^2), N_j is the number of trees in plot j , N_j was either the number of living trees in plot j , or 1111, which is the number of trees in a standard 1-ha plantation, depending on whether the estimate of litter production at the plot level controlled for tree mortality or not.

Litter was also collected on a bi-weekly basis between July and November in 2007 and 2008. In these sampling campaigns, the same 1 m^2 litter traps were positioned under each of 60 individual trees growing in each of the diversity levels (Oelmann et al., 2010) rather than in subplots as in the dry season experiment. The data were used to estimate litter biomass in the wet season. Contrary to our expectation that litter production should increase with the age of the plantation, litter production was not significantly higher in the wet season of 2008 than in 2007. We therefore used the average litter production of these two years in our estimate of yearly litter production. The scaling up of wet season litter production was based on species identity and the number of trees per species in each plot:

$$\text{Litter}_{\text{wet}} = \left(\frac{\sum_k (X_{ij} N_{ij})}{A_j} \right) \cdot N_j \quad (4)$$

where X_{ij} is the mean litter production for 2007 and 2008 of species i in plot j , N_{ij} is the number of trees of species i in plot j , N_j was either the number of living trees in plot j or 1111, which is the number of trees in a standard 1 ha plantation depending on whether the estimate of litter production at the plot level controlled for tree mortality or not.

An approximate estimate of yearly litter biomass was calculated as the sum of dry and wet season litter production, assuming that the dry season lasted 4 months and the wet season lasted 8 months. Months for which we had no data (January, May and June), were filled by the average monthly litter biomass for the dry and wet season mean production, respectively:

$$\text{Total litter} = \left(4 \cdot \left(\frac{\text{Litter}_{\text{dry}}}{3} \right) \right) + \left(8 \cdot \left(\frac{\text{Litter}_{\text{wet}}}{5.5} \right) \right) \quad (5)$$

This assumption seems plausible, because some species (e.g. *Anacardium excelsum*) shed leaves all year round. The Sardinilla plantation includes ten monoculture plots (i.e., two replicates per species). Unfortunately, litter was collected in different monocultures of the same species in the two seasons. Therefore, litter biomass in monoculture is a composite estimate of litter production from the two monocultures of the same species rather than a plot specific value:

$$\text{Total litter}_m = \left(4 \cdot \left(\frac{\text{Litter}_{\text{dry}i}}{3} \right) \right) + \left(8 \cdot \left(\frac{\text{Litter}_{\text{wet}j}}{5.5} \right) \right) \quad (6)$$

where $\text{Litter}_{\text{dry}i}$ refers to the litter production of the first monoculture of a given species, and $\text{Litter}_{\text{wet}j}$ refers to the litter production of the second monoculture of a given species. Finally, litter biomass was converted into litter C pool by using plot- and species-specific C concentrations measured from the dry season litter (Scherer-Lorenzen et al., 2007).

Mean litter production per tree of $233 \pm 60 \text{ g}$ and $122 \pm 15 \text{ g}$, in the wet season of 2007 and 2008 respectively, suggests that although trees allegedly grow through time, factors other than years determine litter C pool. We therefore calculated a single estimate of the litter C pool and used it in the calculation of the aboveground C pool in 2006, 2007 and 2009 assuming no increase in litter production between 2006 and 2009.

2.1.4. Herbaceous biomass

To estimate the biomass of the herbaceous vegetation, each plot was divided into four subplots, giving a total of 96 subplots. Within each subplot, herbaceous vegetation was cut to ground level in one randomly positioned, non-permanent, quadrat (0.5 m^2) twice a year at the beginning and end of the wet season (May/June and November/December). The green and dry (litter) biomass was separated, dried and weighed. The dry and green biomass within each of the four quadrats was summed and scaled up to the plot level, taking into account individual plot size. Herbaceous biomass was then scaled to 1 ha. Here we report data of 2006, 2007 and 2009.

In addition, to estimate the C concentration, herbaceous vegetation was collected with a frame (0.06 m^2) within the area confined by the canopy drip line under each of the 60 focal trees used to estimate litter production in the wet season. The herbaceous vegetation was sorted into grasses and non-leguminous herbs (henceforward termed grasses/herbs) and legumes and the respective weight was recorded. For all samples, the C concentration was measured with an elemental analyzer (Vario EL III, Elemental Analysensysteme, Hanau, Germany). We found no significant diversity effect on C concentration of legumes or grasses/herbs, but the proportion of grasses/herbs was significantly higher ($F_{2,24} = 5.23$, $p < 0.01$) in triplets (69.3%) than in monoculture (46.4%) and six-species mixtures (44.8%). To transform herbaceous biomass into herbaceous C pool, we therefore used the following index:

$$C_{\text{herbs}} = (40.66 \cdot \text{Prop}_{\text{g/h},i}) + (44.78 \cdot \text{Prop}_{\text{l},i}) \quad (7)$$

where 40.66% and 44.78% are the mean C concentration of, respectively, grasses/herbs and legumes under the 60 focal trees, $\text{Prop}_{\text{g},i}$ is the mean proportion of grasses/herbs in each diversity level, and $\text{Prop}_{\text{l},i}$ is the mean proportion of legumes in each of the diversity levels.

2.1.5. Soil measurements

Initial soil sampling was done in July 2001 during plantation establishment, both at the site of the plantation and in an adjacent pasture. This included 225 topsoil samples (0–10 cm) and seven soil profiles (0–100 cm), using a 10 cm cylindrical corer with a diameter of 5 cm (Abraham, 2004). Soil sampling of topsoil (0–10 cm) was repeated in March 2009 using a 10 cm cylindrical corer with a diameter of 6.8 cm and sampling once per plot ($n=22$). Samples were dried for at least 72 h in a drying room at 60°C and were afterwards analyzed for soil organic C concentration (SOC) and $\delta^{13}\text{C}$ with a Flash 1112 Elemental Analyzer coupled to a Delta V Advantage isotope ratio mass spectrometer (Thermo Fisher Scientific, Waltham, USA). Bulk density (d_B) sampling in March 2009 (dry season) resulted in higher values than the sampling in July 2001 (wet season) by Abraham (2004). However, we assume that this is related to seasonal soil contraction due to the large clay content than to inherent changes in d_B . A study by Seitlinger (2008) with sampling in June 2007 (wet season) found similar d_B values to Abraham (2004). Assuming no change in d_B from 2007 to 2009, we used the d_B values reported by Seitlinger (2008) to calculate the soil organic C pool (SOCP) from the C concentrations from samples taken in 2009. To derive the contribution of the source of organic matter in the topsoil, we used a two-member mixing model and the reported values by Abraham (2004), with -14.4% for pasture

litter from the Sardinilla site and –29.5% for tree litter obtained from nearby Barro Colorado Island.

2.2. Fluxes

2.2.1. Decomposition of coarse woody debris

Decomposition of CWD was measured between May 2007 and March 2008 for medium size CWD (~2 cm diameter) for each species in each diversity treatment. Dead branches were collected on the ground in April 2007 and cut into 10 cm stakes. Twenty stakes were cut, weighed, dried and re-weighed to serve as control for no decomposition. Mesh bags were made of mosquito screen (1 mm mesh size) and 10 stakes from one species were put into bags. The stakes that were put in the mesh bags were not dried to ensure that the chemical composition was not changed. Each of the stakes was weighed and identified with a metal tag. For each species, 12 mesh bags were prepared and positioned on the ground at the centre of two randomly chosen subplots of the target species' two monocultures, of two of the triplets where this target species grew and of two randomly chosen six-species plots.

The decomposition of a total of 120 stakes per species was therefore followed through time. Every month, one stake was removed from each mesh bag and both the fresh and dry masses were recorded to calculate the loss in woody biomass. For each species in each diversity level, we calculated the decomposition rate constant, k , from the decay model (Scherer-Lorenzen et al., 2007) over the initial six months period, June to December 2007:

$$X = X_0 \cdot e^{-kt} \quad (8)$$

where X is the mass of CWD remaining at time t , X_0 is the initial mass, k is the exponential decay coefficient, and t is time in months. While it is possible that the mesh bags could have decreased the rate of decomposition by excluding some detritivorous arthropods, the method is recommended by the Long-term Intersite Decomposition Experiment Team (LIDET) (Harmon and Sexton, 1996).

2.2.2. Litter decomposition

Litter decomposition was studied using litter bags as described in Scherer-Lorenzen et al. (2007). Briefly, litter bags (1 mm mesh size) were filled with 10 g of dry litter with the proportion of each species representing their abundance within each plot. Replicate litter bags were retrieved every four weeks during a 116-day period from May to September 2005, corresponding to the wet season, and loss in dry weight was determined.

2.2.3. Soil respiration

Soil respiration measurements were made using a closed chamber system and a PP Systems (Amesbury, MA, USA) EGM-4 Environmental infrared gas analyzer with collars permanently inserted into the ground to 5 cm depth one month prior to sampling. We built a PVC soil respiration chamber of 20.32 cm diameter and 10.16 cm height for a total volume of 3293 cm³. To capture seasonal changes in soil respiration, each collar was sampled up to twice per week over four weeks in March 2004 at the height of the dry season, and again in June 2004 at the onset of the wet season. Soil respiration was measured in the area between two trees in both monoculture and mixture pairs. Overall, we measured respiration of monoculture pairs for all six species and of 12 unique two-species pairs. Monoculture pairs were selected among their corresponding monoculture plots, while two-species pairs were selected randomly from either the triplets or the six-species mixtures (see Murphy et al., 2008 for methodological details). With six monoculture pairs and 12 two-species pairs, each replicated five times, we sampled a total of 90 collars in the biodiversity plots.

Using the combined March and June soil respiration data, we modeled plot level respiration of the six-species mixtures. As a null

hypothesis we considered plot respiration as an additive function of the number of individuals of each species, where the respiration of each species in the plot was calculated from the respiration values of each species in monoculture. Summing the respiration of each species produced a value for plot level respiration (model 1; Eq. (9)):

$$R_{1j} = X_j \cdot N_j \quad (9)$$

where R_{1j} is the respiration of species j in the plot, X is the average respiration of species j in monoculture (1–6), N_j is the number of individuals of species j , and:

$$B_{1m} = \sum R_{i(1-6)} \quad (10)$$

where B_{1m} is the respiration of six-species plot estimated independently for each of the six plots.

Model 2 assumes that plot level respiration is dependent upon the interactions between individual trees and their neighbors of different species. Individual tree respiration is calculated as follows:

$$R_{2i} = X_{ia} \cdot N_{ia} + X_{ib} \cdot N_{ib} \quad (11)$$

where R_{2i} is the respiration of individual i (1–225), x_{ia} is the average respiration of individual i paired with neighbor a , x_{ib} is the average respiration of individual i paired with neighbor b , N_{ia} is the number of individual i with neighbors (a) (1 and 2), and N_{ib} is the number of individual i with neighbors (b) (1 and 2). The sum of all individual tree respiration rates is the plot level respiration rate:

$$B_2 = \sum R_{2(1-225)} \quad (12)$$

To account for spatially explicit differences in the plots, calculations were repeated for each of the six-species plots.

2.3. Calculation and statistical analyses

We estimated NPP as the change in aboveground biomass of four different biomass compartments (trees, litter, herbaceous and CWD) between consecutive years. NPP was therefore calculated from biomass increment for the 2006–2007 (NPP₂₀₀₇) and the 2007–2009 (NPP₂₀₀₉) intervals.

Aboveground C pool size was calculated for each plot in 2006, 2007 and 2009 by summing the C mass of the following ecosystem components: CWD, trees, herbaceous vegetation and litter. These components were scaled up either as observed (i.e., scaled up with existing tree density; observed aboveground C pools), or as maximum (i.e., scaled up assuming 1111 trees per ha; Maximum aboveground C pools). We therefore obtained two measures of ACP for each plot. The relative growth rates of both estimates of ACP were calculated for each plot between 2006 and 2009:

$$RGR_{ACP} = \frac{(\ln(ACP_2) - \ln(ACP_1))}{t} \quad (13)$$

where time interval (t) is defined as a function of the date of two successive measurements: $date_2 - date_1/365.25$ or $date_2 - date_1/730.5$, respectively, for one or two years interval.

We also calculated ecosystem C storage as the sum of aboveground C pool, root C and the topsoil SOC pool (SOCP). Root biomass and associated C were estimated using a site and species-specific root/shoot ratio obtained by excavating entire root systems in 2003 in trees planted previously in 1998 in an adjacent plantation (Coll et al., 2008) and harvested at a similar age at the time of excavation. The root/shoot ratios were 0.29 (Hc), 0.30 (Ls), 0.37 (Ae, Tr) and 0.55 (Co). Finally, ecosystem C gain between 2001 and 2009 was estimated as:

$$\text{Ecosystem C gain} = ACP_{2009} + RC_{2009} + (SOCP_{2009} - SOCP_{2001}) \quad (14)$$

where ACP_{2009} is aboveground C pool, i.e., the sum of the C mass of CWD, trees, herbaceous vegetation and litter in 2009, RC_{2009} is the root C pool estimated from root/shoot ratio for 2009, and $SOC_{2009} - SOC_{2001}$ is the difference in the topsoil organic C pools between 2001 and 2009 and takes a negative value.

Litter C concentration, ecosystem C gain and RGR of C were analyzed by univariate ANOVA (Type III Sums of Squares) with diversity as the main effect of interest. Aboveground ecosystem characteristics measured repeatedly at the plot level through time (e.g. C pools in trees, CWD, herbaceous vegetation as well as aboveground C pool), were tested using an ANOVA with repeated measures (ANOVAR) with diversity as the main between subject effect and years as the main within subject effect. Soil characteristics measured in 2001, prior to the establishment of the plantation, and in 2009 were analyzed by two-way ANOVAs with year, diversity and their interactions as the effects of interest because sampling did not occur at exactly the same position in 2001 and 2009, which prevented us from using ANOVAR. Decomposition of CWD was analyzed by three-way ANOVA with diversity, species and month as the main factors. Because measurements were replicated at the subplot level, the model considered that the appropriate error for diversity was plot (diversity). Month was not considered as a repeated factor since a different bag was measured each time. Pearson's correlation coefficient was used to test the relationship between different C pools and fluxes. For soil respiration data, the assumption of no diversity effect (i.e., $B_1 = B_2$; Eqs. (8) and (10)), was tested using a paired *t*-test with plot-level soil respiration rates for each of the six-species plots estimated by both methods (B_1 and B_2).

Finally, for 2009, we tested for three different path models to relate the observed aboveground C pools and SOC. These paths were:

$$SOC = \text{Trees} + \text{Herbaceous} + \text{CWD} + \text{Litter} + \varepsilon \quad (15)$$

$$SOC = \text{RGR}_{\text{Trees}} + \text{Herbaceous} + \text{CWD} + \text{Litter} + \varepsilon \quad (16)$$

$$\Delta SOC = \text{RGR}_{\text{Trees}} + \text{Herbaceous} + \text{CWD} + \text{Litter} + \varepsilon \quad (17)$$

Data were standardized prior to the analysis. All statistical analyses were performed using SAS v. 9.2. Normality was checked prior to the analysis. The only variable that needed transformation was litter production, which was normalized by calculating the square-root.

3. Results

3.1. Carbon pools

3.1.1. Net primary production and aboveground pools

Overall, NPP ranged from $14.9 \text{ Mg ha}^{-1} \text{ yr}^{-1}$ in monocultures in 2007 to $23.6 \text{ Mg ha}^{-1} \text{ yr}^{-1}$ in triplets in 2009. Year was the only significant difference observed with an increase through time overall, NPP_{2009} being significantly higher ($21.4 \pm 2.1 \text{ Mg ha}^{-1} \text{ yr}^{-1}$) than NPP_{2007} ($15.5 \pm 1.0 \text{ Mg ha}^{-1} \text{ yr}^{-1}$). Observed aboveground C pools were estimated yearly as the sum of trees, CWD, litter and herbaceous C pools for each diversity level. Not surprisingly, the ANOVA unveiled a significant effect of year ($F_{2,38} = 93.48, p < 0.0001$), with C pools increasing from 2006 to 2009 (Fig. 1). Across diversity levels, the general mean for observed aboveground C pools in 2006 were $7.9 \pm 2.5 \text{ Mg ha}^{-1}$, while in 2009 the observed aboveground C pool was $20.4 \pm 7.4 \text{ Mg ha}^{-1}$, a 158% increase. The effect of diversity on the observed aboveground C pools was not significant.

In 2009, the contribution of the four components of aboveground C pools ranked CWD ~ litter < herbaceous < trees (Table 2). Living trees accounted for 59–84% of the total observed aboveground C pool. The herbaceous C pool was an important component of the system, with between 3.6 and 6.3 Mg ha^{-1} among the

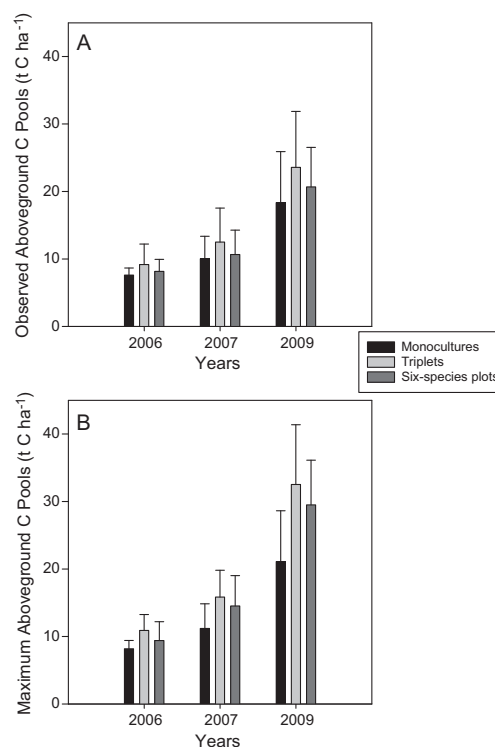


Fig. 1. Observed (A) and maximum (B) aboveground C pools for the three diversity levels for 2006, 2007 and 2009. Data are mean for each diversity level in year with standard deviation.

different plots in 2009. The contribution of CWD to observed aboveground C pools was negligible, being always <1%. Across diversity levels and years, the CWD C pool ranged between 0.008 Mg ha^{-1} for six-species mixtures in 2006 to 0.423 Mg ha^{-1} for triplets in 2007. The CWD C varied markedly among plots. In one of the monoculture plots established with *Luehea seemanii*, the CWD C pool ($0.546 \text{ Mg C ha}^{-1}$) was an order of magnitude greater than the mean of all monoculture plots ($0.112 \text{ Mg C ha}^{-1}$). The pool of C in trees in that particular plot was likewise greater than the mean trees C pool of monocultures ($26.4 \text{ Mg C ha}^{-1}$ vs $13.5 \text{ Mg C ha}^{-1}$, respectively). MANOVA was used to test the effect of diversity on the allocation of C within the different aboveground pools, but no significant effect

Table 2

Estimated contribution (%) of the four C pools measured to estimate observed aboveground C pools (OACP) and maximum aboveground C pool (MACP), controlling for tree mortality. Data are the mean in 2009 for each of the diversity levels with standard deviation in parentheses. CWD, coarse woody debris.

	Monocultures	Triplets	Six-species
OACS			
Trees	68.8 (14.2)	75.0 (8.9)	74.3 (5.3)
Herbaceous	29.2 (14.0)	22.7 (9.7)	24.0 (5.7)
Litter	1.4 (0.8)	1.6 (0.7)	1.0 (0.5)
CWD	0.5 (0.5)	0.8 (0.2)	0.7 (0.2)
MACS			
Trees	73.5 (11.9)	82.9 (5.3)	82.7 (2.8)
Herbaceous	24.7 (11.9)	15.6 (5.3)	16.4 (2.8)
Litter	1.2 (0.4)	0.6 (0.01)	0.7 (0.1)
CWD	0.6 (0.4)	0.8 (0.2)	0.8 (0.2)

Table 3

Results from analysis of variance comparing topsoil characteristics (0–10 cm) in 2001 and 2009. SOC, soil organic C concentration; SOCP, soil organic C pool. Significant effects are shown in *italics*.

Traits	Sources of variation	<i>F</i>	df	<i>p</i>
SOC	Year	51.97	1	<0.0001
	Diversity	0.96	2	0.96
	Year × diversity	2.54	2	0.093
$\delta^{13}\text{C}$	Year	26.23	1	<0.001
	Diversity	0.44	2	0.64
	Year × diversity	1.51	2	0.23
SOCP	Year	52.12	1	<0.001
	Diversity	1.71	2	0.11
	Year × diversity	1.40	2	0.38

was detected. The CWD C pool was stable through time, while the herbaceous C pool increased slightly. The fastest increment in C pool was for trees.

Maximum aboveground C pools, obtained by controlling for tree density, were also estimated (Fig. 1). As for observed aboveground C pools, the maximum aboveground C pools increased significantly through time ($F_{2,38} = 156.1$, $p < 0.0001$). The effects of both diversity and year × diversity on maximum aboveground C pools were also statistically significant ($F_{2,19} = 4.47$, $p = 0.025$ and $F_{4,38} = 398$, $p = 0.0085$ respectively). Maximum aboveground C pools for monocultures was $13.5 \text{ Mg C ha}^{-1}$ compared with $19.8 \text{ Mg C ha}^{-1}$ for triplets, a 46% difference. Through time, maximum aboveground C pools increased significantly less in monocultures than in mixture plots (Fig. 1). Trees C pool was a more important component of maximum aboveground C pool in mixtures than in monocultures, while herbaceous and litter C pools were more important components of maximum aboveground C pools in monocultures than in mixtures (Table 2). Not surprisingly the observed aboveground C pools were always smaller than maximum aboveground C pools.

Analysis of the RGR of aboveground C pools unveiled a marginally significant diversity effect on maximum aboveground C pools ($F_{2,21} = 2.81$, $p = 0.085$) with higher RGR at higher in triplets (36.3%) than in monocultures (30.1%) and six-species (28.8%), but no effect of diversity on observed aboveground C pools.

3.1.2. Soil properties

We observed strong changes in the concentration (SOC), pool (SOCP) and stable carbon isotope ratio ($\delta^{13}\text{C}$) of topsoil C during the establishment phase of the plantation (Fig. 2). Soil C decreased overall by 28.7% between 2001 and 2009. The reduction of SOC was strongest in the triplets (−40%), followed by monocultures (−25%) and the six-species mixtures (−19%). Similarly, SOCP decreased significantly from a mean of $34.5 \pm 2.4 \text{ Mg C ha}^{-1}$ in 2001 to $25.7 \pm 5.7 \text{ Mg C ha}^{-1}$ in 2009 (Table 3). The $\delta^{13}\text{C}$ decreased from −16.9‰ in 2001 to −20.8‰ in 2009. In 2001, about 80% of the organic matter in the soil was derived from C_4 pasture vegetation, whereas by 2009 this contribution had decreased to 49%, indicating increased inputs of organic matter by trees. On average, this means that the 2001 soil contained $27.6 \text{ Mg C ha}^{-1}$ of C_4 -derived C, which decreased to $12.6 \text{ Mg C ha}^{-1}$ in 2009, whereas the C_3 -derived C component increased from 6.9 to $13.1 \text{ Mg C ha}^{-1}$. These changes indicate the speed with which soil organic C turns over in this system. None of the soil characteristics that we measured showed a significant effect of diversity, but SOC responded marginally to the interaction between year and diversity (Table 3).

3.2. Carbon fluxes

3.2.1. Coarse woody debris decomposition

Besides changing through time, monthly CWD decomposition, measured as the proportional loss in CWD biomass, varied sig-

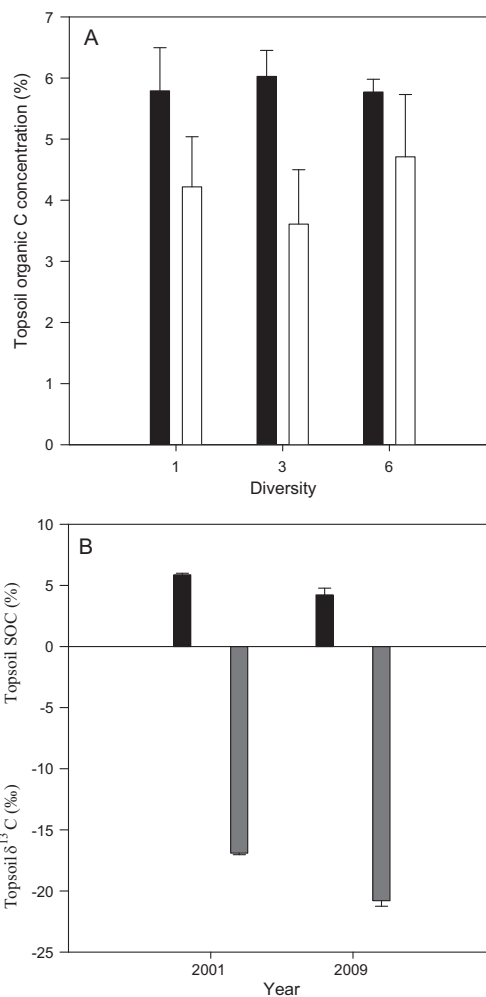


Fig. 2. (A) Comparison of topsoil (0–10 cm) soil organic C concentration (SOC) for the three diversity levels in 2001 and in 2009. The filled bars are data from 2001 and the empty bars are for 2009; (B) Mean value, across all diversity treatment for SOC and $\delta^{13}\text{C}$ values in 2001 and 2009. The black bars denote SOC and the grey bars are $\delta^{13}\text{C}$ values.

nificantly as function of diversity, species and their interaction (Table 4). Monthly decomposition was significantly faster in monocultures, with a mean of $35 \pm 24.1\%$ compared with $31.3 \pm 21.0\%$ and $31.9 \pm 26.8\%$ for triplets and six-species mixtures, respectively. Across species, wood decomposition was slowest for *Luhea seemanii* ($27.7 \pm 26.5\%$) and highest for *Hura crepitans* ($42.1 \pm 21.8\%$), the other species having intermediate values of $29.1 \pm 22.3\%$ (*Tabebuia rosea*), $32.1 \pm 14.5\%$ (*Cedrela odorata*) and $33.6 \pm 30.8\%$ (*Anacardium excelsum*). After one month in the field, the woody stakes had lost, on average, between 19% (in six-species mixtures) and 29% (in monocultures) of the initial mass. It took six months to lose up to 40% of the initial mass and, after 10 months, the overall loss in biomass was $48 \pm 20.5\%$. As time passed, the water content of the stakes increased to ~60%. Of the 600 stakes monitored in the experiment, only 21 stakes fully decomposed: nine were Hc, six Co, five Tr and one was Ae. The decay rate, *k*, did not differ significantly

G Model

FORECO-12439; No. of Pages 11

ARTICLE IN PRESS

C. Potvin et al. / Forest Ecology and Management xxx (2010) xxx–xxx

7

Table 4

Results of the ANOVA for the decomposition of coarse woody debris (CWD) between May 2007 and March 2008. Note that because data were replicated within a plot, the effect of diversity was tested against the appropriate error term plot (diversity). Significant effects are in italics.

Sources	df	SS	F	p
<i>Diversity</i>	2	0.20	15.93	0.025
<i>Species</i>	4	1.36	15.92	0.0001
<i>Div × sp</i>	8	0.85	4.99	0.0001
<i>Month</i>	9	14.84	77.05	0.0001
<i>Div × month</i>	18	0.57	1.48	0.09
<i>Sp × month</i>	36	1.94	2.53	0.0001
<i>Div × sp × month</i>	71	2.36	1.56	0.0048
Plot (div)	3	0.01	0.30	ns
Error	393	8.41		

among diversity levels, but responded significantly to the effect of species (diversity) ($F_{12,59} = 22.03$, $p < 0.0001$). Decay rate, k , ranged between -3.22 ± 0.39 for *Hura crepitans* grown in monocultures to -0.85 ± 0.20 for *Anacardium excelsum* in monocultures.

3.2.2. Litter decomposition

Data on litter decomposition were published previously (Scherer-Lorenzen et al., 2007). In brief, diversity had no significant effect on decomposition of the entire litter mixture (i.e., mixing species resulted in purely additive effects), although within mixtures, individual species decomposed at different rates depending on litter diversity. These results also highlighted the importance of species-specific effects on ecosystem processes.

3.2.3. Soil respiration

Soil respiration rates measured between pairs of trees were scaled to the plot level in the diversity plots to compare plot-level diversity effects. Using average respiration values from the monoculture pairs (model 1), respiration at the plot level was estimated to be $0.99 \pm 0.09 \mu\text{mol CO}_2 \text{ m}^{-2} \text{ s}^{-1}$. When scaling up using respiration of the mixed-species pairs (model 2), plot respiration was estimated to be $0.84 \pm 0.08 \mu\text{mol CO}_2 \text{ m}^{-2} \text{ s}^{-1}$. Our scaling-up calculations show that, at the plot level, there was a significant difference between the purely additive model and the model considering neighboring species interactions ($t = 15.35$, $df = 11$, $p < 0.001$), using the combined dry and early wet season data. This pattern was consistent across plots (Fig. 3).

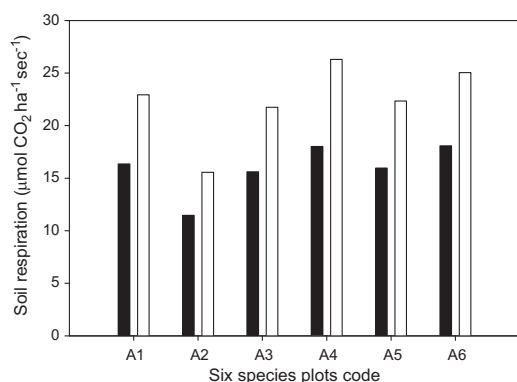


Fig. 3. Plot level soil respiration for each of the six-species mixtures using two scaling procedures. Empty bars represent plot respiration using monoculture scaling and filled ones using multipair scaling. For details see Murphy et al. (2008). Data used to estimate soil respiration at the plot level were obtained in March (dry season) and June (early wet season) of 2004.

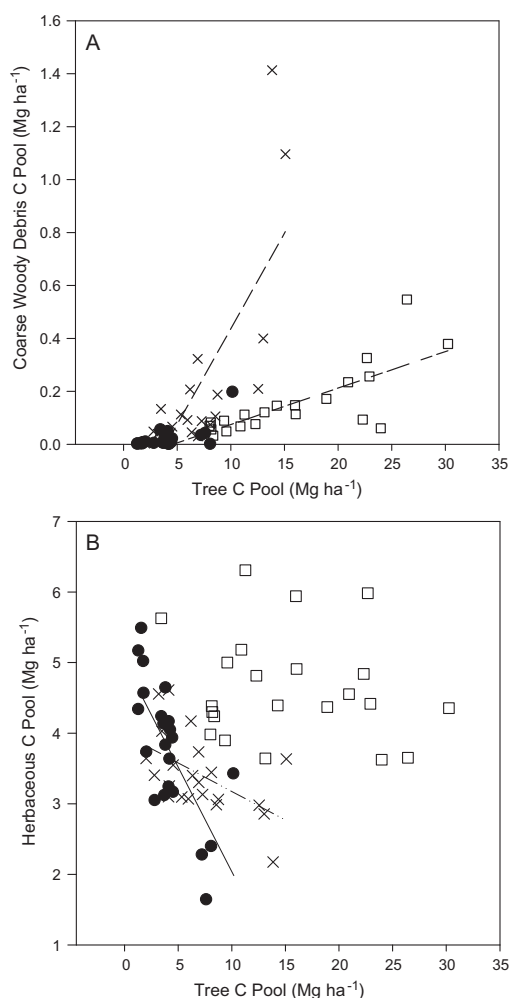


Fig. 4. Correlation between (A) the herbaceous vegetation and (B) coarse woody debris C pools and the trees C pools in 2006, 2007 and 2009. Symbols are: (●) 2006; (X) 2007; (□) 2009.

3.3. The ecosystem perspective

The relationship among the different components of the above-ground C pools was examined by correlation analyses, which revealed that the CWD C pool was significantly and positively correlated with the tree C pool in 2007 and 2009, but not in 2006 (2006: $r = 0.397$, $p = 0.225$; 2007: $r = 0.840$, $p = 0.001$; 2009: $r = 0.694$, $p = 0.017$). For the herbaceous C pool, we observed a significant negative correlation with the tree C pool in both 2006 and 2007 ($r = -0.724$, $p < 0.0001$, and $r = -0.539$, $p < 0.05$ respectively), but not in 2009 ($r = -0.168$, $p = 0.45$) (Fig. 4).

At the ecosystem level, three of the four aboveground C pools that were measured (trees, herbaceous vegetation and CWD) had their highest values in triplets and their lowest values in monocultures (Table 5). This pattern was also observed for litter production in the dry season of 2005 (Scherer-Lorenzen et al., 2007). Our results also indicate higher fluxes in monocultures than in mix-

Table 5

Magnitude and direction of diversity effects on observed C pools (OACP) and fluxes in the Sardinilla plantation. For trees, herbaceous and coarse woody debris (CWD), we compared mean C pools in 2009. For litter production, the difference was for our yearly estimate. Litter decomposition data are from Scherer-Lorenzen et al. (2007). Soil respiration data are from 2004 and for soil we calculated the difference in the loss of SOC between 2001 and 2009. Variables for which either the diversity or the time by diversity effects were statistically significant are in italics.

OACP components		Fluxes		Soil	
Tree	Triplets > monocultures +35%	Litter decomposition	Monocultures > triplets +5%	<i>Loss in SOC</i>	Triplets > monocultures +15.1%
Herbaceous	Triplets > monocultures +5%	<i>CWD decomposition</i>	Monocultures > triplets +11.8%		
Litter	Triplets > monocultures +7%	<i>Soil respiration</i>	Monocultures > mixture +17%		
CWD	Triplets > monocultures +73%				

tures, both for CWD decomposition and soil respiration. Finally, while the entire system lost SOC through time, the loss was most important in triplets and least important in six-species mixtures (Table 5).

Eight years after planting, the ecosystem C storage in the plantation, including tree roots and mineral topsoil C, ranged between $50.2 \pm 11.4 \text{ Mg C ha}^{-1}$ for monocultures and $54.5 \pm 8.7 \text{ Mg C ha}^{-1}$ for six-species plots (Fig. 5), triplets showing an intermediate value ($51.8 \pm 8.1 \text{ Mg C ha}^{-1}$), triplets showing an intermediate value ($51.8 \pm 8.1 \text{ Mg C ha}^{-1}$), then the plantation gained in C, on average, ~ 20 and lost $\sim 9 \text{ Mg ha}^{-1}$ in biomass and soil respectively, for an overall gain of $\sim 11 \text{ Mg ha}^{-1}$ over 8 years. The plantation gained C during this period, with a mean accumulation of $16.1 \pm 10.6 \text{ Mg C ha}^{-1}$ in monocultures, $17.4 \pm 9.5 \text{ Mg C ha}^{-1}$ in triplets and $19.2 \pm 8.6 \text{ Mg C ha}^{-1}$ in six-species mixtures. Differ-

ences among the diversity levels were not statistically significant for either ecosystem C storage or gain. The two plots that gained most C between 2001 and 2009 were a six-species plot ($35.3 \text{ Mg C ha}^{-1}$) and a triplet established with *Luhea seemanii*, *Anacardium excelsum* and *Tabebuia rosea* ($32.9 \text{ Mg C ha}^{-1}$) (Fig. 5). Three monocultures also showed high C gains between 2001 and 2009: two were planted with *Tabebuia rosea* ($31.2 \text{ Mg C ha}^{-1}$ and $27.3 \text{ Mg C ha}^{-1}$) and the third one with *Cedrela odorata* ($26.5 \text{ Mg C ha}^{-1}$). The plots with the lowest ecosystem C gain were the monocultures of *Hura crepitans* (1.3 and 1.8 Mg C ha^{-1}), in which the increments in C pools aboveground (12.8 and 9.3 Mg C ha^{-1} , respectively) were cancelled by losses of soil C of 13.9 and 8.4 Mg C ha^{-1} , respectively. Interestingly, *Hura* also had the highest leaf litter decomposition rate, presumably due to its low ratios of C:N and lignin:N (Scherer-Lorenzen et al., 2007).

We used path analyses to obtain a better understanding of the ecosystem response to diversity. We tested three models (Eq. (15)–(17)) to relate either SOC in 2009 or changes in SOC between 2001 and 2009, with four main aboveground C pools (trees, herbs, litter and CWD). The path model described in Eq. (15) had the highest explanatory power, with adjusted r^2 values of 0.136, 0.532 and 0.996 for monocultures, triplets and six-species mixtures, respectively. In monocultures, none of the paths were statistically significant, while two and four paths were statistically significant for triplets and six-species mixtures, respectively (Fig. 6). This suggests that, as diversity increases, the cycling of C is more tightly coupled among the different components of the ecosystem. In six-species mixtures, tree C is positively related to both CWD and litter production. Litter production, in turn, is positively correlated with SOC.

4. Discussion

4.1. Planting for carbon: an ecosystem approach

Eight years after reforestation in Sardinilla, the aboveground tree C pool and the topsoil organic C pool were found to be highly dynamic. We observed an increase in the size of the trees C pool concurrent with a decrease in the size of the soil C pool in the top 10 cm. As stated by other researchers (Catovsky et al., 2002; Körner, 2000), but often ignored, our results show that NPP, estimated from aboveground biomass, is not a good index of ecosystem C storage. The decreasing size of the topsoil C pool during the initial years following reforestation in Sardinilla shows that inputs to the topsoil C pool were smaller than the outputs. In the plantation, inputs to the soil are derived mainly from fine roots, litter production (Valverde-Barrantes, 2007) and CWD (Kirby and Potvin, 2007), while C is most probably lost through the decomposition of the previous grassland species and their root biomass. The observed changes in $\delta^{13}\text{C}$ provide some information on the source of the organic matter in the soil, showing clearly a changing contribution from C_4 pasture to C_3 trees. By 2009, about half of the soil organic matter in the topsoil was derived from trees, and this fraction is likely to increase with progressing plantation establishment. After plantation establishment in Sardinilla, the topsoil continued

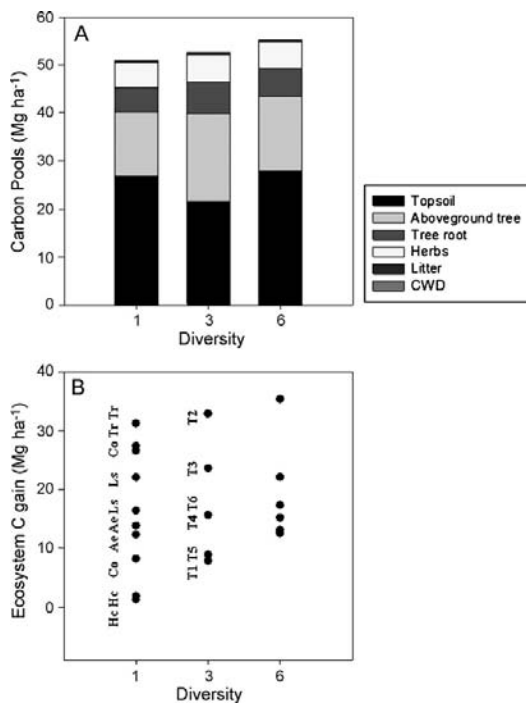


Fig. 5. (A) Total ecosystem C storage broken down in its different above- and below-ground components in 2009 and (B) ecosystem C gain between 2001 and 2009 for each of the three different diversity levels. In (A) data are the mean of all plots established with the same number of species while, for (B), each circle represents an individual plot. Species planted in monocultures are abbreviated as follows: Ae, *Anacardium excelsum*, Co, *Cedrela odorata*, Hc, *Hura crepitans*, Ls, *Luhea seemanii*, Tr, *Tabebuia rosea*. The triplets are abbreviated as T1–T6 and were established with T1: Co–Hc and *Cordia alliodora* (Ca) that massively died after planting, T2: Ae–Ls–Tr, T3: Co–Ls–Ae, T4: Co–Hc–Ls, T5: Hc–Tr–Ca and T6: Ae–Tr–Ca.

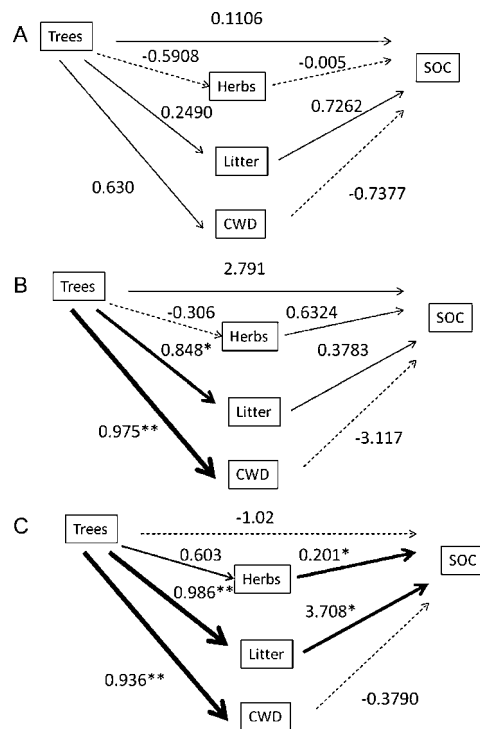


Fig. 6. Solved path diagram relating aboveground C pools with SOC for (A) monocultures, (B) triplets and (C) six-species mixtures. Solid lines represent positive relationships and dashed ones negative effects. Increasing width of the lines denotes statistically significant paths. The numbers are the path coefficients for each step of the model. Path significance: * $p < 0.05$ and ** $p < 0.01$.

to lose pasture SOC, which has not been replaced by plantation SOC. It should be noted that the decline in soil carbon is likely to be an underestimate, because we did not account for C in deeper soil horizons. These can contain a considerable proportion of the total soil C. In 2001, for example, seven soil profiles to a depth of 1 m contained 100–120 Mg C ha⁻¹, so that between 25% and 30% of the 1 m-deep SOC is contained in the top 10 cm (Abraham, 2004). In nearby Barro Colorado Island, for example, only 25% of the total soil C down to 1 m depth is found in the upper 10 cm, falling to 15% if 3 m depth is considered (B.L. Turner, unpublished data). Despite this, the biggest changes following perturbation can be expected in the topsoil as deeper soil carbon pools are considered fairly stable (Malhi and Davidson, 2009). We therefore assume that the majority of the changes following afforestation are captured in our dataset.

In the early years of plantation establishment a large proportion of tree productivity is allocated to developing storage organs (trunks and roots), rather than to yearly tissues such as leaves, thus reducing C flux to the soil C (Nair et al., 2009b; Yang et al., 2007). The magnitude and direction of changes in the soil C pool following reforestation can be highly variable and dependent on a variety of factors, including previous land use, species and soil properties (Epron et al., 2009). Meta-analysis have indicated a 10% reduction of soil C pools with land conversion from pasture to plantation (Guo and Gifford, 2002) and reductions in soil C between 6.7% and 15% across 153 sites with diverse plantation types (Berthrong et al., 2009). Both studies indicated that *Pinus* plantations in particular reduced soil N due to rapid plant uptake. In comparison, broadleaf tree plantations reduced soil C pools (Guo and Gifford, 2002). Don

et al. (2009) reported a significant C loss (41% reduced gross primary production) only during the first year after conversion from pasture to tree plantation due to site preparation, including ploughing. In Sardinilla, however, the soil was not ploughed before planting. Standard reforestation practice in Panama is to hand clean the field and open a hole, the size of seedling's roots, thus minimizing ecosystem disruption.

The precipitation regime might provide a possible explanation for the observed loss of SOC during reforestation in Sardinilla. Guo and Gifford (2002) reported that plantations established in areas with >1500 mm yr⁻¹ rainfall showed an average -23% decreases in SOC. Precipitation at the nearby meteorological station of Salamanca, about 5 km to the northeast of the Sardinilla plantation, has a long term mean (1972–2009) of 2289 mm, raising the possibility that an important amount of C might be lost from the site after heavy rains. Net ecosystem production that ultimately determines C storage has been described as the balance between autotrophic C uptake by photosynthesis and respiration (Catovsky et al., 2002), although in the humid tropics C loss via runoff as dissolved organic C must also be accounted for (Schwendenmann and Veldkamp, 2005; Goller et al., 2006; Fujii et al., 2009).

Root biomass and dynamics are important unknown in global C pools (Nair et al., 2009a). Robinson (2007) suggested that available data on root biomass underestimate their contribution to the total biomass by 40%. We used site- and species-specific allometric relationships to estimate root biomass and, therefore, the root C pool, although this approach suffered from several shortcomings. First, we assumed that the root/shoot ratio remained identical as trees grew and that these ratios were also not sensitive to neighborhood-effects, although these assumptions that were not tested. Furthermore, due to the clay-rich nature of the soil, we were unable to sample and weigh fine roots (Coll et al., 2008). According to Nair et al. (2009a) fine roots could represent as much as 33% of global NPP, although high turnover of fine roots imply that this part of NPP will not strongly affect long-term C sequestration into the soil C pool. The root/shoot ratios that we used to estimate the root C pool did not account for fine roots, thus underestimating the true size of this pool.

In 2009, the aboveground tree C pool in Sardinilla ranged between 30.2 Mg C ha⁻¹ for a triplet established with Ae, Ls and Tr and 3.4 Mg C ha⁻¹ for a monoculture plot of Hc, with a mean value of 15.7 Mg C ha⁻¹. These values compare well with data from a 9–14-year-old native tree plantation in Costa Rica that reported a range of 12.4–79.1 Mg C ha⁻¹ (Redondo-Brenes, 2007) and are in line with an early report of C pools in the aboveground plant component of tropical plantations (Schroeder, 1992). Overall, despite the reduction in the size of the topsoil C pool, the Sardinilla plantation has acted as a net C sink since its establishment, with an average of 18.39 Mg C ha⁻¹ gained over 8 years. Further, the observed exponential tree growth suggests that the sink strength will increase through time, at least in the medium term. Our results show clearly that the aboveground tree C pool represents only half of the observed ecosystem C storage with the mineral topsoil (not including soil carbon > 10 cm deep), with herbs and tree roots being other important C pools.

4.2. Biodiversity and C pools

The possibility that mixed-species plantations might increase ecosystem C storage has been often cited as a reason for the promotion of reforestation with native species (Diaz et al., 2009; Piotto et al., 2010; Caspersen and Pacala, 2001). A variety of hypotheses have been proposed to explain the expected relationship between tree diversity and ecosystem C storage. Diaz et al. (2009), along with Catovsky et al. (2002), stated that biodiversity could affect (1) the rates of C gain or loss, (2) the size of C pool, and (3) temporal sta-

bility and hence the lifespan or stability of C pools. In other words, if biodiversity influences either the size of C pools or fluxes, it will affect ecosystem C storage. However, in Sardinilla, the strongest diversity effects that we uncovered were on the links between the different pools of C, rather than on the pools themselves. The C pools, whether ecosystem or aboveground only, did not respond significantly to diversity.

Results from other mixed-species plantations suggest that the identity of the dominant species plays an important role in determining C gained by the trees (Redondo-Brenes, 2007; Valverde-Barrantes, 2007). For example Piotto et al. (2010) found positive biodiversity effects in one of three 15–16-year-old native plantations and showed that, in economical terms, mixed species plantations outperformed monocultures. Ewel and Mazzarino (2008) suggested that traits such as leaf phenology could explain the outcome of mixed species plantations and argued that no unique outcome of planting mixed species was to be expected. In Sardinilla, mixtures forming a stratified canopy (e.g. with the fast-growing Ls in the upper canopy, the moderately growing Ae in the middle canopy, and the late successional and slow-growing species Tr in the lower canopy) are especially promising. Such stratification is often mentioned as a prerequisite for complementary resource use in mixed stands, leading to higher productivity (Kelly, 1992; Scherer-Lorenzen et al., 2005a). Furthermore, the inclusion of species with rather high limits of litter decomposition (Berg and McClaugherty, 2003), such as those with recalcitrant litter, would also allow for sustained accumulation of humus and hence C in the soil. Data from litter production and decomposition from our plantation suggest that admixing Ls and Ae would also contribute to C sequestration, due to their high rates of litter and CWD production, combined with rather low decomposition rates and low N concentrations in litter (Scherer-Lorenzen et al., 2007).

It has been noted elsewhere that tree mortality plays an important role in determining the biomass of a plantation (Vila et al., 2007; Paquette and Messier, 2010). Mortality was species-specific in Sardinilla, and we provided strong evidence for species complementarity when controlling for tree mortality (Potvin and Gotelli, 2008). Following these results we chose to report aboveground C pools as either observed or maximum values. To calculate observed aboveground C pools, the data was scaled up to a standard area, chosen as one hectare, to correct for different plot sizes. The second estimate of aboveground C pools assumed no mortality and used the average biomass value of living trees of each species to estimate plot-level tree biomass. Maximum aboveground C pools, controlling for tree density and associated RGR, were shown to respond significantly to diversity, yet observed aboveground C pool did not. Mortality apparently obscured the diversity effect as reported elsewhere (Erskine et al., 2006; Petit and Montagnini, 2006), despite the possibility that dead trees might free resources allowing living trees to grow bigger. The important work done by Ewel and collaborators in La Selva, Costa Rica, could provide an explanation (Haggard and Ewel, 1997; Ewel and Mazzarino, 2008). In 1991, they established monocultures and polycultures of three native tree species (*Hyeronima alchorneoides*, *Cedrela odorata* and *Cordia alliodora*) in association with *Euterpe oleracea* and *Heliconia imbricata* forming a sub-canopy cover. After 13 years of growth, their results show that deciduousness of the tree species is a key characteristic determining the productivity of the ecosystem. *Hyeronima*, being evergreen, was able to maintain a high aboveground net primary production, while the net aboveground production of *Cordia*, and to a lesser extent *Cedrela*, was severely limited by *Euterpe* and *Heliconia*. We suggest that tree mortality in Sardinilla stimulated the herbaceous layer rather than growth of the remaining living trees.

We nevertheless uncovered three significant or marginally significant effects of diversity or its interaction (CWD decomposition,

soil respiration, and the reduction of SOC) and used path analyses to examine relationships between these different pools and fluxes. The results unequivocally showed that, as diversity increases, the links between the different C pools and fluxes become significantly stronger. The strongest diversity effects in the Sardinilla plantations were on the links between the different pools of C, rather than on the size of the pools themselves. Eight years after establishment of the tree plantation on a former pasture, tree diversity affected the processes governing the changes in C pools and fluxes related to the land-use change. We conclude that the choice of tree mixtures for afforestation in the tropics alters ecosystem C storage. Our ability to make stronger inferences from this finding is curtailed by the quality of some of the estimates that we used (e.g. for litter production) and because of the temporal variation in some of the data used (e.g. soil respiration data from 2004). Our results, however, strongly suggest that an integrated ecosystem approach, in which all ecosystem characteristics linked to both C pools and C cycling are included, is required to gain an accurate representation of the effect of biodiversity on this important ecosystem function. We are currently planning such an integrated effort in Sardinilla for the 10th year of the plantation in 2011.

Acknowledgements

The Sardinilla plantation was established with the help to a grant from the Ministère de la Recherche, de la Science et de la Technologie du Québec. Continuous support from the Smithsonian Tropical Research Institute was invaluable in our ability to maintain this site on the long term. C.P. acknowledges the support from a Discovery grant of the Natural Sciences and Engineering Council of Canada. Jose Luis Bonnilla collected litter fall and analyzed the litter decomposition bags in 2005. In 2007 and 2008 litter fall and the herbaceous vegetation were sampled by Simone Taperon, Timo Mark, and Lisa Werther, while Volker Hahn helped in measuring soil respiration. This research was funded by the German Research Foundation (DFG Wi 1601/6-1) which we gratefully acknowledge. N.B. and S.W. appreciate funding from the North-South Centre (former Swiss Centre for International Agriculture) of ETH Zurich, Switzerland. Financial support was provided to M.S.-L. and Jan Jansa (ETH Zurich) by the Swiss National Science Foundation (3100A0-110031/1).

References

- Abraham, M., 2004. Spatial variation in soil organic carbon and stable carbon isotope signature in a pasture and a primary forest in Central Panama. M.Sc. thesis, Department of Geography, McGill University, 91 pp.
- Berthrong, S.T., Jobbágy, E.G., Jackson, R.B., 2009. A global meta-analysis of soil exchangeable cations, pH, carbon, and nitrogen with afforestation. *Ecological Applications* 19, 2228–2241.
- Caspersen, J.P., Pacala, S.W., 2001. Successional diversity and forest ecosystem function. *Ecological Research* 16, 895–903.
- Catovsky, S., Bradford, M.A., Hector, A., 2002. Biodiversity and ecosystem productivity: implications for carbon storage. *Oikos* 97, 443–448.
- Coll, L., Potvin, C., Messier, C., Delagrangé, S., 2008. Carbon storage, allocation patterns and root architecture of tropical trees with contrasting shade tolerance in young mixed plantations. *Trees—Structure and Function* 22, 585–596.
- Delagrangé, S., Coll, L., Messier, C., Potvin, C., 2008. Linking multiple-level tree traits with biomass accumulation in native tree species used for reforestation in Panama. *Trees—Structure and Function* 22, 337–349.
- Diaz, S., Hector, A., Wardle, D.A., 2009. Biodiversity in forest carbon sequestration initiatives: not just a side benefit. *Current Opinion in Environmental Sustainability* 1, 55–60.
- Don, A., Rebmann, C., Kolle, O., Scherer-Lorenzen, M., Schulze, E.D., 2009. Impact of afforestation-associated management changes on the carbon balance of grassland. *Global Change Biology* 15, 1990–2002.
- Elias, M., Potvin, C., 2003. Assessing intra- and inter-specific variation in trunk carbon concentration for 32 neotropical tree species. *Canadian Journal of Forest Research* 33, 1039–1045.

G Model

FORECO-12439; No. of Pages 11

ARTICLE IN PRESS

C. Potvin et al. / Forest Ecology and Management xxx (2010) xxx–xxx

11

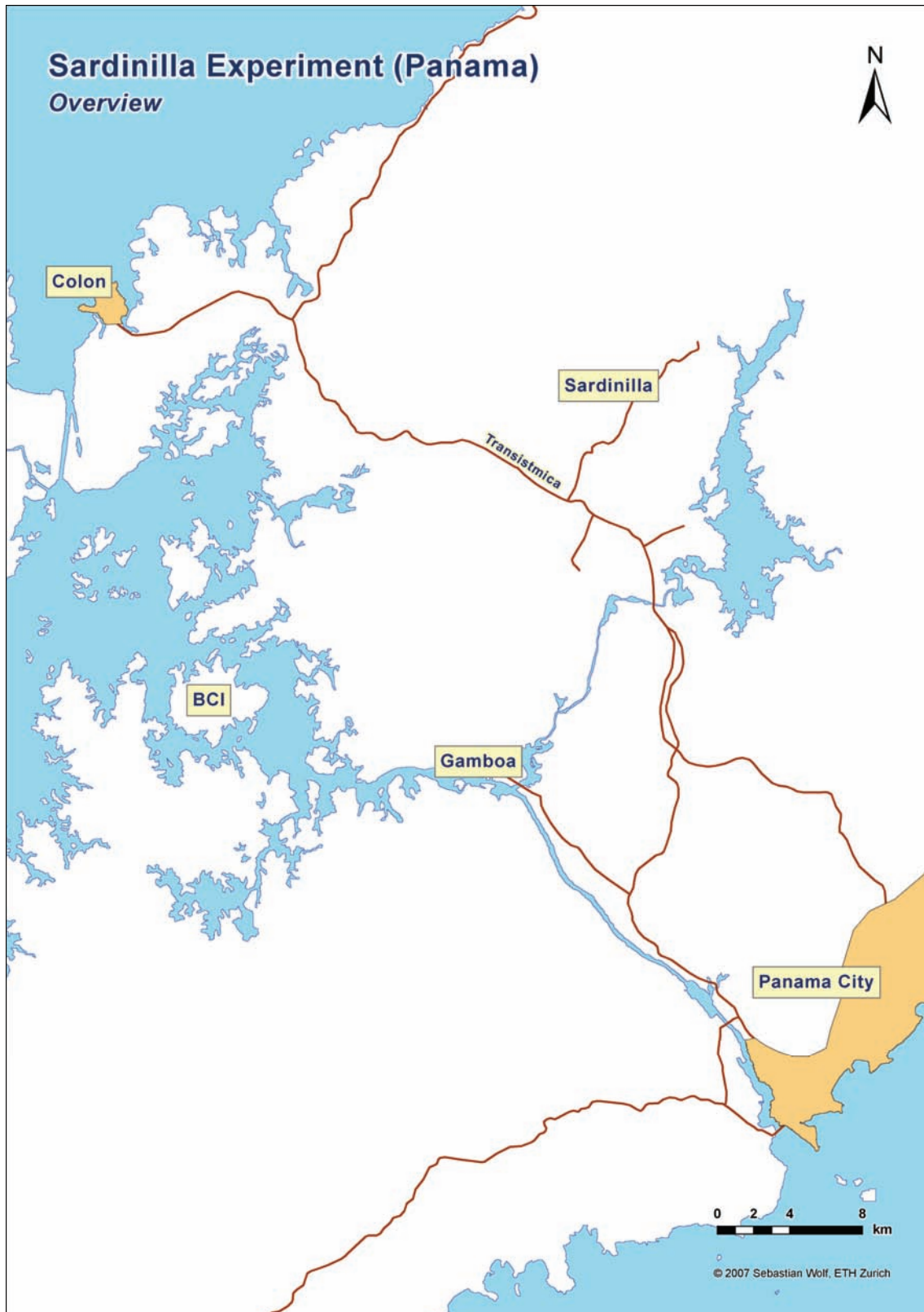
- Epron, D., Marsden, C., M'Bou, A.T., Saint-André, L., d'Annunzio, R., Nouvellon, Y., 2009. Soil carbon dynamics following afforestation of a tropical savannah with *Eucalyptus* in Congo. *Plant and Soil* 323, 309–322.
- Erskine, P.D., Lamb, D., Bristow, M., 2006. Tree species diversity and ecosystem function: can tropical mixed-species plantations generate greater productivity? *Forest Ecology and Management* 233, 205–210.
- Ewel, J.J., Mazzarino, M.J., 2008. Competition from below for light and nutrients shifts productivity among tropical species. *Proceedings of the National Academy of Sciences (USA)* 105, 18836–18841.
- Firn, J., Erskine, P.D., Lamb, D., 2007. Woody species diversity influences productivity and soil nutrient availability in tropical plantations. *Oecologia* 154, 521–533.
- Fujii, K., Uemura, M., Hayakawa, C., Funakawa, S., Sukartiningih, Kosaki, T., Ohta, S., 2009. Fluxes of dissolved organic carbon in two tropical forest ecosystems of East Kalimantan, Indonesia. *Geoderma* 152, 127–136.
- Goller, R., Wilcke, W., Fleischbein, K., et al., 2006. Dissolved nitrogen, phosphorus, and sulfur forms in the ecosystem fluxes of a montane forest in Ecuador. *Biogeochemistry* 77, 57–89.
- Guo, L.B., Gifford, R.M., 2002. Soil carbon stocks and land use change: a meta analysis. *Global Change Biology* 8, 345–360.
- Haggar, J.P., Ewel, J.J., 1997. Primary productivity and resource partitioning in model tropical ecosystems. *Ecology* 78, 1211–1221.
- Harmon, M.E., Sexton, J., 1996. Guidelines for Measurements of Woody Detritus in Forest Ecosystem LTER Network Office. University of Washington, Seattle, WA.
- Kelty, M.J., 1992. Comparative productivity of monocultures and mixed-species stands. In: Kelty, M.J., Larson, B.C., Oliver, C.D. (Eds.), *The Ecology and Silviculture of Mixed-species Forests*. Kluwer Academic Publishers, Dordrecht/Boston/London, pp. 125–141.
- Kirby, K.R., Potvin, C., 2007. Species-level management in carbon sink projects: a case study from an Embera territory in eastern Panama. *Forest Ecology and Management* 246, 208–221.
- Körner, Ch., 2000. Biosphere responses to CO₂ enrichment. *Ecological Applications* 10, 1590–1619.
- Körner, C., 2003. Slow in, rapid out—carbon flux studies and Kyoto targets. *Science* 300, 1242–1243.
- Malhi, Y., Baldocchi, D.D., Jarvis, P.G., 1999. The carbon balance of tropical, temperate and boreal forests. *Plant Cell and Environment* 22, 715–740.
- Malhi, Y., Davidson, E.A., 2009. Biogeochemistry and ecology of terrestrial ecosystems in Amazonia. In: Keller, M., Bustamante, M., Gash, J., Dias, P.S. (Eds.), *Amazonia and Global Change*. American Geophysical Union, Washington, DC, pp. 293–298.
- Malmer, A., Murdiyasar, D., Bruijnzeel, L.A., Ilstedt, U., 2010. Carbon sequestration in tropical forests and water, a critical look at the basis for commonly used generalizations. *Global Change Biology* 16, 599–604.
- Murphy, M., Balsler, T., Buchmann, N., Hahn, V., Potvin, C., 2008. Linking tree biodiversity to belowground process in a young tropical plantation: impacts on soil CO₂ flux. *Forest Ecology and Management* 255, 2577–2588.
- Nair, P.K.R., Nair, V.D., Kumar, B., Hailé, S.G., 2009a. Soil carbon sequestration in tropical agroforestry systems: a feasibility appraisal. *Environmental Science and Policy* 12, 1099–1111.
- Nair, P.K.R., Kumar, B., Nair, V.D., 2009b. Agroforestry as a strategy for carbon sequestration. *Journal of Plant Nutrition and Soil Science* 172, 10–23.
- Oelmann, Y., Potvin, C., Mark, T., Werther, L., Tapernon, S., Wilcke, W., 2010. Tree mixture effects on aboveground nutrient pools of trees in an experimental plantation in Panama. *Plant and Soil* 326, 199–212.
- Paquette, A., Messier, C., 2010. The role of plantations in managing the world's forests in the Anthropocene. *Frontiers in Ecology and the Environment* 8, 27–34.
- Petit, B., Montagnini, F., 2006. Growth equations and rotation ages of ten native tree species in mixed and pure plantations in the humid Neotropics. *Forest Ecology and Management* 199, 243–257.
- Piotto, D., Craven, D., Montagnini, F., Alice, F., 2010. Silvicultural and economic aspects of pure and mixed native tree species plantations on degraded pasturelands in humid Costa Rica. *New Forests* 39, 369–385.
- Potvin, C., Gotelli, N., 2008. Biodiversity enhances individual performance but does not affect survivorship in tropical trees. *Ecology Letters* 11, 217–223.
- Redondo-Brenes, A., 2007. Growth, carbon sequestration, and management of native tree plantations in humid regions of Costa Rica. *New Forests* 34, 253–268.
- Robinson, D., 2007. Implications of a large global root biomass for carbon sink estimates and for soil carbon dynamics. *Proceedings of the Royal Society B* 274, 2753–2759.
- Scherer-Lorenzen, M., Bonilla, J.L., Potvin, C., 2007. Tree species richness affects litter production and decomposition dynamics in a tropical biodiversity experiment. *Oikos* 116, 2108–2124.
- Scherer-Lorenzen, M., Körner, C., Schulze, E.-D., 2005a. The functional significance of forest diversity: a synthesis. In: Scherer-Lorenzen, M., Körner, C., Schulze, E.-D. (Eds.), *Forest Diversity and Function: Temperate and Boreal Systems*. Ecological Studies, vol. 176. Springer, Berlin, Heidelberg, New York, pp. 377–389.
- Scherer-Lorenzen, M., Potvin, C., Koricheva, J., Schmid, B., Hector, A., Bornik, Z., Reynolds, G., Schulze, E.D., 2005b. The design of experimental tree plantations for functional biodiversity research. In: Scherer-Lorenzen, M., Kivner, C., Schulze, E.-D. (Eds.), *The Functional Significance of Forest Diversity*. Ecological Studies, vol. 176. Springer, Heidelberg/New York, pp. 347–376.
- Schwendenmann, L., Veldkamp, E., 2005. The role of dissolved organic carbon, dissolved organic nitrogen, and dissolved inorganic nitrogen in a tropical wet forest ecosystem. *Ecosystems* 8, 339–351.
- Seitlinger, T., 2008. Einfluss der Artenzahl auf die Phosphorgehalte der oberirdischen Biomasse und auf die Phosphorverfügbarkeit im Boden. Master thesis, Department of Geography, University of Zurich, 58 pp.
- Schlapfer, F., Schmid, B., 1999. Ecosystem effects of biodiversity: a classification of hypotheses and exploration of empirical results. *Ecological Applications* 9, 893–912.
- Schlesinger, W.H., Lichter, J., 2001. Limited carbon storage in soil and litter of experimental forest plots under increased atmospheric CO₂. *Nature* 411, 466–469.
- Schroeder, P., 1992. Carbon storage potential of short rotation tropical tree plantations. *Forest Ecology and Management* 50, 31–41.
- Schulze, E.-D., Wirth, C., Heimann, M., 2000. Climate change: managing forests after Kyoto. *Science* 289, 2058–2059.
- Valverde-Barrantes, O.J., 2007. Relationships among litterfall, fine-root growth and soil respiration for five tropical tree species. *Canadian Journal of Forestry Research* 37, 1954–1965.
- Vila, M., Vayareda, J., Comas, L., Ibanez, J.J., Mata, T., Obon, B., 2007. Species richness and wood production: a positive association in Mediterranean forests. *Ecology Letters* 10, 241–250.
- Wishnie, M.H., Dent, D.H., Mariscal, E., Deago, J., Cedeno, N., Ibarra, D., Condit, R., Ashton, P.M.S., 2007. Initial performance and reforestation potential of 24 tropical tree species planted across a precipitation gradient in the Republic of Panama. *Forest Ecology and Management* 243, 39–49.
- Yang, Y.-S., Chen, G.-S., Guo, J.-F., Xie, J.-S., Wang, X.-G., 2007. Soil respiration and carbon balance in a subtropical native forest and two managed plantations. *Plant Ecology* 193, 71–84.

Appendix D – GIS Maps

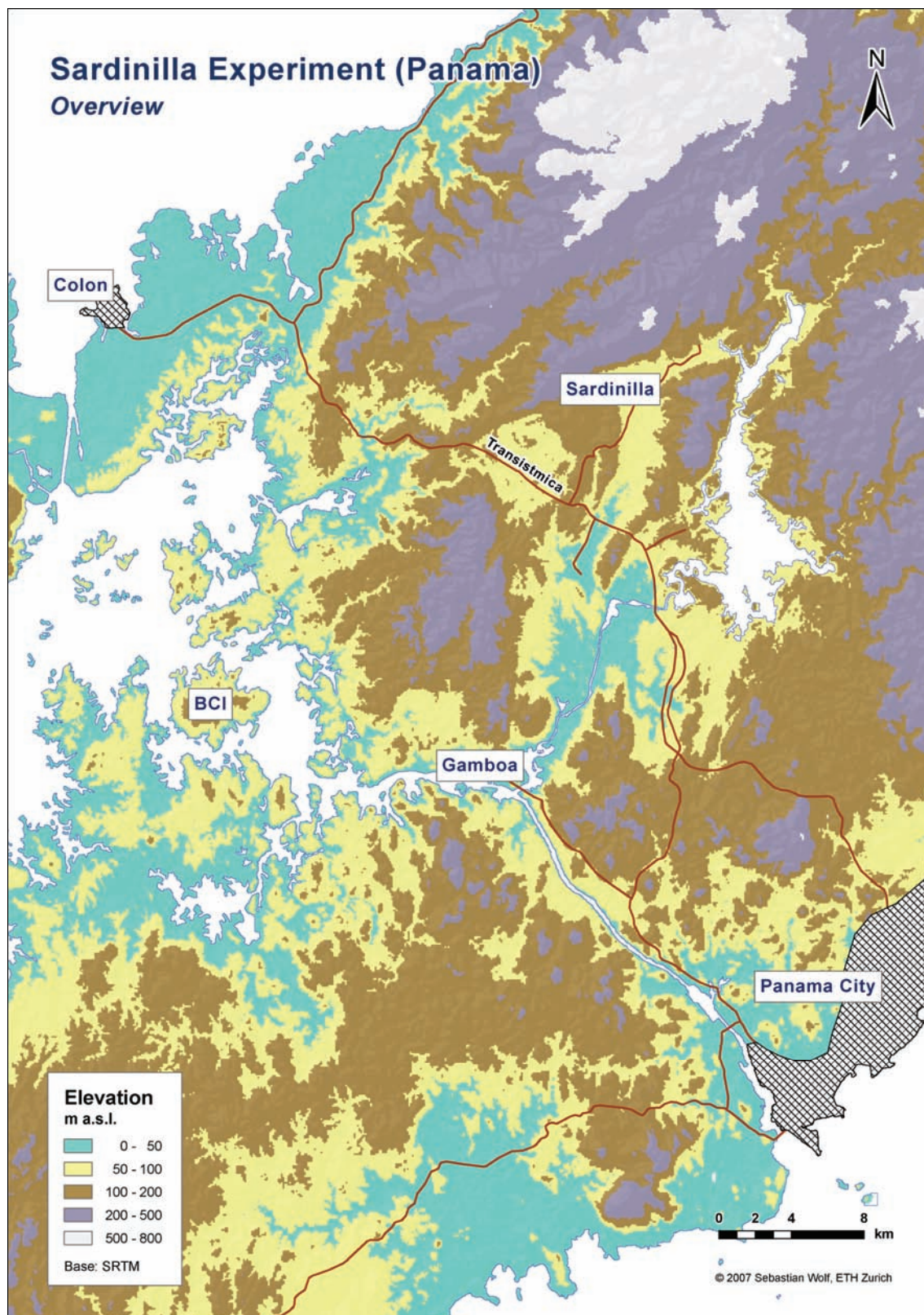
The assembly of a Geographic Information System (GIS) of the Sardinilla site was based on an extensive surveying and mapping campaign in February and March 2007. Elevation data was surveyed using a Vertex Laser VL400 (Hagloef, Langsele, Schweden) with 245 measurement points within the 12 ha Sardinilla Plantation. The digital elevation model was generated using ordinary kriging. Location data was surveyed using a handheld Geck 301 PDC receiver (Garmin, Graefelfing, Germany). The software Fugawi 4.0 (Northport Systems Inc., Toronto, Ontario, Canada) was used to extract mapping data from the handheld GPS receiver and convert them into ESRI shapefiles. The software ArcGIS 9.1 (ESRI, Redlands, California, USA) was used for digitizing, analyzing data and for the map design.

GIS Maps

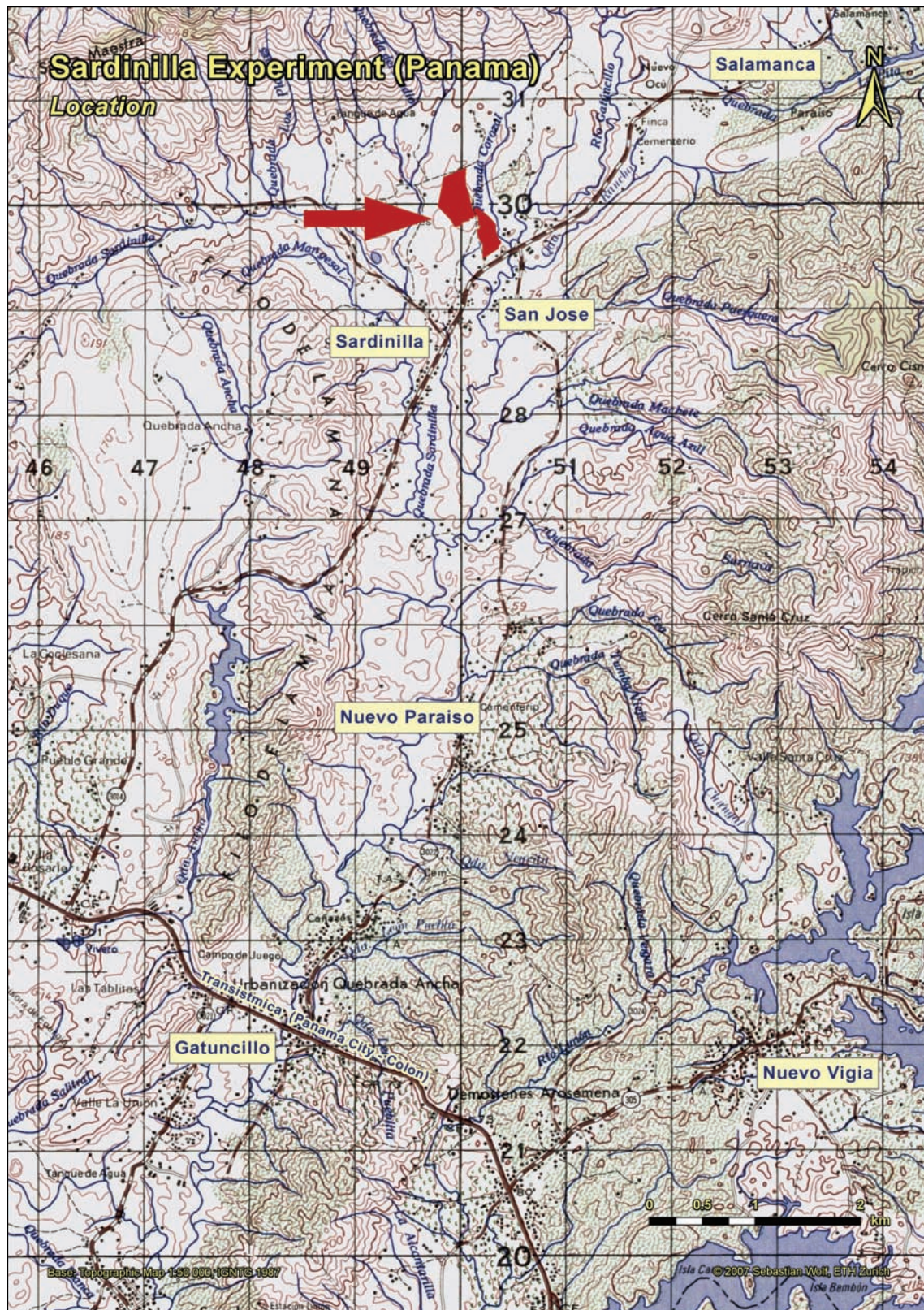
- D1: Overview of Central Panama
- D2: Topography of Central Panama
- D3: Location of the Sardinilla site
- D4: Geology of the Sardinilla site
- D5: Surroundings of the Sardinilla site
- D6: Infrastructure of the Sardinilla Plantation and Pasture
- D7: Orthophoto of the Sardinilla site
- D8: Land use of the Sardinilla Plantation and Pasture
- D9: Tree species richness in the Sardinilla Plantation
- D10: Relief in the Sardinilla Plantation
- D11: Slope angle in the Sardinilla Plantation
- D12: Slope aspect in the Sardinilla Plantation
- D13: Modelled surface runoff in the Sardinilla Plantation
- D14: GIS geometries of the Sardinilla Plantation



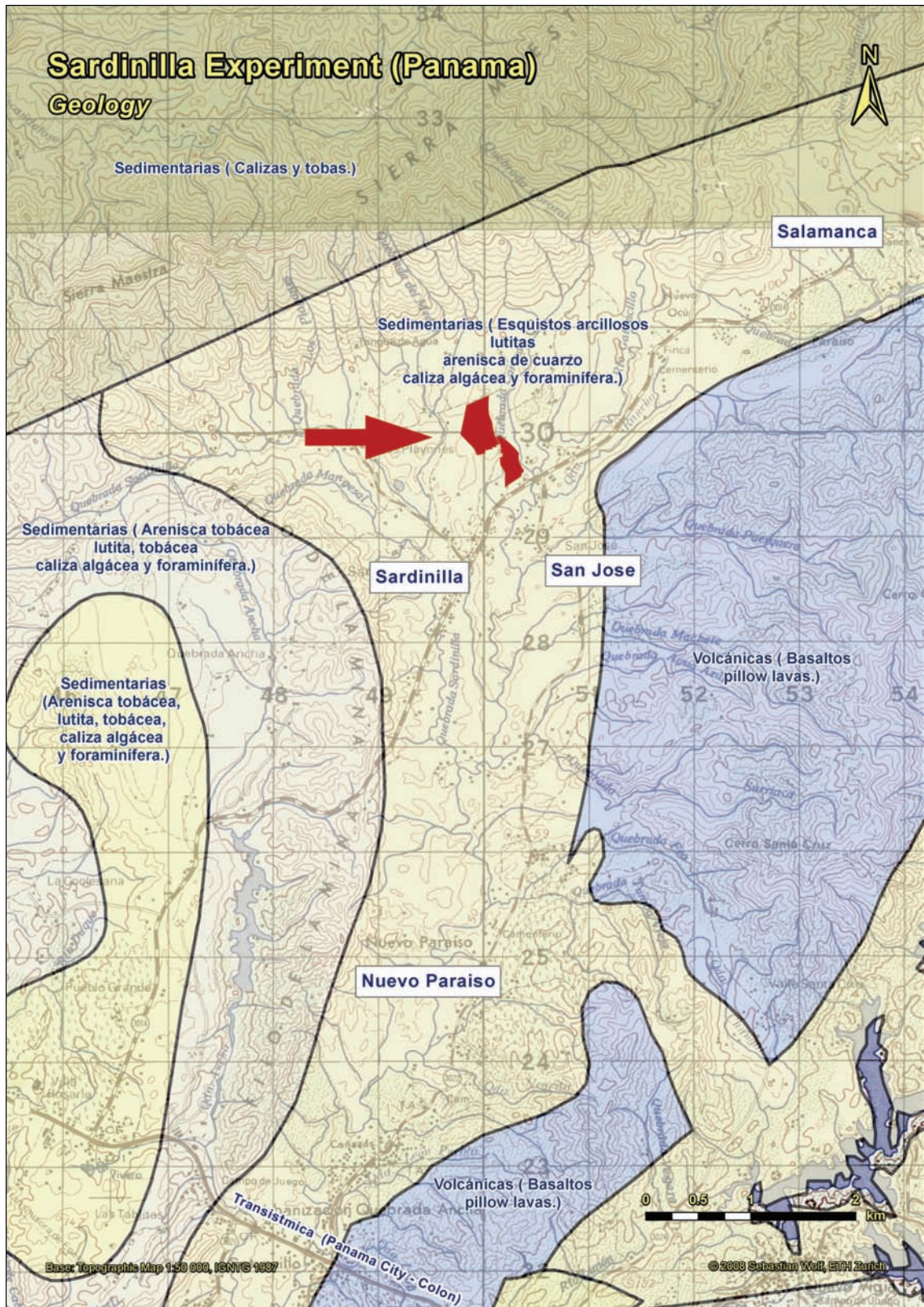
D1. Overview of Central Panama. Vector data is based on VMAP1 from the National Imagery and Mapping Agency (NIMA).



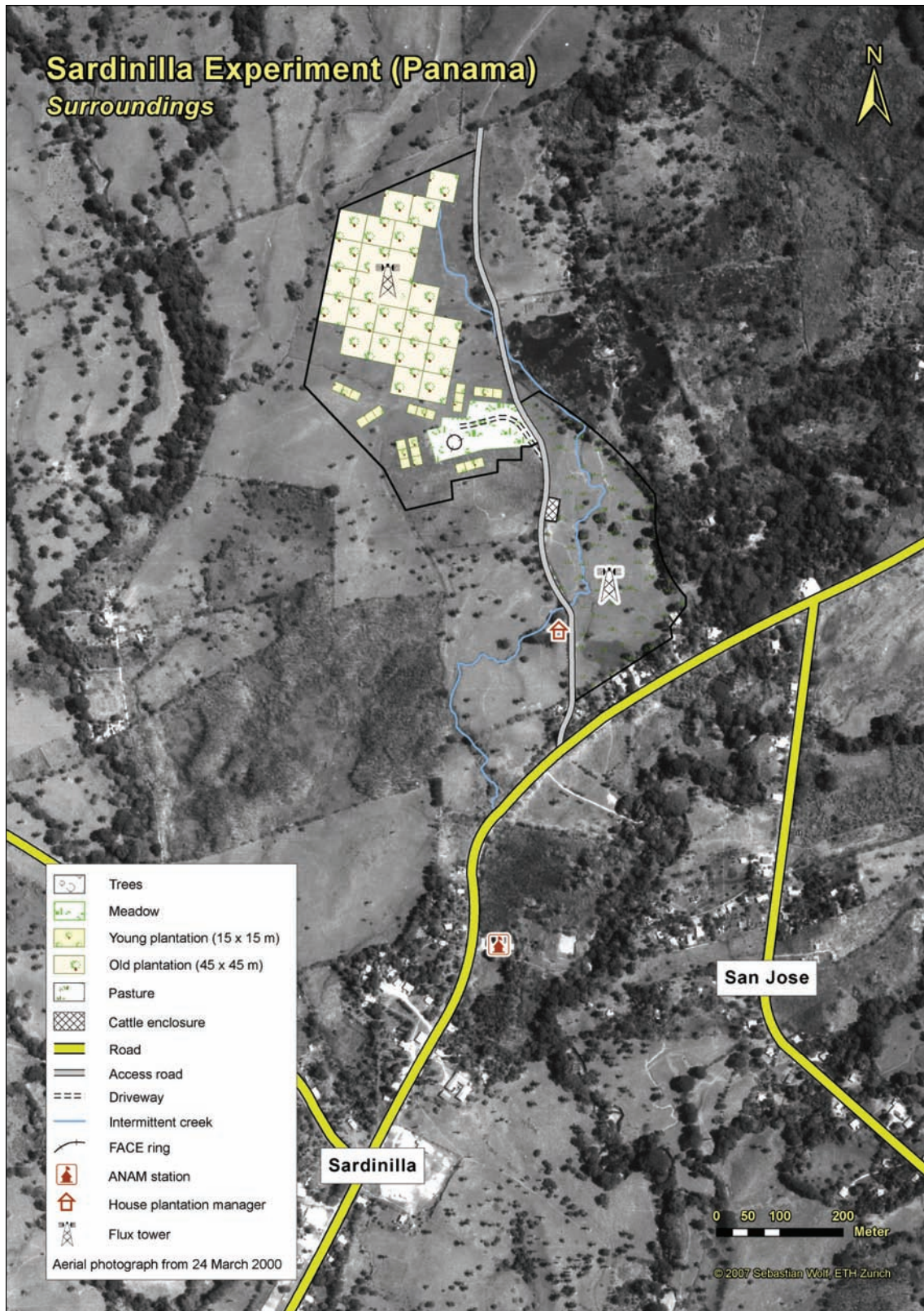
D2. Topography of Central Panama. The topography is derived from the digital elevation model of the Shuttle Radar Topography Mission (SRTM) by NASA. Vector data is based on VMAP1 from the National Imagery and Mapping Agency (NIMA).



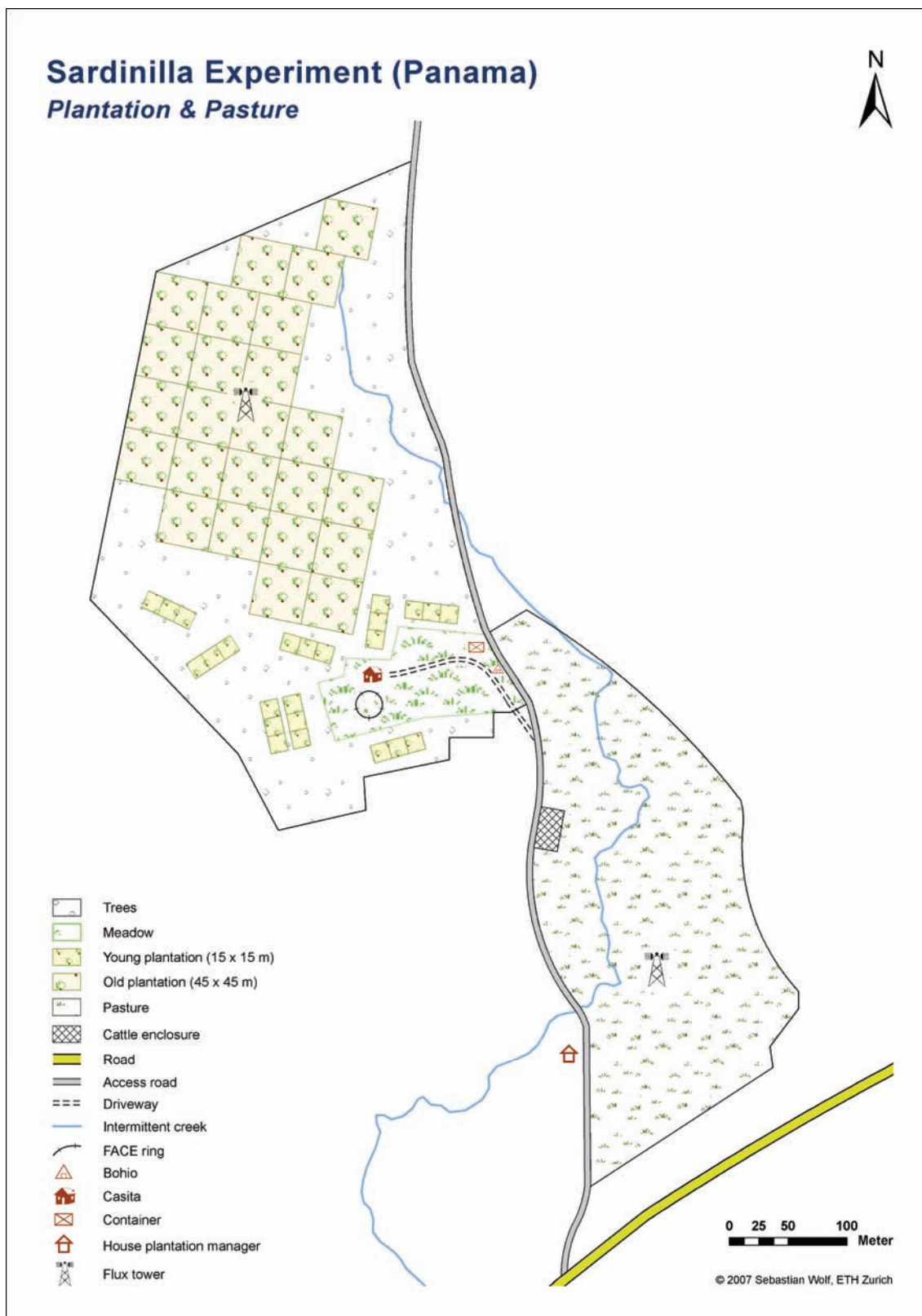
D3. Location of the Sardinilla site. The topographic map 1:50 000 was provided by the Instituto Geográfico Nacional Tommy Guardia (IGNTG).



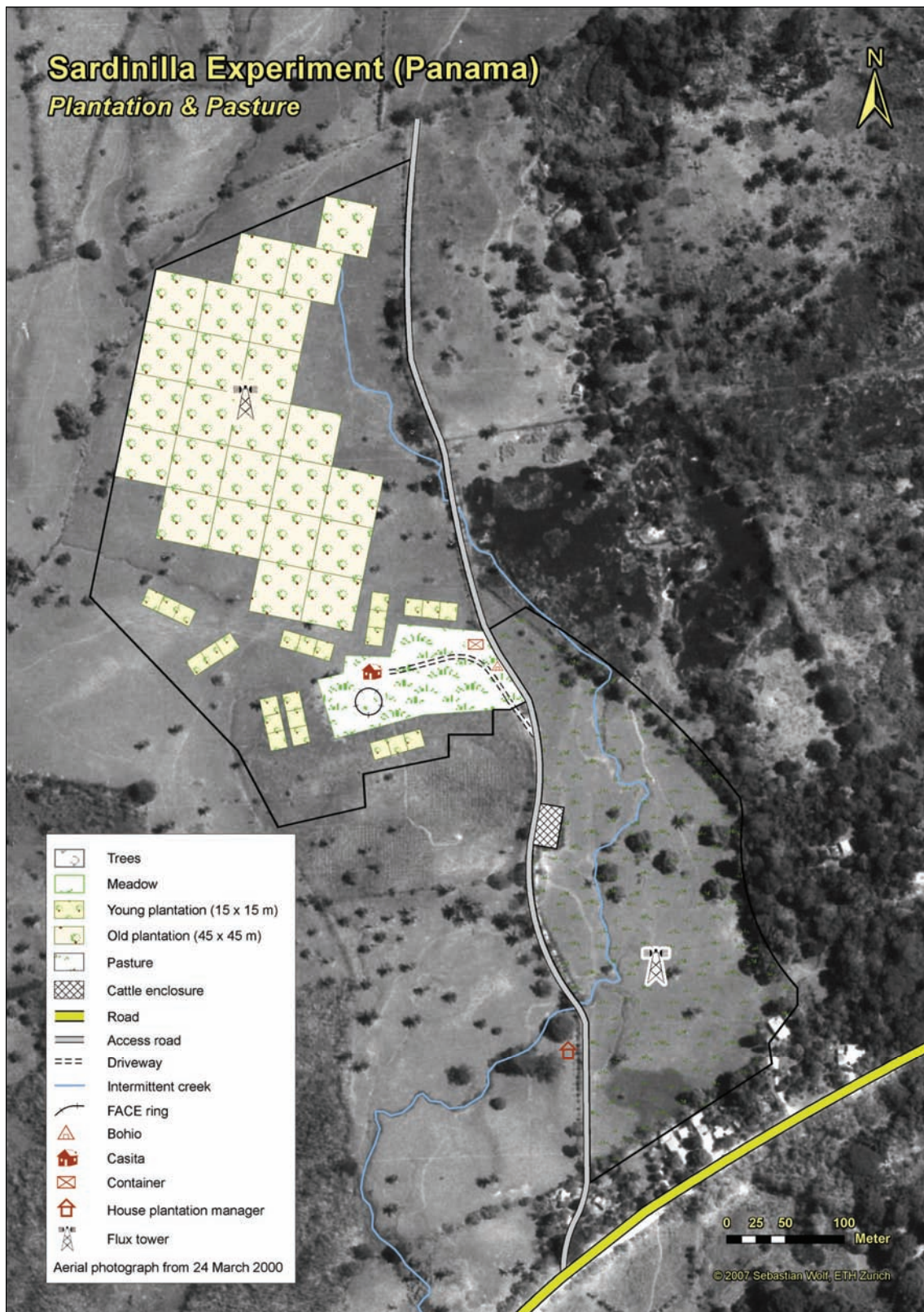
D4. Geology of the Sardinilla site, which translates from the Spanish notation to ‘Sediments consisting of clayey schist, pelite, quartz sandstone and limestone from algae and foraminifera’. Geology data was provided by the Autoridad Nacional del Ambiente of Panama (ANAM, 2010). The topographic map 1:50 000 was provided by the Instituto Geográfico Nacional Tommy Guardia (IGNTG).



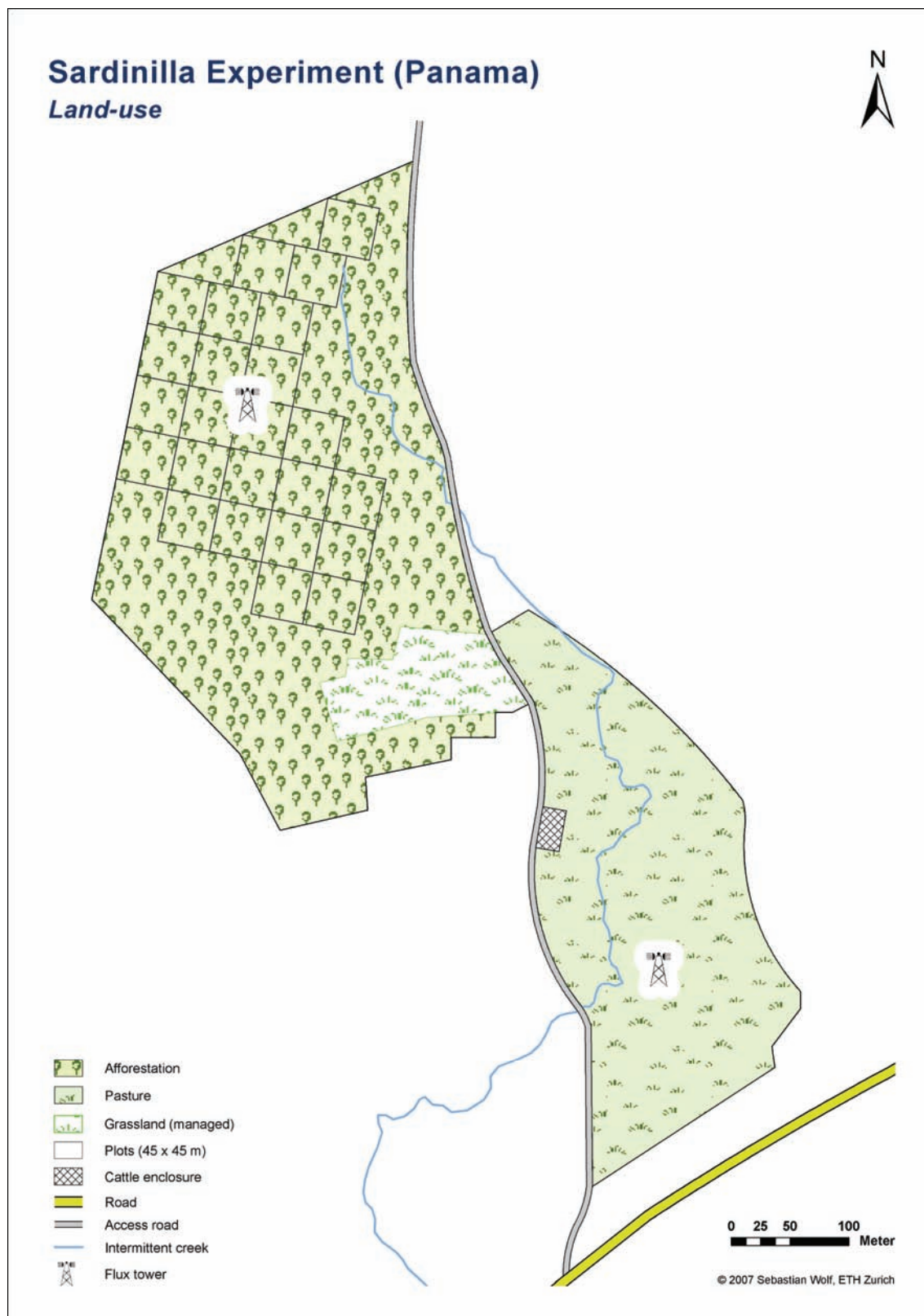
D5. Surroundings of the Sardinilla site. The aerial photograph was provided by the Instituto Geográfico Nacional Tommy Guardia (IGNTG).



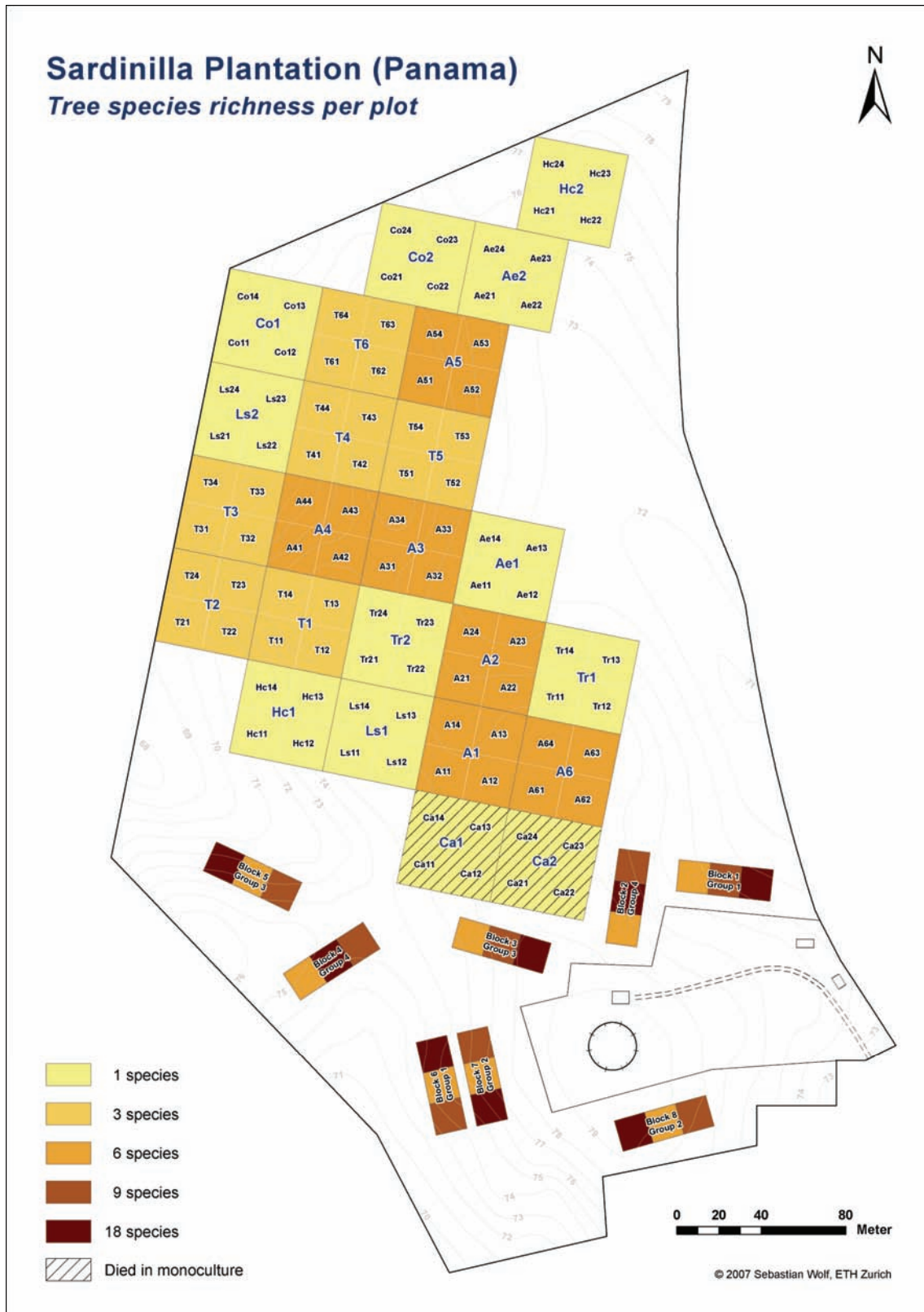
D6. Infrastructure of the Sardinilla Plantation and Pasture.



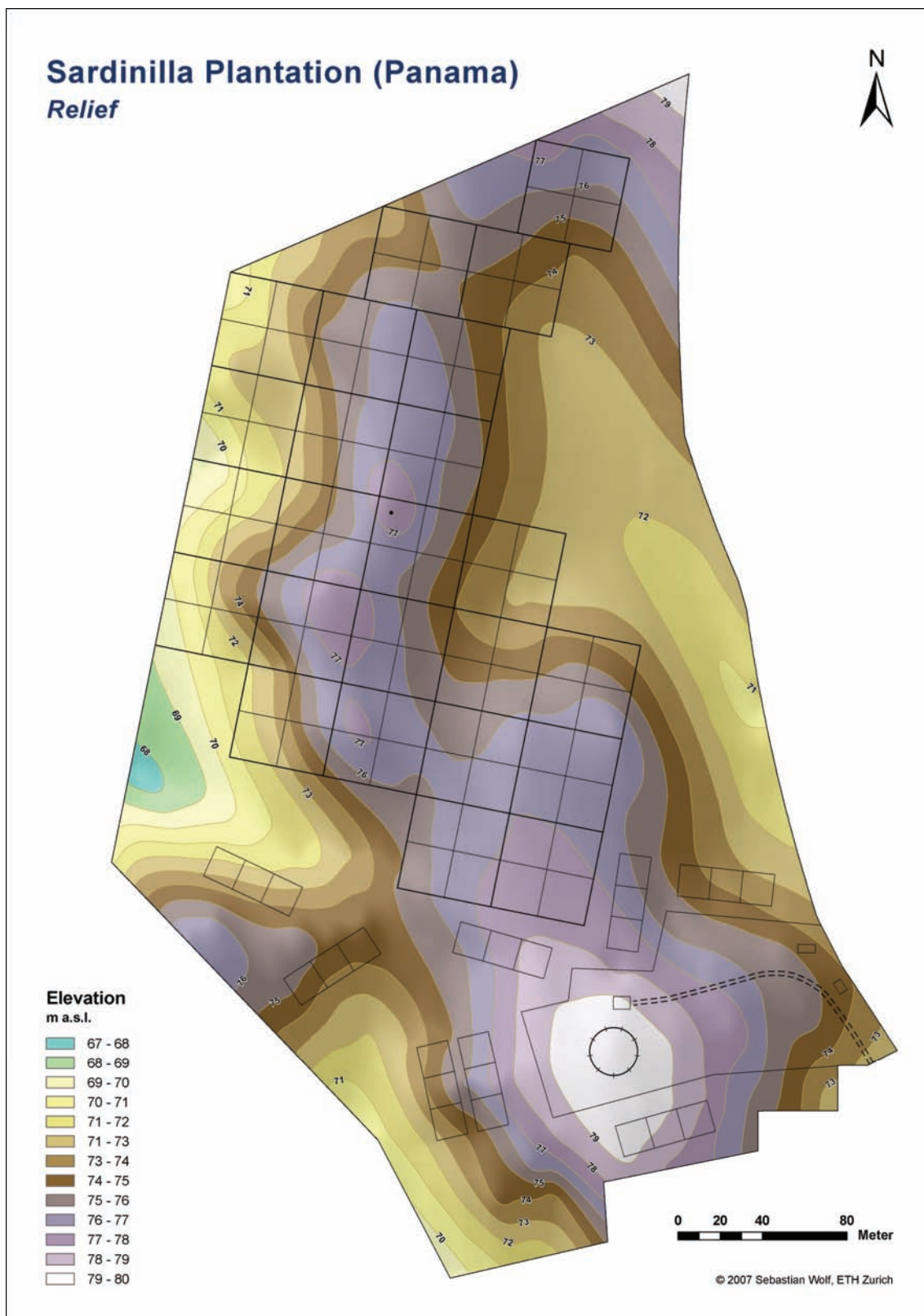
D7. Orthophoto of the Sardinilla site. The aerial photograph was provided by the Instituto Geográfico Nacional Tommy Guardia (IGNTG).



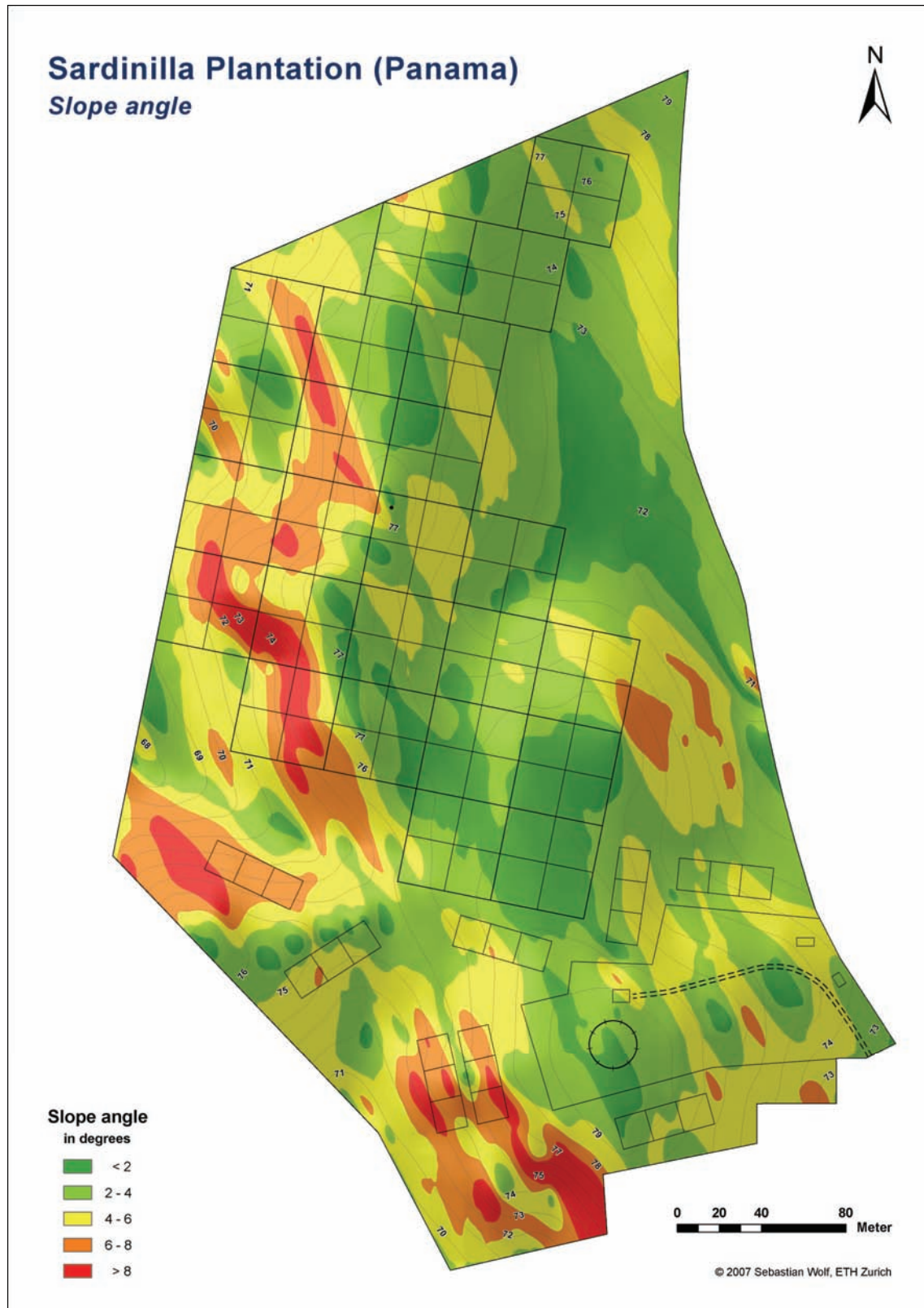
D8. Land use of the Sardinilla Plantation and Pasture. The surrounding areas are predominantly pasture land with occasional patches of secondary forest.



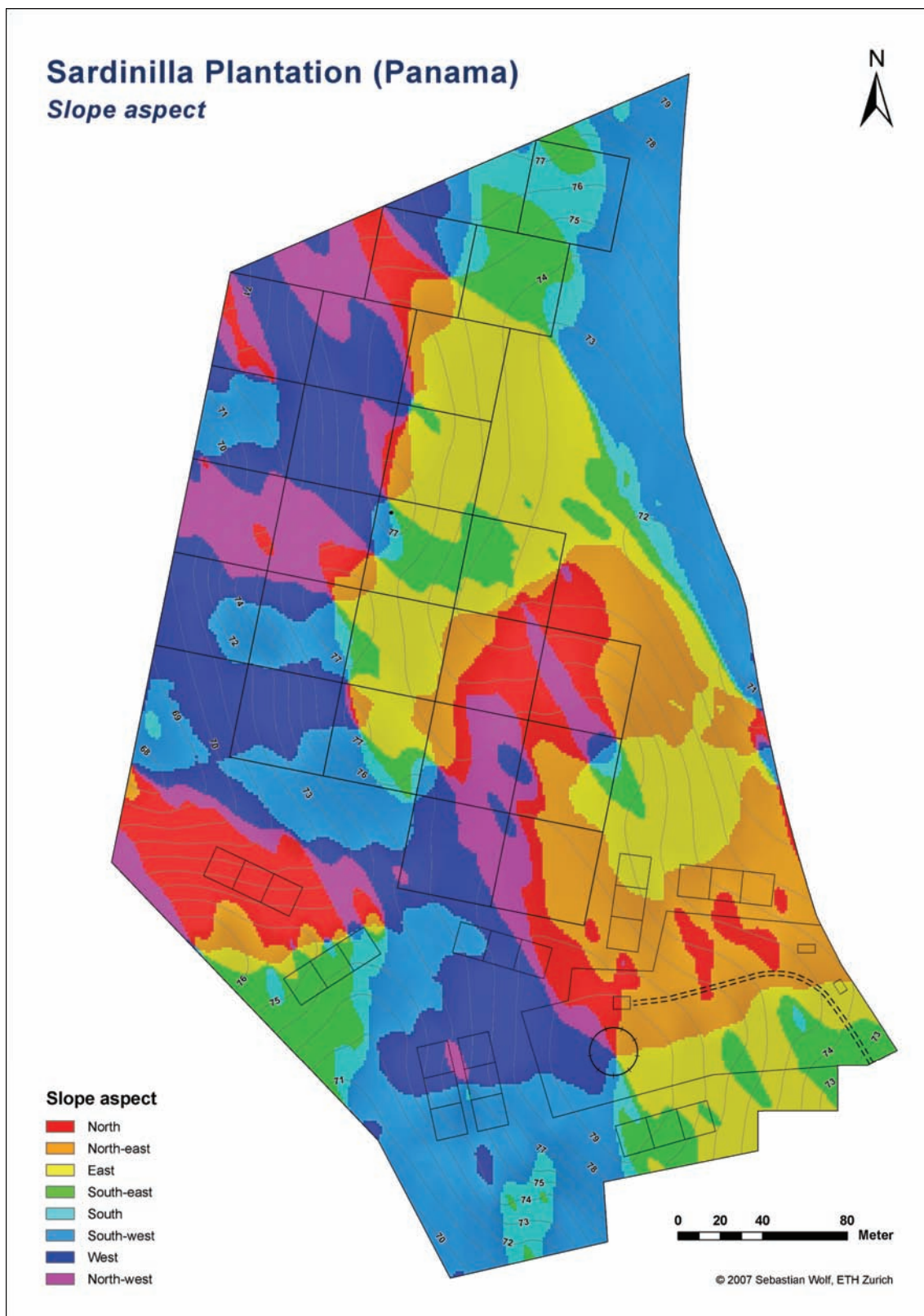
D9. Tree species richness in the Sardinilla Plantation. Large labels denote the plot and small labels denote the subplot names.



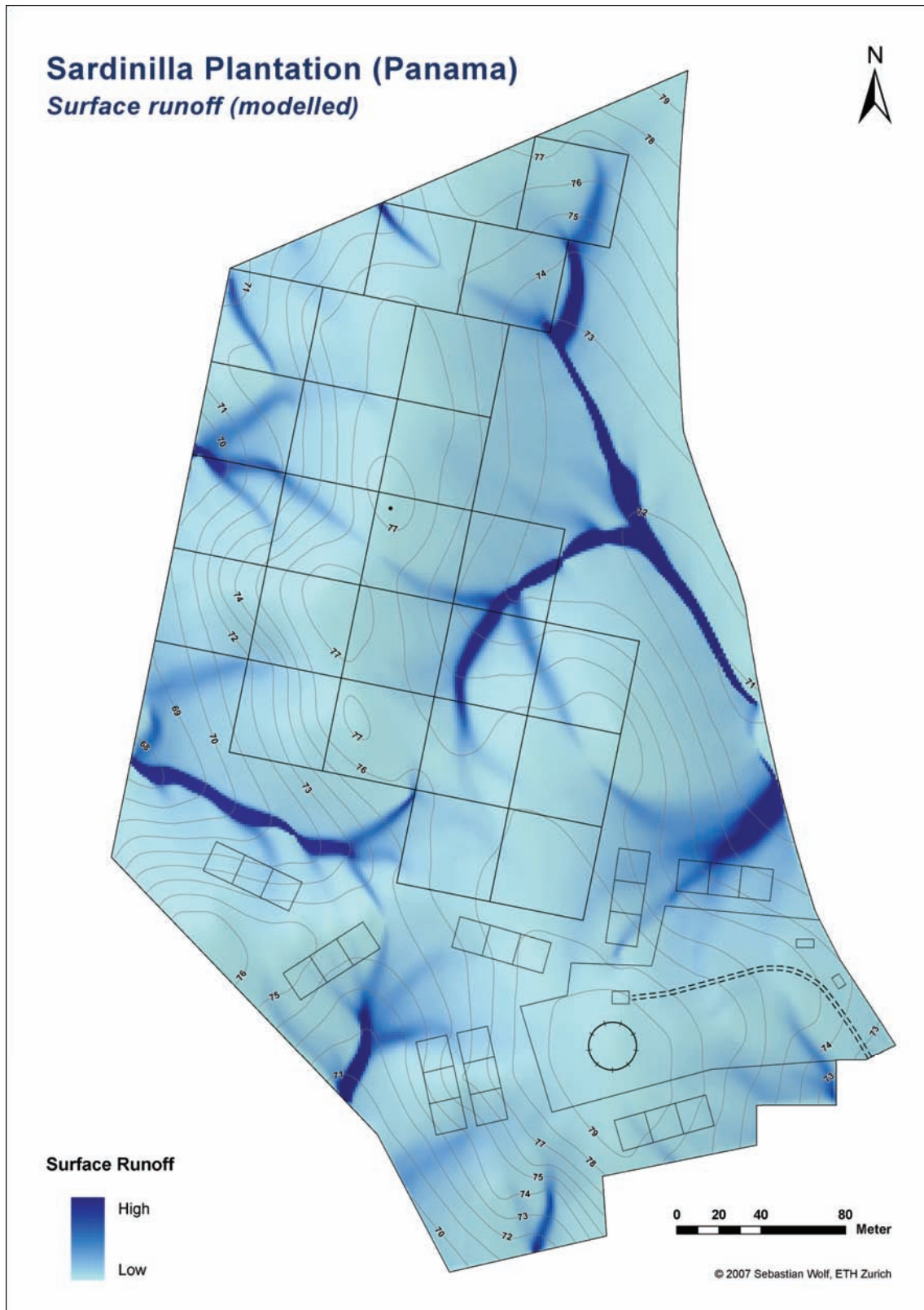
D10. Relief in the Sardinilla Plantation



D11. Slope angle in the Sardinilla Plantation



D12. Slope aspect in the Sardinilla Plantation



D13. Modelled surface runoff in the Sardinilla Plantation using the multiple flow direction algorithm FD8 after Freeman (1991).



D14. GIS geometries of the Sardinilla Plantation. The blue lines and numbers denote the silvopastoral plots of Mirco Plath (Applied Entomology Group, ETH Zurich).

Acknowledgements

This thesis would not have been possible without the scientific, technical and personal support of various people during the four years of my research at ETH Zurich.

First of all, I would like to thank **Nina Buchmann** and **Werner Eugster** for being my supervisors, mentors, for providing continuous support that reached far beyond science and for being exemplary role models of scientific supervisors.

Nina: Thank you very much for your confidence in me, the opportunity to do research in your group, for giving me the freedom to work independently, the encouragement to never stop questioning, countless challenging and inspiring discussions, valued advices, and for your persistent support of my community service outside of science. With your passion and dedication, you have an invaluable share in my motivation of continuing in science.

Werner: Thank you very much for your tremendous support with flux measurements, data analysis, programming in R and for very constructive feedbacks. Your outstanding patience and constant encouragements were invaluable, and I admire your broad and profound knowledge of ecology, micrometeorology, computer sciences *et cetera* – for me, you are a truthful Geographer. I am also very grateful for your more or less successful introduction to the art of ‘Swiss diplomacy’.

Thanks also to **Nicolas Gruber** for being my very supportive co-examiner, who always found a way of convincing me to see my results from another perspective. This was a great benefit for my thesis work and I really appreciated the inspiring discussions.

Many thanks to all my colleagues from the **Grassland Sciences and TEP Group**, for the pleasant working environment and the supportive atmosphere, especially to:

Peter Plüss, for the outstanding technical support combined with a constant positive attitude.

Patrick Flüttsch, for manufacturing various prefabricated parts for my fieldwork.

Claudine, for managing all the administrative, travelling and accounting issues.

Alexander Knohl, for many inspiring discussions and feedbacks on posters.

Ansgar Kahmen, Albin Hammerle, Patrick Sturm and Dörte Bachmann for proof-reading and Lutz Merbold for manuscript feedback.

Sonja Majorek, for many inventive discussions on water fluxes.

Rebecca Hiller, for providing R support, for many informative flux measurement discussions and for valuable comments on manuscripts.

Sophia Etzold, my long-term roommate in the basement of the LFW building, for helpful discussions on flux measurements and R.

Sincere thanks to Catherine Potvin for hosting my fieldwork at the Sardinilla site and to Ben Turner for many inspiring discussions on soil data. Doing research in Panama would have been very difficult without the support of the Smithsonian Tropical Research Institute (STRI) and I am particularly grateful to Raineldo Urriola, who repeatedly solved logistic problems even when I was far away from Panama.

Thanks to Rodrigo Vargas for constructive manuscript feedback and the stimulating cooperation in organizing the FLUXNET Young Scientist Network. Furthermore, I would like to thank Timothy Seipel, for regularly pulling me away from the desk for magnificent adventures in the Swiss mountains and valuable comments on manuscripts. Thanks also to Katharine Seipel for helpful language editing.

Particular thanks go to **José Monteza** for his outstanding support in the field and for reliable tower maintenance while I have been far away from Panama. Thanks also to Iliana Monteza for family-like board and logging in Sardinilla.

Very special thanks to **Matthias (Matti) Barthel** for all the inspiring philosophical and personal conversations, for enlightening my biological understanding of plants, for innumerable visits to the ‘Tanne’, and for all the cheerful time spend together. Without you, my PhD time would have been not half that enjoyment.

Finally, special thanks go to **my parents**, Dorothee and Hans-Dieter Wolf, for invaluable support in following my own path and for giving me the opportunity to spend most of my childhood outdoors. This was without doubt the foundation of my curiosity and fascination for nature that attracted me to sciences. Therefore, this thesis is not only to my credit but to a large extend also your accomplishment.

Abschließend möchte ich **meinen Eltern**, Dorothee und Hans-Dieter Wolf, ganz herzlich danken. Von Euch hatte ich die unbegrenzte Unterstützung meinen eigenen Weg zu gehen und die wertvolle Möglichkeit, einen Großteil meiner Kindheit draußen in der Natur verbringen zu können. Dies war ohne Zweifel die Grundlage für meine Neugierde und Faszination für die Natur, welche mich letztendlich für die Naturwissenschaften begeistert hat. Diese Doktorarbeit ist somit nicht alleine mein Verdienst, sondern Ihr habt in entscheidendem Maß zum Gelingen dieser Arbeit beigetragen.

The research presented in this thesis was funded by the North-South Centre (former Swiss Centre for International Agriculture) of ETH Zurich, Switzerland. Furthermore, I acknowledge financial support for conferences and fieldwork by the Huber-Kudlich-Foundation, the Fonds Agro-Alimentaire, the Association Suisse de Géographie and the Professor Dr. Zerweck-/ Cassella-Foundation.

SEBASTIAN WOLF

Born on 25th of December 1978
Dresden, Germany



Education

- 2006 – 2010 **PhD student**, ETH Zurich (Switzerland),
Institute of Plant, Animal and Agroecosystem Sciences,
Grassland Sciences Group
Thesis: *"Carbon dioxide and water vapour fluxes of tropical
pasture and afforestation: seasonal variations of net eco-
system exchange and carbon sequestration potentials"*
- 1999 – 2006 **M.Sc. in Geography**, Dresden University of Technology,
Dresden (Germany)
Thesis: *"Effects of changing land-use patterns on soil
erosion in the Saxon Switzerland National Park Region"
(in collaboration with the Leibniz Institute of Ecological and
Regional Development)*
Specialisations: *Physical Geography, Cartography,
Remote Sensing, Computer Science, Geographic
Information Systems (GIS)*
Research topics: *Soil erosion modelling, landscape
fragmentation, thematic mapping in remote areas*
- 1997 **High school degree**, Johann-Andreas-Schubert
Gymnasium, Dresden (Germany)

Professional Experience

- 2007 – 2010 **Visiting Scientist**, Smithsonian Tropical Research Institute
(STRI), Panama City (Panama)
Extensive fieldwork at the Sardinilla research site
- 10/2003 – 09/2005 **Teaching Assistant**, Dresden University of Technology,
04/2001 – 07/2002 Institute of Geography, Dresden (Germany)
*Preparation for undergraduate and graduate courses; Mark-
ing of essays; Leading and preparing geographical excursions*
- 10/2004 – 02/2005 **Teaching Assistant**, Dresden University of Technology,
10/2002 – 02/2004 Institute of Photogrammetry and Remote Sensing,
Dresden (Germany)
*Teaching and course preparation for undergraduate and
graduate level in Remote Sensing; Maintaining systems and
data; Revision of e-learning platform*
- 11/2002 – 05/2003 **Research Assistant**, Simon Fraser University,
Department of Geography, Burnaby / Vancouver (Canada)
*Research project on the early detection of Mountain Pine
Beetle infestation using airborne remote sensing; Editorial
assistance for the 'International Journal of Remote Sensing'*

-
- 08–09/2002 **Leader of scientific mapping expedition**,
Dresden University of Technology, Institute of Cartography,
Dresden (Germany)
*Leading and organising of scientific mapping expedition
to Tien Shan Mountains (Kyrgyzstan)*
- 02–03/2002 **Participant of scientific mapping expedition**,
Dresden University of Technology, Institute of Cartography,
Dresden (Germany)
*Participating in scientific mapping expedition
to Ojos del Salado (Atacama Desert, Chile)*
- 09/2001 **Leader of scientific surveying expedition**,
Dresden University of Technology, Institute of Cartography,
Dresden (Germany)
*Leading and organising of scientific surveying expedition
to Dachstein South Face Cave (Austrian Alps)*
- 10/2000 – 07/2002 **Teaching Assistant**, Dresden University of Technology,
Institute for Software and Multimedia Technology,
Dresden (Germany)
Undergraduate teaching for application software
- 03/1998 – 04/1999 **Civilian Service**, German Multiple Sclerosis Society,
Dresden (Germany)
Care for handicapped people
- 10/1997 – 12/1997 **Internship**, Saxony National Association of the
German Alpine Association, Dresden (Germany)
Thematic mapping of rock formations

Community Service

- since 2009 **Organizer**, FLUXNET Young Scientist Network
- since 2005 **Federal Education Team**, German Alpine Association
Teaching instructor of youth guides
- 2003 – 2008 **Executive board**, Saxony National Association of the
German Alpine Association
Fundraising, mentoring, advanced training of youth guides
- since 1995 & 2004 **Youth guide & Instructor for Alpine Climbing**, Saxony
Mountaineering Federation of the German Alpine Association
*Instructor of children, teenager and adults; public relations,
Fundraising, editorial work, organisation of events*

Publications

Peer reviewed

- Wolf S**, Eugster W, Potvin C, Turner BL, Buchmann N (accepted) Carbon sequestration potential of tropical afforestation compared to pasture in Panama. *Global Change Biology*
- Wolf S**, Eugster W, Potvin C, Buchmann N (accepted) Strong seasonal variations in net ecosystem CO₂ exchange of a tropical pasture and afforestation in Panama. *Agricultural and Forest Meteorology*
- Schneebeil M, **Wolf S**, Kunert N, Eugster W, Mätzler C (accepted) Relating the X-Band opacity of a tropical tree canopy to sapflow, rain interception and dew formation. *Remote Sensing of Environment*
- Potvin C, Manzilla L, Buchmann N, Monteza J, Moore T, Murphy M, Oelmann Y, Scherer-Lorenzen M, Turner, B.L., Wilcke W, Zeugin F, **Wolf S** (in press) An ecosystem approach to biodiversity effects: carbon pools in a tropical tree plantation. *Forest Ecology and Management*. doi: 10.1016/j.foreco.2010.11.015
- Wolf S**, Walz U, Kleber A (2009) Effects of land-cover change on soil erosion in the Saxon Switzerland National Park Region. *Die ERDE* 140(2): 155–174
- Schneebeil M, Mätzler C, **Wolf S**, Eugster W (2008) X-band opacity of a tropical tree canopy and its relation to intercepted rain, eddy fluxes and other meteorological variables. *Microwave Radiometry and Remote Sensing of the Environment, MICRORAD 2008*. doi: 10.1109/MICRAD.2008.4579514. 223–235

Book chapters, Monographs and Reports

- Walz U, **Wolf S**, Neubert M (2008) Impact of Landscape Change on Landscape Functions in the Saxon Switzerland. In: Csaplovics E, Wagenknecht S, Seiler U (Eds.): *Spatial Information Systems for Transnational Environmental Management of Protected Areas and Regions in the Central European Space*. Rhombus, Berlin. pp 105–117
- Wolf S**, Walz U (2007) Auswirkungen einer veränderten Landnutzungsstruktur auf die Bodenerosion. In: Strobl J, Blaschke TH, Griesebner G (Hrsg.): *Angewandte Geoinformatik 2007. Beiträge zum 19. AGIT-Symposium Salzburg*. Wichmann, Heidelberg, pp 867–872
- Wolf S** (2006) Bodenerosion als Funktion veränderter Landnutzungsstruktur – Modellierung der Entwicklung am Beispiel der Nationalparkregion Sächsische Schweiz. *Diploma / Masters thesis*, Dresden University of Technology, Institute of Geography, 177 p
- Wolf S** (2004) Landschaftszerschneidung – Grenzüberschreitende Untersuchung der Entwicklung und ihrer Auswirkungen für das Gebiet der Sächsisch-Böhmischen Schweiz. *Studienarbeit (Research Assignment)*, Dresden University of Technology, Institute of Geography, 40 p
- Roberts A, Dragicevic S, Northrup J, **Wolf S**, Li Y, Coburn C (2003) Mountain Pine Beetle Detection and Monitoring – Remote Sensing Evaluations. *Forestry Innovation Investment Operational Report*, 45 p
- Roberts A, Northrup J, **Wolf S**, Li Y (2003) Mountain Pine Beetle Detection and Monitoring – Interpretation and Evaluation of Airborne Imagery. *West Fraser Sawmills Report*, 22 p

Miscellaneous

- Wolf S**, Eugster W, Buchmann N (2009) What happens with the carbon? *Newsletter of Smithsonian Tropical Research Institute*, 13.11.2009: 4
- Wolf S**, Eugster W, Buchmann N (2009) CO₂ fluxes of tropical ecosystems with different land-use in Panama. *FluxLetter* 2(3): 14–16
- Vargas R, **Wolf S**, Zeeman M (2009) FLUXNET Young Scientists Network. *FluxLetter* 2(3): 9

- Wolf S**, Walz U (2005) Grenzüberschreitende Untersuchung der Landschaftszerschneidung in der Sächsisch-Böhmischen Schweiz. *Mitteilungen des Landesvereins Sächsischer Heimatschutz e.V.* 3: 33–39
- Wolf S** (2003) Tien Shan Mountains, mapping expedition. *American Alpine Journal* 77: 346–347
- Wolf S** (2002) Kartieren in Eis, Geröll und hohen Bergen. *Dresdner Universitätsjournal* 16: 3
- Wolf S** (2002) Topographische Kartierung am höchsten Vulkan der Erde. *Der neue Sächsische Bergsteiger* 2: 48–49

DISS. ETH NO. 19415

ISBN 978-3-909386-16-1

